

Veejendra K. Yadav

# Steric and Stereoelectronic Effects in Organic Chemistry

 Springer

# Steric and Stereoelectronic Effects in Organic Chemistry

Veejendra K. Yadav

# Steric and Stereoelectronic Effects in Organic Chemistry

 Springer

Veejendra K. Yadav  
Department of Chemistry  
Indian Institute of Technology Kanpur  
Kanpur, Uttar Pradesh  
India

ISBN 978-981-10-1138-2      ISBN 978-981-10-1139-9 (eBook)  
DOI 10.1007/978-981-10-1139-9

Library of Congress Control Number: 2016938380

© Springer Science+Business Media Singapore 2016

This work is subject to copyright. All rights are reserved by the Publisher, whether the whole or part of the material is concerned, specifically the rights of translation, reprinting, reuse of illustrations, recitation, broadcasting, reproduction on microfilms or in any other physical way, and transmission or information storage and retrieval, electronic adaptation, computer software, or by similar or dissimilar methodology now known or hereafter developed.

The use of general descriptive names, registered names, trademarks, service marks, etc. in this publication does not imply, even in the absence of a specific statement, that such names are exempt from the relevant protective laws and regulations and therefore free for general use.

The publisher, the authors and the editors are safe to assume that the advice and information in this book are believed to be true and accurate at the date of publication. Neither the publisher nor the authors or the editors give a warranty, express or implied, with respect to the material contained herein or for any errors or omissions that may have been made.

Printed on acid-free paper

This Springer imprint is published by Springer Nature  
The registered company is Springer Science+Business Media Singapore Pte Ltd.



*To Arpita, Dhananjay and Dhruv with love*

# Preface

The aim of this book is to offer a decent understanding of the principles of steric and stereoelectronic effects in organic chemistry and their consequences on product selectivity and reaction rates. This book differs from most other books of the same level. In this book, strong emphasis is placed on logical evolution of the subject in a streamlined manner to aid structured comprehension of the intricacies. This book is intended for the honors undergraduate and graduate students, and the teachers.

The discussion is spread over seven chapters. Chapter 1 lays the stress on the important aspects of steric and stereoelectronic effects and their control on the conformational profile and reactivity features of the molecules. Chapter 2 describes the geometrical requirements for reactions at saturated and unsaturated carbons, and the resultant stereochemical features. Application of the said geometrical requirements to intramolecular instances results in remarkable control on diastereoselectivity. Chapter 3 deals with the facial selectivity of nucleophilic additions to acyclic and cyclic carbonyl compounds, and it explains how the steric and stereoelectronic effects control the same through elaborate discussions. The selectivity profile is explained using models such as Cram's model, Anh–Felkin modification of Cram's model, Houk's transition structure and electrostatic models, Cieplak's  $\sigma \rightarrow \sigma^*$  model, and cation coordination model. Chapter 4 comments on allylic strain and its effect on the conformational profile and related stereochemical outcomes of reactions. The high diastereoselectivity observed in the reactions of Evans enolates is solely on account of allylic strain. The conservation of orbital symmetry rules is presented in Chap. 5. After defining the bonding and antibonding orbitals of different types, reactions such as  $\pi^2 + \pi^2$ ,  $\pi^4 + \pi^2$ , and electrocyclic processes have been used to demonstrate the application of the rules. Chapter 6 is an amalgamation of the conservation of orbital symmetry rules and orbital overlap effect, which serves as a very powerful tool to reliably predict the stereochemical course of pericyclic reactions. It is demonstrated by examples how the orbital overlap factor allows one of the otherwise two symmetry-controlled pathways to predominate. Chapter 7 is a must read to understand some of those control elements that did not find mention in the earlier chapters. The prominent among these elements are

spiroconjugation, periselectivity, torquoselectivity,  $\alpha$ -effect, Hammett constants, Hammond postulate, and Curtin–Hammett principle. A set of questions are provided at the end to challenge the reader by allowing an evaluation of the comprehension level.

The book is based mainly on the lecture notes prepared for the classes at IIT Kanpur. I am grateful to the authors of many books that I have used in preparing the notes. Important among these books are: (a) Stereoelectronic Effects in Organic Chemistry by Pierre Deslongchamps, (b) Molecular Orbitals and Organic Chemical Reactions by Ian Fleming, (c) Modern Physical Organic Chemistry by Eric V. Anslyn and Dennis A. Dougherty, (d) Mechanism and Theory in Organic Chemistry by Thomas H. Lowry and Kathleen S. Richardson, and (e) The Physical Basis of Organic Chemistry by Howard Maskill. I thank Prof. J.N. Moorthy for reading the chapters critically and suggesting changes to improve the quality of presentation. I thank Prof. M.L.N. Rao for his pleasant company and stimulating discussions over numerous coffee sessions. Last but not least, I thank Dr. Arpita Yadav, my better half, and Dhananjay and Dhruv, our sons, for bearing with me while I have been busy with drawing the structures and also for their never-ending enthusiasm and support.

I would appreciate and gratefully acknowledge criticism, suggestion for improvement, and detection of errors from the readers. I thank the Publishers, Springer (India) Pvt. Ltd., for bringing out the book in the present form.

Veejendra K. Yadav

# Contents

<b>1 Steric and Stereoelectronic Control of Organic Molecular Structures and Organic Reactions</b> . . . . .	1
1 Influence of Steric Effects on Structures . . . . .	1
2 Influence of Stereoelectronic Effects on Reactions . . . . .	6
3 Evaluation of the Numerical Value of Anomeric Effect . . . . .	28
4 Influence of Anomeric Effect on Conformational Preferences . . . . .	29
5 Influence of Anomeric Effect on Conformational Reactivities . . . . .	35
6 Conformations of Mono and Dithioacetals . . . . .	40
7 Conformations of Mono and Diazaacetals . . . . .	43
References . . . . .	44
<b>2 Reactions at Saturated and Unsaturated Carbons</b> . . . . .	47
References . . . . .	68
<b>3 Diastereoselectivity in Organic Reactions</b> . . . . .	71
1 Cram's Model for Asymmetric Synthesis . . . . .	72
2 Anh–Felkin Modification of Cram's Model for Asymmetric Synthesis . . . . .	72
3 Cieplak's Model for Diastereoselectivity . . . . .	76
4 Houk's Transition State and Electrostatic Models for Diastereoselectivity . . . . .	83
5 Cation Coordination Model for Diastereoselectivity . . . . .	86
References . . . . .	100
<b>4 A<sup>(1,2)</sup> and A<sup>(1,3)</sup> Strains</b> . . . . .	103
1 Introduction . . . . .	103
2 A <sup>(1,2)</sup> Strain . . . . .	105
3 Stereocontrol in Reactions on Account of A <sup>(1,2)</sup> Strain . . . . .	109
4 A <sup>(1,3)</sup> Strain . . . . .	111
5 Stereocontrol in Reactions on Account of A <sup>(1,3)</sup> Strain . . . . .	113

6	A <sup>(1,3)</sup> Strain in Amides and Its Consequences on Diastereoselectivity . . . . .	122
	References . . . . .	124
<b>5</b>	<b>The Conservation of Orbital Symmetry (Woodward–Hoffmann Rules) . . . . .</b>	<b>127</b>
1	Introduction . . . . .	127
2	Orbitals and Symmetry Considerations . . . . .	128
3	$\pi^2 + \pi^2$ Reaction . . . . .	131
4	Electrocyclic Ring Closure and Ring Opening Reactions . . . . .	139
5	Diels–Alder Reaction ( $\pi^4 + \pi^2$ Reaction) . . . . .	144
	References . . . . .	146
<b>6</b>	<b>The Overlap Component of the Stereoelectronic Factor</b>	
	<b>Vis-à-Vis the Conservation of Orbital Symmetry Rules . . . . .</b>	<b>147</b>
1	Introduction . . . . .	147
2	Steric Effects in the Thermal Fragmentation of <i>Cis</i> -3,6-Dimethyl-3,6-Dihydropyridazine . . . . .	149
3	Orbital Overlap Effects in the Thermal Fragmentation of Cyclopropanated and Cyclobutanated <i>Cis</i> -3,6-Dimethyl-3,6-Dihydropyridazine . . . . .	149
4	Orbital Overlap Effects in [1,5] Sigmatropic Shifts . . . . .	151
5	Difficulties Experienced with the [1,5] Sigmatropic Shift in Cyclobutanated Species . . . . .	153
	References . . . . .	155
<b>7</b>	<b>Miscellaneous . . . . .</b>	<b>157</b>
1	Spiroconjugation . . . . .	157
2	Periselectivity . . . . .	159
3	Torquoselectivity . . . . .	167
4	Ambident Nucleophiles . . . . .	169
5	Ambident Electrophiles . . . . .	172
6	$\alpha$ -Effect . . . . .	182
7	Carbenes . . . . .	184
8	Hammett Substituent Constants . . . . .	187
9	Hammond Postulate . . . . .	195
10	Curtin–Hammett Principle . . . . .	196
11	Diastereotopic, Homotropic, and Enantiotopic Substituents . . . . .	197
	References . . . . .	200
	<b>Questions . . . . .</b>	<b>203</b>

## About the Author

**Veejendra K. Yadav** earned his Ph.D. under the mentorship of Dr. Sukh Dev in 1982. He has carried out his postdoctoral research at University of Calgary, Memorial University of Newfoundland, University of Ottawa, and University of Southern California over the years 1983–1990 before joining Indian Institute of Technology Kanpur (IITK) as Assistant Professor in the late 1990. Over the years, he rose through ranks and became full professor in 2001. He has taught both undergraduate and postgraduate students at IITK over the past 25 years, and has remained a popular teacher among the students throughout. His research focuses on the development of new reactions with emphasis on the construction of pharmacophores, synthesis of biologically active molecules, and computational-cum-experimental investigation of facial selectivity. He has two international patents and 80 research papers in peer-reviewed journals to his credit. More details may be found on the link: <http://home.iitk.ac.in/~vijendra>.

# Chapter 1

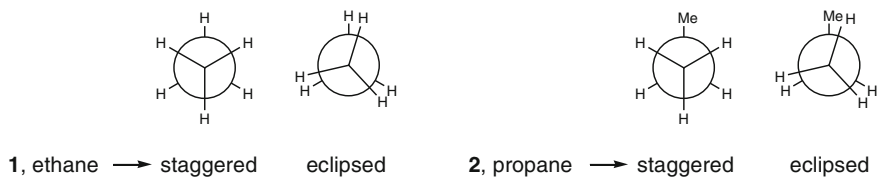
## Steric and Stereoelectronic Control of Organic Molecular Structures and Organic Reactions

**Abstract** This chapter emphasises on the important aspects of steric and stereoelectronic effects and their control on the conformational and reactivity profiles. The conformational effects in ethane, butane, cyclohexane, variously substituted cyclohexanes, and *cis*- and *trans*-decalin systems allow a thorough understanding. Application of these effects to E2 and E1cB reactions followed by anomeric effect and mutarotation is discussed. The conformational effects in acetal-forming processes and their reactivity profile, carbonyl oxygen exchange in esters, and hydrolysis of orthoesters have been discussed. The application of anomeric effect in 1,4-elimination reactions, including the preservation of the geometry of the newly created double bond, is elaborated. Finally, a brief discussion on the conformational profile of thioacetals and azaacetals is presented.

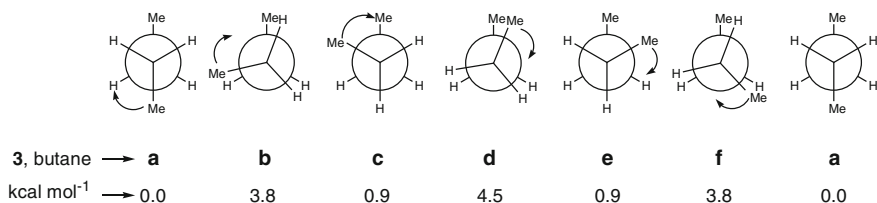
**Keywords** Conformational profile • Steric effect • E2 reaction • E1cB reaction • Anomeric effect • Mutarotation • Acetal hydrolysis • Acetal formation • Carbonyl oxygen exchange in esters • Ozonation of acetals • Orthoester and hydrolysis • Numerical value of anomeric effect • Relative energy of acetals • 1,4-elimination • Mono and dithoacetals • Mono and diazaacetals

### 1 Influence of Steric Effects on Structures

With all the substituents as hydrogen, consider the staggered and eclipsed conformations of ethane **1** as shown below. The staggered conformation is more stable than the eclipsed conformer by  $3.0 \text{ kcal mol}^{-1}$ . The electron pairs of the eclipsed bonds repel each other to raise the energy of the system by  $1.0 \text{ kcal mol}^{-1}$ . Three such interactions make up to  $3.0 \text{ kcal mol}^{-1}$ .

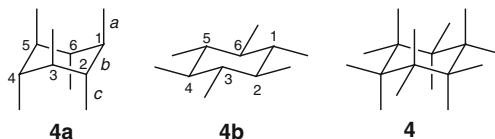


With one of the hydrogen atoms replaced by methyl, we arrive at the staggered and eclipsed conformations of propane **2**. Other than the three repulsive electron pair–electron pair interactions, each contributing  $1.0 \text{ kcal mol}^{-1}$ , there is also the methyl-hydrogen van der Waals repulsion (steric interaction) that contributes  $0.4 \text{ kcal mol}^{-1}$  in the eclipsed conformer. Thus, the eclipsed conformer is less stable by  $(3 \times 1.0) + 0.4 = 3.4 \text{ kcal mol}^{-1}$  than the staggered conformer. On either side of the methyl group in the staggered conformer, there is a hydrogen atom on the front carbon with a dihedral (torsion) angle of  $60^\circ$ . Methyl and hydrogen are said to be *gauche* to each other with no repulsive interaction between them. However, the *gauche* methyl–methyl interaction contributes by  $0.9 \text{ kcal mol}^{-1}$ . Also, the eclipsing methyl–methyl van der Waals repulsion is estimated to be  $1.5 \text{ kcal mol}^{-1}$ . One encounters the last two interactions below in the discussion of conformations of butane.



Different conformers **3a–f** of butane **3** across the central  $\sigma_{C-C}$  bond are shown above. Beginning from the staggered conformer **3a** that has two methyl groups with torsion angle of  $180^\circ$ , one can write the other important conformers by rotation about the central  $\sigma_{C-C}$  bond by  $60^\circ$  each time in the clockwise manner as shown. Note that the conformers **3b** and **3f**, and **3c** and **3e** are one and the same as far as their energies are concerned. There are no issues related to either eclipsing electron pair–electron pair repulsion or van der Waals repulsion in **3a**. Hence, **3a** is the most stable conformer and let us assume its energy as  $0.0 \text{ kcal mol}^{-1}$ . Now, we can calculate the energies of other conformers as follows: **3b** and **3f**:  $3.8 \text{ kcal mol}^{-1}$ ; **3c** and **3e**:  $0.9 \text{ kcal mol}^{-1}$ ; **3d**:  $4.5 \text{ kcal mol}^{-1}$ . All these values are, in fact, so small that butane exists as an equilibrium mixture of all the conformers at STP (standard temperature and pressure). The equilibrium distribution, as expected, is a function of the relative energies; the more stable a conformer, the more is its contribution.

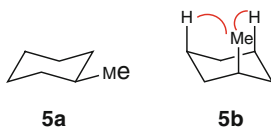




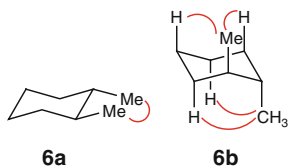
Consider the structure **4a** for cyclohexane. The axial bonds on any two adjacent ring positions, such as C1 and C2, are parallel and also anti to each other. The three bonds involved in this relationship are *a*, *b*, and *c* and they could also be viewed to be in the same plane geometrically. The ‘anti’, the ‘parallel’, and the ‘same plane’ are put together is termed ‘antiperiplanar’. So, the axial bonds on two adjacent cyclohexane ring positions are antiperiplanar.

The equatorial bonds on any two consecutive ring positions, such as C1 and C2, are gauche to each other with a torsion angle of  $60^\circ$  as shown in **4b**. With these substituents as methyl, the situation is exactly the same as in the gauche butane conformers **3c** and **3e**. Therefore, this will raise the energy by  $0.9 \text{ kcal mol}^{-1}$ . Another important structural feature stems from the observation that an equatorial bond is antiperiplanar to two ring bonds. For instance, the bond on C1 is antiperiplanar to  $\sigma_{\text{C2-C3}}$  and  $\sigma_{\text{C5-C6}}$ . Likewise, the bond on C2 is antiperiplanar to  $\sigma_{\text{C3-C4}}$  and  $\sigma_{\text{C1-C6}}$ . A special note should be made of the orientations of the bonds on C3 and C6; other than being antiperiplanar to each other across a hypothetical  $\sigma_{\text{C3-C6}}$  bond, both the bonds are antiperiplanar to  $\sigma_{\text{C1-C2}}$  and  $\sigma_{\text{C4-C5}}$  as well.

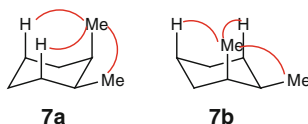
A good knowledge of the structural relationship of axial and equatorial bonds on cyclohexane ring will help us understand the underlying stereoelectronic and conformational effects on reactivity issues. Methylcyclohexane can adopt, in principle, the two chair conformations **5a** and **5b**. The conformer **5b** is obtained from **5a** after ring flip. The conformer **5a** is fully devoid of van der Waals interactions. However, one discovers two butane gauche interactions in the conformer **5b** as shown, each raising the energy by  $0.9 \text{ kcal mol}^{-1}$ . Thus, **5b** is less stable than **5a** by  $2 \times 0.9 = 1.8 \text{ kcal mol}^{-1}$ . In other words, mono-substituted cyclohexane ring should prefer the conformer that allows the substituent to occupy equatorial position.



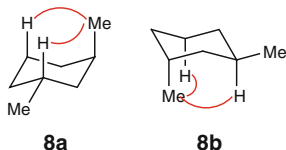
Consider *trans*-1,2-dimethylcyclohexane **6**. In the conformer **6a**, the two equatorial methyl groups are gauche to each other, which will raise the energy by  $0.9 \text{ kcal mol}^{-1}$ . In the conformer **6b**, the product of chair inversion of **6a**, each axial methyl group is engaged in two butane gauche interactions. This will raise the energy by  $2 \times (2 \times 0.9) = 3.6 \text{ kcal mol}^{-1}$ . The conformer **6a**, therefore, is more stable than **6b** by  $3.6 - 0.9 = 2.7 \text{ kcal mol}^{-1}$ . Thus, *trans*-1,2-disubstituted cyclohexane must prefer the conformer in which both the substituents occupy equatorial positions.



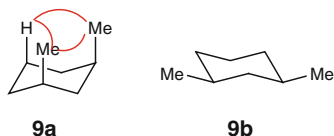
Consider *cis*-1,2-dimethylcyclohexane. In either of the two conformers **7a** and **7b**, one methyl is axial and the other equatorial. The two methyl groups are mutually gauche to each other and the ax-methyl is further gauche to two axial H atoms as shown. Both the conformers are one and the same. In the event that one substituent is different from the other, the molecule will largely adopt the conformer in which the larger substituent occupies the equatorial position.



*Trans*-1,3-dimethylcyclohexane can adopt either of the conformers **8a** and **8b**. In both, one methyl is axial and the other equatorial. Both the conformers, therefore, are one and the same. The equatorial methyl does not involve in any van der Waals interaction. However, the axial methyl is engaged in two butane gauche interactions as indicated. Thus, compared to methylcyclohexane, *trans*-1,3-dimethylcyclohexane is higher on the energy scale by  $2 \times 0.9 = 1.8 \text{ kcal mol}^{-1}$ .

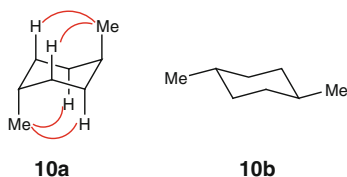


*Cis*-1,3-dimethylcyclohexane can adopt two conformers. In the conformer **9a**, both the methyl groups are axial and gauche to each other. Further, each methyl group is gauche to an axial hydrogen atom as shown. The total increase in the energy of this conformer will therefore be  $2.5 + 0.9 + 0.9 = 4.3 \text{ kcal mol}^{-1}$ . In **9b**, the two methyl substituents are equatorial and there are no issues arising from gauche interactions. Thus, **9b** is more stable than **9a** by  $4.3 \text{ kcal mol}^{-1}$ . Also, the more stable *cis*-1,3-dimethylcyclohexane conformer **9b** is more stable than *trans*-1,3-dimethylcyclohexane **8a/8b** by  $1.8 \text{ kcal mol}^{-1}$ .

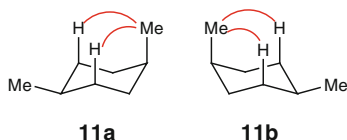


The two possible conformers of *trans*-1,4-dimethylcyclohexane are **10a** and **10b**. From the foregoing discussions, it is obvious that the conformer **10b** is more

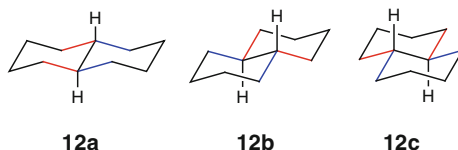
stable than the conformer **10a** by  $2 \times (2 \times 0.9) = 3.6 \text{ kcal mol}^{-1}$ . In **10a**, each axial methyl group is engaged in two gauche interactions as shown.



Each conformer of *cis*-1,4-dimethylcyclohexane, **11a** or **11b**, has one methyl group axial and the other equatorial. The axial methyl group is engaged in two gauche interactions as shown, raising the energy of the system by  $2 \times 0.9 = 1.8 \text{ kcal mol}^{-1}$ . In comparison, the more stable conformer of *trans*-1,4-dimethylcyclohexane, **10b**, is more stable than *cis*-1,4-dimethylcyclohexane **11** by  $1.8 \text{ kcal mol}^{-1}$ .

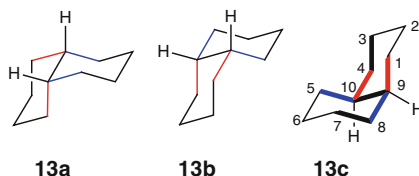


There are three different representations of *trans*-decalin, **12a–c**. Note that the bonds in both red and blue colors are equatorial to the other ring, leaving the hydrogen atoms on the ring-junctions axial. We have previously understood that the 1,2-diequatorial substituents are gauche to each other. Two such interactions raise the energy of the system by  $1.8 \text{ kcal mol}^{-1}$ . These interactions are present in *cis*-decalin as well, but now between one axial and one equatorial substituent (see below). For the purpose of relative energy calculation, these gauche interactions are therefore not counted. The ring flip in *trans*-decalin is not permitted for the reason that it requires two current equatorial bonds to turn axial and then get connected by a two carbon chain without subjecting the ring to strain. This is just not possible.



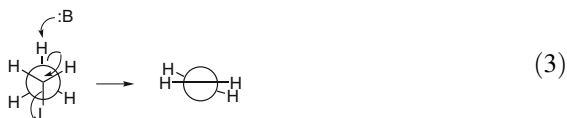
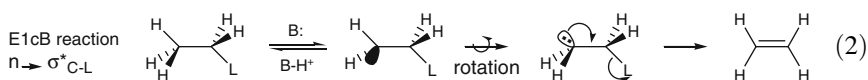
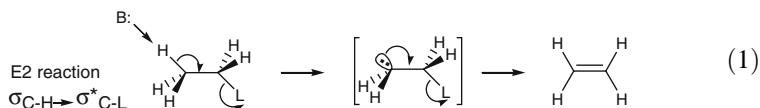
The three different representations of *cis*-decalin are **13a–c**. Of the two red bonds, one is axial and the other equatorial to the other ring. The same is true of the two blue bonds in the other ring. Consequently, one of the two hydrogen atoms on the ring junction is axial and the other equatorial to one of the two rings. One may note that the three gauche interactions present in *cis*-decalin are distinct from those present in *trans*-decalin. These are the interactions across C1–C9–C10–C5, C1–C9–C8–C7, and C5–C10–C4–C3 for having the C1- and C5-methylene groups axial to the other ring system. These gauche interactions may be traced in other representations also. Unlike in *trans*-decalin, ring flip in *cis*-decalin, which reduces

the energy of the system by  $0.4 \text{ kcal mol}^{-1}$ , is allowed. This energy corresponds to entropy. Thus, *trans*-decalin turns out to be more stable than *cis*-decalin by  $(3 \times 0.9) - 0.4 = 2.3 \text{ kcal mol}^{-1}$ . The conformational mobility in *cis*-decalin is only slightly below that of cyclohexane.



## 2 Influence of Stereoelectronic Effects on Reactions

Let us first define stereoelectronic effect. In Eq. 1, we note the progress of an E2 (elimination bimolecular) reaction. The axis of the electron pair orbital of the base B is collinear with  $\sigma_{\text{C-H}}$  to allow abstraction of H as  $\text{H}^+$ . It is like  $\text{S}_{\text{N}}2$  reaction, wherein a base attacks H from one side and the electron pair of  $\sigma_{\text{C-H}}$  bond leaves from the other side. The resultant carbanion has only a transient life, if at all, as it undergoes yet another  $\text{S}_{\text{N}}2$  reaction wherein the above electron pair orbital attacks the carbon bearing the leaving group L, as shown, and an olefin is formed. It may be noted that the axes of the carbanion electron pair orbital and the electron-deficient  $\sigma_{\text{C-L}}$  bond in the transient species are antiperiplanar, leading to the possibility of a strong  $n \rightarrow \sigma^*_{\text{C-L}}$  interaction. An interaction of this sort is termed *anomeric effect* in the study of sugars and *stereoelectronic effect* elsewhere. One may choose to call it *antiperiplanar effect* as well just because the said stereoelectronic effect is in place necessarily because of the antiperiplanar disposition of the electron pair orbital or electron-rich bond and the electron-deficient bond.



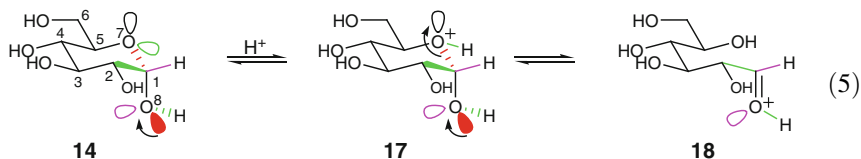
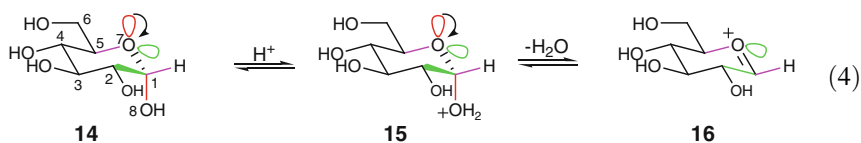
For the E2 reaction to succeed,  $\sigma_{\text{C-H}}$  and  $\sigma_{\text{C-L}}$  bonds must be antiperiplanar to each other as shown. This structural feature allows for  $\sigma_{\text{C-H}} \rightarrow \sigma^*_{\text{C-L}}$  interaction which is responsible for the enhanced acidic character of the hydrogen to allow its

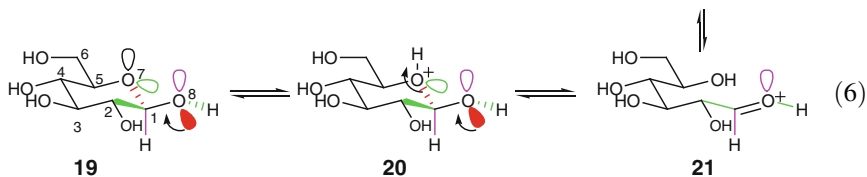
abstraction as  $H^+$  by the base in the rate determining step. The rate of the E2 reaction is therefore dependent on the concentrations of both the substrate and the base. The E2 reaction using Newman projection is shown in Eq. 3.

In contrast to the E2 reaction, the rate of the E1cB reaction (elimination unimolecular through conjugate base) is dependent only on the concentration of the carbanion formed on deprotonation of the substrate by the base, see Eq. 2. However, to begin with, the  $\sigma_{C-H}$  bond is not required to be antiperiplanar to the  $\sigma_{C-L}$  bond. The resultant carbanion (conjugate base of the substrate) survives until it collapses to an olefin by ejecting the leaving group through a transition state similar to that for the E2 reaction. The attainment of the TS may require rotation around the  $\sigma_{C-C}$  bond to orient the electron pair orbital antiperiplanar to the  $\sigma_{C-L}$  bond.

From the above discussions of E2 and E1cB reactions, we learn one very important point: an electron-rich bond such as  $\sigma_{C-H}$  or an electron pair orbital antiperiplanar to an electron-deficient bond such as  $\sigma_{C-L}$  constitutes an energy-lowering prospect. This is necessarily because of the partial electron donation from the electron-rich bond or electron pair orbital to the antibonding orbital corresponding to the electron-deficient bond ( $\sigma^*_{C-L}$ ). This lowers the antibonding orbital and, thus, raises the corresponding bonding orbital on the energy scale. As a result, the bonding orbital is weakened and its cleavage takes place with increased ease. We shall now exploit this information to understand the reactivity profiles of select class of molecules to strengthen our knowledge base.

Note the antiperiplanar relationship of the axial electron pair orbital on the ring oxygen and the  $\sigma_{C1-O8}$  bond in ( $\alpha$ )-D-glucopyranose **14**. This relationship leads to  $n \rightarrow \sigma^*_{C1-OH}$  interaction, also called *anomeric effect*. The consequence of this interaction is facile cleavage of  $\sigma_{C1-OH}$  bond after protonation to generate the oxonium ion **16** as shown in Eq. 4. Likewise, we notice an electron pair orbital on O8, which is antiperiplanar to the  $\sigma_{C1-O7}$  bond. This relationship results in yet another anomeric effect called *exo-anomeric effect* in distinction from the above anomeric effect. The consequence of *exo-anomeric effect* ought to be smooth cleavage of the  $\sigma_{C1-O7}$  bond on protonation of the ring oxygen as shown in Eq. 5. However, the reaction shown in Eq. 5 will otherwise be less facile than the reaction shown in Eq. 4 for reasons of additional energy required for ring-cleavage.





An electron pair orbital that is not engaged in anomeric effect is more electron rich and, hence, more vulnerable to protonation than an electron pair orbital that is involved in anomeric effect. This translates into the understanding that two electron pair orbitals on the same heteroatom are likely to be different from each other on account of whether or not the electron pair is engaged in anomeric effect.

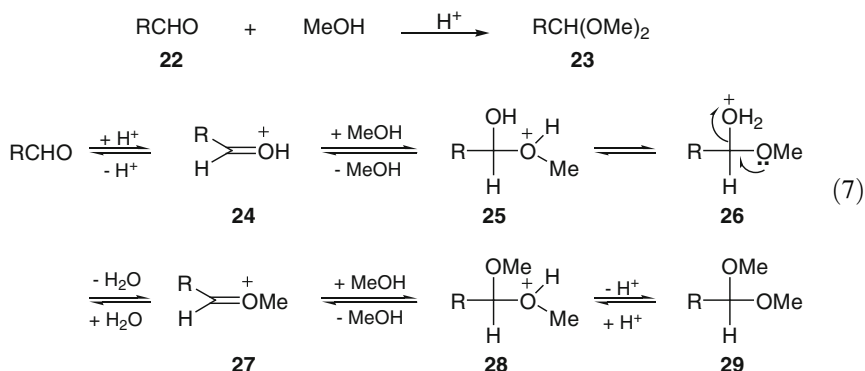
Let us now consider  $\beta$ -(D)-glucose **19**. It turns out from the given color codes that neither of the two electron pair orbitals on the ring oxygen is antiperiplanar to the  $\sigma_{C1-O8}$  bond. The cleavage of  $\sigma_{C1-OH}$  bond after protonation will therefore occur without assistance from any anomeric effect, i.e., the cleavage will be slower than the cleavage shown in Eq. 4. Alternatively, O8 has an electron pair orbital antiperiplanar to the  $\sigma_{C1-O7}$  bond. Therefore,  $\sigma_{C1-O7}$  bond can cleave after protonation of O7 with assistance from anomeric effect arising from O8, as shown in Eq. 6, and generate the oxonium ion **21**, which is essentially a rotamer of the oxonium ion **18**.

It should be noted from Eq. 5 that the species **18** is in equilibrium with  $\alpha$ -(D)-glucose **14**. Thus, under slightly acidic conditions,  $\alpha$ -(D)-glucose and  $\beta$ -(D)-glucose will be predicted to equilibrate with each other and lead to what we popularly know as *mutarotation*. The specific optical rotation of  $\alpha$ -D-glucose is different from that of  $\beta$ -D-glucose. Thus, commencing from  $\alpha$ -(D)-glucose (aqueous solution), the optical rotation will change with time and become static at the equilibrium. Of course, the equilibrium will be established fast if one begins with  $\alpha$ -(D)-glucose because the changes **14**  $\rightarrow$  **17**  $\rightarrow$  **18**  $\rightarrow$  **21** lead to relief from steric strain arising from the axial OH group in **14**. Alternatively, the oxonium ion **16** could be attacked by water from both axial and equatorial sites to generate, respectively,  $\alpha$ -D-glucose and  $\beta$ -D-glucose. Of course, the axial attack will be favored over the equatorial attack due to the stabilizing nature of the resultant anomeric effect.

In the transformation **16**  $\rightarrow$  **14**, water attacks the oxonium ion on the axial face. The electron pair of the cleaved  $\pi$  bond ends up in the axial orbital on the ring oxygen that exerts anomeric effect on the  $\sigma_{C-O}$  bond that is just formed. An attack from the equatorial site will generate **19**, where the new  $\sigma_{C-O}$  bond formed is not in anomeric effect with any of the electron pair orbitals of the ring oxygen. Both the formation and the cleavage of a bond under anomeric control are more facile than when the anomeric effect is absent. We shall continue to learn this aspect through the discussions below as well.

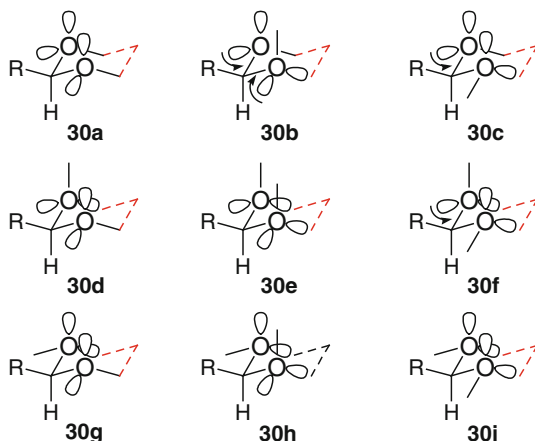
We know that the reaction of an aldehyde with an alcohol under dehydrating conditions generates an acetal as shown in Eq. 7. The details regarding the progress

of the reaction are shown below Eq. 7. As can be seen, one molecule of water is released for every molecule of the acetal formed in the step **26**  $\rightarrow$  **27** and that the proton used in the very beginning of the reaction is released in the end, making the reaction therefore catalytic in the proton source. It should be noted that each step leading to the acetal is reversible, which necessitates removal of the water formed from the reaction mixture to drive it to completion. The proton transfer from one oxygen to the other oxygen in the species **25**, leading to **26**, is very facile given the geometrical closeness of the two oxygen atoms on a tetrahedral carbon.

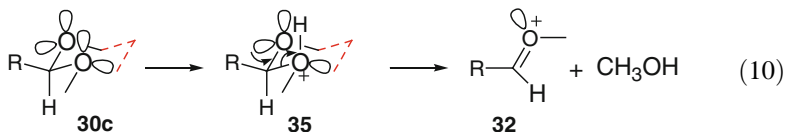
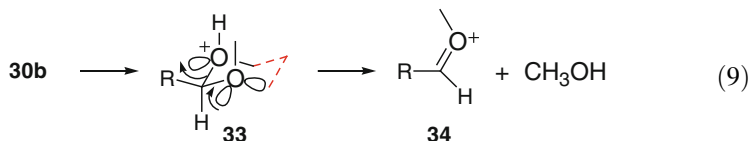
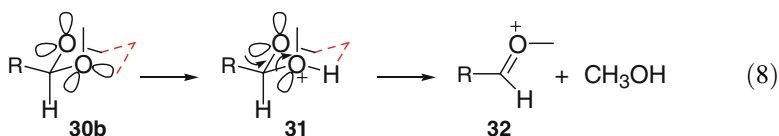


Let us consider the reverse of acetal formation, i.e., acid hydrolysis of an acetal within the ambit of stereoelectronic effects and explore the underlying features. We begin by understanding the conformational profile and the associated conformational effects by representing the acetal in such a way that it appears to be part of a cyclohexane chair. In doing so, we understand the geometrical relationship of various bonds on this ring system much better.

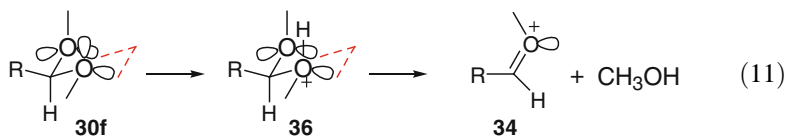
The acetal  $\text{RCH(OMe)}_2$  can have a total of nine conformers, **30a–30i**. We may ignore the broken red bonds, which are included to allow a quick conformational match with that of the cyclohexane chair and, thus, ascertain the geometrical relationships rather easily. The conformers **30a** and **30e** have two methyl groups within van der Waals distance and, hence, their contributions to the overall conformational equilibrium will be small, if not zero. We can therefore eliminate these conformers from further discussion. The conformers **30b** and **30d**, **30c** and **30g**, and **30f** and **30h** are mirror images and, thus, we need to consider only one conformer of each pair. Thus, we are left with four distinct conformers, namely **30b**, **30c**, **30f**, and **30i**, to consider for acid hydrolysis. The relative contributions of these conformers could be estimated from the understanding that they are laced with two, one, one and zero stereoelectronic effects, respectively. The conformers **30b** and **30i** are, respectively, the most contributing and the least contributing. The conformers **30c** and **30f** contribute at the medium level.



The acid hydrolysis of the conformer **30b** is presented in Eqs. 8 and 9. Note that both the oxygen atoms in **30b** have one electron pair orbital that does not participate in any stereoelectronic effect. Protonation of such an electron pair on the front oxygen leads to **31** that can easily undergo  $\sigma_{C-O}$  bond cleavage under stereoelectronic control arising from the other oxygen, as shown, to generate methanol and the *O*-methylated aldehyde **32**. Likewise, protonation of the rear oxygen coupled with the  $\sigma_{C-O}$  bond cleavage, as shown in Eq. 9, will generate methanol and the *O*-methylated aldehyde **34**. The *O*-methylated aldehyde **32** is of *E*-configuration while **34** is of *Z*-configuration. With R being that is small in size and, contributing to marginal van der Waals interaction with the *O*-methyl in **34**, both the cleavage pathways will be expected to be, more or less, equally facile. However, with R that is large, the pathway shown in Eq. 8 must predominate.

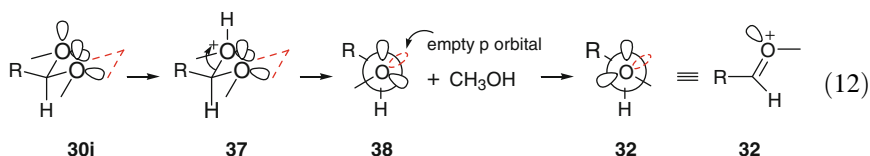




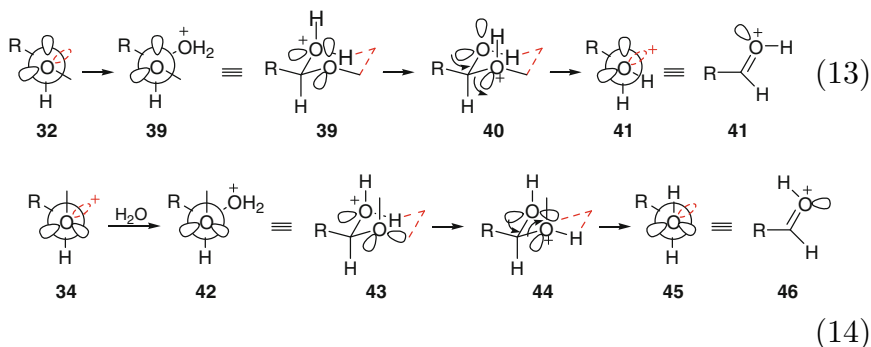


Protonation of the front oxygen in **30c** followed by cleavage of the  $\sigma_{\text{C-O}}$  bond under the stereoelectronic control of the rear oxygen, as shown in Eq. 10, generates **32**. Cleavage of the rear  $\sigma_{\text{C-O}}$  bond after protonation will be expected to be an inefficient process because it is not supported by any stereoelectronic effect arising from the front oxygen. Likewise, **30f** will generate **34** as shown in Eq. 11.

Finally, we discuss the conformer **30i** that lacks any stereoelectronic effects. The molecule is symmetrical and, hence, either of the two  $\sigma_{\text{C-O}}$  bonds can cleave after protonation. However, any such cleavage will take place without the assistance of stereoelectronic effect and, as shown in Eq. 12, the species **38** will be formed. The most notable characteristic of the species **38** is that the axis of the empty orbital (red) is antiperiplanar not to an electron pair orbital on the oxygen but to a  $\sigma_{\text{O-C}}$  bond. The species **38** will, therefore, be a high energy species. Conformational change, while keeping the methyl as far from R as possible (possible through anticlockwise rotation only), will allow formation of the stable species **32** as it has an oxygen electron pair orbital antiperiplanar to the empty orbital required for oxonium ion formation. Since the formation of a high energy species like **38** is involved, the conformer **30i** may be safely predicted to be a neutral conformer, *i.e.*, resistant to hydrolysis.

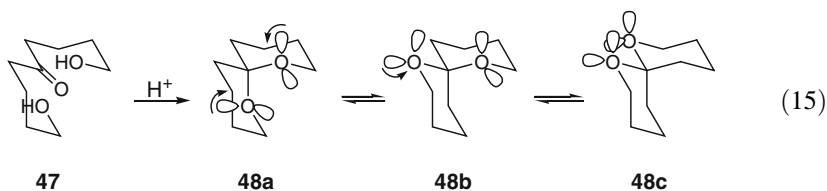


We have so far understood that protonation of one of the two oxygen atoms followed by cleavage of the  $\sigma_{\text{C-O}}$  bond in the important acetal conformers generates the oxonium ion **32** and/or **34**, depending upon the size of R. We will now consider the reactions of these oxonium ions with water. The reaction of **32** is outlined in Eq. 13. Capture of the empty orbital, of course under the stereoelectronic effect of an oxygen electron pair, generates **39**. Note the antiperiplanar relationship of R with the methyl in both **32** and **39**. Proton transfer from one oxygen to the other, taking advantage of the 1,3-diaxial proximity, will generate **40**. Now, cleavage of the  $\sigma_{\text{C-O}}$  bond with stereoelectronic effect, as shown, will generate **41** which is actually the protonated aldehyde. Loss of proton from **41** to another acetal molecule or even water, which is present in large excess, will generate RCHO, the end product of hydrolysis. Considering a similar pathway, the reaction of **34** with water is shown in Eq. 14.



We have noticed above that one of the two electron pair orbitals on the same oxygen is engaged in stereoelectronic effect, whereas the other electron pair orbital is not. The electron density in the former orbital is therefore less than the electron density in the latter orbital. Alternatively, the former orbital is less basic than the latter orbital and, thus, protonation of the latter orbital will be favored kinetically.

We have understood the stereoelectronic effect as a stabilizing effect that lowers the energy of a system by  $1.4 \text{ kcal mol}^{-1}$  and that it originates from the interaction of an oxygen electron pair orbital and a  $\sigma_{\text{C-O}}$  bond. Let us take notes of the following as well: (a) a methylene group axial to a cyclohexane ring contributes equivalent to two gauche butane interactions, i.e.,  $2 \times 0.9 = 1.8 \text{ kcal mol}^{-1}$ , and (b) an oxygen atom axial to a cyclohexane ring contributes  $2 \times 0.4 = 0.8 \text{ kcal mol}^{-1}$ . With a knowledge of these values, we may now begin to calculate the relative energies of the three conformers **48a**, **48b**, and **48c**, Eq. 15, and predict the conformer that will predominate at equilibrium.



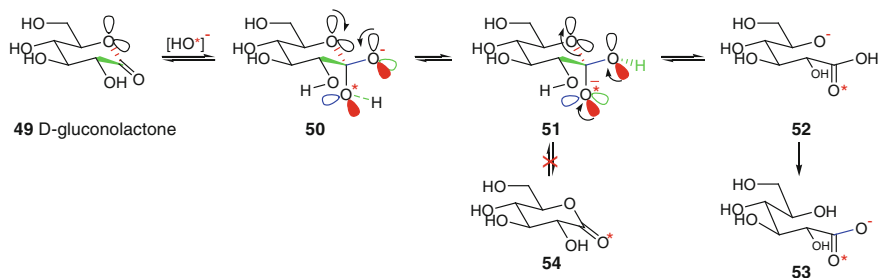
The conformer **48a** benefits from two stereoelectronic effects that will contribute  $-(1.4 \times 2) = -2.8 \text{ kcal mol}^{-1}$ . Each ring in this conformer also has an oxygen atom axial to the other six-membered ring, which will contribute  $+2 \times (2 \times 0.4) = +1.6 \text{ kcal mol}^{-1}$ . Therefore, the net change in the relative energy, is  $-2.8 + 1.6 = -1.2 \text{ kcal mol}^{-1}$ . The conformer **48b** has only one stereoelectronic effect to contribute  $-1.4 \text{ kcal mol}^{-1}$ . One ring has an oxygen atom axial to the other ring and this will contribute  $+0.8 \text{ kcal mol}^{-1}$ . This conformer also has one methylene group axial to the other ring system and this will contribute  $1.8 \text{ kcal mol}^{-1}$ . Thus, the net change in the relative energy is  $-1.4 + 0.8 + 1.8 = +1.2 \text{ kcal mol}^{-1}$ . The number of stereoelectronic effects in the conformer **48c** is nil. However, each ring has one methylene group axial to the other ring to contribute, collectively,

$+(2 \times 1.8) = +3.6 \text{ kcal mol}^{-1}$ . Thus, the net change in the relative energy is  $+ 3.6 \text{ kcal/mol}$ .

From the above discussion, it is obvious that the conformer **48a** will predominate and the conformer **48c** will contribute insignificantly to the equilibrium mixture. In other words, 1,9-dihydroxy-5-nonanone **47** will generate, on being subjected to intramolecular acetal formation reaction under acidic condition, an equilibrium mixture of the three spiroacetals wherein the conformer **48a** must predominate.

In the discussion of acid hydrolysis of an acetal, the cleavage of a  $\sigma_{\text{C-O}}$  bond with the assistance of a single stereoelectronic effect was considered facile. The leaving species was positively charged, which rendered the  $\sigma$  bond weak. Should the leaving species be neutral, at least two stereoelectronic effects are required for  $\sigma$  bond cleavage as we will note in the reaction of D-gluconolactone with hydroxide ion. To a good approximation, the weakness rendered to the  $\sigma_{\text{C-O}}$  bond by a positive charge on the leaving group appears equal to the weakness rendered by one stereoelectronic effect.

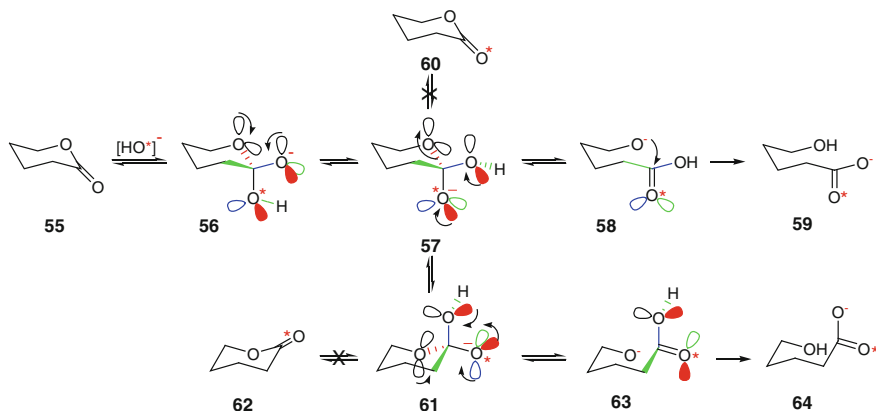
The reaction of D-gluconolactone **49** with  $\text{O}^{18}$ -labeled hydroxide ion under stereoelectronic control (which is axial attack) will furnish **50**. Note that the  $\sigma_{\text{C-O}^*\text{H}}$  bond formed is antiperiplanar not only to an electron pair orbital on the resultant oxy anion, but also to the axial electron pair orbital on the ring oxygen. This reaction is reversible because the  $\sigma_{\text{C-O}^*\text{H}}$  can also cleave very rapidly with the assistance of the same two stereoelectronic effects that facilitated its formation in the first place. Intramolecular proton transfer culminating in the transformation **50**  $\rightarrow$  **51** is also reversible. The  $\sigma_{\text{C-OH}}$  bond in **51** cannot cleave because it is antiperiplanar to only one electron pair orbital on the oxy anion  $[\text{O}^*]^-$  and, thus, **54** that retains the labeled oxygen will not form. In other words, if the hydrolysis reaction is interrupted (quenched by an aqueous acid) before completion and the unreacted D-gluconolactone is examined for the presence of  $\text{O}^{18}$ , it will be discovered to be absent.



However, the ring  $\sigma_{\text{C-O}}$  bond in **51** is under stereoelectronic control of two electron pair orbitals (solid red) and, hence, it can cleave to generate **52**. The transformation **51**  $\rightarrow$  **52** is also reversible because the intramolecular attack of the oxy anion in **52** onto the carbonyl group to result in **52**  $\rightarrow$  **51** conversion is just as

efficient as the **51** → **52** conversion for exactly the same reason(s). Intramolecular proton transfer from the carboxylic acid to the oxy anion in **52** will generate **53**. The reversal of **53** to **52** is difficult because a carboxylate ion is resonance stabilized and, hence, its base-like character is considerably compromised.

D-gluconolactone is an example of *E*-ester wherein the carbonyl oxygen and the substituent on the ethereal oxygen are anti to each other across the intervening  $\sigma_{C-O}$  bond. In the hydrolysis of D-gluconolactone, we did not consider conformational flip from one chair to the other chair because all the equatorial bonds will turn axial, leading to a very large steric strain. To allow for such a conformational flip for the consideration of carbonyl oxygen exchange during *E*-ester hydrolysis, we shall discuss the simplest example of the  $\delta$ -lactone **55**.



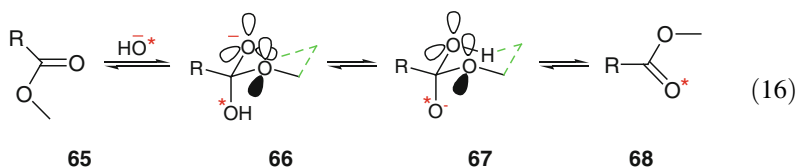
An argument similar to that for the hydrolysis of D-gluconolactone leads us to **59** as the final product, wherein the label  $O^{18}$  has been incorporated. The transformation **57** → **60** is not allowed for the lack of support by the requisite two stereoelectronic effects. Conformational ring flip from **57** to **61** is energy requiring. It may therefore be claimed not to compete with the fast cleavage of **57** to **58** because the latter is supported by two stereoelectronic effects. Let us see the turn of events assuming that the said conformational flip does compete and **61** is indeed formed.

The  $\sigma_{C-OH}$  bond in **61** is antiperiplanar to two electron pair orbitals, one on each of the two other oxygen atoms. It renders the cleavage of  $\sigma_{C-OH}$  bond facile and, hence, the  $O^{18}$ -containing  $\delta$ -lactone **62** may form. However, a close inspection of **61** reveals an alternate possibility as well. Like the  $\sigma_{C-OH}$  bond, the ring  $\sigma_{C-O}$  bond is also antiperiplanar to two electron pair orbitals. The ring  $\sigma_{C-O}$  bond could therefore also cleave with just as much ease as the above  $\sigma_{C-OH}$  bond. However, there is a characteristic difference.

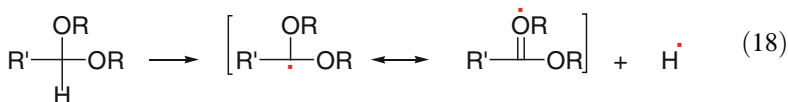
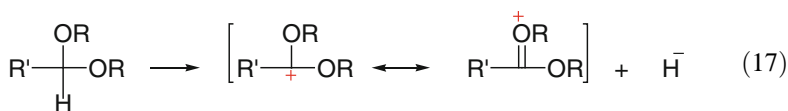
The cleavage of ring  $\sigma_{C-O}$  bond leads to the formation of **63**, wherein the carboxylic acid function is in *Z*-configuration. A *Z*-carboxylic acid benefits from two stereoelectronic effects, whereas an *E*-ester such as **62** derives advantage from only one stereoelectronic effect, vide infra. For this reason, the transition state energy for the

change **61**  $\rightarrow$  **63** will be smaller than that for the change **61**  $\rightarrow$  **62**. The pathway **61**  $\rightarrow$  **63**  $\rightarrow$  **64** predominates. The label is incorporated in the product **64** and the  $\delta$ -lactone **62** with  $O^{18}$  label is not formed. Thus, even if the ring flip **57**  $\rightarrow$  **61** competes with the cleavage **57**  $\rightarrow$  **58**, carbonyl oxygen exchange is not likely to occur. The *E*-esters indeed do not undergo carbonyl oxygen exchange during base hydrolysis.

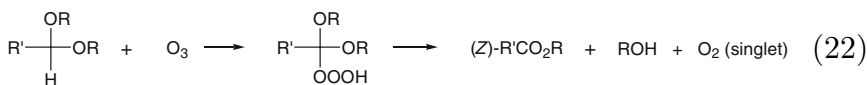
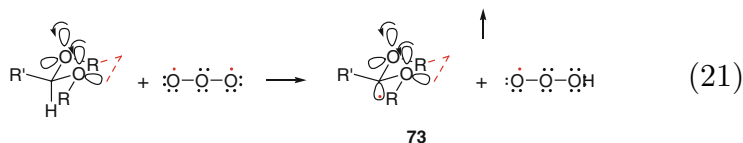
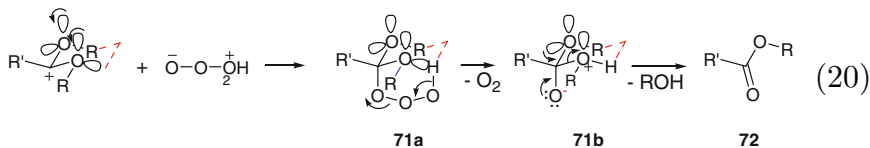
However, acyclic esters such as **65** necessarily exist in the *Z*-configuration and they do undergo carbonyl oxygen exchange. The  $\sigma_{C-OH}$  bond in the tetrahedral conformer **67**, obtained on proton exchange in **66**, is antiperiplanar to two electron pair orbitals, one on each of the two other oxygen atoms, to allow its facile cleavage and the  $O^{18}$ -incorporated *Z*-ester **68** is formed as shown in Eq. 16. Of course, the cleavage of  $\sigma_{C-OMe}$  bond under the influence of two stereoelectronic effects leads to an  $O^{18}$ -containing carboxylic acid as well.



Having understood the consequences of stereoelectronic effects and the requirement of minimum two such effects for the cleavage of a neutral  $\sigma_{C-O}$  bond, we shall now attempt to understand the fate of an acetal in its reaction with ozone and discover yet another important stereochemical feature. The two electron pair orbitals antiperiplanar to the  $\sigma_{C-H}$  bond could arguably polarize the latter to allow the carbon acquire partial positive charge ( $\delta^+$ ) and the hydrogen acquire partial negative charge ( $\delta^-$ ). In the presence of a hydride ion acceptor, a complete departure of hydrogen as hydride ion leading to formation of a stabilized carbocation, as shown in Eq. 17, is therefore conceivable. Since a carbon-centered radical is also stabilized by a heteroatom linked to it, the radical character of the above  $\sigma_{C-H}$  bond, as shown in Eq. 18, is also equally conceivable.



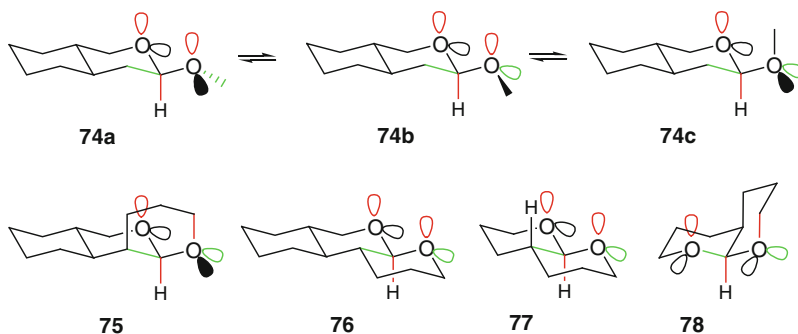
Ozone could also be considered as either 1,3-dipole or 1,3-diradical species. The dipolar form of ozone will exploit the dipolar character of the  $\sigma_{C-H}$  bond and, likewise, the radical form of ozone will exploit the radical character of the  $\sigma_{C-H}$  bond. These notions and their consequences are summarized in the Eqs. 19–21. Let us consider each of these in detail.



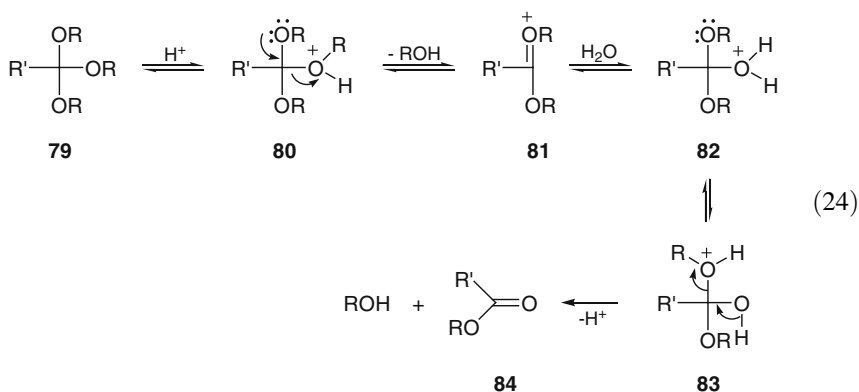
The dipolar form of ozone reacts through abstraction of the acetal hydrogen as hydride ion to generate a hydrotrioxide ion and the carbocation **70** as shown in Eq. 19. A combination of these two species under the stereoelectronic control of the acetal's two oxygen atoms will generate the hydrotrioxide **71a**. Direct insertion of the dipolar ozone into the  $\sigma_{\text{C-H}}$  bond can also take place to generate the above hydrotrioxide as shown in Eq. 20. Hydrogen atom abstraction by the diradical form of ozone will generate the radical species **73** and a hydrotrioxy radical as shown in Eq. 21. A combination of the two will lead to the hydrotrioxide **71a**. Fragmentation of **71a** in the manner shown by the arrows leads to the formation of the oxyanion **71b** and dioxigen. Further cleavage under stereoelectronic control leads to the *Z*-ester **72**. The net reaction is shown in Eq. 22. *The oxygen gas evolved has been found to be in its singlet excited state and the hydrotrioxide formation has been confirmed by its detection at low temperature [1].*

From the above discussion, it is easy to identify those acetals that will react with ozone and also those acetals that either do not react or react, but with great difficulty. Note the three different conformers of **74**. The conformers **74a** and **74b** meet the requirement for reaction with ozone for having two electron pair orbitals antiperiplanar to the  $\sigma_{\text{C-H}}$  bond. The conformer **74c** does not meet this requirement, as it has only one such electron pair orbital. To test whether **74c** indeed does not react or reacts with ozone but slowly in comparison to the conformers **74a** and **74b**, one needs to freeze the conformer **74c** as in **75**. The species **75** was indeed discovered to be inert to ozone. Likewise, the reactive conformer **74b** could be frozen as in **76** and **77**. Note that the key structural features of the three conformers of **74** resemble that of a  $\beta$ -glycoside. Also note further the stereo-functional similarity between **75** and **78**; the  $\sigma_{\text{C-H}}$  bond in each is antiperiplanar to one oxygen electron

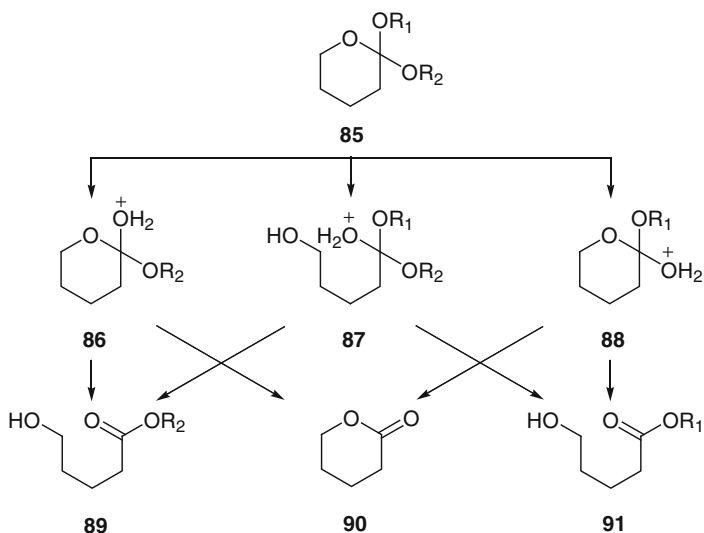
pair orbital and one  $\sigma_{C-O}$  bond. One may like to reason that the conformationally rigid  $\alpha$ -glycosides will be expected to be inert to ozone.



Orthoesters such as **79** are protected forms of esters. The hydrolysis of orthoesters to carboxylic acid esters is easily achieved on exposure to an aqueous acid as shown in the Eq. 23. The stepwise progress of the hydrolysis, given in Eq. 24, is illustrative of the possible stereoelectronic control elements. Protonation followed by bond cleavage assisted by the stereoelectronic effect(s) will generate **81**. The cleavage taking place with the assistance from two stereoelectronic effects will arguably be faster than the cleavage taking place with the assistance from only one such effect. The combination of **81** and water will generate **82**. Undoubtedly, if the stereoelectronic effects are to control this addition, water must occupy the same place that was vacated in the previous step. Intramolecular proton transfer from one oxygen to the other oxygen leads to **83** whose obvious fate is cleavage under stereoelectronic control to generate the ester **84** and an alcohol. The initially engaged  $H^+$  has now been released to allow it to be reengaged for the hydrolysis all over again. The catalytic nature of  $H^+$  is thus established.

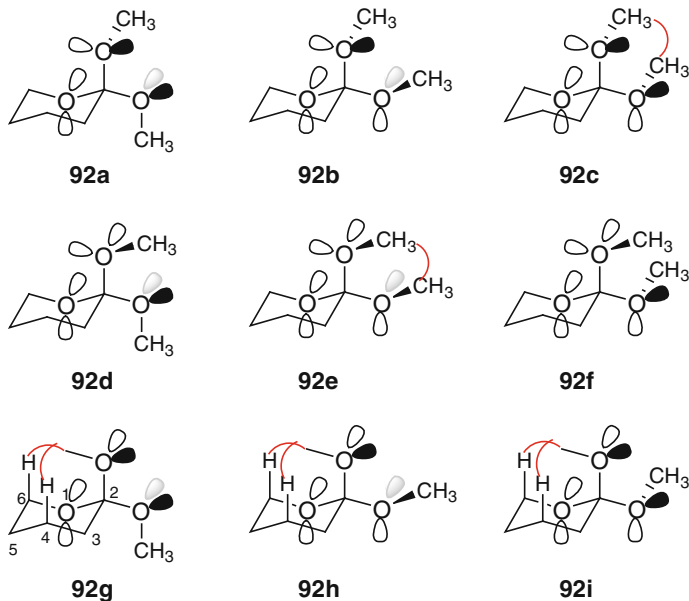


The importance of stereoelectronic effect in orthoester hydrolysis could be gleaned from the reaction of **85**. Should the stereoelectronic effects not be invoked, the reaction could generate all three different products, **89–91**. When  $R_1$  and  $R_2$  are same, there will be only two products, **89** and **90**. We shall learn below from a meaningful consideration of the prevailing stereoelectronic effects that only the **89**-like product is expected to predominate.



Let us examine each step of the orthoester hydrolysis under the operating stereoelectronic effects that vary with the variation in the conformational profile. Consider the acetal **92** and the nine well-defined conformers **92a–92i**. The conformers **92c** and **92e** suffer from severe steric interactions between the methyl groups as shown and, hence, their concentration at equilibrium should be expected to be negligible. Likewise, conformers **92g–92i** also suffer from severe steric interactions between the methyl of the axial methoxy group and the axial hydrogen atoms on ring positions 4 and 6 as shown for **92g**. The equilibrium concentration of each of these conformers also should be expected to be negligible like those of **92c** and **92e**. We may eliminate all these conformers from further discussion.



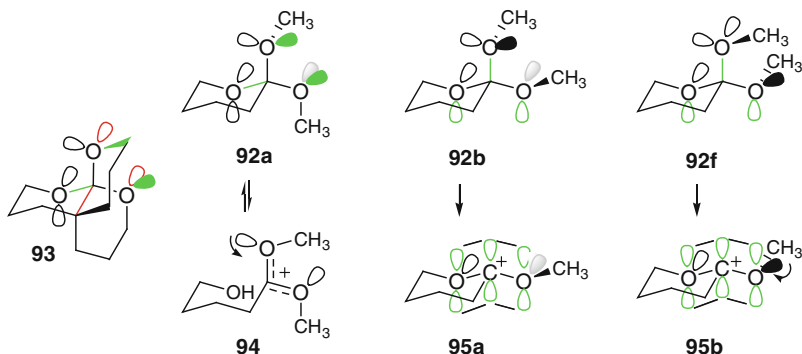


The loss of an alkoxy group, after protonation, is the starting point of hydrolysis. An orthoester can provide for this loss to take place with the assistance from one or two stereoelectronic effects, the latter being obviously favored over the former. The conformer **92d** does not allow any  $\sigma_{C-O}$  bond to cleave with the assistance from two stereoelectronic effects. This conformer may therefore be treated as the slow reacting or even as the neutral conformer. This prediction has been verified experimentally by studying the hydrolysis of **93**, a rigid **92d** conformer, which was found to be stable to the normally employed mild acidic conditions for orthoester hydrolysis [2–5]. Therefore, the conformer **92d** is also eliminated from further discussion.

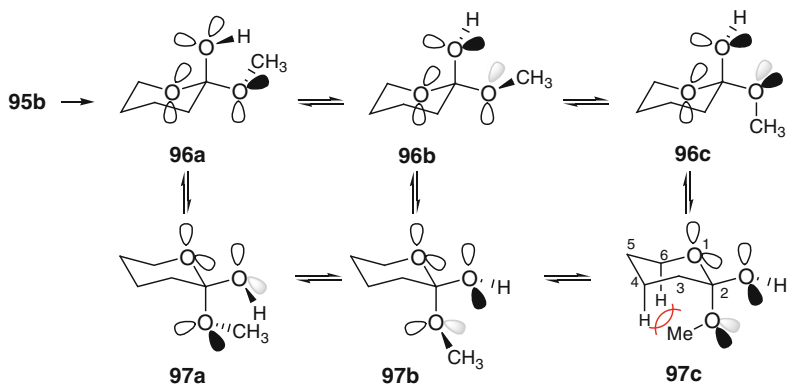
The conformer **92a** is set to undergo cleavage of only the ring  $\sigma_{C-O}$  bond to form **94**, a species that still has one stereoelectronic effect as shown and will be treated as an *E,Z*-dialkoxycarbonium ion. The conformers **92b** and **92f** will collapse to **95a** and **95b**, respectively, by the loss of the axial methoxy group. These species can be regarded as *E,E*- and *E,Z*-lactonium ions, respectively. The species **95b** has one stereoelectronic effect left in it, whereas **95a** has none. Obviously, on account of the remaining stereoelectronic effect(s), the transformations **92a**  $\rightarrow$  **94** and **92f**  $\rightarrow$  **95b** will be favored over the transformation **92b**  $\rightarrow$  **95a**.

There is no entropic gain in the transformation **92a**  $\rightarrow$  **94**, as a single molecule is formed from a single molecule and the ring is cleaved. In contrast, in each of the other two transformations, two molecules are formed from one, leading to entropic gain, and, moreover, the rings are not cleaved. Thus, the transformations **92b**  $\rightarrow$  **95a** and **92f**  $\rightarrow$  **95b** are predicted to be energetically more favorable than the transformation **92a**  $\rightarrow$  **94**, where the internal return **94**  $\rightarrow$  **92a** may be significant.

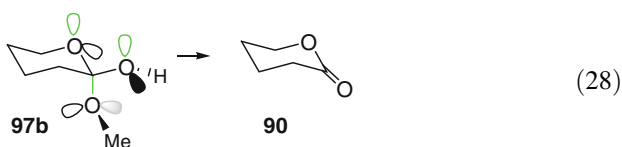
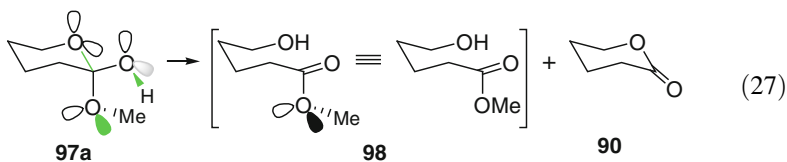
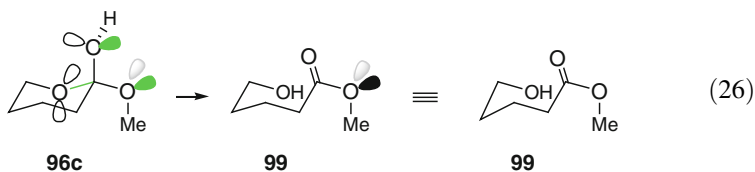
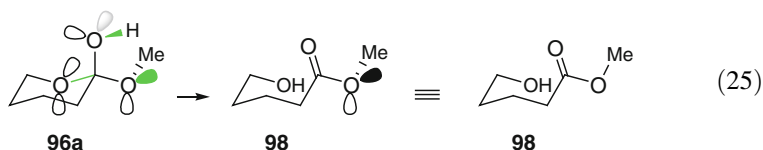
Again, out of  $92b \rightarrow 95a$  and  $92f \rightarrow 95b$ , the latter transformation ought to be more efficient than the former for retaining one stereoelectronic effect. Thus, the orthoester **92** should undergo hydrolysis via the conformer **92f** predominantly.



Stereoelectronically controlled hydration of the *E,Z*-lactonium ion **95b** will generate the hemi-orthoester **96a** wherein the new  $\sigma_{C-O}$  bond is antiperiplanar to the two oxygen electron pair orbitals. In instances where the tetrahydropyran ring cannot easily undergo chair inversion, **96a** will exist in equilibrium with **96b** and **96c**. In instances where the tetrahydropyran ring can easily undergo chair inversion, the conformers **97a**, **97b**, and **97c** will also be present at equilibrium. However, the relative concentration of **97c** will be negligible because of the strong steric interactions between the methyl group and the axial hydrogen atoms on ring positions 4 and 6, as shown. Note that the conformers **96a**, **96b**, and **96c** resemble the conformers **92f**, **92b**, and **92a**, respectively. The exact orientation of  $\sigma_{O-H}$  is to be neglected because proton exchange is a fast process and, as such, the O–H bond may be considered to be equivalent to an electron pair orbital.



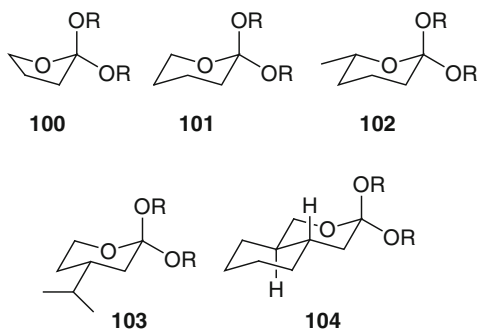
We shall now consider the cleavage of each of the above hemi-orthoester conformers under stereoelectronic control just as we dealt previously with the cleavage of the important orthoester conformers: first, **96a** will cleave to the hydroxy Z-ester **98**, as shown in Eq. 25; second, **96b** will not cleave and constitute the neutral conformer; third, **96c** will cleave to the hydroxy E-ester **99**, as shown in Eq. 26. Interestingly, neither of **96a** and **96c** can cleave to a lactone because no ring oxygen electron pair orbital is in stereoelectronic effect with the equatorial  $\sigma_{C-OMe}$  bond. Thus, in instances where the tetrahydropyran ring cannot easily undergo chair inversion, lactone will not be formed. Additionally, since the Z-ester is more stable than the E-ester, hydrolysis will take place preferentially via the conformer **96a** and the hydroxy Z-ester **98** will be formed.



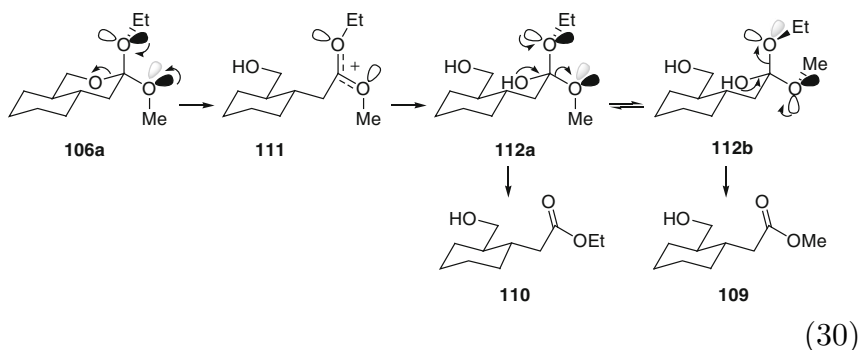
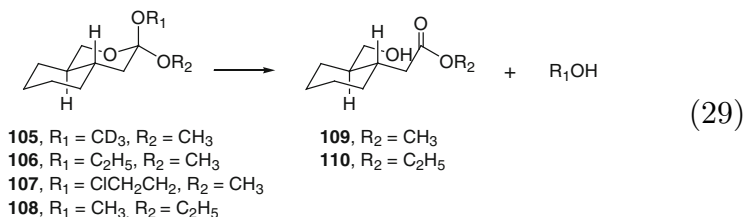
The conformer **97a** can cleave to both the hydroxy Z-ester **98** and the lactone **90**, Eq. 27. The conformer **97b** can cleave only to the lactone **90**, Eq. 28. The cleavage **97a** to the hydroxy Z-ester will be favored over cleavage to the lactone because the hydroxy Z-ester enjoys one additional stereoelectronic effect. Thus, even in instances where the tetrahydropyran ring can easily undergo ring inversion, lactone will not be formed and the preferred product of hydrolysis will still be the hydroxy Z-ester **98**. The overall hydrolysis pathway for conformationally labile cyclic orthoesters therefore is **92f**  $\rightarrow$  **95b**  $\rightarrow$  **96a/97a**  $\rightarrow$  **98**. However, keeping in view that the formation of a hydroxy ester through ring opening is opposed by its reversibility and assuming that this reversibility factor is as important as one

*stereoelectronic effect, the lactone formation may compete to a varying degree depending upon the orthoester in question and also the hydrolytic conditions.*

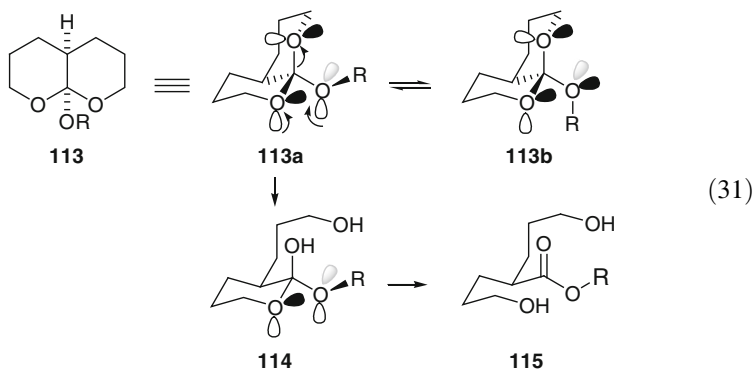
Mild acid hydrolyses of the conformationally labile orthoesters **100** and **101** are reported to yield 70:30 mixtures of the corresponding hydroxy Z-ester and lactone [6, 7]. The conformationally rigid orthoesters **102–104** furnish only the corresponding hydroxy Z-esters. The orthoesters **102** and **103** are conformationally rigid because chair inversion causes severe 1,3-diaxial interactions between the axial alkoxy group and the axial methyl group in **102** and the axial isopropyl group in **103**. The molecule **104** is conformationally rigid because it conforms to a *trans*-decalin system. The results from both the conformationally labile **100** and **101** and the conformationally rigid **102–104** confirm the conclusions drawn above, i.e., mild acid hydrolysis of (a) conformationally rigid cyclic orthoester should generate a hydroxy Z-ester exclusively and (b) conformationally labile cyclic orthoester may give both a hydroxy Z-ester and a lactone with the former probably formed more predominantly than the latter. Entropy factor favors lactone formation.

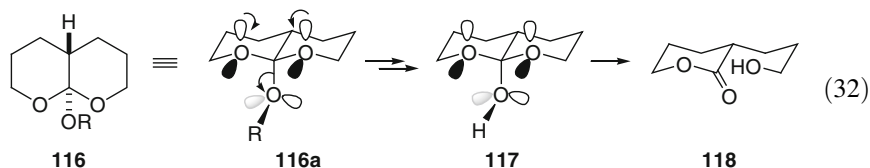


In evidence for the preferred cleavage of the axial alkoxy group, the results of hydrolyses of **105–108** (rigid conformers) are quite illustrative, Eq. 29. The hydrolysis in each instance generates the same hydroxy methyl ester **109**. However, hydrolysis of **108** generates the hydroxy ethyl ester **110**. That the hydrolysis does not proceed via the pathway **92a**  $\rightarrow$  **94** is conclusively demonstrated by the observation that such a pathway for the orthoester **106a** (an equivalent of the conformer **92a**) is likely to lead to both the ethyl and methyl esters as shown in the Eq. 30. Cleavage of the ring oxygen, after due protonation (not shown), under stereoelectronic control will generate **111**. Hydration of **111** under the same two stereoelectronic effects that allowed a smooth cleavage of the ring  $\sigma_{C-O}$  bond will lead to **112a**, which will be expected to exist in equilibrium with the conformer **112b**. Cleavage of the hemi-orthoesters **112a** and **112b** will generate the ethyl ester **110** and the methyl ester **109**, respectively. Only the methyl ester **109** is obtained from experiments.

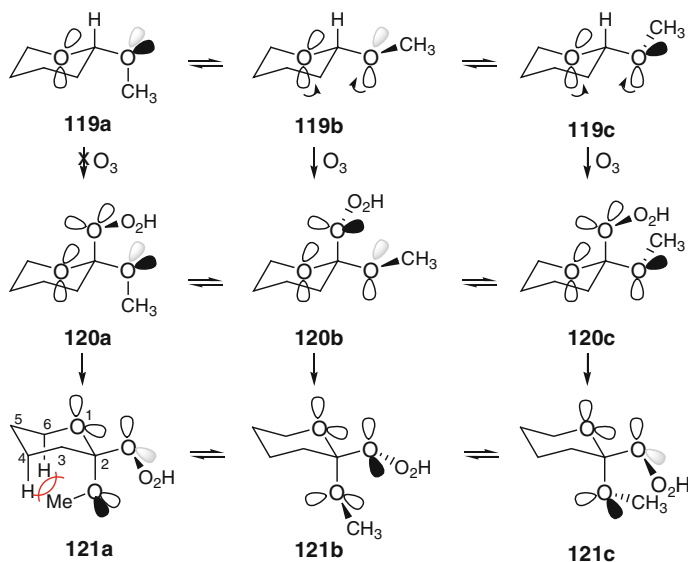


The bicyclic *cis*-ester **113** can exist as an equilibrium mixture of **113a** and **113b**. The conformer **113b** is the nonreacting conformer corresponding to **92d**. The conformer **113a** can undergo cleavage of only one of the two ring  $\sigma_{\text{C-O}}$  bonds which, following hydration of the resultant lactonium ion, will give the hemi-orthoester **114**. Further cleavage of **114** will give the dihydroxy *Z*-ester **115**. It is to be noted that chair inversion in **114** is not allowed because the inversion will place the large hydroxyalkyl substituent axial, leading to severe steric interactions. The *trans*-ester **116** will exist as **116a** to allow cleavage-cum-hydration to form **117** that can cleave only to the lactone **118**. However, the transformation **117**  $\rightarrow$  **118** will take place with the assistance from only one stereoelectronic effect arising from the external oxygen atom. The energy barrier for the transformation **117**  $\rightarrow$  **118** is therefore higher than that for the transformation **114**  $\rightarrow$  **115**.

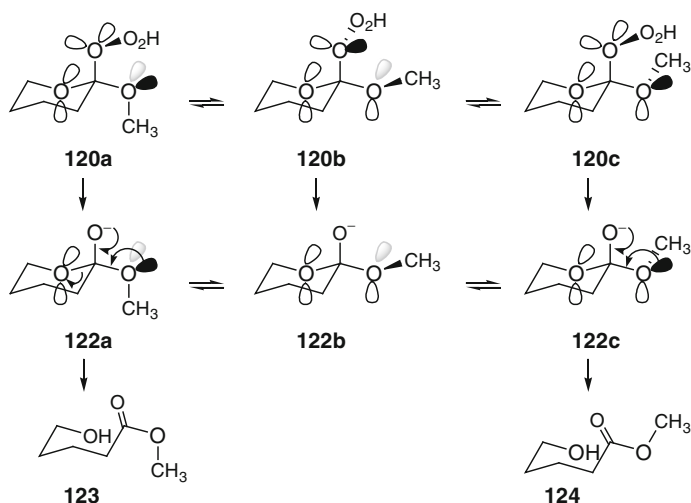




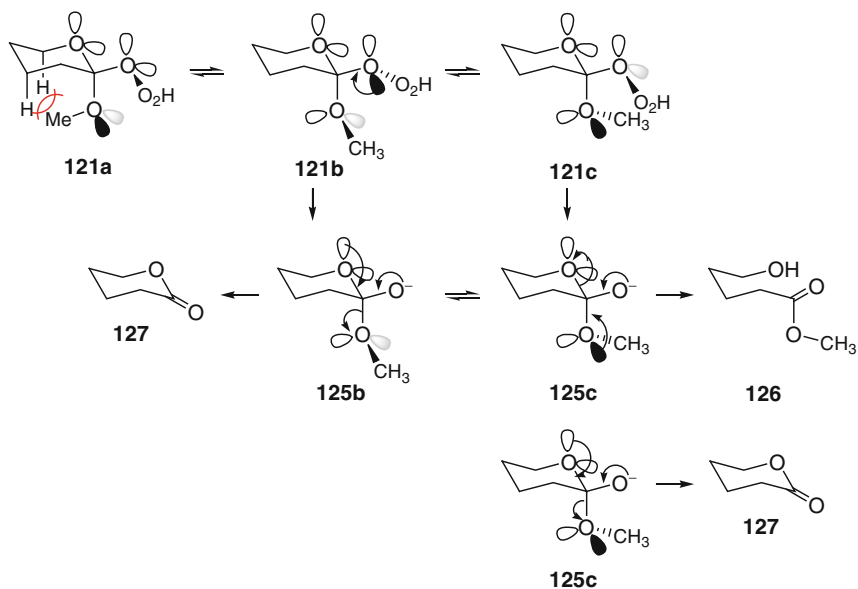
The reaction of ozone with tetrahydropyranyl ether is similar to the reaction of ozone with an acetal. Since the hydrotrioxide cleaves to an oxy anion, the control elements that influence the chemistry of hemi-orthoesters will also control the chemistry of such hydrotrioxides. The relative orientation of the hydrotrioxide functional group is therefore not important. However, the steric interactions need to be considered in arriving at the predominant conformers **120a**, **120b**, and **120c**.



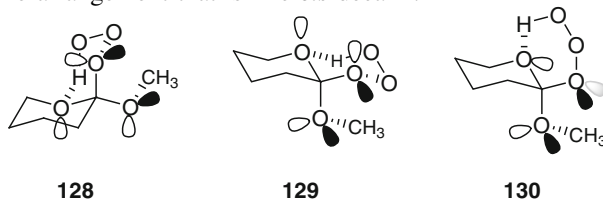
The conformer **119a** is the nonreacting conformer. The conformers **119b** and **119c** will react with ozone to generate, respectively, **120b** and **120c** that will be in equilibrium with each other and also with **120a**. These are the three important hydrotrioxide conformers that one needs to consider must the chair inversion not be allowed. The conformers **120a** will form, via the oxy anion **122a**, the *E*-ester **123** on cleavage of the ring  $\sigma_{C-O}$  bond. The conformer **120b** may break down to the oxy anion **122b**, but **122b** itself cannot cleave any further due to the lack of the required two stereoelectronic effects on any one of the two neutral  $\sigma_{C-O}$  bonds. The conformer **120c** will cleave to the *Z*-ester **124**. Thus, for species that do not allow chair inversion, the conformer **120c** is the most reacting conformer and the product formed from this conformer is a hydroxy *Z*-ester. A *Z*-ester is more stable than the corresponding *E*-ester on account of the presence of one additional stereoelectronic effect in the former.



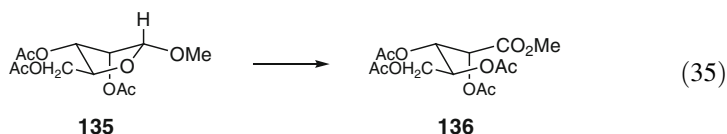
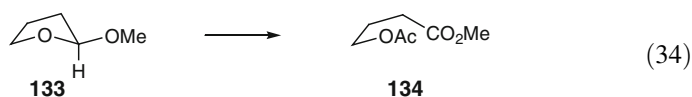
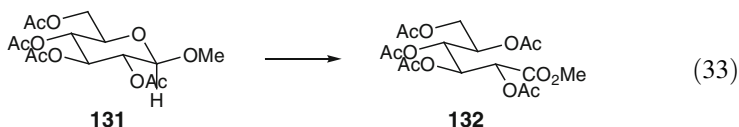
Should the chair inversion be allowed, the other three conformers to consider would be **121a**, **121b**, and **121c**. The conformer **121a** suffers from severe steric interactions, as shown, resulting in low concentration at the equilibrium. The conformer **121b** can cleave only to the  $\delta$ -lactone **127**, cyclic form of an *E*-ester, via the oxy anion **125b**. Finally, the conformer **121c** can cleave to both the hydroxy *Z*-ester **126** and the  $\delta$ -lactone **127**, via the oxy anion **125c**. Since the formation of an *E*-ester/ $\delta$ -lactone is more energy requiring than the formation of a *Z*-ester, cleavage of **121c**, via **125c**, to the hydroxy *Z*-ester **126** is expected to predominate.



Must the formation of a hydrogen bond between the hydrotrioxide and the leaving group be preferred over the steric interactions of the kind present in **92c** and **92e**, the reacting conformer corresponding to **120c** will be **128**. Likewise, the hydrogen-bonded conformer corresponding to **121c** will be one or both of **129** and **130**. Having considered that the axial electron pair orbital on the ring oxygen is engaged with an anomeric effect with the external  $\sigma_{C-OMe}$  bond, the equatorial electron pair orbital on the ring oxygen is more electron rich and, hence, the **129**-like arrangement must be more suited than the **130**-like arrangement. Additionally, the **129**-like arrangement is like *trans*-decalin that is more favorable than the **130**-like arrangement that is like *cis*-decalin.

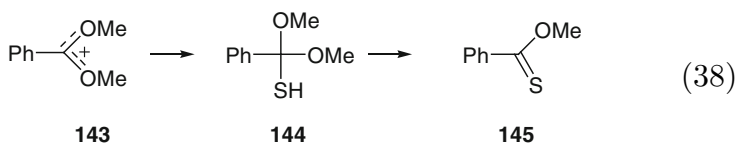
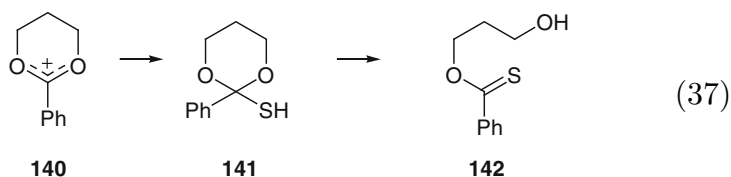
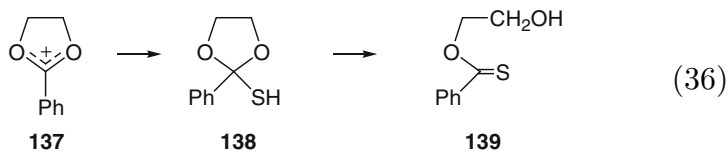


The reactions of ozone with simple tetrahydropyranyl ethers and conformationally rigid  $\beta$ -glycosides were indeed discovered to give the corresponding hydroxy *Z*-esters exclusively under kinetically controlled conditions; lactone formation was not observed [8–10]. For instance,  $\beta$ -D-glucopyranoside **131** reacted under acetylating conditions to form **132** exclusively, Eq. 33. The reactions of the tetrahydrofuranyl ethers **133**, Eq. 34, and **135**, Eq. 36, were similar to that of **131**; only the esters **134** and **136** were obtained, respectively.

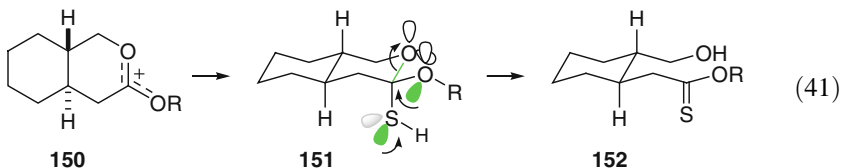
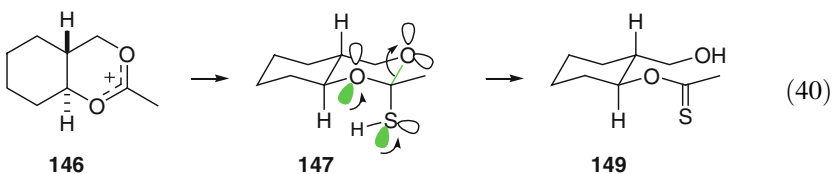
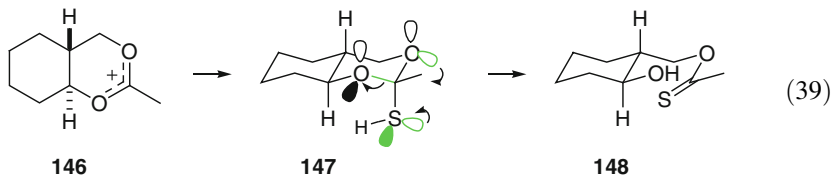


The cleavage of a hemi-ortho-thiol ester, formed from the combination of a hydrosulfide ion with a dialkoxycarbocation, was found to occur under stereoelectronic control. The cyclic dialkoxycarbocations **137**, Eq. 36, and **140**, Eq. 37, and the acyclic dialkoxycarbocation **143**, Eq. 38, were reacted with sodium hydrosulfide to give the monothioesters **139** and **142**, and the thionobenzoate **145**, respectively [11–13].





Likewise, the reactions given in the Eqs. 39–41 could be analyzed and the formation of **148** and **149** from **146** and the formation of **152** from **150** understood [14]. Likewise, the intermediate hemithio-orthoesters **147** and **151** are formed from axial attack of the hydrosulfide ion on the cationic species **146** and **150**, respectively.

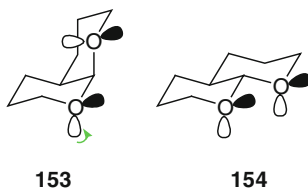


### 3 Evaluation of the Numerical Value of Anomeric Effect

We will now quantify the anomeric effect and ascertain that it indeed is  $-1.4 \text{ kcal mol}^{-1}$ , a number that we have previously used in other calculations. However, before we proceed to do this, let us understand how we can calculate the energy difference of any two conformers, given their equilibrium distribution under a set of experimental parameters. From the law of thermodynamics,  $\Delta E = -RT \ln K$ ; where  $\Delta E$  is the difference in the energies of the two conformers,  $R$  the gas constant and  $T$  the reaction temperature in Kelvin at which the ratio of the conformers at equilibrium is  $K$ .

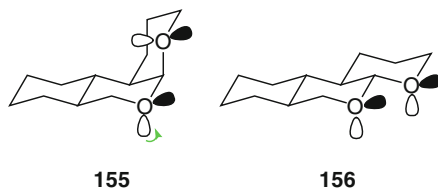
Descotes et al. [15] studied the acid-catalyzed isomerization of the *cis*- and *trans*-bicyclic acetals **153** and **154**, at  $80 \text{ }^\circ\text{C}$  and discovered the mixture to contain 57 % of *cis*-**153** and 43 % of *trans*-**154** at the equilibrium. This gives a value of  $57/43 = 1.3256$  to  $K$ . On substituting this value and also the values of the gas constant  $R$  ( $1.98 \text{ cal mol}^{-1} \text{ K}^{-1}$ ) and  $T$  in the above equation, a value of  $-0.17 \text{ kcal mol}^{-1}$  for  $\Delta E$  was obtained. In other words, *cis*-**153** is more stable than *trans*-**154** at  $80 \text{ }^\circ\text{C}$  by  $0.17 \text{ kcal mol}^{-1}$  or the difference of the energies of *cis*-**153** and *trans*-**154** is  $-0.17 \text{ kcal mol}^{-1}$ .

*Cis*-**153** has one anomeric effect, as shown, and *trans*-**154** has no anomeric effect at all. Putting together the anomeric effect (say,  $x \text{ kcal mol}^{-1}$ ), steric interactions and the conformational effects, the energies of *cis*-**153** and *trans*-**154** were computed to be, respectively,  $x + 0.85 \text{ kcal mol}^{-1}$  (one  $\text{CH}_2$  group axial to the other ring) +  $0.80 \text{ kcal mol}^{-1}$  (one OR group axial to the other ring)  $-0.42 \text{ kcal mol}^{-1}$  (the stabilizing entropy factor associated with *cis*-decalin) and  $0.0 \text{ kcal mol}^{-1}$  on the relative energy scale. Since *cis*-**153** is more stable than *trans*-**154** by  $0.17 \text{ kcal mol}^{-1}$ , the mathematical correspondence  $x + 0.85 + 0.80 - 0.42 = -0.17$  holds and one obtains a value of  $-1.40 \text{ kcal mol}^{-1}$  for  $x$ .



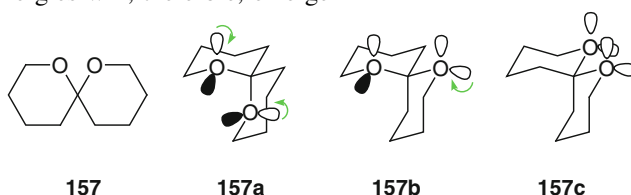
Deslongchamps et al. [16] rigidified **153** and **154** as in the structures **155** and **156** and found the equilibrium distribution (MeOH, *p*-TsOH, reflux) to be 45 and 55 %, respectively. This distribution corresponds to an energy difference of  $0.14 \text{ kcal mol}^{-1}$ , i.e., **155** is less stable than **156** by  $0.14 \text{ kcal mol}^{-1}$ . The species **156** is free from anomeric effects and also from steric effects and, thus, its energy could be placed at  $0.0 \text{ kcal mol}^{-1}$  on the relative energy scale. The energy of **155** will then add up to  $x \text{ kcal mol}^{-1}$  (one anomeric effect) +  $0.85 \text{ kcal mol}^{-1}$  (one  $\text{CH}_2$  group axial to the other ring) +  $0.8 \text{ kcal mol}^{-1}$  (one OR group axial to the other ring). On putting together the energies of **155** and **156**, one arrives at the relationship  $x + 0.85 + 0.8 = 0.14$ , which lends a value of  $-1.51 \text{ kcal mol}^{-1}$  to  $x$ . This

value is close to the value obtained above by Descotes and coworkers. Henceforth, we shall consider the anomeric effect and the gauche *n*-butane interaction to be contributing by  $-1.4 \text{ kcal mol}^{-1}$  and  $0.9 \text{ kcal mol}^{-1}$ , respectively, and make their use to analyze the conformational effects in other structure types.



#### 4 Influence of Anomeric Effect on Conformational Preferences

The spiroacetal **157** can exist as an equilibrium mixture of the three conformers **157a**, **157b**, and **157c**. We will now calculate the relative energies of these conformers and see how these numbers could be reliably used to predict conformer distributions in compliance with the experimental observation. The conformers **157a**, **157b**, and **157c** possess two, one, and zero anomeric effects, respectively, as shown. In the conformer **157a**, each ring has one OR axial to the other ring. This will raise the energy of the conformer by  $2 \times (2 \times 0.4) \text{ kcal mol}^{-1}$ . In the conformer **157b**, there are two gauche *n*-butane interactions by virtue of having an axial  $\text{CH}_2$  group, which will contribute  $2 \times 0.9 \text{ kcal mol}^{-1}$ . The conformer **157b** also has one OR group axial to the other ring and this will contribute  $2 \times 0.4 \text{ kcal mol}^{-1}$ . In the conformer **157c**, each ring has one  $\text{CH}_2$  group axial to the other ring to contribute  $2 \times (2 \times 0.9) \text{ kcal mol}^{-1}$ . The following pictures of the conformational energies will, therefore, emerge



$$E_{157a} = 2(-1.4) \text{ kcal mol}^{-1} + (2 \times 0.4) \text{ kcal mol}^{-1} + (2 \times 0.4) \text{ kcal mol}^{-1} = -1.2 \text{ kcal mol}^{-1}$$

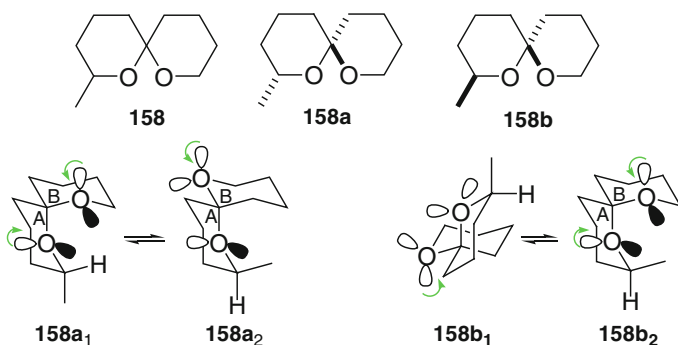
$$E_{157b} = 1(-1.4) \text{ kcal mol}^{-1} + (2 \times 0.9) \text{ kcal mol}^{-1} + (2 \times 0.4) \text{ kcal mol}^{-1} = 1.2 \text{ kcal mol}^{-1}$$

$$E_{157c} = (2 \times 0.9) \text{ kcal mol}^{-1} + (2 \times 0.9) \text{ kcal mol}^{-1} = 3.6 \text{ kcal mol}^{-1}$$

The conformer **157a** is therefore more stable than the conformers **157b** and **157c** by  $2.4 \text{ kcal mol}^{-1}$  ( $E_{151a} - E_{151b}$ ) and  $4.8 \text{ kcal mol}^{-1}$  ( $E_{151a} - E_{151c}$ ), respectively. This conformational analysis leads one to predict that the spiroacetal **157** must exist essentially as the conformer **157a**. This result has indeed been verified

experimentally by  $^{13}\text{C}$  NMR study and X-ray analysis by Deslongchamps and coworkers [17, 18].

Deslongchamps et al. [17, 18] have also studied the methyl substituted spiro-system **158**, formed from decan-1,9-diol-5-one, for which the two isomers **158a** and **158b** are possible. While the methyl substituent is *trans* to the  $\sigma_{\text{C-O}}$  bond of the other ring at the spiro-carbon in **158a**, it is *cis* in **158b**. The isomer **158a** can further exist either as the conformer **158a<sub>1</sub>** or **158a<sub>2</sub>** or as an equilibrium mixture of both. One obtains the conformer **158a<sub>2</sub>** on flipping the ring A in **158a<sub>1</sub>**. Likewise, the two different conformers for the isomer **158b** are **158b<sub>1</sub>** and **158b<sub>2</sub>**. The magnitudes of the steric interactions of a methyl group 1,3-diaxial to another methyl (or methylene) and to oxygen have been estimated to be  $4.0 \text{ kcal mol}^{-1}$  and  $3.0 \text{ kcal mol}^{-1}$ , respectively. Now, we can put together the operating anomeric and steric effects for each conformer and calculate the net relative energies.



### 158a<sub>1</sub>

- two anomeric effects to contribute  $2 \times (-1.4) \text{ kcal mol}^{-1}$
- ring A's OR in 1,3-diaxial interactions with two hydrogen atoms of ring B to contribute  $(2 \times 0.4) \text{ kcal mol}^{-1}$
- ring B's OR in 1,3-diaxial interactions with two hydrogen atoms of ring A to contribute  $(2 \times 0.4) \text{ kcal mol}^{-1}$ .

All the above interactions add up to  $-1.2 \text{ kcal mol}^{-1}$ .

### 158a<sub>2</sub>

- one anomeric effect to contribute  $-1.4 \text{ kcal mol}^{-1}$
- ring A's OR in 1,3-diaxial interactions with two hydrogen atoms of ring B to contribute  $(2 \times 0.4) \text{ kcal mol}^{-1}$
- ring B's one  $\text{CH}_2$  group axial to ring A and in 1,3 diaxial interactions with a hydrogen atom to contribute  $0.9 \text{ kcal mol}^{-1}$  and with a methyl group to contribute  $4.0 \text{ kcal mol}^{-1}$

All these interactions add up to  $4.3 \text{ kcal mol}^{-1}$ .

**158b<sub>1</sub>**

- (a) one anomeric effect to contribute  $-1.4 \text{ kcal mol}^{-1}$
- (b) vertical ring's OR in 1,3-diaxial interactions with two hydrogen atoms of the horizontal ring to contribute  $(2 \times 0.4) \text{ kcal mol}^{-1}$
- (c) ring B's one CH<sub>2</sub> group is axial to the vertical ring and it is in 1,3-diaxial interactions with two hydrogen atoms of ring A to contribute  $(2 \times 0.9) \text{ kcal mol}^{-1}$

All these interactions add up to  $1.2 \text{ kcal mol}^{-1}$ .

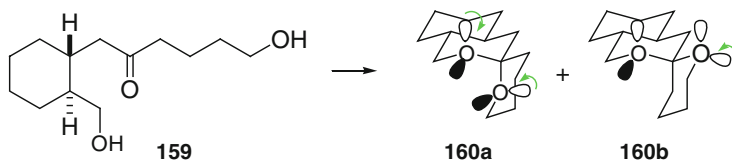
**158b<sub>2</sub>**

- (a) two anomeric effects to contribute  $2 \times (-1.4) \text{ kcal mol}^{-1}$
- (b) ring A's OR in 1,3-diaxial interactions with two hydrogen atoms of ring B to contribute  $(2 \times 0.4) \text{ kcal mol}^{-1}$
- (c) ring B's OR in 1,3-diaxial interaction with a hydrogen atom of ring A to contribute  $(1 \times 0.4) \text{ kcal mol}^{-1}$  and with a methyl group to contribute  $3.0 \text{ kcal mol}^{-1}$

All these interactions add up to  $1.4 \text{ kcal mol}^{-1}$ .

Thus, **158a<sub>1</sub>** is more stable than **158a<sub>2</sub>** by  $4.3 - (-1.2) = 5.5 \text{ kcal mol}^{-1}$ . With such a large energy difference, the isomer **158a** must exist as the conformer **158a<sub>1</sub>** predominantly. Since the conformers **158b<sub>1</sub>** and **158b<sub>2</sub>** differ from each other by a mere  $0.2 \text{ kcal mol}^{-1}$ , the isomer **158b** will be expected to exist as an almost 1:1 equilibrium mixture of the two. However, since the isomers **158a** and **158b** are interconvertible through acid-catalyzed acetal-opening to decan-1,9-diol-5-one and re-ring closure and since **158a<sub>1</sub>** is the most stable of all the conformers, only **158a** will be predicted to form under thermodynamically controlled conditions, and it should exist exclusively as the conformer **158a<sub>1</sub>**. This prediction has been confirmed experimentally.

Cyclization of **159** can give rise to, in principle, a mixture of the two conformationally rigid isomeric acetals **160a** and **160b**. These isomers benefit from two and one anomeric effects, respectively, as shown. In the isomer **160a**, each ring of the spiroacetal has an axial OR group, each contributing by  $(2 \times 0.4) \text{ kcal mol}^{-1}$ . In the isomer **160b**, while one spiroacetal ring has an axial CH<sub>2</sub> group to contribute by  $(2 \times 0.9) \text{ kcal mol}^{-1}$ , the other spiroacetal ring has an axial OR group to contribute by  $(2 \times 0.4) \text{ kcal mol}^{-1}$ . When these anomeric and steric effects are put together for each isomer, the net relative energies of these isomers are as follows

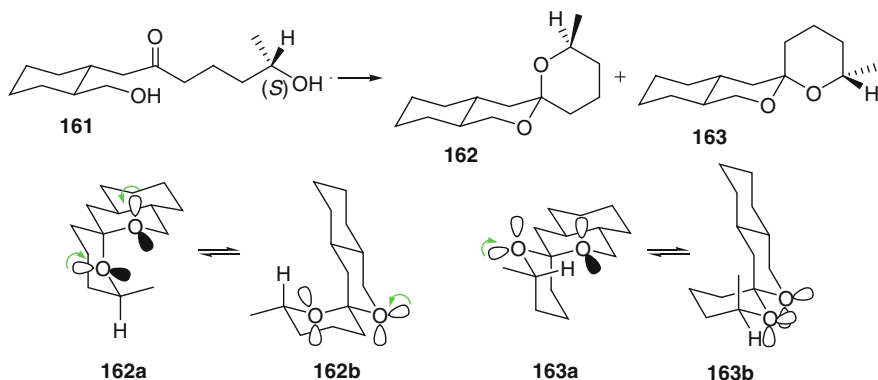


$$E_{160a}: 2(-1.4) + (2 \times 0.4) + (2 \times 0.4) = -2.8 + 1.6 = -1.2 \text{ kcal mol}^{-1}$$

$$E_{160b}: 1(-1.4) + (2 \times 0.9) + (2 \times 0.4) = -1.4 + 2.6 = +1.2 \text{ kcal mol}^{-1}$$

Thus, the isomer **160a** is more stable than the isomer **160b** by 2.4 kcal mol<sup>-1</sup>. Since **160a** and **160b** are interconvertible under the acidic conditions of cyclization of **159**, the isomer **160a** will be predicted to form predominantly under thermodynamically controlled conditions. Deslongchamps and coworkers have indeed shown that the cyclization of **159** under acidic conditions (0.1 *N* HCl/CH<sub>3</sub>OH) furnished only **160a**. From the cyclization under mild acidic conditions (catalytic *p*-TSA in CHCl<sub>3</sub>), a small amount of **160b** was isolated and shown to convert irreversibly and completely into **160a** on exposure to 1.0 *N* HCl in acetone [17].

The dihydroxy ketone **161**, with the (*S*)-configuration at the secondary carbinol center, will be expected to give a mixture of the two isomeric spiroacetals **162** and **163**. The acetal **162** can exist as an equilibrium mixture of **162a** and **162b**. Likewise, the acetal **163** can exist as an equilibrium mixture of **163a** and **163b**. The two conformational isomers are to be achieved by flipping the methyl-containing ring from one chair to the other chair. When these operating anomeric and steric effects are put together for each isomer, the net relative energies of these isomers are as follows:



$$E_{162a} : 2 \times (-1.4) + (2 \times 0.4) + (1 \times 0.4) + 3.0 = 1.4 \text{ kcal mol}^{-1}$$

$$E_{162b} : 1 \times (-1.4) + (2 \times 0.4) + (2 \times 0.9) = 1.2 \text{ kcal mol}^{-1}$$

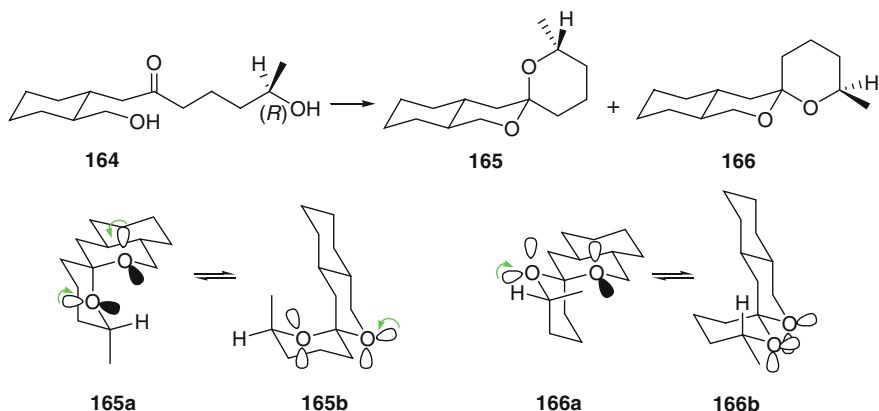
$$E_{163a} : 1 \times (-1.4) + (2 \times 0.4) + (2 \times 0.9) = 1.2 \text{ kcal mol}^{-1}$$

$$E_{163b} : 0 \times (-1.4) + (1 \times 0.9) + 4.0 = 4.9 \text{ kcal mol}^{-1}$$

From the above relative energies, the isomers **162** and **163** must be formed in nearly equal amounts. Further, the isomer **162** should exist, within a small approximation, as a 1:1 mixture of the conformers **162a** and **162b** due to very small energy difference. Because of very large energy difference (3.7 kcal mol<sup>-1</sup>), the

isomer **163** must exist as the only conformer **163a**. These predictions bear well with the observed experimental results [17].

Let us now consider the dihydroxy ketone **164** which is enantiomeric to **161** at the secondary carbinol center. Cyclization is expected to lead to the formation of two isomeric acetals **165** and **166**. The isomer **165** may be expected to exist as an equilibrium mixture of **165a** and **165b**. Likewise, the isomer **166** may be expected to exist as an equilibrium mixture of **166a** and **166b**. Whether both **165** and **166** or just one of them, and also whether each of these could indeed exist as an equilibrium mixture of the two possible conformational isomers will be governed by their relative energy differences, calculated as follows:



$$E_{165a} : 2 \times (-1.4) + 0.8 + 0.8 = -1.2 \text{ kcal mol}^{-1}$$

$$E_{165b} : 1 \times (-1.4) + 0.8 + 0.9 + 4.0 = 4.3 \text{ kcal mol}^{-1}$$

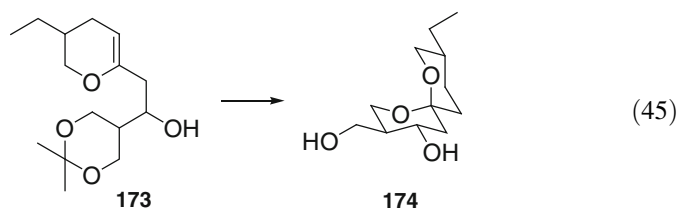
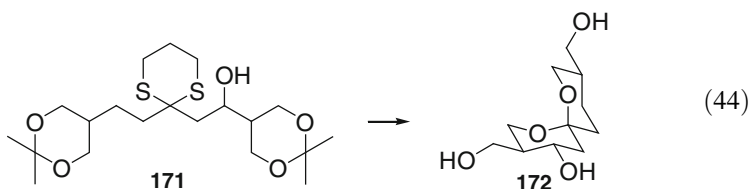
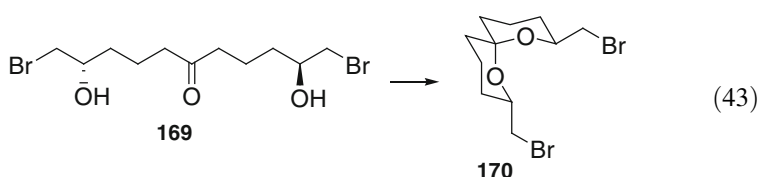
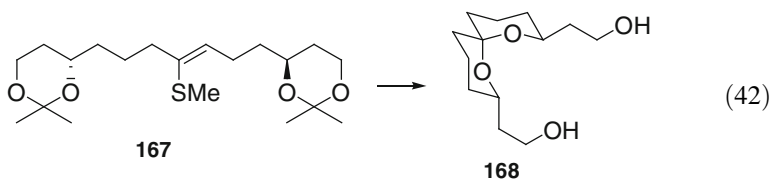
$$E_{166a} : 1 \times (-1.4) + 0.4 + 3.0 + (2 \times 0.9) = 3.8 \text{ kcal mol}^{-1}$$

$$E_{166b} : (2 \times 0.9) + (2 \times 0.9) = 3.6 \text{ kcal mol}^{-1}$$

Obviously, only the isomer **165** will be expected to form, and that too must exist predominantly as the conformer **165a**. Since **161** and **164** are noninterconvertible, but **162** and **163**, and **165** and **166** are interconvertible, one will expect **162a**, **162b**, **163a**, and **165a** to form from an enantiomeric mixture of **161** and **164**. This is very well corroborated by the experiments carried out by Deslongchamps and coworkers [17]. Further, under the acidic conditions of the reaction, while the isomer **162a** or **163a** was converted into an approximately 1:1 mixture of **162a** and **163a**, the isomer **165a** was found not to equilibrate. References [17, 18] provide mines of information, and may be referred to by the reader with serious stereochemical inclination.

We have learnt above enough about the anomeric effect and its implications on conformational preferences. Let us take a look at the examples from the general literature given in Eqs. 42–45 and analyze them in the manner as above. The

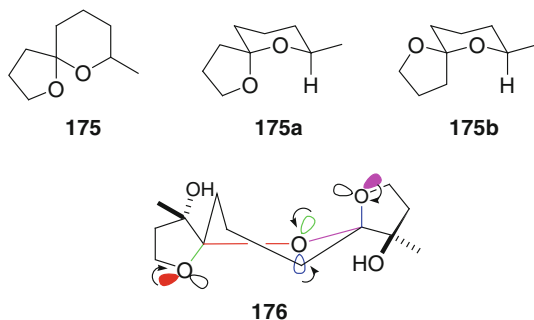
masked tetrahydroxyketone **167** [19], dibromodihydroxyketone **169** [20] and masked pentahydroxyketone **171** [21] cyclized exclusively to **168** (Eq. 42), **170** (Eq. 43), and **166** (Eq. 44), respectively. A cyclization similar to **171**  $\rightarrow$  **172** was adopted by Kozikowski and coworkers for the synthesis of ( $\pm$ )-talaromycin B [23]. In yet another successful synthesis of talaromycin B, Kocienki and Yates have achieved the transformation **173**  $\rightarrow$  **174**, Eq. 45 [24]. In the products of all these transformations, the stereochemistry at the spiroacetal carbon is the same as that in the predicted predominant conformer **157a**.



We have discussed above the conformational profile of 1,7-dioxaspiro[5.5]undecane skeleton. There are examples of 1,6-dioxaspiro[4.5]decane skeleton as well, a skeleton that has been encountered in products of natural origin including the ionophores. Cottier et al. [25] have prepared several derivatives of 1,6-dioxaspiro[4.5]decane and shown that **175** exists as the conformer **175a** in preference to **175b**. These authors have also reported that the compound **176** exists in the conformation as shown, each ring oxygen having an electron pair orbital antiperiplanar to a polar

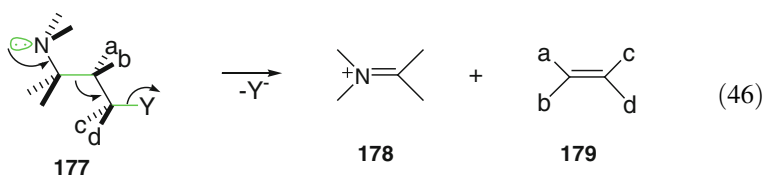


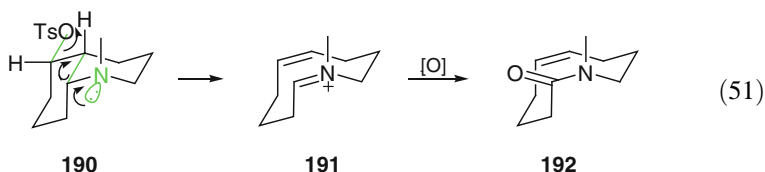
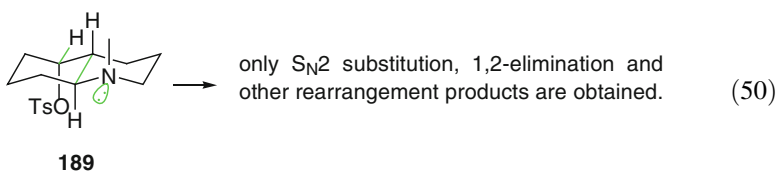
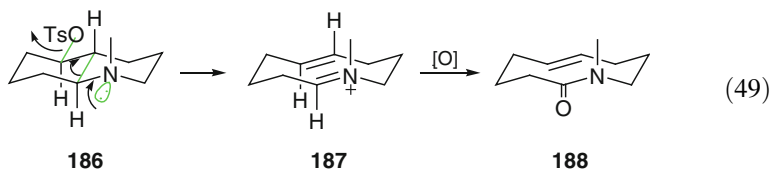
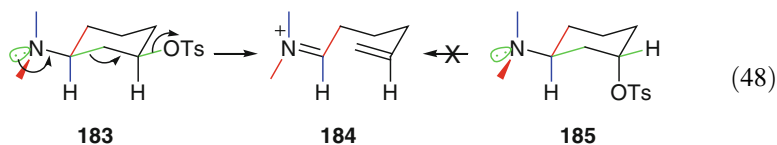
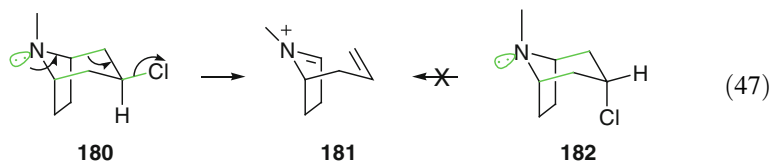
$\sigma_{C-O}$  bond. The existence of the central tetrahydropyran ring in a twist-boat conformation to accommodate as many as four  $\sigma_{C-O}$  bonds antiperiplanar to different electron pair orbitals represents a very strong case of conformational control by the anomeric effect.



## 5 Influence of Anomeric Effect on Conformational Reactivities

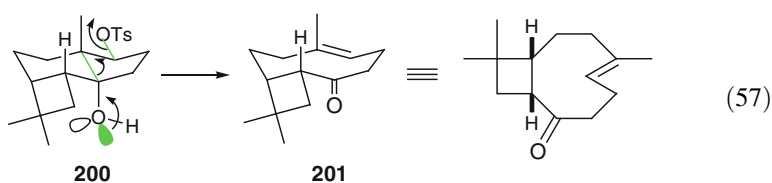
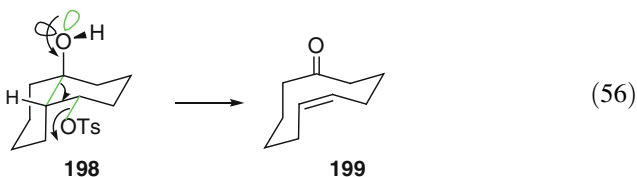
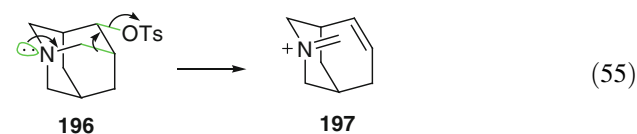
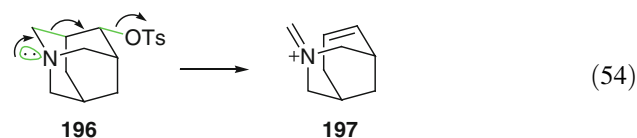
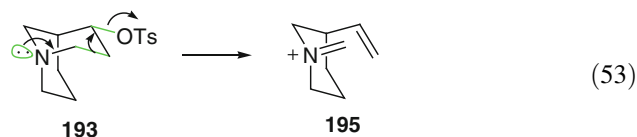
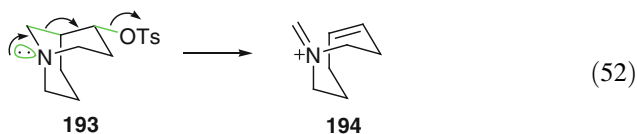
Having understood the anomeric effect well from the foregoing discussions, we shall now analyze the 1,4-eliminations shown in Eqs. 46–51. These eliminations are rendered possible by the antiperiplanar relationship of the breaking central  $\sigma_{C-C}$  bond with the electron pair orbital on the heteroatom and the  $\sigma_{C-X}$  bond, X being a leaving group such as a halogen and OTs. Note that while the species **183** generates **184** under the conditions of solvolysis, the species **185** undergoes  $S_N2$  reaction, 1,2-elimination, and rearrangement to generate species other than **184**. The ring expansion through the transformation **186**  $\rightarrow$  **187** is remarkable. In contrast, the isomer **189** undergoes alternate reactions. Also, compare the transformations **186**  $\rightarrow$  **188** and **190**  $\rightarrow$  **192** and note the geometry of the resultant olefins. The geometry of this olefin is *trans* in **188** and *cis* in **192** because of (a) the differences in the ring junction geometry, and (b) stereoelectronic control of the two intramolecular  $S_N2$  processes that take place during the 1,4-elimination. The intermediate iminium ions formed from these reactions were oxidized after hydrolysis on aqueous workup to isolate carbonyl compounds as the end products.



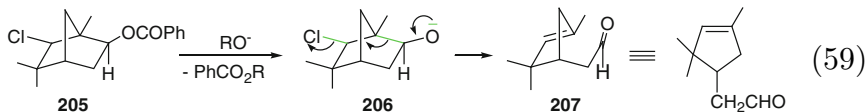
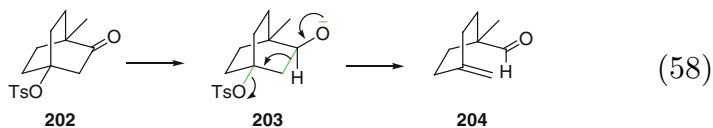


The 1,4-elimination of **193**, given in the Eqs. 52 and 53, represents two pathways leading to two different iminium ions **194** and **195**, whose relative distribution will depend on whether the reaction is performed under thermodynamic or kinetic control. The species **194** is a cyclooctene derivative and the species **195** a cyclohexane derivative. The cyclohexane derivative **195** must, of course, predominate in a thermodynamically controlled reaction. Like the species **193**, the species **196** also represents two pathways for 1,4-elimination as shown in Eqs. 54 and 55. Fortunately, both the pathways yield the same product **197**. The reactions shown in Eqs. 56 and 57 are examples of elimination resulting from the 1,3-diol mono-tosylate system. An electron pair orbital on the hydroxylic oxygen that is antiperiplanar to the cleaving central  $\sigma_{C-C}$  bond provides the necessary electronic push in which the former makes the latter weak, and therefore labile for cleavage. The reaction shown in Eq. 57 was used by Corey and coworkers in a synthesis of

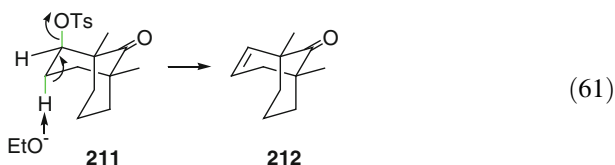
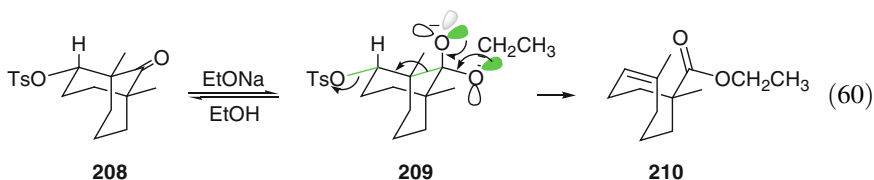
$\alpha$ -caryophyllene [26]. The *trans* geometry of the olefinic bond in the product **201** must be noted.



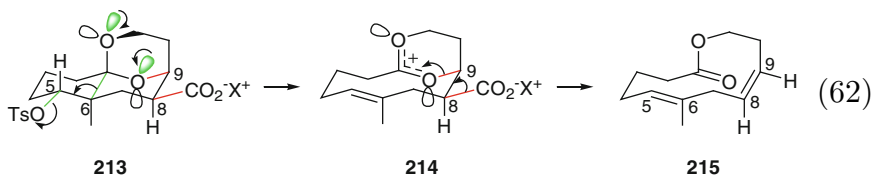
In the Eqs. 58 and 59, an oxy anion provides the necessary electronic push for the 1,4-elimination to take place smoothly. In Eq. 58, this oxy anion was generated in situ by hydride reduction of the carbonyl group [27]. The in situ oxy anion generation in Eq. 59 was achieved by the cleavage of the ester group on reaction with an alkoxide ion in a protocol that is typical of transesterification [28].



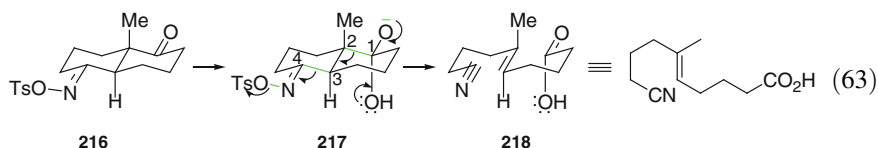
The reactions shown in the Eqs. 60 and 61 are also illustrative of the power of anomeric effect and the geometrical relationship of the participating bonds. In Eq. 60, ethoxide ion attack on the carbonyl group in **208** generates the tetrahedral intermediate **209**, wherein both the oxy anion and the ethereal oxygen have one electron pair orbital antiperiplanar to a common ring bond. Further, this ring bond is antiperiplanar to the equatorial  $\sigma_{\text{C-OTs}}$  bond. These geometrical features together fulfill the necessary requirement for 1,4-elimination and the cyclooctene derivative **210** is formed. In the event that the  $\sigma_{\text{C-OTs}}$  bond is axial, as in **211**, the 1,4-elimination is avoided altogether and the simple 1,2-elimination takes place under the otherwise identical reaction conditions to form **212** [29].



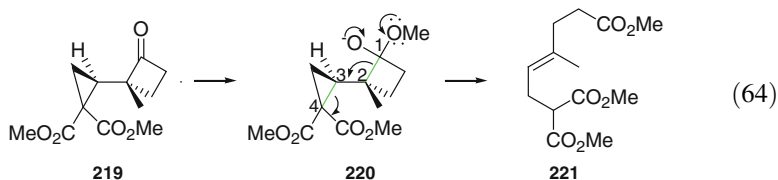
The reaction shown in the Eq. 62 is an example of 1,4-elimination that is followed by decarboxylation of the respective amidinium carboxylates ( $X = \text{amidinium ion}$ ) to obtain the same *E,Z*-macrolide [30, 31]. The fragmentation was considered by Eschenmoser to take place in two consecutive steps: (a) both the ring oxygen atoms have one electron pair orbital each in an antiperiplanar orientation to stereoelectronically eject the tosylate ion via cleavage of the ring  $\sigma_{\text{C-C}}$  bond and generate the dipolar ions **214**, and (b) the  $\pi_{\text{C}_8\text{-C}_9}$  bond in **215** emerges from the stereoelectronically controlled decarboxylation for having  $\sigma_{\text{C}_8\text{-CO}_2^-}$  bond antiperiplanar to  $\sigma_{\text{C}_9\text{-O}}$  bond.

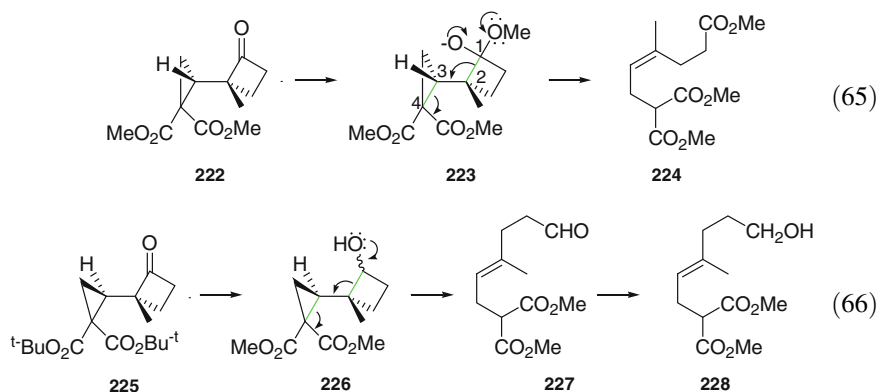


As shown in Eq. 63, the bicyclic species **216** is quantitatively transformed into the  $\omega$ -cyanocarboxylic acid **218** [32]. The intermediate species **217** formed from the reaction with hydroxide ion has two electron pairs, one on each of the two oxygen atoms located on C1, antiperiplanar to the  $\sigma_{C1-C2}$  bond. The antiperiplanar relationship between  $\sigma_{C1-C2}$  and  $\sigma_{C3-C4}$  and also between  $\sigma_{C3-C4}$  and  $\sigma_{N-OTs}$  are the other requirements for the overall fragmentation to be successful. Note that the nitrile function emerges from a process of anti-elimination.

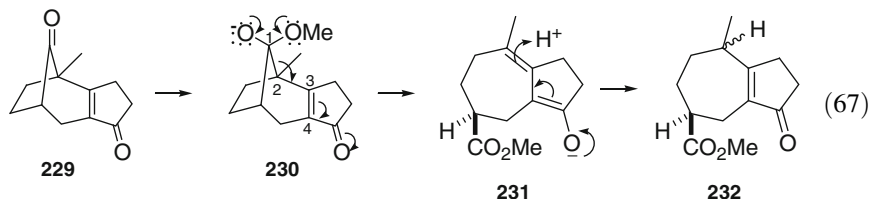


The simultaneous cleavage of both a cyclopropane ring and a cyclobutane ring in **219** in a highly stereospecific manner leads to the formation of **221**, wherein the double bond has *E*-geometry, Eq. 64. Note that the anti relationship of the methyl substituent on the cyclobutane ring and the shown hydrogen on the cyclopropane ring is retained in the product olefin. Compare this with a similar cleavage of **222** that leads to **224** with *Z*-double bond, Eq. 65 [33]. Fragmentations of **219** and **222** proceed through stereoelectronically favored cleavages of the intermediates **220** and **223**, respectively. Also note that the antiperiplanar relationship between  $\sigma_{C1-C2}$  and  $\sigma_{C3-C4}$  and also between  $\sigma_{C1-C2}$  and the two electron pair orbitals, one on each of the two oxygen atoms on C1, allow the smooth cleavage. The reaction of **225** with sodium borohydride in methanol in the presence of magnesium methoxide furnished **228**, Eq. 66 [33]. This reaction involves transesterification from *tert*-butyl ester to methyl ester, reduction of ketone to alcohol, fragmentation under full stereoelectronic control and, finally, reduction of the resultant aldehyde to alcohol.



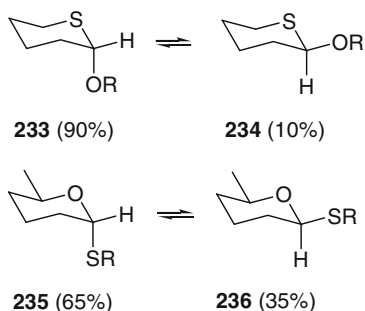


Methoxide ion-catalyzed transformation of the tricyclic enedione **229** into the isomeric mixture of the ester **232**, Eq. 67, is yet another interesting example. The  $\sigma_{C1-C2}$  bond is weakened by the two antiperiplanar electron pair orbitals, one on each the two oxygen atoms on C1. Moreover,  $\sigma_{C1-C2}$  bond is nearly parallel to the  $p$  orbitals of the  $\pi_{C=C}$  bond that allows their electron densities to mix well enough to facilitate formation of the dienolate as in **231** [34]. Protonation on either face of the dienolate is responsible for formation of the isomeric mixture of the end product **232**.

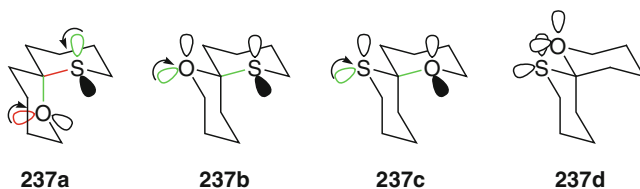


## 6 Conformations of Mono and Dithioacetals

2-Alkoxytetrahydrothiopyrans were studied by Zefirov and Shekhtman [35] and the axial conformer **233** was found to predominate (90 %) over the equatorial conformer **234** when R was a methyl or a propyl group. The equilibrium of the isomeric mixture of **235** and **236** under acidic conditions was studied by Eliel and Giza [36]. The axial isomer **235** was found to constitute almost 65 % of the mixture. These examples indicate that a monothioacetal function benefits from anomeric effect arising from sulfur, which is possibly a bit weaker than that offered by oxygen.



1-Oxa-7-thiaspiro[5.5]undecane **237** can exist in four different conformations **237a–237d** that possess two, one, one and zero anomeric effects, respectively. Taking into account the steric effects as before (0.9 kcal mol<sup>-1</sup> for a gauche form of *n*-butane, 0.4 kcal mol<sup>-1</sup> for a gauche form of X-CH<sub>2</sub>-Y-CH<sub>2</sub> (X = S or O, Y = S or O or CH<sub>2</sub>) and -1.4 kcal mol<sup>-1</sup> for an anomeric effect arising from both the oxygen and the sulfur, the relative stabilities turn out to be 0.0, 2.4, 2.4 and 4.8 kcal mol<sup>-1</sup> (add 1.2 kcal mol<sup>-1</sup> to each of the final values). On this account, **239** must exist predominantly as the conformer **237a**.



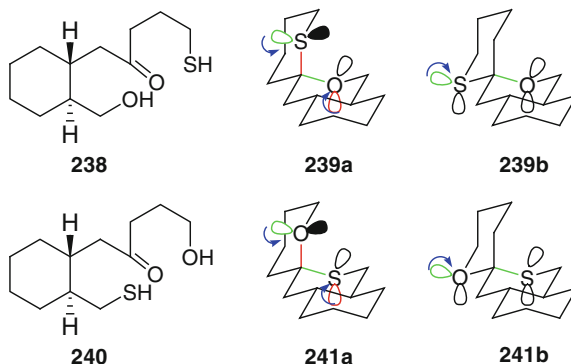
$$E_{237a} : 2 \times (-1.4) + (2 \times 0.4) + (2 \times 0.4) \text{ kcal mol}^{-1} = -1.2 \text{ kcal/mol}$$

$$E_{237b} : 1 \times (-1.4) + (2 \times 0.4) + (2 \times 0.9) = 1.2 \text{ kcal mol}^{-1}$$

$$E_{237c} : 1 \times (-1.4) + (2 \times 0.4) + (2 \times 0.9) = 1.2 \text{ kcal mol}^{-1}$$

$$E_{237d} : 0 \times (-1.4) + (2 \times 0.9) + (2 \times 0.9) = 3.6 \text{ kcal mol}^{-1}$$

The above analysis gains support from the cyclization results of the compounds **238** and **240**. The compound **238** furnished the conformer **239a** rather than **239b**. In the conformer **239a**, each heteroatom exerts an anomeric effect on the other heteroatom, whereas only the sulfur atom exerts an anomeric effect on the oxygen atom in the conformer **239b**.



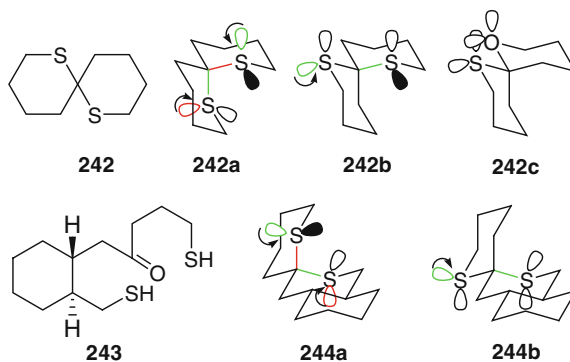
Taking the anomeric effects together with the operating steric factors, the following energy profile emerges:

$$E_{239a} : [-1.4 - 1.4 + (2 \times 0.4) + (2 \times 0.4) = -1.2 \text{ kcal mol}^{-1}$$

$$E_{239b} : [-1.4 + (2 \times 0.4) + (2 \times 0.9) = 1.2 \text{ kcal mol}^{-1}$$

Thus, **239a** is more stable than **239b** by a margin of  $2.4 \text{ kcal mol}^{-1}$ . Likewise, the cyclization of **240** furnished only the conformer **241a** and none of the conformer **241b** [18, 37]. The conformers **241a** and **241b** may also be calculated, like above, to differ in energy by  $2.4 \text{ kcal mol}^{-1}$ .

1,7-Dithiaspiro[5.5]undecane **242** may be expected to exist in three conformations **242a**, **242b**, and **242c** that have, respectively, two, one, and zero anomeric effects. Taking into account the prevailing steric effects and the stabilizing anomeric effect worth  $1.4 \text{ kcal mol}^{-1}$  exerted by the sulfur, the relative energies of these conformers are as follows:



$$E_{242a} : 2 \times (-1.4) + (2 \times 0.4) + (2 \times 0.4) = -1.2 \text{ kcal mol}^{-1}$$

$$E_{242b} : 1 \times (-1.4) + (2 \times 0.4) + (2 \times 0.9) = +1.2 \text{ kcal mol}^{-1}$$

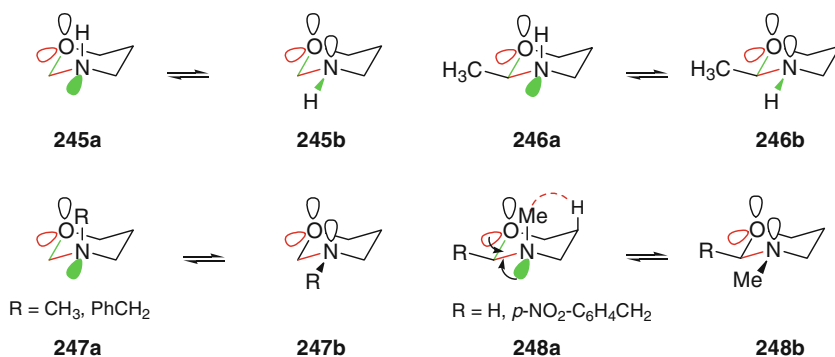
$$E_{242c} : 0 \times (-1.4) + (2 \times 0.9) + (2 \times 0.9) = +3.6 \text{ kcal mol}^{-1}$$



The conformer **242a** is more stable than the conformers **242b** and **242c** by, respectively, 2.4 and 4.8 kcal mol<sup>-1</sup>. On this basis, **242** must exist predominantly as the conformer **242a**. This prediction was verified experimentally and also by achieving the cyclization of **243** under acid-catalyzed conditions when the product was discovered to exist predominantly as the conformer **244a** at equilibrium [18, 37]. The conformer **244a** [ $2 \times (-1.4) + (2 \times 0.4) + (2 \times 0.4) = -1.2$  kcal mol<sup>-1</sup>] is 2.4 kcal mol<sup>-1</sup> more stable than the conformer **244b** [ $-1.4 + (2 \times 0.4) + (2 \times 0.9) = 1.2$  kcal mol<sup>-1</sup>]. The anomeric effect due to the sulfur atom must also therefore be of the order of -1.4 kcal mol<sup>-1</sup>.

## 7 Conformations of Mono and Diazaacetals

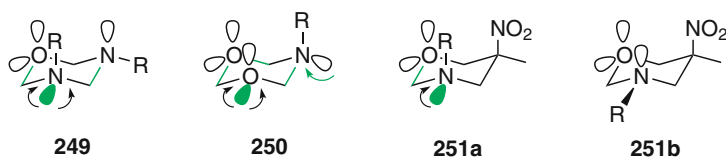
The acetals **245** and **246** have been discovered from low temperature NMR studies to exist largely as the conformers **245a** and **246a**, respectively [38]. Both these conformers benefit from two anomeric effects as compared to the conformers **245b** and **246b** that have only one such effect. The one additional anomeric effect in the conformers **245a** and **246a** therefore appears to be responsible for their better stabilities. The conformer **247a** with an axial alkyl substituent, methyl or benzyl, on the nitrogen has been suggested to be more stable than the conformer **247b** with an equatorial alkyl substituent on the nitrogen [39]. Again, **247a** benefits from one additional anomeric effect than the conformer **247b**.



The acetal **248** that bears a methyl group on the nitrogen and either an equatorial hydrogen atom or a *p*-nitrobenzyl group on the ring carbon in between the two heteroatoms was discovered to exist as 1:1 equilibrium mixture of the conformers **248a** and **248b** [40]. This result demonstrates that both the conformers are of equal energy and, hence, it was used for an evaluation of the anomeric effect arising from the nitrogen. The conformer **248a** is raised in energy from one *n*-butane gauche interaction as shown (0.9 kcal mol<sup>-1</sup>) and another interaction due to one gauche

form of  $\text{CH}_3\text{-N-CH}_2\text{-O}$  ( $0.4 \text{ kcal mol}^{-1}$ ). Let us assume that the contribution from the anomeric effect caused by the equatorial electron pair orbital on the nitrogen atom is  $x \text{ kcal mol}^{-1}$ , then  $x + 0.9 + 0.4 = 0$ . This lends a value of  $-1.3 \text{ kcal mol}^{-1}$  to  $x$ . This value is very close to the value of the anomeric effect arising from oxygen electron pair orbital.

1-Oxa-3,5-diaza- and 1,3-dioxo-5-azacyclohexanes exist in the conformations **249** and **250**, respectively [41]. With the axial alkyl group on the nitrogen atom, both the conformers gain two anomeric effects as shown. The conformer **251a** with an axial methyl, ethyl, or propyl substituent on the nitrogen atom is favored over the conformer **251b** possessing the substituent on nitrogen equatorial. However, the conformer **251b** is favored over the conformer **251a**, when the substituent on nitrogen is a large isopropyl, cyclohexyl, or *tert*-butyl group [39].



## References

1. Kovak F, Plesnikar B (1978) *J Chem Soc Chem Comm*, 122
2. Pocker Y, Green E (1974) *J Am Chem Soc* 96:166
3. Bouab O, Lamaty G, Moreau C, Pomares O, Deslongchamps P, Ruest L (1980) *Can J Chem* 58:567
4. Beaulieu N, Deslongchamps P (1980) *Can J Chem* 58:875
5. McElvain SM, McKay GR Jr (1955) *J Am Chem Soc* 77:5601
6. Capon B, Grieve DM (1982) *Tetrahedron Lett* 23:4823
7. Deslongchamps P, Chenevert R, Taillefer RJ, Moreau C, Saunders JK (1975) *Can J Chem* 53:1601
8. Deslongchamps P, Moreau C (1971) *Can J Chem* 49:2465
9. Deslongchamps P, Moreau C, Fréhel D, Atlani P (1972) *Can J Chem* 50:3402
10. Deslongchamps P, Atlani P, Fréhel D, Malaval A, Moreau C (1974) *Can J Chem* 52:3651
11. Khouri F, Kaloustian MK (1978) *Tetrahedron Lett* 5067
12. Khouri F, Kaloustian MK (1979) *J Am Chem Soc* 101:2249
13. Kaloustian MK, Khouri F (1981) *Tetrahedron Lett* 22:413
14. Kaloustian MK, Khouri F (1980) *J Am Chem Soc* 102:7579
15. Descotes G, Lissac M, Delmau J, Duplax J (1968) *CR Acad Sci Ser C* 267:1240
16. Beaulieu N, Dickinson RA, Deslongchamps P (1980) *Can J Chem* 58:2531
17. Deslongchamps P, Rowan DD, Pothier N, Sauvé G, Saunders JK (1981) *Can J Chem* 59:1105
18. Pothier N, Rowan DD, Deslongchamps P, Saunders JK (1981) *Can J Chem* 59:1132
19. Evans DA, Sacks CE, Whitney RA, Mandel NG (1978) *Tetrahedron Lett* 727
20. Cresp TM, Probery CL, Sondheimer F (1978) *Tetrahedron Lett* 3955
21. Schreiber SL, Sommer TJ (1983) *Tetrahedron Lett* 24:4781
22. Schreiber SL, Sommer TJ, Satake K (1985) *Tetrahedron Lett* 26:17
23. Kozikowski AP, Scripko JG (1984) *J Am Chem Soc* 106:353

24. Kocienki P, Yates C (1984) *J Chem Soc Chem Commun* 151
25. Cottier L, Descotes G, Grenier MF, Metras F (1981) *Tetrahedron* 37:2515
26. Corey EJ, Mitra RB, Uda H (1964) *J Am Chem Soc* 86:485
27. Kraus W (1966) *Angew Chem Int Ed* 5:316
28. Schmidt H, Muehlstaedt M, Son P (1966) *Chem Ber* 99:2736
29. Martin J, Parker W, Raphael RA (1964) *J Chem Soc* 289
30. Sternbach DD, Shibuya M, Jaisli F, Bonetti M, Eschenmoser A (1979) *Angew Chem Int Ed Engl* 18:634
31. Shibuya M, Jaisli F, Eschenmoser A (1979) *Angew Chem Int Ed Engl* 18:636
32. Eisele W, Grob CA, Renk E, von Tschammer W (1968) *Helv Chim Acta* 51:816
33. Trost BM, Frazee WJ (1977) *J Am Chem Soc* 99:6124
34. Buchanan GL, Young GAR (1971) *J Chem Soc, Chem Commun* 643
35. Zefirov NS, Shekhtman NM (1968) *Dokl Akad Nauk SSSR* 180:1363
36. Eliel EL, Giza CA (1968) *J Org Chem* 33:3754
37. Deslongchamps P, Rowan DD, Pothier N, Saunders JK (1981) *Can J Chem* 59:1122
38. Booth H, Limeux RU (1971) *Can J Chem* 49:777
39. Allingham Y, Cookson RC, Crabb TA, Vary S (1968) *Tetrahedron* 24:4625
40. Riddell FG, Lehn JM (1968) *J Chem Soc B* 1224
41. Baker VJ, Ferguson IJ, Katritzky AR, Patel R, Rahimi-Rastgoo S (1978) *J Chem Soc Perkin Trans* 2:377

## Chapter 2

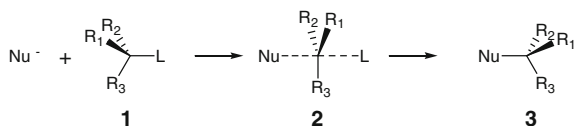
# Reactions at Saturated and Unsaturated Carbons

**Abstract** This chapter covers the geometrical requirements for reactions at saturated and unsaturated carbons in both acyclic and cyclic systems with related stereochemical features. The nucleophilic attacks in  $S_N2$  and  $S_N2'$  processes, involving the necessary geometrical requirements, are discussed. The resonance-driven activation of cyclopropane is of much significance in synthetic chemistry. The mode of activation and its consequences on the product profile are amply reasoned. The  $S_N2$ -originated 1,2-migration within the geometrical constraints of the reactant and neighboring group participation under solvolysis conditions have been explained with emphasis on product distribution. The activation of oxiranes by Lewis acids, followed rearrangement with stereochemical effects, is elaborated. Given the suitable geometrical disposition of substituents and functional groups in a given molecule, many 1,2-migrations take place in tandem to generate fascinating skeletons. This chemistry has been described by the construction of several steroidal skeletons. Baldwin rules and the preferential 5-*exo*-trig over 5-*endo*-trig cyclization are demonstrated using kinetics and related product analysis with examples. The stereoelectronically controlled addition reactions have been highlighted.

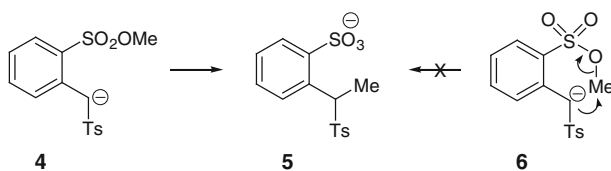
**Keywords**  $S_N2$  and  $S_N2'$  reactions • Baldwin rules • Oxirane opening • Activation of a cyclopropane • 1,2-rearrangement • Ring contraction • Ring expansion • Solvolysis • Neighboring group participation • Oxirane rearrangement • Classical and nonclassical carbocations • 5-*exo*- vis-à-vis 5-*endo* cyclization • Addition and elimination reactions

The concerted bond formation and bond cleavage in  $S_N2$  reactions proceeds with full stereoelectronic control. In the transition structure **2** for the reaction, both the nucleophile and the leaving group are bonded to the central carbon atom, which has acquired  $sp^2$  character. One lobe of the p orbital on the carbon overlaps with the incoming nucleophile and the other lobe with the leaving group. Since the nucleophile approaches the carbon from the direction opposite to the leaving group, the result is Walden inversion or inversion of configuration. The reaction is, thus,

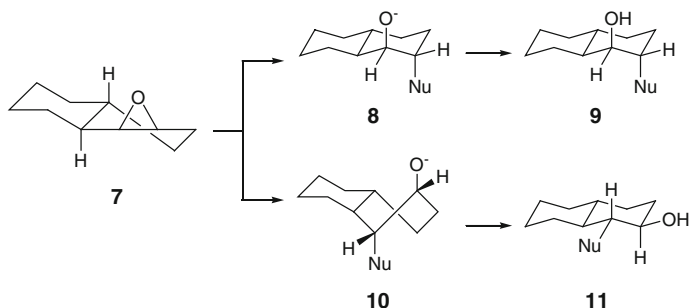
controlled by electronic effects that impose a definite geometrical restraint in the transition structure.



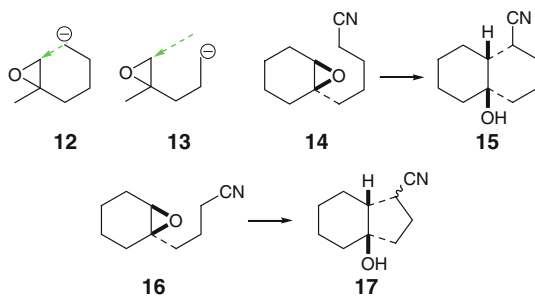
The evidence as to the fact that the nucleophile is indeed aligned in a collinear arrangement to the leaving group is provided from the transformation **4** → **5**, which was discovered to take place via an intermolecular process rather than the formally appealing intramolecular version shown in **6**. The intramolecular version does not allow the said collinear arrangement [1]. The reaction was found indeed to be bimolecular.



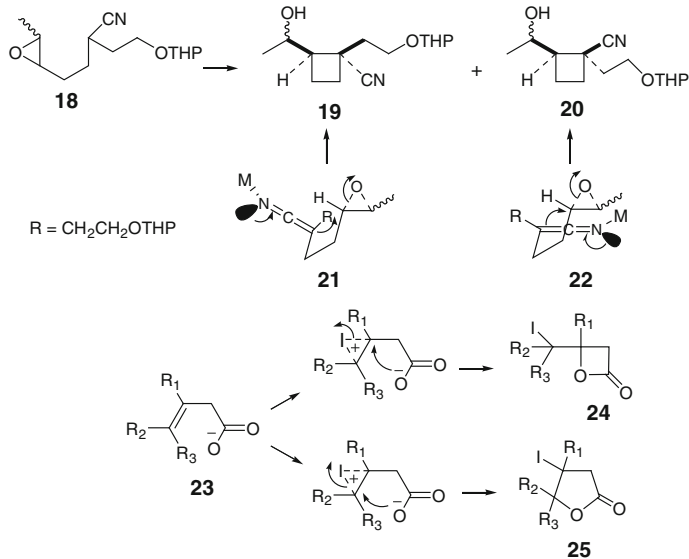
In accordance with the collinear requirement, epoxides react with nucleophiles and open up to give products of well-defined stereochemistry. We shall investigate this by considering the conformationally rigid unsymmetrical epoxide **7**, which may form two different products **9** and **11** by following different pathways. While the diaxial product **9** results from axial attack at C3 and proceeds through the chair-like intermediate **8**, the diequatorial product **11** results from equatorial attack at C2 and proceeds through the twist boat-like intermediate **10**. Since the equatorial attack at C2 proceeds through a higher energy twist-boat transition structure than the chair transition structure arising from axial attack at C3, the product **9** must form in preference to **11** under kinetically controlled conditions. It should be noted that the 1,2-diequatorial product is thermodynamically more stable than 1,2-diaxial product on account of the possible 1,3-diaxial interactions in the latter. Indeed, epoxide opening to give the diaxial product is very well known.



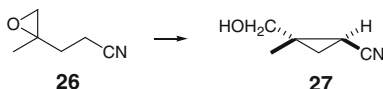
The intramolecular  $S_N2$  opening of epoxides must also follow the above stereoelectronic requirement within the geometrical constraints of the system. It is solely based on the collinear requirement of the  $S_N2$  reaction that Stork favored intramolecular opening leading to a six-membered ring more than that leading to a five-membered ring. While the nucleophile is perfectly aligned for a rear collinear attack in the formation of the six-membered in **12**, it is poorly aligned in the formation of the five-membered ring in **13**. The trajectory requires the nucleophile to be on the dotted line which, in turn, requires considerable bond distortion. From the reactions of the epoxynitriles **14** and **16** under basic conditions, it was indeed discovered that the transformation **14**  $\rightarrow$  **15** leading to a six-membered ring is significantly easier than the transformation **16**  $\rightarrow$  **17** leading to a five-membered ring [2].



A similar analysis of the transition state requirement allowed Stork to realize that it was easier to achieve collinearity in the formation of a four-membered ring than in the formation of a five-membered ring. Thus, for a given situation where both the four- and five-membered rings could form, the former was considered to prevail. Indeed, the reaction of the epoxynitrile **18** with a base (required for deprotonation to generate the requisite carbanion) in benzene furnished a 95:5 mixture of the isomeric cyclobutanes **19** and **20** only [3]. No five-membered ring product was formed. One may note that the major isomer **19** is less stable due to two large substituents being *cis* to each other than in the minor isomer **20**. This result indicates that the transition state structure **21**, leading to **19**, is of lower energy than the transition state structure **22** that leads to **20**. In the transition state structure **22**, the nitrogen atom along with the large solvated metal ion comes close to the far end of the epoxide carbon to cause significant van der Waals interactions. In yet another interesting example, iodolactonization of the  $\beta,\gamma$ -unsaturated carboxylic acid salts **23** were found to yield the butyrolactones **24** in preference to the otherwise more stable  $\gamma$ -lactones **25**. The internal opening of the three-membered ring iodonium ion (equivalent to an epoxide) by the carboxylate ion leading to a four-membered ring product, **23**  $\rightarrow$  **24**, is preferred over the opening leading to a five-membered ring product, **23**  $\rightarrow$  **25**.



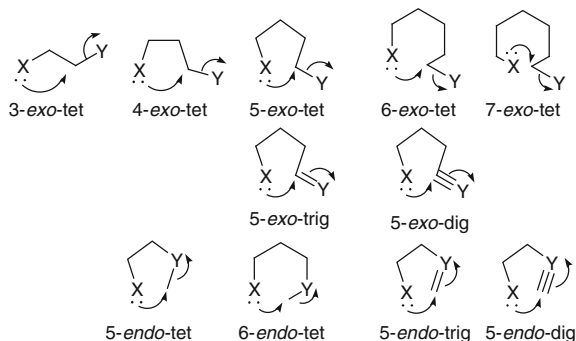
Finally, in regard to the internal opening of an epoxide ring, cyclopropane formation is preferred over cyclobutane formation, regardless of the relative degree of substitution of the ring. For instance, the reaction of **26** with a suitable base generated the cyclopropane **27** exclusively [3]. The transition state structure for this transformation resembles the transition state structure **21** above, but with one carbon less in the chain linking the nitrile group and the ring.



In summary, in internal epoxide ring opening, six-membered ring formation does not require bending of any of the  $\sigma$  bonds of the chain, while the formation of five-, four-, and three-membered rings requires the simultaneous bending of four, three, and two such  $\sigma$  bonds, respectively, in addition to the electron pair orbital of the carbanion. Though the degree of bending is more pronounced in the formation of the three-membered ring than in others, the number of bonds that must bend simultaneously is more important than the degree of bond bending. Thus, the simultaneous bending of three  $\sigma$  bonds leading to cyclobutane formation is less difficult than the simultaneous bending of four  $\sigma$  bonds leading to cyclopentane formation, but more difficult than the bending of two  $\sigma$  bonds leading to cyclopropane formation. In other words, the facility of ring formation in the internal opening of epoxides decreases in the order: six-membered ring > three-membered ring > four-membered ring > five-membered ring.

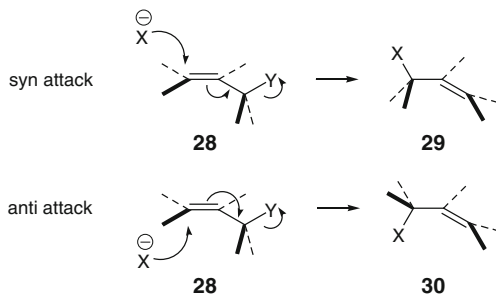
We shall now turn to the internal  $S_N2$  reaction on a  $sp^3$  carbon. Purely on account of geometrical constraints imposed in achieving the collinear alignment,

Baldwin proposed a set of rules for such ring closure reactions [4]. The reactions were designated by a numerical prefix which denotes the size of the ring to be formed, followed by the term *exo* or *endo* depending upon whether the bond breaking is exocyclic or endocyclic to the ring thus formed. Now, a suffix such as *tet* (for a tetrahedral or  $sp^3$  carbon), *trig* (for a trigonal or  $sp^2$  carbon), or *dig* (for a diagonal or  $sp$  carbon) describes the state of hybridization of the electrophilic carbon. A collection of many such reactions are given below.



While all the reactions from 3-*exo-tet* to 7-*exo-tet* are favored, the 5-*endo-tet* and 6-*endo-tet* reactions are disfavored on stereoelectronic grounds, i.e., on account of the collinear requirement of  $S_N2$  reactions. The relative ease of these processes is 3-*exo-tet* > 4-*exo-tet* < 5-*exo-tet* > 6-*exo-tet* > 7-*exo-tet*. It is important to recognize that the intramolecular  $S_N2$  process proceeding through the transition structure resembling **6** constitutes a 6-*endo-tet* process and, hence, unfavorable.

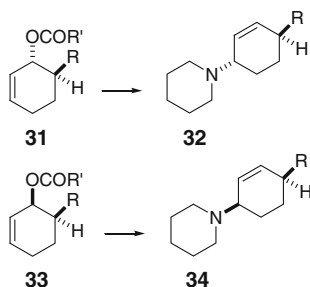
The  $S_N2'$  reaction involves nucleophilic attack on the terminal  $sp^2$  carbon with a shift in the position of the double bond. The nucleophile may attack either *anti* or *syn* to the leaving group as shown in the transformations **28**  $\rightarrow$  **29** and **28**  $\rightarrow$  **30**, respectively. The *syn* attack is preferred over the *anti* attack because the *syn* attack displaces the  $\pi$  electrons in the direction that is *anti* to the  $\sigma_{C-Y}$  bond and, thus, suitable for the next rear side attack.



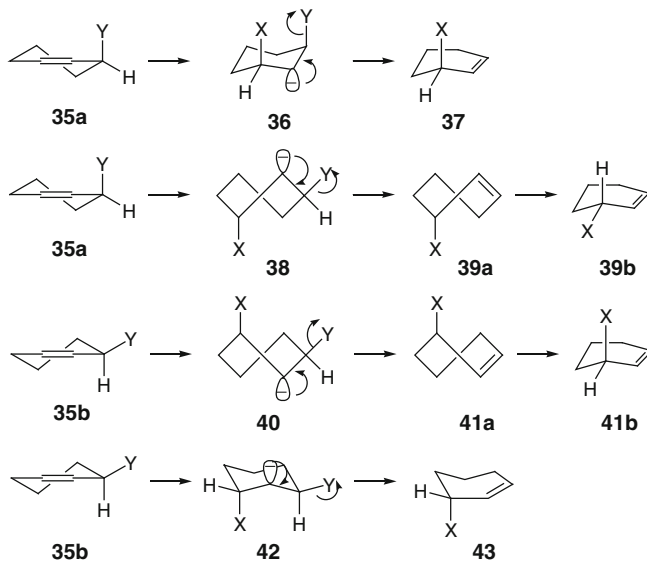
In confirmation of the above preferred *syn* attack, reactions of the cyclohexenyl dichlorobenzoates **31** ( $R = \text{Me}, i\text{-Pr}, t\text{-Bu}; R' = \text{Cl}_2\text{C}_6\text{H}_3$ ) with piperidine afforded **32**. Likewise, the *trans* and *cis* mesitoates **31** and **33** ( $R = i\text{-Pr}, R' = \text{C}_6\text{H}_2\text{Me}_3$ )



reacted with piperidine to form **32** and **34**, respectively [5, 6]. The difference in the relative dispositions of the two substituents on the cyclohexene core should be noted.

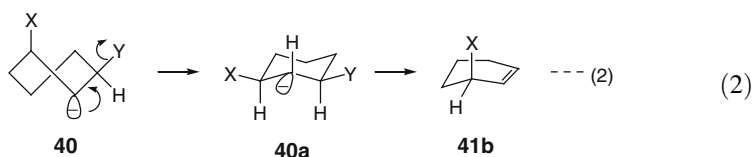
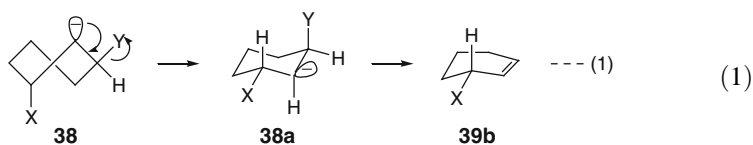


The story of the cyclohexenyl system is a little more complicated than from the above two reactions, because the cyclohexenyl system can exist in two conformations such as **35a** and **35b**. A *syn* attack on **35a** will proceed through the chair-like transition state resembling **36** and generate **37**. In the transition state structure **36**, the electron pair orbital is disposed *anti* to the leaving group Y and, thus, the subsequent elimination (or intramolecular  $S_N2$  reaction) is facile. In the alternate *anti* attack, the transition state structure resembles the twist-boat structure **38**, wherein the electron pair orbital is *syn* to the leaving group and, thus, not facile. Thus, the difficulties in the transformation **35a**  $\rightarrow$  **39b** are: (a) energy-requiring twist-boat transition structure **38**, (b) stereoelectronically unsupported *syn* elimination leading to the transformation **38**  $\rightarrow$  **39a**, and (c) the energy requiring flip of the twist-boat olefin **39a** to the half chair product **39b**. Out of these two processes, the process **35a**  $\rightarrow$  **36**  $\rightarrow$  **37** appears to be the better choice.

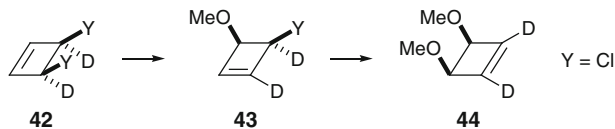


In the alternate conformer **35b**, the *syn* attack will proceed through the twist-boat conformer resembling **40**, wherein the axes of the electron pair orbital and  $\sigma_{C-Y}$  are *anti* but not antiperiplanar to allow a smooth elimination to **41a**, going over to **41b** through ring flip. However, in comparison, this transformation must be more facile than the transformation **35a**  $\rightarrow$  **39b**. Though the *anti* attack to **35b** does proceed through a chair-like transition structure resembling **42**, the final elimination reaction leading to **43** is not supported stereoelectronically for the *syn* dispositions of the electron pair orbital and the leaving group Y. Overall, the *syn* process **35a**  $\rightarrow$  **36** **37** is the most energy conserving process and it will be expected to prevail.

It is also conceivable that the twist-boat transition state structures **38** and **40** may undergo ring flip to **38a** and **40a** before collapsing through the elimination pathways to form **39b** and **41b** as shown in Eqs. 1 and 2, respectively.

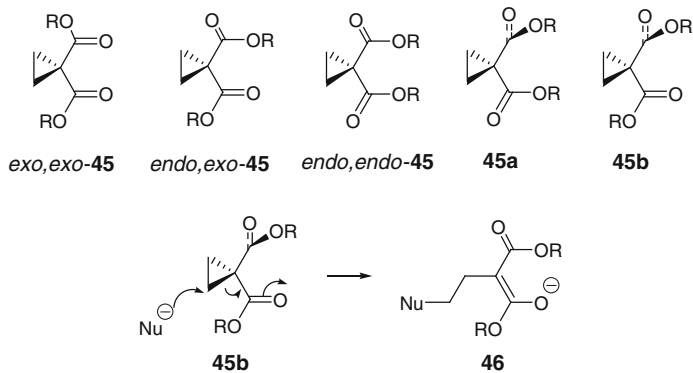


A fascinating example of two consecutive *syn* additions is expressed from the overall transformation **42**  $\rightarrow$  **44** via **43**, the product of the first *syn* addition, on reaction of **42** with sodium methoxide [7]. Note that the methoxy substituents in the product are *syn*, which could be easily established by nOe measurements.

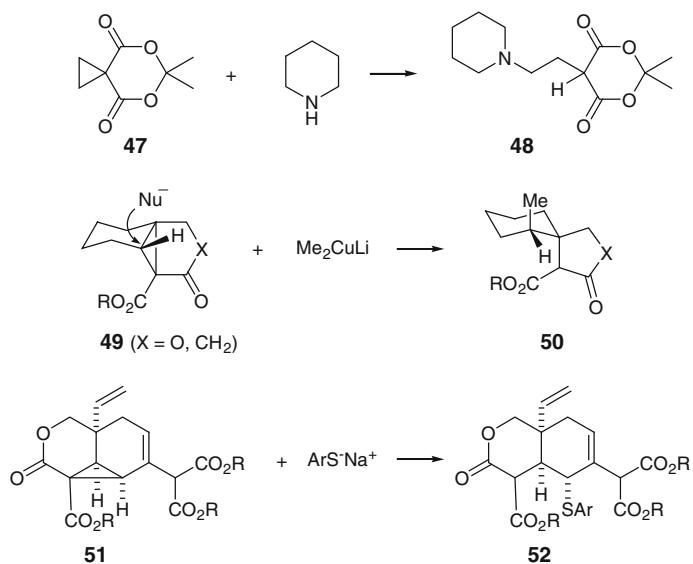


It is conceivable that cyclopropane 1,1-dicarboxylate can adopt either of the three conformations *exo,exo*-**45**, *endo,exo*-**45**, and *endo,endo*-**45**. When the carbonyl group and the cyclopropane ring are *anti* across the intervening  $\sigma_{C-C}$  bond, we will consider the orientation to be *exo*. Likewise, when the carbonyl group and the cyclopropane ring are *syn* across the intervening  $\sigma_{C-C}$  bond, we will consider the orientation to be *endo*. However, all the above conformations are disfavored on dipolar and/or steric grounds. It is therefore assumed that **45** adopts preferably the conformer **45a** or **45b** to avoid the said interactions, on one hand, and still have the *p* orbital of the in-plane carbonyl function parallel to the adjacent  $\sigma_{C-C}$  bond. This arrangement activates the  $\sigma_{C-C}$  bond and allows a nucleophilic attack on the remote carbon. The resultant carbanion delocalizes into the carbonyl group as shown in the

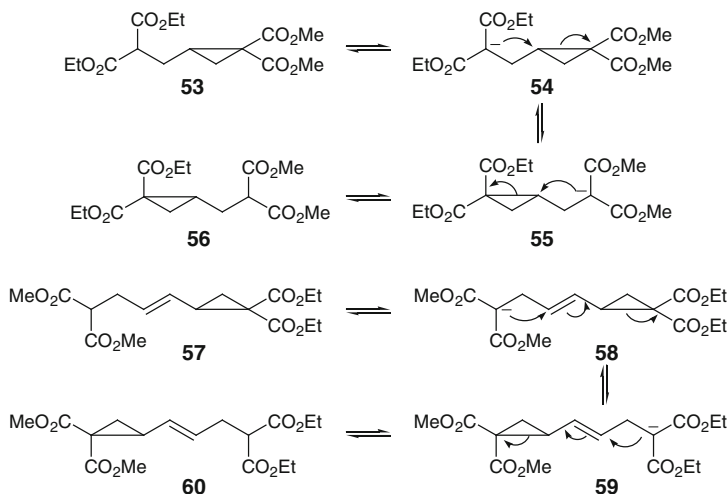
transformation **45b**  $\rightarrow$  **46**. The conformer **45b** is preferred over **45a** if one is to rely upon the anti-transition state structure theory. It is also evident that if the compound is locked in either of the conformations *exo,exo*-**45**, *endo,exo*-**45**, and *endo,endo*-**45** for geometrical reasons, it will display heightened reactivity toward nucleophiles.



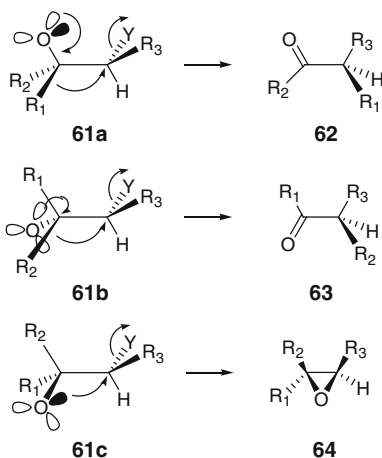
Indeed, when **47** is mixed with piperidine in benzene at room temperature, an exothermic reaction takes place to form the adduct **48** [8]. For substrates enjoying activation by a single carbonyl function, please see the transformations **49**  $\rightarrow$  **50** [9] and **51**  $\rightarrow$  **52** [10].



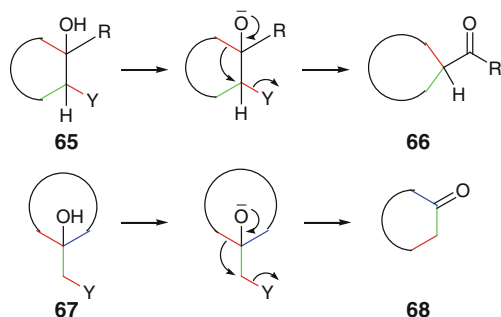
It is the consequence of the above activation mechanism that **53** equilibrates with **56** via **54** and **55**, and likewise, **57** equilibrates with **60** upon addition of a catalytic amount of  $\text{CH}_3\text{S}(\text{O})\text{CH}_2\text{Na}$  in DMSO as the solvent [11, 12].



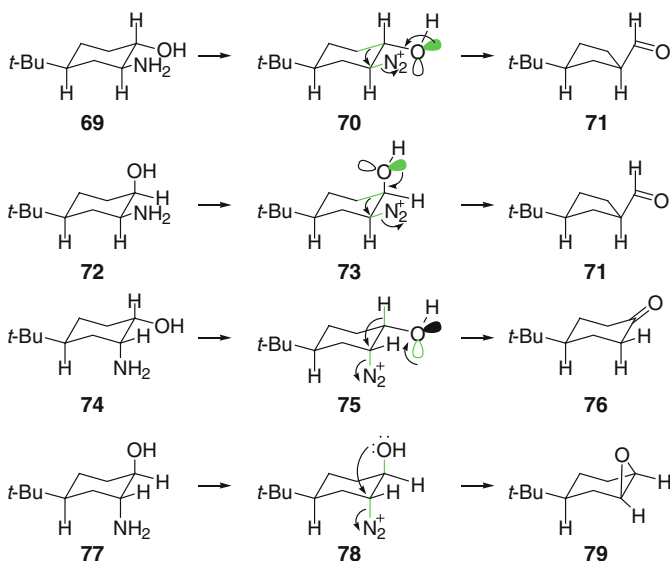
Now, we shall consider rearrangement reactions that involve two or more intramolecular  $\text{S}_{\text{N}}2$  processes before reaching the product. Let us begin with the reaction of tertiary alcohols bearing a leaving group at the  $\beta$  carbon. Note that in the general transformation **61a**  $\rightarrow$  **62**, the group  $\text{R}_1$  that migrates from the oxygen-bearing carbon to the carbon bearing the leaving group  $\text{Y}$  is disposed in an anti relationship with both  $\sigma_{\text{C-X}}$  and electron pair orbital on the oxygen atom. If for some reason, steric or otherwise, the molecule adopts the conformation as in **61b**, it is  $\text{R}_2$  that will migrate and yield the isomeric compound **63**. Finally, the conformer **61c**, wherein  $\sigma_{\text{C-O}}$  is anti to the leaving group  $\text{Y}$ , will lead to the epoxide **64**.



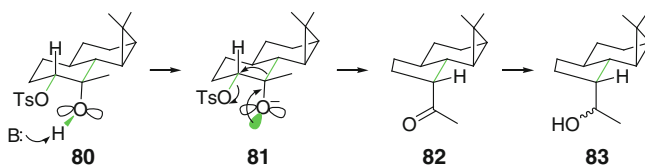
We can now apply the above general concepts to a system wherein both the hydroxyl group and the leaving group Y are located at positions 1 and 2 on a ring system, such as in **65**, and to a system wherein the hydroxyl function is located on a ring carbon and the leaving group Y on a carbon outside the ring, such as in **67**. We shall notice ring contraction in the transformation **65**  $\rightarrow$  **66** and ring expansion in the transformation **67**  $\rightarrow$  **68**. The carbon bearing the hydroxyl group in **65** comes out of the ring in the product **66** and, thus, the number of atoms in the ring gets reduced by one. In contrast, the carbon outside the ring in **67** becomes part of the ring in the product **68** and, thus, the ring gets enlarged by one.



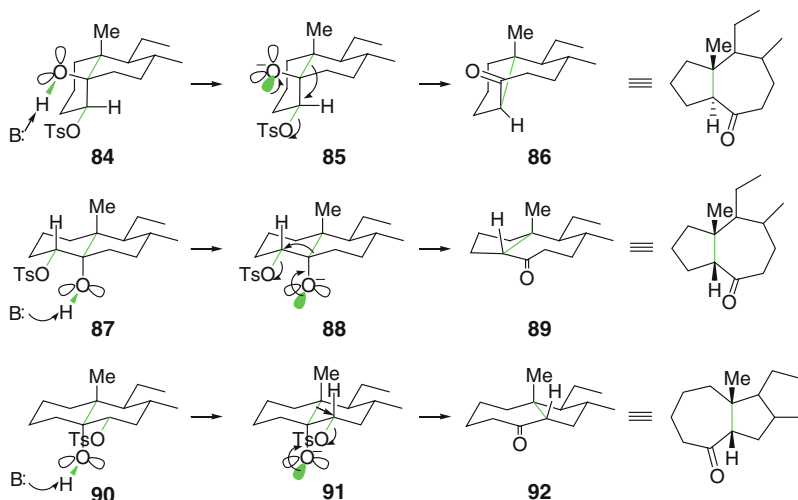
Let us now apply the above concepts to the deamination of vicinal aminoalcohols on a cyclohexane backbone. Four different situations arise from the structures of **69**, **72**, **74**, and **77**. The amino group is transformed into a diazonium species to act as a leaving group as in structures **70**, **73**, **75** and **78**, respectively. It is easy to note the antiperiplanar relationship of the ring bond in green color with an electron pair orbital on the oxygen in green color and the  $\sigma_{C-N}$  bond, also in green color, in structures **70** and **73**. The rearrangement, as shown, occurs to furnish the ring-contracted aldehyde **71** in each instance. In the diazonium species **75**, it is the axial hydrogen on the carbinol carbon that is antiperiplanar to the  $\sigma_{C-N}$  bond and, thus, the hydrogen migrates and the cyclohexanone **76** is formed. In the species **78**, the carbinol oxygen itself is antiperiplanar to the  $\sigma_{C-N}$  bond, which allows an intramolecular nucleophilic displacement of the diazonium group and the epoxide **79** is formed. It is important to recall that the transformations **70/73**  $\rightarrow$  **71** and **75**  $\rightarrow$  **76** are typical of the transformations **61a/b**  $\rightarrow$  **62/63** and, likewise, the transformation **78**  $\rightarrow$  **79** is typical of the transformation **61c**  $\rightarrow$  **64**.



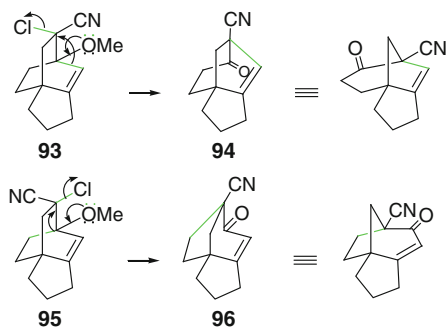
We will now consider some more such examples. Attempted reduction of **80** with  $\text{LiAlH}_4$  furnished the ring-contracted product **83** [13]. The basic character of  $\text{LiAlH}_4$  was responsible for deprotonation of the carbinol to generate the corresponding oxy anion **81**, which triggers the rearrangement to **82**. The carbonyl product **82** is reduced further by the hydride to yield the observed alcohol **83**.



The transformations **84**  $\rightarrow$  **86**, **87**  $\rightarrow$  **89** and **90**  $\rightarrow$  **92** are some of the other steroid-based examples wherein one ring is contracted and the other is enlarged by virtue of the structural design of the substrates [14].



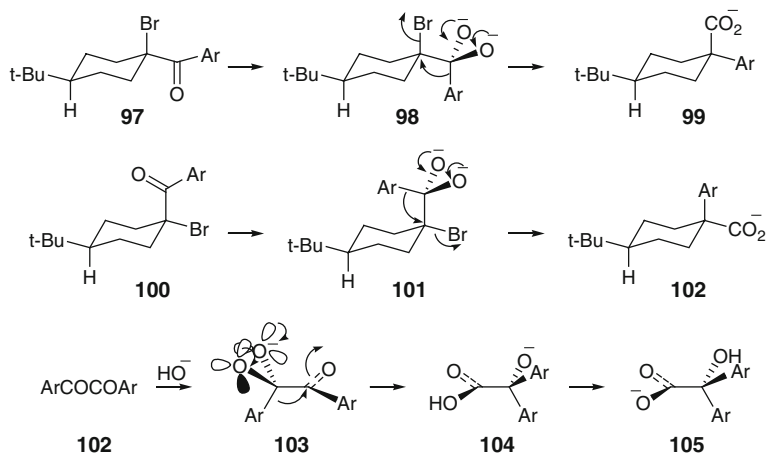
A consequence of the relative orientational differences could also be seen from the changes **93**  $\rightarrow$  **94** and **95**  $\rightarrow$  **96** [15]. These changes are brought about upon treatment with a silver salt,  $\text{AgBF}_4$ , which weakens the  $\sigma_{\text{C-Cl}}$  bond to allow the  $\sigma_{\text{C-C}}$  bond antiperiplanar to it (green color bonds in the bicyclic system) to migrate. Of course, in each substrate, one electron pair orbital on the oxygen atom is antiperiplanar to the migrating bond as well to provide the much necessary push.



We learnt above that an oxygen atom (for that matter, a heteroatom) on one carbon and a leaving group on the adjacent carbon constituted a situation for bond migration from the oxygen-bearing carbon to the carbon bearing a leaving group with the loss of the latter. Throughout, an electron pair orbital on the oxygen was antiperiplanar to the migrating bond and the migrating bond, in turn, was antiperiplanar to the bond connecting the leaving group to the adjacent carbon. Let us consider a situation wherein there are two oxygen atoms on the same carbon and

each oxygen atom has one electron pair orbital antiperiplanar to the migrating bond on the same very carbon. This allows the migration to occur faster, probably twice as fast as the migration in a case with just one oxygen atom. Such situations arise in reactions of  $\alpha$ -halo ketones and aryl-substituted 1,2-dicarbonyl compounds with oxygen-based nucleophiles such as the hydroxide ion.

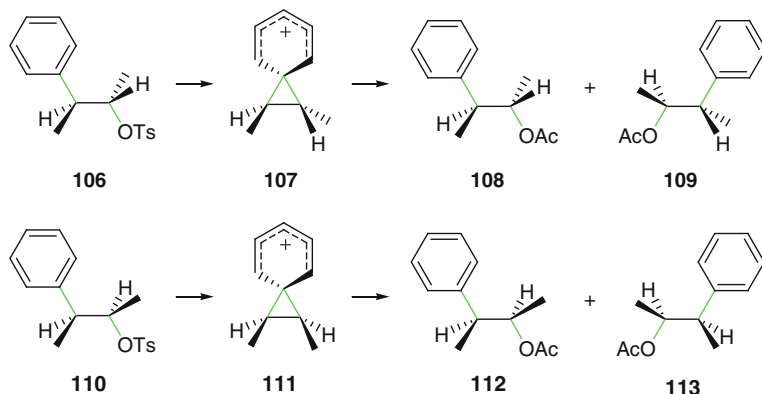
For instance, **97** generates **98** on reaction with sodium hydroxide, wherein each oxygen has one electron pair antiperiplanar to the  $\sigma_{\text{C-Ar}}$  bond and, thus, making it labile for cleavage. Further, the  $\sigma_{\text{C-Ar}}$  bond is antiperiplanar to the  $\sigma_{\text{C-Br}}$  bond on the adjacent carbon. The combined consequence of these two geometrical dispositions is cleavage of the  $\sigma_{\text{C-Ar}}$  bond and attack of the aryl group on the carbon bearing bromine in  $\text{S}_{\text{N}}2$  fashion in quick succession to form **99** as the sole product. The reaction is, therefore, stereoelectronically controlled. The story with the transformation **100**  $\rightarrow$  **102** is similar. The transformation **102**  $\rightarrow$  **105** constitutes what we know as benzil-benzilic acid rearrangement, and it proceeds by following the same stereoelectronic principles as the other rearrangements.



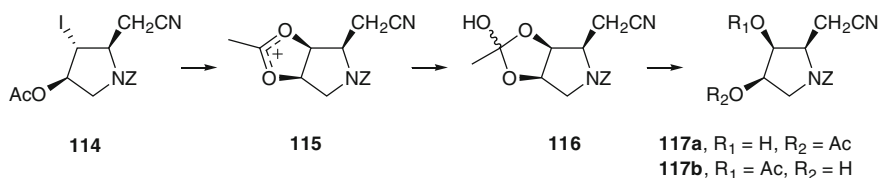
Solvolysis with neighboring group participation in the presence of a nucleophile may be viewed as a reaction on a saturated carbon. There is, however, a difference: the carbon under attack by the external nucleophile in the present instance carries substantial positive charge on account of charge distribution through the neighboring group. We will understand this process by considering the solvolysis of the *erythro*-tosylate **106** in comparison with the solvolysis of the *threo*-tosylate **110** in acetic acid. Neighboring group participation in **106** leads to the chiral phenonium ion **107**, which is captured by acetate ion on either of the two carbon atoms of the three-membered ring, as shown, and a 50:50 mixture of the *erythro*-acetates **108** and **109** is formed. Please note that **108** and **109** are one and the same (try



superimposing one onto the other) and, thus, the resultant product is optically active. A similar analysis of the solvolysis of **110** allows us to arrive at the two *threo* products **112** and **113** through the achiral phenonium ion **111**. Since **112** is mirror image of **113**, the resultant product mixture is optically inactive overall.

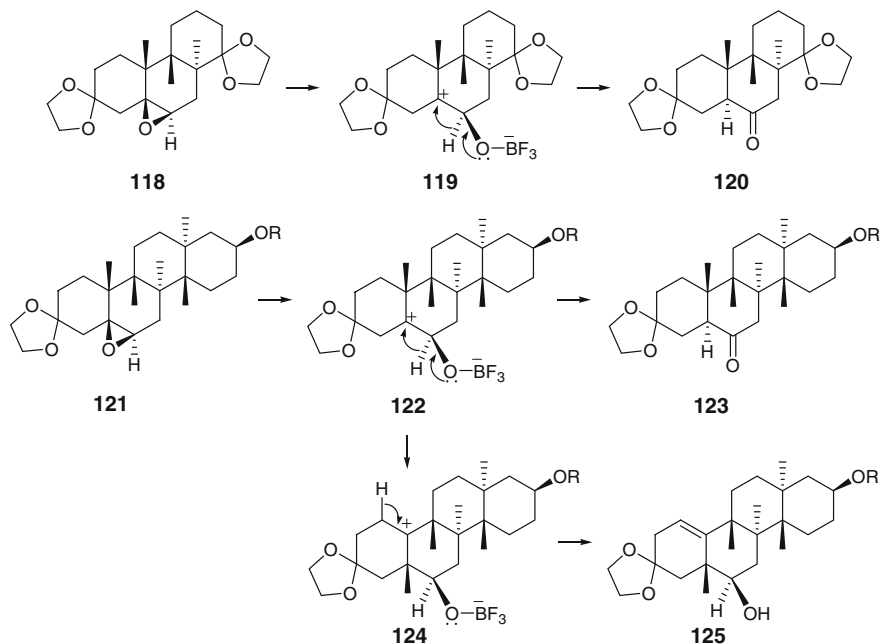


When the iodoacetate **114** was subjected to solvolysis in wet acetic acid containing silver acetate, the products were the *cis*-diol monoacetates **117a** and **117b**. Weakening of the  $\sigma_{C-I}$  bond through association of silver ion with the iodine atom is closely followed by the intramolecular capture of the incipient carbocation by the acetoxy group on the adjacent carbon to generate the acetoxonium ion **115**. This is captured by water to generate **116**, which collapses to a mixture of **117a** and **117b**. The compound **117** was used in the synthesis of (+)-crotanecine, a naturally occurring alkaloid [16].

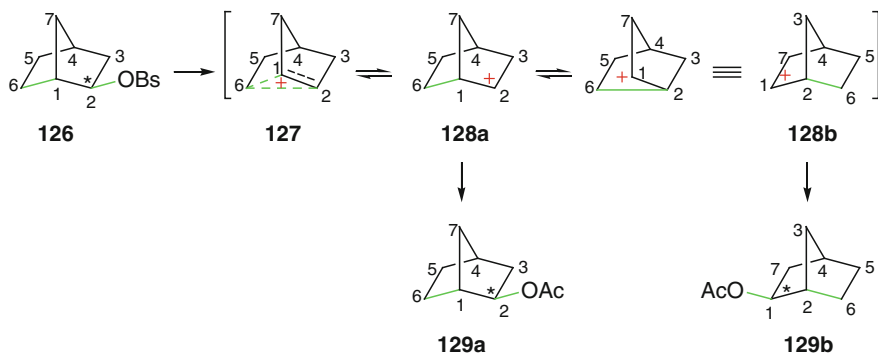


The rearrangement of oxiranes to carbonyl species on treatment with Lewis acids provides yet another elegant example of neighboring group participation that culminates into excellent diastereocontrol. For instance, the oxirane **118** is smoothly transformed into **120** on treatment with  $\text{BF}_3 \cdot \text{OEt}_2$ . The key to the formation of a single product is concurrent heterolysis of the  $\sigma_{C-O}$  bond from the  $\beta$ -face and migration of the hydrogen as a hydride on the  $\alpha$ -face is as shown. Contrast to this is the formation of both **123** and **125** from **121**. In this case, a small time lag between

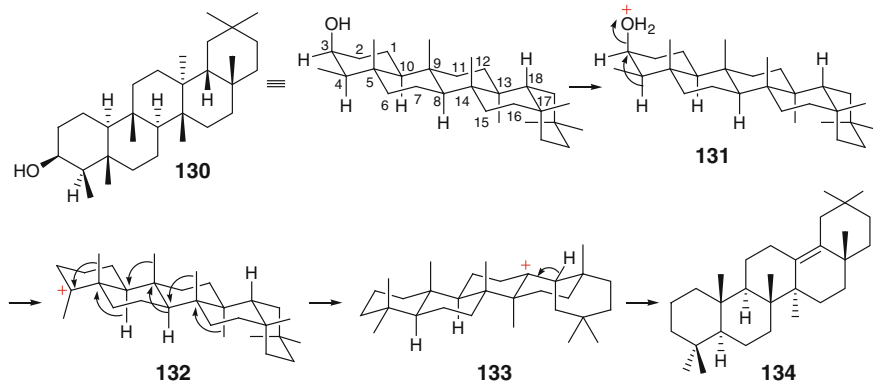
the cleavage of the  $\sigma_{C-O}$  bond and the migration of hydrogen allows transient formation of the discrete carbocation **122**, which allows migration of the angular methyl group, as shown, and the new carbocation **124** is formed. The loss of a proton from **124** leads to the formation of **125**.



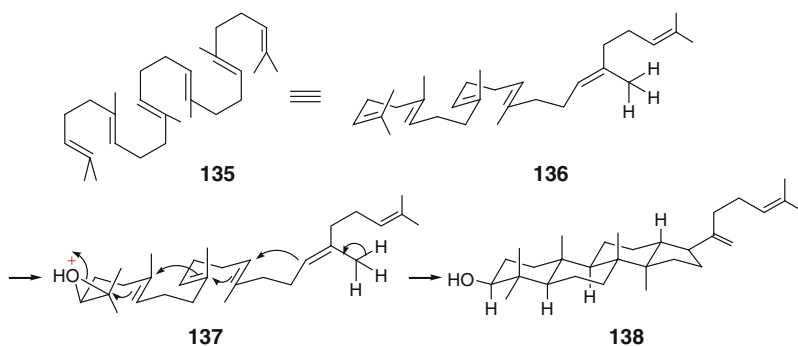
In the *exo*-2-norbornyl brosylate **126**, the  $\sigma_{C-OBs}$  bond is antiperiplanar to  $\sigma_{C1-C6}$  bond. This allows acetolysis to proceed with neighboring group participation, as shown, leading to the formation of a 50:50 mixture of **129a** and **129b** from an optically active brosylate. Since **129a** is mirror image of **129b**, the product is optically inactive overall. The cleavage of  $\sigma_{C-OBs}$  bond under neighboring group participation of  $\sigma_{C1-C6}$  bond allows formation of the nonclassical carbocation [17, 18] **127** which could be viewed as a fast equilibrating 50:50 mixture of the classical carbocations [19] **128a** and **128b**, one being mirror image of the other. The *exo*-capture of **128a** and **128b** forms **129a** and **129b**, respectively.



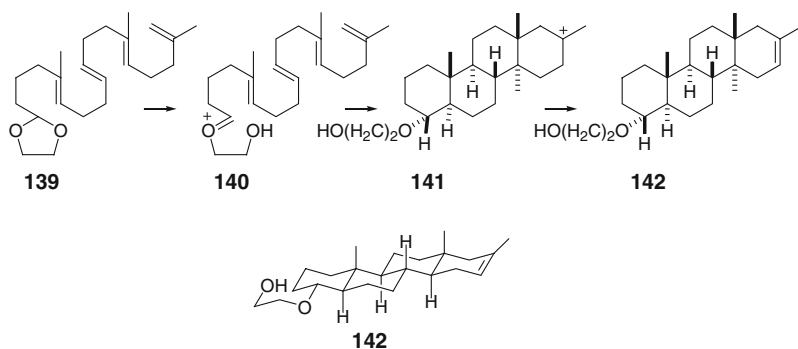
The effect of an antiperiplanar arrangement of an electron-deficient bond and an electron-rich bond is so dramatic that several rearrangements can occur one after the other in quick succession. The acid-catalyzed 3- $\beta$ -friedelanol (**130**)  $\rightarrow$  13(18)-oleanene (**134**) transformation is one such example among many. Protonation of the carbinol oxygen converts it into a strong leaving group. The  $\alpha$ -hydrogen on C4, which is anti to the  $\sigma_{C-O}$  bond, migrates, leading to the tertiary cation **132**. Soon after, many angular group migrations take place to arrive at the angular tertiary cation **133**, whose fate is only to undergo deprotonation, as shown, to form **134**.



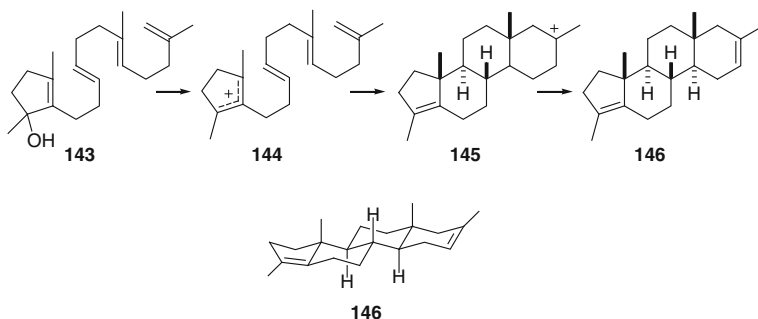
The enzyme-catalyzed polycyclization of squalene **135** produces dammaradienol **138**, which is known to be the precursor of cholesterol. In the process, squalene oxide is the intermediate, which adopts the conformation as shown in **137**, and rearranges, under acid catalysis, to **138** [20, 21]. Note that in the transformations **131**  $\rightarrow$  **133** and **137**  $\rightarrow$  **138**, many  $S_N2$  reactions take place in tandem for the sole reason of stereoelectronically driven well-organized geometrical orientations of the reacting functional groups. Note that all the double bonds are *trans*, and also that two such consecutive bonds are 1,5-related to each other.



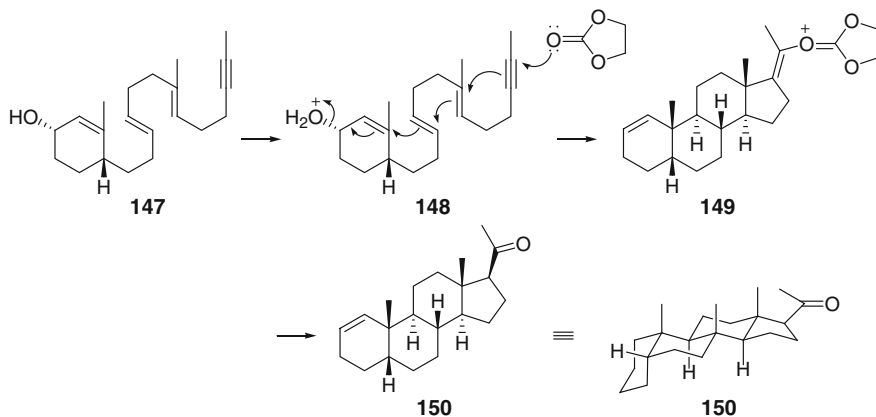
A cationic center may be derived from a variety of other sources such as acetal and alcohol on mixing with an acid. Treatment of the polyolefinic acetal **139** with stannic chloride in pentane gives an almost 50:50 mixture of the two racemic D-homosteroidal tetracyclic isomers **142**. The first formed cationic species **140** is not chiral and, hence, the two faces of the nearest olefinic bond can react with it at equal ease. The conversion of the open chain **139** having no chiral centers into the tetracyclic species **142** having seven such centers and yet producing only two out of the total possible 64 racemates (i.e., four out of  $2^7 = 128$  diastereomers) is a striking tribute to the power of stereoelectronic effects [22].



The allylic alcohol **143** furnishes the tetracyclic product **146** on treatment with stannic chloride in nitroethane at  $-80\text{ }^\circ\text{C}$ . The first formed allylic cation **144** undergoes tandem cyclization with the remaining olefinic bonds to form the tertiary cation **145**, which loses a proton to generate **146** [23].

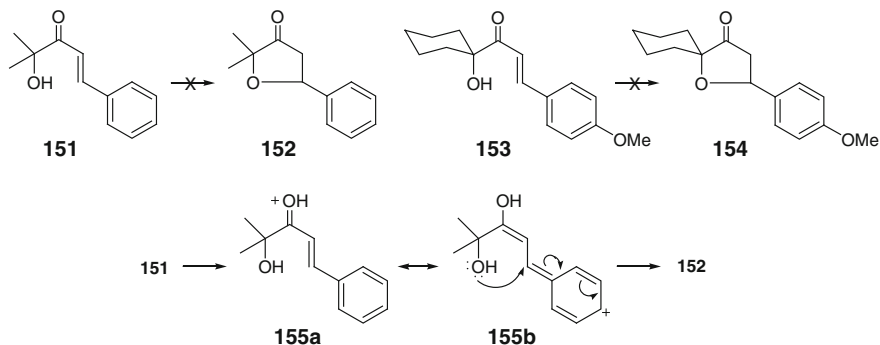


In a more impressive polyene cyclization, reaction of the optically active allylic alcohol **147** with trifluoroacetic acid and ethylene carbonate followed by workup with  $K_2CO_3$  in aqueous methanol furnished the optically active product **150**. The reaction is initiated by a *syn*-selective  $S_N2$  reaction with allylic rearrangement ( $S_N2'$ ) and proceeds through the carbonate-trapped intermediate **149**. Likewise, the reaction of the enantiomer of **147** furnished the enantiomer of **150**. The cyclization step was essentially enantiospecific. The process involves total asymmetric synthesis due to a single chiral center in the starting allyl alcohol [24].

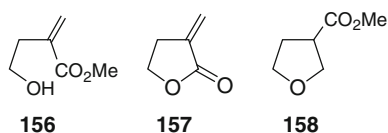


We have learnt that (a) the dihedral angle requirement for  $S_N2$  reactions is  $180^\circ$  or close to it, (b) the *5-exo-trig* reaction is favored over the *5-endo-trig* reaction, and (c) axial electrophilic or nucleophilic attack on a double bond present in cyclohexene is favored over the corresponding equatorial attack. Keeping these principles in mind, we can proceed to analyze a few reactions that involve attack on a  $sp^2$  center. Substrates such as **151** and **153** fail to react under basic conditions to form the furanones **152** and **154**, respectively. Obviously, the oxy anion formed from the alcohol does not react with the enone in *5-endo-trig* manner, a pathway that one

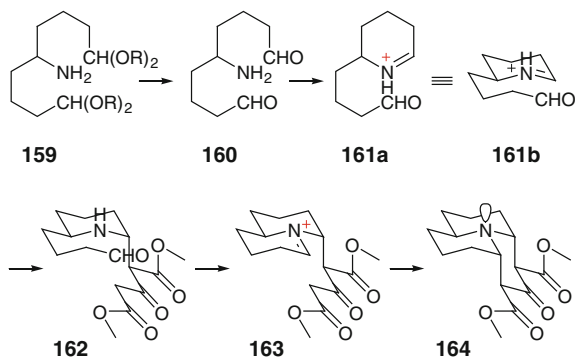
finds formally very appealing. Remember that oxy anions add rapidly to enones in bimolecular processes under otherwise similar reaction conditions. In contrast, **152** and **154** are formed readily under acidic conditions, and we must understand the compelling reason for the same. Under the acidic conditions of the reaction, protonation of the carbonyl oxygen in **151** leads to a resonance mixture of **155a** and **155b**. It is this **155b** that allows now the 5-*exo*-trig closure, as shown, and the product **152** is formed with a great facility [25, 26].



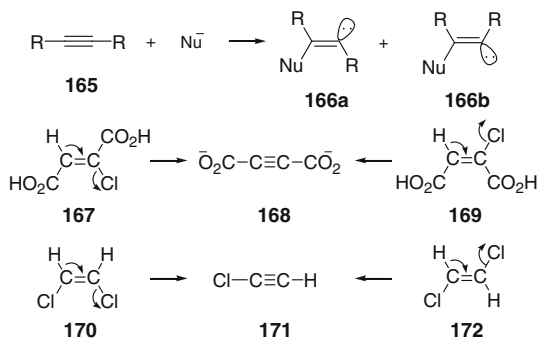
In further revelation of the strong stereoelectronic requirement for the intramolecular  $S_N2$  reaction, the hydroxy ester **156** furnished the lactone **157** only and none of the tetrahydrofuran product **158** on reaction with a base. Whereas the product **157** arises from the 5-*exo*-trig process involving attack of the oxy anion on the ester carbonyl function, the difficult 5-*endo*-trig process involving attack of the oxy ion at the olefinic carbon in conjugate fashion is required for the formation of **158** [25, 26].



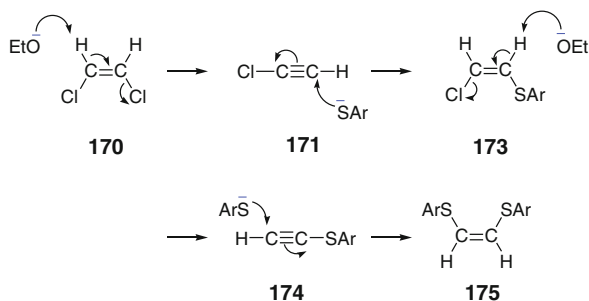
When the species **159** and dimethyl 3-oxo-pentan-1,5-dicarboxylic acid (dimethyl acetone dicarboxylate) are taken together in aqueous acid, **164** is formed as the sole product. Hydrolysis leads to the dialdehyde **160**, which undergoes intramolecular condensation to generate the iminium ion **161a**, rewritten as **161b** in the three-dimensional form. The enol from the dicarboxylate acts as a nucleophile and reacts with the above iminium ion on the axial face to generate **162**, releasing the secondary amine function simultaneously. Intramolecular condensation of this secondary amine with the other aldehyde function forms the iminium ion **163**, which is captured by the other enol form of the dicarboxylate, again on the axial face, and **164** is formed [27].



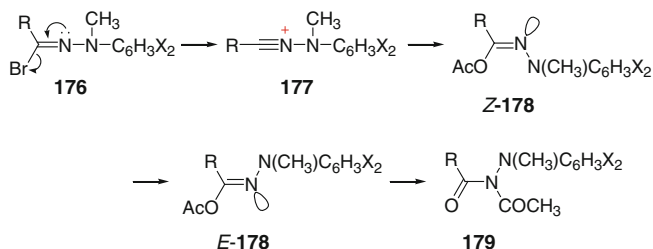
Addition of a nucleophile to a triple bond as in **165** may, in principle, lead to two different products **166a** and **166b**. The added nucleophile is anti to the released electron pair orbital in **166a** and *syn* in **166b**. The stereoelectronic effects favor the formation of **166a**. That being the case, the process **166a**  $\rightarrow$  **165** must also be faster than the process **166b**  $\rightarrow$  **165**; both of these processes are E1cB reactions. Following this, the transformation **167**  $\rightarrow$  **168** under basic conditions was indeed discovered to be 50 times faster than the corresponding transformation **169**  $\rightarrow$  **168** [28, 29]. Also, *cis*-dichloroethylene **170** is transformed into chloroacetylene **171** about 20 times faster than *trans*-dichloroethylene **172** [30].



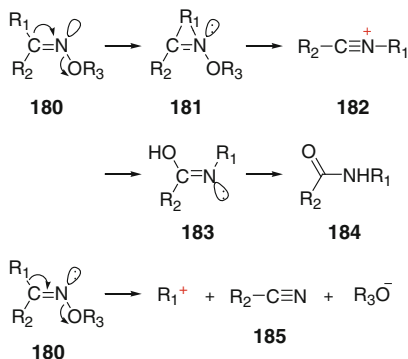
The *cis*-dichloroethylene **170** reacts with sodium *p*-toluenethiolate ( $p\text{-CH}_3\text{C}_6\text{H}_4\text{SNa}$ ) in the presence of sodium ethoxide to give *cis*-1,2-*bis-p*-tolylmercaptoethylene **175**. This is in contrast to the behavior of *trans*-dichloroethylene which is recovered unchanged. The transformation **170**  $\rightarrow$  **175** proceeds as shown, and there is evidence in favor of **171**, **173**, and **174** as the intermediates during the course of the reaction [31–33]. *Trans*-elimination is therefore favored over *cis*-elimination, indicating a decisive role of the stereoelectronic effects in such reactions.



Addition of a nucleophile to a nitrilium ion generates a product in which the released electron pair occupies the position on the nitrogen that is *anti* to the nucleophile. For instance, the *N*-anilnonitrilium ion **177**, formed from solvolysis of the hydrazonyl bromide **176** in the presence of sodium acetate, gives *Z*-**178**. On heating, *Z*-**178** is rapidly transformed into the amide **179** via isomerization to *E*-**178** [34, 35]. Note that the acyl group migration from oxygen to nitrogen takes place in the last step of the whole process.

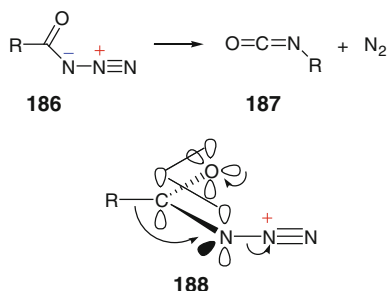


In the widely used Beckman rearrangement [36] that converts oximes and derivatives into amides, the group that migrates is the one that is *anti* to the  $\sigma_{\text{N-O}}$  bond. Also, the stereochemical integrity of the migrating group is completely retained in the product. Thus, the migration of  $\text{R}_1$  in **180** generates the nitrilium ion **182**, which hydrolyses, via **183**, to form the amide **184**. When the migrating group can form a stable cation, fragmentation to the corresponding nitrile such as **180**  $\rightarrow$  **185** takes place instead of the above migration.





In the Curtius rearrangement in which the acylazide **186** is transformed into the isocyanate **187** and molecular nitrogen, the migrating group retains its stereochemical integrity just as in the Beckman rearrangement. Stereoelectronic effects therefore control the reaction because the migrating group is necessarily anti to the  $\sigma_{\text{N}-\text{N}_2^+}$  bond and, also, the migrating group is anti to an electron pair orbital on the carbonyl oxygen as illustrated in **188**.



Thus, both the *trans*-addition and *trans*-elimination are strongly favored over the corresponding *cis*-variants due to stereoelectronic effects. In 1,2-migrations, the migrating group is always anti to the leaving group on the adjacent carbon.

## References

1. Tenud L, Farooq S, Seibl J, Eschenmoser A (1970) *Helv Chim Acta* 53:2059
2. Stork G, Cama LD, Coulson DR (1974) *J Am Chem Soc* 96:5268
3. Stork G, Cohen JF (1974) *J Am Chem Soc* 96:5270
4. Baldwin JE (1976) *J Chem Soc Chem Commun* 738
5. Stork G, White WN (1956) *J Am Chem Soc* 78:4609
6. Stork G, Kreft III AF (1977) *J Am Chem Soc* 99:3850, 8373
7. Kirmse W, Scheidt F, Vater H-J (1978) *J Am Chem Soc* 100:3945
8. Singh RK, Danishefsky S (1975) *J Am Chem Soc* 97:3239
9. Clark RD, Heathcock CH (1975) *Tetrahedron Lett* 16:529
10. Isobe M, Iio H, Kawai T, Goto T (1940) *J Am Chem Soc* 1978:100
11. Danishefsky S, Dynak J, Yamamoto M (1973) *J Chem Soc Chem Commun* 81
12. Danishefsky S, Tsai MY, Dynak J (1975) *J Chem Soc Chem Commun* 7
13. Bates RB, Buchi G, Matsuura T, Shaffer RR (1960) *J Am Chem Soc* 82:2327
14. Nussim M, Mazur Y (1968) *Tetrahedron* 24:5337
15. Yamada Y, Kimura M, Nagaoka H, Ohnishi K (1977) *Tetrahedron Lett* 2379
16. Yadav VK, Rueger H, Benn M (1984) *Heterocycles* 22:2735
17. Winstein S, Trifan DS (1949) *J Am Chem Soc* 71:2953
18. Winstein S, Trifan DS (1952) *J Am Chem Soc* 74:1147, 1154
19. Brown HC (1973) *Acc Chem Res* 6:377
20. van Tamelan EE, Willett JD, Clayton RB, Lord KE (1966) *J Am Chem Soc* 88:4752
21. Corey EJ, Russey WE, de Montellano PRO (1966) *J Am Chem Soc* 88:4750
22. Johnson WS, Wiedhaup K, Brady SF, Olson GL (1968) *J Am Chem Soc* 90:5277
23. Johnson WS, Semmelhack MF, Sultanbawa MUS, Dolak LA (1968) *J Am Chem Soc* 90:2994
24. Johnson WS, McCarry BE, Markezich RL, Boots SG (1980) *J Am Chem Soc* 102:352

25. Baldwin JE, Cutting J, Dupont W, Kruse L, Silberman L, Thomas RC (1976) *J Chem Soc Chem Commun* 736
26. Baldwin JE, Kruse LI (1977) *J Chem Soc Chem Commun* 233
27. Stevens RV, Lee AWM (1979) *J Am Chem Soc* 101:7032
28. Michael A (1895) *J Prakt Chem* 52:308
29. Price CC, Karabinos JV (1940) *J Am Chem Soc* 62:1159
30. Chavanne G (1912) *Bull Soc Chim Belg* 26:287
31. Truce WE, Mcmanimie RJ (1954) *J Am Chem Soc* 76:5745
32. Truce WE, Boudakian MM, Heine RF, McManimie RJ (1956) *J Am Chem Soc* 78:2743
33. Truce WE, Sims JA (1956) *J Am Chem Soc* 78:2756
34. Hegarty AF, McCormack MT (1976) *J Chem Soc Perkin Trans 2* 2:1701
35. Hegarty AF (1980) *Acc Chem Res* 13:448
36. Donaruma IG, Heldt WZ (1960) *Org React* 11:1

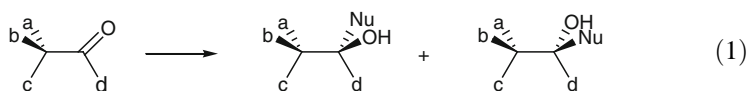
## Chapter 3

# Diastereoselectivity in Organic Reactions

**Abstract** This chapter deals with the facial selectivity of nucleophilic additions to carbonyl compounds. This is explained using models such as the Cram's model, Anh–Felkin modification of Cram's model, Houk's transition structure model, Houk's electrostatic model, Cieplak's  $\sigma \rightarrow \sigma^*\#$  model, and cation coordination model. The intricacies, variations, and predicted selectivities of these models are elaborated with examples. It has been argued that the Cieplak's  $\sigma \rightarrow \sigma^*\#$  model is applicable to only those reactions that proceed through product-like transition structures. Using the cation coordination model, the facial selectivities of a number of substrates, including the better *anti*-selectivity of *endo,endo*-2,3-diethyl-7-norbornanone in comparison to that of *endo,endo*-2,3-dimethyl-7-norbornanone, have been convincingly explained.

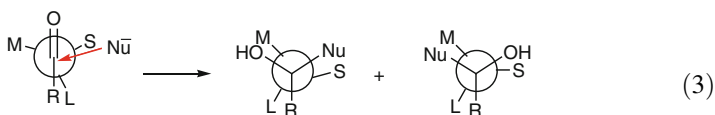
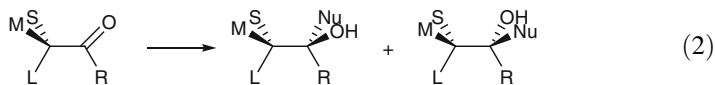
**Keywords** Cram's model • Anh–Felkin modification • Houk's transition structure model • Houk's electrostatic model • Cieplak's  $\sigma \rightarrow \sigma^*\#$  model • Cation coordination model ( $\sigma \rightarrow \pi^*$  model) • Carbonyl pyramidalization •  $\sigma \rightarrow \pi^*$  interaction • Reactant-like and product-like transition structures

The addition of a nucleophile to a carbonyl compound with a chiral  $\alpha$  carbon generates a mixture of two diastereoisomers. The ratio of these diastereoisomers depends on the relative bulks of the (non-coordinating) substituents on the chiral center, the effective bulkiness of the nucleophile as well and the reaction conditions. By effective bulkiness, we mean the bulk of the solvated nucleophile, if the same is imminent. The reaction is schematically represented in Eq. 1.



## 1 Cram's Model for Asymmetric Synthesis

From a close scrutiny of the results of several such reactions, Cram proposed a model to explain the predominant diastereoselectivity [1]. The model relies on the relative bulks of the three substituents on the  $\alpha$  carbon, and envisages approach of the nucleophile to the carbonyl group *syn* to the small substituent. The carbonyl species was considered to adopt a conformation wherein the carbonyl group was flanked by the small- and medium-sized groups as shown in Eq. 2. The attack *syn* to the medium-sized group generates the minor diastereoisomer. Understandably, the difference between the relative bulks of the small and medium size groups is the sole determinant of the observed diastereoselectivity. This model was so successful at reliably predicting the major diastereoisomer from a host of reactions that it came to be known as *Cram's model for asymmetric synthesis*. The reaction expressed by Eq. 2 could also be expressed by Eq. 3 using Newman projections for both the reactant and the product.



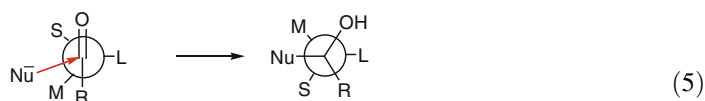
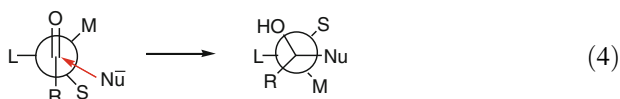
S = small group, M = medium group, L = large group

The difficulty with Cram's model, however, was threefold: (a) the product was formed in the eclipsed conformation which is higher in energy than the product in the staggered conformation, (b) the alkyl group R interacts sterically with the large substituent L in the suggested reacting conformer, and (c) the angle of nucleophilic attack at the carbonyl carbon ( $\text{Nu}\dots\text{C}\dots\text{O}$ ) is less than  $90^\circ$ , which supposedly leads to a substantial raise in the energy of the TS due to the electrostatic repulsion between the similarly charged nucleophile and the carbonyl oxygen (both carry net negative charges). It was later that the quantum mechanical calculations suggested that the angle of nucleophilic attack at the carbonyl carbon must be close to the tetrahedral angle.

## 2 Anh–Felkin Modification of Cram's Model for Asymmetric Synthesis

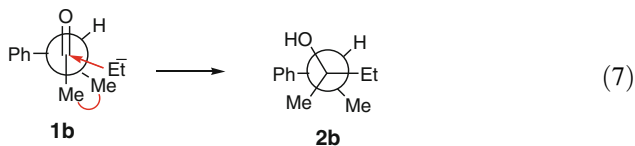
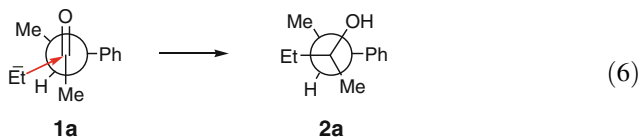
Even if one ignores the difficulty related to the angle of attack, the first two factors which destabilize the TS were serious liabilities of the Cram's model and needed to be addressed. Anh and Felkin considered a different reactant conformer in which

the large substituent was disposed orthogonally to the carbonyl group and the nucleophile was allowed to approach along a trajectory that is opposite to it, and yet somewhat closer to the small substituent to render a tetrahedral attack as shown in Eq. 4 [2, 3]. Such a geometrical arrangement avoids steric interactions between the nucleophile and the large group by keeping them opposite to each other, allows the product to be formed directly in the staggered conformation, and, of course, ensures the angle of attack being tetrahedral as required by the quantum mechanical calculations. This approach came to be known as the *Anh–Felkin modification of Cram’s model for asymmetric synthesis*. The minor diastereoisomer is therefore derived from the alternate conformer shown in Eq. 5. However, this conformer is of higher energy than the conformer shown in Eq. 4 for the geometrical vicinity of R and M.



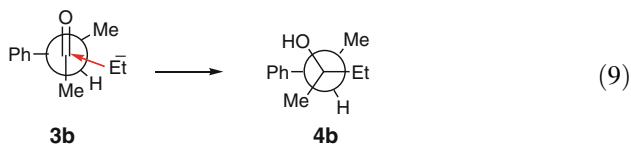
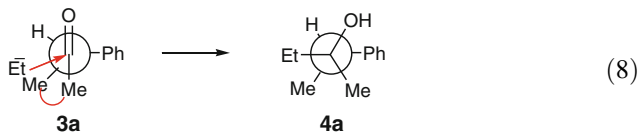
S = small group, M = medium group, L = large group

Let us consider the reaction of (*S*)-3-phenyl-2-butanone, **1**. The two conformers of the reactant are **1a** (Eq. 6) and **1b** (Eq. 7), following the Anh–Felkin modification of Cram’s model. The conformer **1a** will predominate over **1b** because the latter suffers from steric interactions between the two methyl groups that are gauche to each other. The conformers **1a** and **1b** will generate the products (*S,S*)-**2a** and (*R,S*)-**2b**, respectively, on reaction with ethyl magnesium iodide. Since **1a** is the predominant conformer, (*S,S*)-**2a** is formed as the major product, and (*R,S*)-**2b** constitutes the minor product.

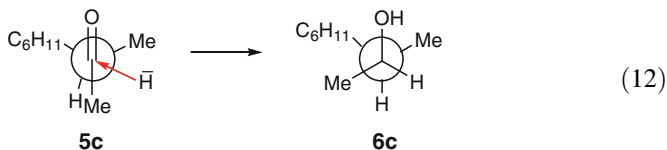
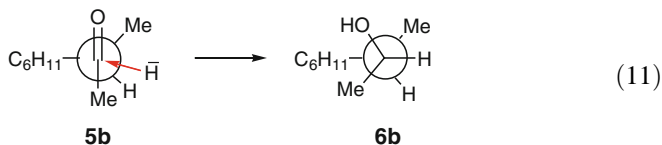
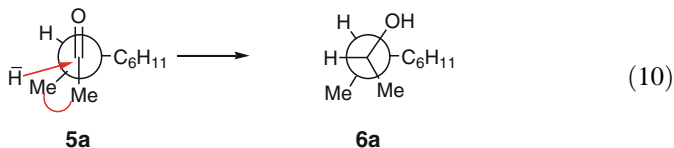


For (*R*)-3-phenyl-2-butanone, **3**, the two reacting Anh–Felkin conformers are **3a** and **3b**. These conformers are expected to generate predominantly the products (*S*,

*R*)-**4a** and (*R,R*)-**4b** as shown in Eqs. 8 and 9, respectively, on reaction with EtMgI. Since the conformer **3b** is more stable than **3a** on account of methyl–methyl interaction in the latter, the product (*R,R*)-**4b** predominates. Note that the products (*S,S*)-**2a** and (*R,R*)-**4b** and (*R,S*)-**2b** and (*S,R*)-**4a** are enantiomers of each other.



Let us extend the above analysis to (*R*)-3-cyclohexyl-2-butanone, **5**. The two reacting Ahn–Felkin conformers emerge to be **5a** (Eq. 10) and **5b** (Eq. 11), with the latter predominating. The predominant product expected from each of these on reaction with a hydride reagent is (*R,R*)-**6a** and (*S,R*)-**6b**, respectively. Because the conformer **5b** is more stable than the conformer **5a** on account of methyl–methyl gauche interaction in the latter, the product (*S,R*)-**6b** must predominate over (*R,R*)-**6a**. Indeed, (*S,R*)-**6b** and (*R,R*)-**6a** are formed in 72:28 ratio on reduction using LiAlH<sub>4</sub> [1].



Although the predominant product from the reaction of **5** with LiAlH<sub>4</sub> is well explained by the Ahn–Felkin modification of Cram’s model, the question that arises is what truly guarantees the conformation **5b**? An ab initio calculation of (*R*)-**5** at HF/6-31G\* level of theory predicts the conformer **5c** (Eq. 12) to be the lowest on the potential energy surface. In this conformer, the  $\sigma_{C-H}$  bond on the asymmetric

carbon is nearly eclipsing with the  $\sigma_{\text{C-Me}}$  bond on the carbonyl carbon (torsion angle =  $16^\circ$ ). This is not the conformer which Cram had considered to be the reacting conformer either. Therefore, it turns out that both Cram, and Anh and Felkin considered different but less stable conformers as the reacting conformers to explain the predominant product. Arguably, the conformers are in dynamic equilibrium with one another, and it is likely that the less stable conformer **5b** reacts faster than the more stable conformer **5c**.

Additionally, one may be tempted to allow **5c** to react with nucleophiles along the trajectory shown by the arrow. This trajectory is not only *anti* to the largest substituent, cyclohexyl, on the asymmetric carbon but it also fulfills the requirement of near tetrahedral angle for such an attack. Additionally, the product is formed directly in the staggered conformation as one allows for a gradual rotation (clockwise in the present instance) during the event that the carbonyl carbon changes its hybridization from  $sp^2$  to  $sp^3$ . The product **6c** is the same product as **6b**.

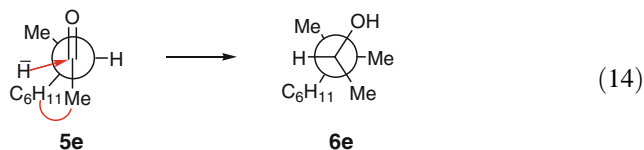
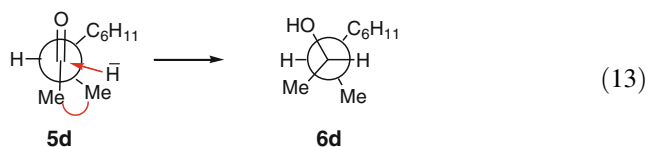
In the indicated approach of the nucleophile to conformer **5c**, the nucleophile is *gauche* to the methyl group on the adjacent  $sp^3$  carbon to raise the energy of the TS. Such an energy contribution will be higher in the alternate TS wherein the nucleophile is allowed to enter from the other side of the carbonyl group due to the large bulk of the cyclohexyl group in comparison to that of methyl. Thus, the reaction represented by Eq 12 may very well be the minimum energy reaction pathway.

One may also wish to invoke the competitive  $\sigma \rightarrow \pi^*_{\text{C=O}}$ <sup>1</sup> interactions arising from the substituents on the  $\alpha$  carbons to support a particular conformation of the reactant and, thus, control the selectivity of nucleophilic addition. Since it is an established fact that a  $\sigma_{\text{C-H}}$  bond is more electron-donating than a  $\sigma_{\text{C-C}}$  bond [4–6], the two possible scenarios are **5d** (Eq. 13) and **5e** (Eq. 14), wherein  $\sigma_{\text{C-H}}$  and  $p_{\text{C=O}}$  are parallel to each other to allow for  $\sigma_{\text{C-H}} \rightarrow \pi^*_{\text{C=O}}$  interaction. The nucleophile enters from the opposite side, as shown by the arrows [7, 8].

This model favors approach of a nucleophile to an electrophilic center from the direction opposite to the most electron-donating substituent at the adjacent carbon. However, from the discussion above, both **5d** and **5e** are high energy conformers. While both the methyl groups are *gauche* to each other in **5d**, methyl on the carbonyl carbon is *gauche* to the cyclohexyl group in **5e**. For the differential bulks of methyl and cyclohexyl groups, the conformer **5d** will be expected to be somewhat lower in energy than the conformer **5e**. Interestingly, both the conformers **5d** and **5e** fall to **5c** on attempted geometry optimization. Thus, **5c** is the most stable conformer with the torsion angle of  $99.2^\circ$  between the two methyl groups.

---

<sup>1</sup> $\sigma \rightarrow \pi^*_{\text{C=O}}$  interaction causes pyramidalisation at the carbonyl carbon in such a way that the larger coefficient of the electron-deficient orbital on the carbonyl carbon is on the side opposite to the more electron-donating  $\sigma$  bond on the  $\alpha$  carbon to attract a nucleophile during the course of the reaction. More application of this concept will be found later in this chapter.



Indeed, a TS resembling **5d** will generate the product **6d** with correct (*S,R*)-stereochemistry. The TS resembling **5e** will generate a product of (*R,R*)-stereochemistry. Though it is heartening to arrive at the correct product stereochemistry, due diligence must be exercised in recognizing the prevailing steric interactions in the TS. In maintaining the tetrahedral angle of attack, the nucleophile must approach the carbonyl carbon from the direction which is in between the methyl and cyclohexyl groups, but closer to the methyl group, on the  $sp^3$  carbon. However, such a TS has not been calculated to warrant further comments. We will learn, later in this chapter, more about  $\sigma \rightarrow \pi^*_{C=O}$  control on diastereoselection.

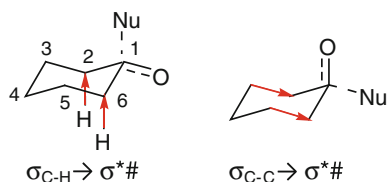
### 3 Cieplak's Model for Diastereoselectivity

To explain the stereochemical outcome in nucleophilic additions to substituted cyclohexanones, Cieplak advocated for  $\sigma \rightarrow \sigma^*_{\#}$  interaction ( $\sigma_{\#}$  is the incipient bond that is being formed between the nucleophile and the carbonyl carbon in the TS and  $\sigma^*_{\#}$  is the corresponding antibonding orbital) as a TS-stabilizing factor, and suggested the approach of a nucleophile from the direction which is anti to the more electron-donating  $\sigma$  bond on the  $\alpha$ -carbon. For instance, a nucleophile will approach largely on the axial face to result predominantly in the equatorial alcohol, as observed indeed from the experiments, due to the fact that the axial  $\sigma_{C-H}$  bonds on C<sub>2</sub> and C<sub>6</sub> of cyclohexanone are better electron-donating than  $\sigma_{C_2-C_3}$  and  $\sigma_{C_5-C_6}$  ring bonds. The  $\sigma \rightarrow \sigma^*_{\#}$  concept became so popular that it invited many researchers to explore new substrates in efforts to judge its validity. Cieplak's approach to discern the axial versus equatorial selectivity of cyclohexanone is summarized in Fig. 1.

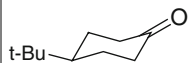
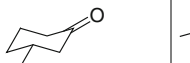

The reduction of 4-*tert*-butylcyclohexanone by LiAlH<sub>4</sub> in THF at 0 °C affords a mixture of the *trans*- and *cis*-alcohols in 88.5:11.5 ratio (Table 1) [9]. The predominant attack takes place obviously from the axial direction as predicted above by the Cieplak model. This selectivity is expected to diminish when the ring carries an equatorial methyl group on C<sub>3</sub> because it will (a) not introduce an element of steric interaction during the course of the nucleophilic addition, and (b) raise



**Fig. 1** Cieplak's  $\sigma \rightarrow \sigma^*$  model to explain axial versus equatorial selectivity of cyclohexanones



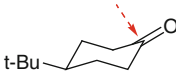
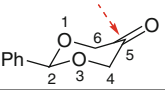
**Table 1** Relative yields of equatorial approach of the nucleophile in nucleophilic additions to 4-*tert*-butyl-, 3-methyl- and 3,5-dimethylcyclohexanones [reproduced from reference 7]

Nucleophile and reaction condition (°C)			
LiAlH <sub>4</sub> , THF, 0	11.5 [9]	15.4 [9]	17.0 [9]
MeLi, Et <sub>2</sub> O, 0	65 [9]	66 [9]	
EtMgBr, Et <sub>2</sub> O, 0	69 [10]	72 [11]	

somewhat the donor ability of  $\sigma_{C2-C3}$  to support equatorial attack. In other words, the difference of the sum of interactions  $\sigma_{C2-H} \rightarrow \sigma^*_{\#}$  and  $\sigma_{C6-H} \rightarrow \sigma^*_{\#}$  (supporting axial attack) and  $\sigma_{C2-C3} \rightarrow \sigma^*_{\#}$  and  $\sigma_{C5-C6} \rightarrow \sigma^*_{\#}$  (supporting equatorial attack) is somewhat reduced, leading to somewhat increased equatorial attack. Indeed, within a small approximation, 3-methylcyclohexanone exhibits 15.4 % preference for equatorial attack as compared to 11.5 % for 4-*tert*-butylcyclohexanone under the otherwise identical reaction conditions [9]. From an extrapolation of this argument, *cis*-3,5-dimethylcyclohexanone is expected to exhibit better preference for equatorial attack in comparison to 3-methylcyclohexanone. Indeed, the observed equatorial preference of *cis*-3,5-dimethylcyclohexanone is more than that of 3-methylcyclohexanone by 1.6 % [9].

Since a nucleophile must approach the carbonyl group at a tetrahedral angle, the axial substituents on C<sub>3</sub> and C<sub>5</sub> offer resistance to the reaction on the axial face. Two scenarios emerge: (a) an increase in the size of the nucleophile may lead to enhanced equatorial attack for a given set of axial substituents, including hydrogen atoms, on C<sub>3</sub> and C<sub>5</sub>, and (b) an axial substituent larger than hydrogen may cause enough steric resistance to the axial approach of even a relatively small nucleophile to allow the equatorial attack to be favored. In support of the scenario (a), reaction of 4-*tert*-butylcyclohexanone with MeLi in Et<sub>2</sub>O at 0 °C generates a 65:35 mixture of *cis*-4-*tert*-butyl-1-methylcyclohexanol (the product of equatorial attack) and *trans*-4-*tert*-butyl-1-methylcyclohexanol (the product of axial attack). Compare this with the 11.5:88.5 composition of the *cis*- and *trans*-4-*tert*-butylcyclohexanols obtained on reaction with LiAlH<sub>4</sub> in THF at 0 °C [9]. Likewise, the reaction of 4-*tert*-butylcyclohexanone with C<sub>2</sub>H<sub>5</sub>MgBr in Et<sub>2</sub>O at 0 °C generates a 69:31 mixture of *cis*- and *trans*-4-*tert*-butyl-1-ethylcyclohexanols [10]. The dimeric and/or multimeric nature of the alkyllithiums and also the Grignard reagents increase their bulk enough to turn the attack on equatorial face significant.

**Table 2** The yields of axial approach of Grignard reagents to 4-*tert*-butylcyclohexanone and 2-phenyl-1,3-dioxan-5-one [reproduced from reference 7]

Grignard reagent		
CH <sub>3</sub> MgI	45	98
CH <sub>3</sub> CH <sub>2</sub> MgI	31	98
(CH <sub>3</sub> ) <sub>2</sub> CHMgI	18	96
(CH <sub>3</sub> ) <sub>3</sub> CMgCl	0	No addition

The effect of a gradual increase in the bulk of a given type of nucleophile on the facial selectivity of a given cyclohexanone could also be gleaned from a measurement of the relative axial approach. The axial selectivity decreases in the order 45 % → 31 % → 18 % → 0 % on changing the nucleophilic reagent from CH<sub>3</sub>MgI → CH<sub>3</sub>CH<sub>2</sub>MgI → (CH<sub>3</sub>)<sub>2</sub>CHMgI → (CH<sub>3</sub>)<sub>3</sub>CMgCl in the reaction with 4-*tert*-butylcyclohexanone as shown in Table 2. The steric effect arising from (CH<sub>3</sub>)<sub>3</sub>CMgCl is so significant that absolutely no reaction occurs on the axial face and, hence, the *cis*-alcohol is isolated as the sole product.

Let us now consider 2-phenyl-1,3-dioxan-5-one and compare its selectivity profile with that of 4-*tert*-butylcyclohexanone in reactions with Grignard reagents, see Table 2. In 2-phenyl-1,3-dioxan-5-one,  $\sigma_{C4-O3} \rightarrow \pi^*_{C=O}$  and  $\sigma_{C6-O1} \rightarrow \pi^*_{C=O}$  interactions destabilize the eq-TS because the participating  $\sigma$  bonds are electron-deficient due to the significantly electronegative character of oxygen [12]. The  $\sigma_{C4-Hax} \rightarrow \pi^*_{C=O}$  and  $\sigma_{C6-Hax} \rightarrow \pi^*_{C=O}$  interactions stabilize the ax-TS and the corresponding product is formed almost exclusively. These results are included in Table 2. In the reaction with *tert*-butylmagnesium chloride, the axial addition is denied completely because of the steric interactions between the phenyl group on C2 and the large *tert*-butylmagnesium chloride.

On replacing the ring oxygen in 6-phenyl-1-oxan-3-one by sulfur, the selectivity profile is expected to change in favor of equatorial attack because  $\sigma_{S-C}$  is strongly electron-donating. The direction of electron donation is from sulfur to carbon. Likewise, by replacing both the ring oxygen atoms in 2-phenyl-1,3-dioxan-5-one by sulfur, the equatorial approach of the nucleophile is expected to constitute the major pathway. In relative quantitative terms,  $(\sigma_{S-C2} \rightarrow \sigma^*_{\#} + \sigma_{C4-C5} \rightarrow \sigma^*_{\#}) > (\sigma_{C2-Hax} \rightarrow \sigma^*_{\#} + \sigma_{C4-Hax} \rightarrow \sigma^*_{\#})$  in 6-phenyl-1-thian-3-one and  $(\sigma_{S-C4} \rightarrow \sigma^*_{\#} + \sigma_{S-C6} \rightarrow \sigma^*_{\#}) \gg (\sigma_{C4-Hax} \rightarrow \sigma^*_{\#} + (\sigma_{C6-Hax} \rightarrow \sigma^*_{\#}))$  in 2-phenyl-1,3-dithian-5-one. These predictions are in good qualitative and quantitative agreement with the experimental results collected in Fig. 2 [13, 14].

The electron-donating power of  $\sigma_{C2-C3}$  and  $\sigma_{C5-C6}$  bonds in cyclohexanone could also be modified by incorporating equatorial electron-withdrawing substituents at C3 and C5 positions. The consequent decrease in  $\sigma_{C2-C3} \rightarrow \sigma^*_{\#}$  and  $\sigma_{C5-C6} \rightarrow \sigma^*_{\#}$  interactions imply more axial attack of the nucleophile than the equatorial attack. This explains the opposite effects of the methyl and cyano

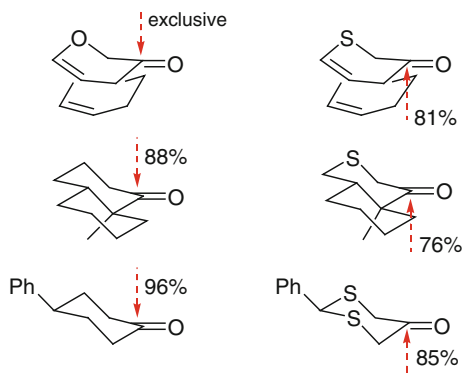


**Fig. 2** The axial versus equatorial approach of nucleophile in reductions with a metal hydride

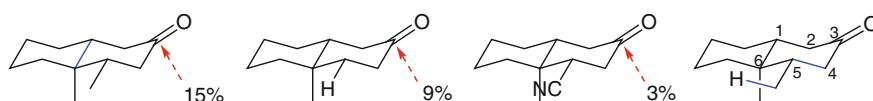


**Fig. 3** The relative equatorial approach of a nucleophile in the reductions of 3-decalones bearing different C5-substituents

substituents on the stereochemistry of reduction of *trans*-3-decalones by lithium *tert*-butoxyaluminum hydride,  $\text{LiAl}(\text{OCMe}_3)_3\text{H}$ . While the methyl derivative allows 15 % equatorial attack, it is diminished to just 3 % in the nitrile (Fig. 3) [15]. Why does the methyl derivative allow larger equatorial approach (15 %) than the unsubstituted derivative (9 %) even when a  $\sigma_{\text{C-H}}$  is better electron-donor than a  $\sigma_{\text{C-C}}$ ? The origin of the observed effect may be traced to the extended hyperconjugation effect arising from the  $\sigma_{\text{C-H}}$  of the methyl group, which is antiperiplanar to  $\sigma_{\text{C4-C5}}$  bond, as shown in the last structure in Fig. 3. This results in  $\sigma_{\text{C-H}} \rightarrow \sigma_{\text{C4-C5}}^*$  interaction worth  $3.31 \text{ kcal mol}^{-1}$ . This raises the electron density of the  $\sigma_{\text{C4-C5}}$  bond, which, in turn, supports enhanced equatorial attack of the nucleophile.

Different heteroatoms in 4-heterocyclohexanones alter the electron densities of  $\sigma_{\text{C2-C3}}$  and  $\sigma_{\text{C5-C6}}$  bonds differently. However, Cieplak invoked transannular electron delocalization of the sort depicted in Fig. 4 and argued in favor of increased axial attack as a consequence of increasing electron-donating ability of the heteroatom lone pair. It is to be remembered that the electron-donating ability of a heteroatom lone pair is opposite of its electronegativity, i.e., the less electronegative a heteroatom, the more electron-donating will its lone pair be and vice versa. Accordingly, sulfur, nitrogen, and oxygen atoms display decreasing donor ability because the electronegativity increases in the same order.

Following the Cieplak model, the ease of axial approach of a given nucleophile must therefore decrease in the same order. However, from the experimental results

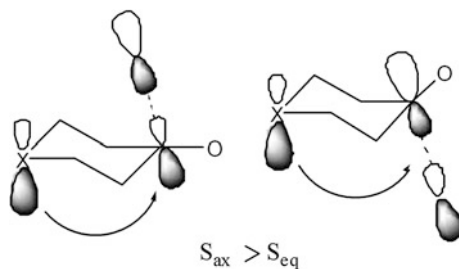
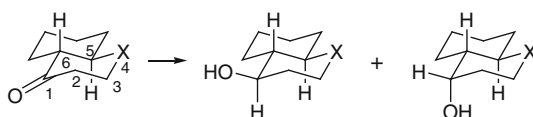


**Fig. 4** Cieplak's  $n \rightarrow \sigma^*$  overlap hypothesis to explain the axial versus equatorial selectivity of 4-heterocyclohexanones;  $S_{ax}$  and  $S_{eq}$  indicate axial and equatorial approach, respectively

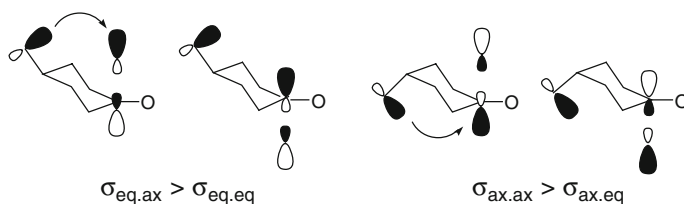
**Table 3** Experimental selectivities of *trans*-2-heterobicyclo[4.4.0]decan-5-ones in reductions with  $\text{NaBH}_4$  and  $\text{Na}(\text{CN})\text{BH}_3$



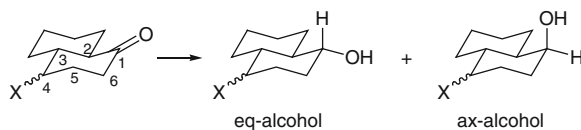
Heteroatom X	Hydride	Temperature ( $^{\circ}\text{C}$ )	Time (min)	Attack (ax:eq)
NBn	$\text{NaBH}_4$	0	60	>30:1
	$\text{Na}(\text{CN})\text{BH}_3$	25	60	>34:1
O	$\text{NaBH}_4$	0	30	6.3:1
	$\text{Na}(\text{CN})\text{BH}_3$	25	60	13:1
S	$\text{NaBH}_4$	0	40	3.9:1
	$\text{Na}(\text{CN})\text{BH}_3$	25	60	9.5:1

collected in Table 3, the trend for axial approach is  $\text{N} > \text{O} > \text{S}$  [16]. Cieplak's hypothesis based on  $n \rightarrow \sigma^*$  overlap is thus unable to explain the observed trend. Therefore, there is a need to look for an alternate explanation.

There occurs a variation in the electron densities of ring bonds in cyclohexanone by introducing a polar substituent on C4 as well. According to Cieplak, the impact of such a substituent is controlled by through-space  $n \rightarrow \sigma^*$  overlap as shown in Fig. 5, and a predominance of axial attack is expected for both axial and equatorial substituents. The experimental results obtained by Houk [17] for substituents such as OH, OAc, Br, Cl, and F support this hypothesis, see Table 4. A substituent



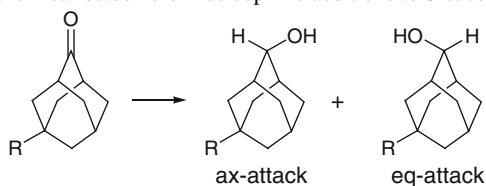
**Fig. 5** Pictorial presentation of the effect of a polar C4 substituent on cyclohexanone on the axial versus equatorial diastereoselectivity based on  $n \rightarrow \sigma^*$  overlap (reproduced from reference 7)

**Table 4** Stereoselectivities in the reduction of 4-substituted *trans*-decalones with NaBH<sub>4</sub> in MeOH at 25 °C

X	(eq:ax)-alcohol	X	(eq/ax)-alcohol
H	60:40		
eq-OH	61:39	ax-OH	85:15
eq-OAc	71:29	ax-OAc	83:17
eq-Br	66:34		
eq-Cl	71:29	ax-Cl	88:12
		ax-F	87:13

occupying the axial position was found to be a better axial director than when occupying the equatorial position. The through-space  $n \rightarrow \sigma^*$  overlap, however, has not been confirmed by quantum mechanical calculations. If the  $\sigma \rightarrow \sigma^*$  interaction turns out being the ultimate control element, a polar electron-attracting substituent on C4 should be expected to inductively reduce the electron densities of  $\sigma_{C2-C3}$  and  $\sigma_{C5-C6}$  bonds to inhibit equatorial approach of a nucleophile and, thus, result in enhanced axial selectivity. The axial selectivity is primarily supported by the  $\sigma_{C2-H_{ax}} \rightarrow \sigma^*$  and  $\sigma_{C6-H_{ax}} \rightarrow \sigma^*$  interactions.

The 5-substituted 2-adamantanones constitute a class of molecules belonging to the category of 4-substituted cyclohexanones. William le Noble studied the reduction of several of this class of compounds by different hydride sources and noted the selectivity profile. These results are collected in Table 5 [18]. Although the reaction conditions are not exactly the same for direct comparison of the results

**Table 5** Stereochemical outcome of nucleophilic additions to 5-substituted 2-adamantanones

R	Reaction conditions	ax:eq selectivity
C <sub>6</sub> H <sub>5</sub>	LiAlH <sub>4</sub> , Et <sub>2</sub> O, rt	56:44
C <sub>6</sub> H <sub>5</sub>	LiAl(OBu <sup>t</sup> ) <sub>3</sub> H, Et <sub>2</sub> O, rt	49:51
F	NaBH <sub>4</sub> , <i>i</i> -PrOH, rt	62:38
Cl	NaBH <sub>4</sub> , <i>i</i> -PrOH, rt	59:41
<b>OH</b>	<b>NaBH<sub>4</sub>, MeOH, 0°C</b>	<b>43:57</b>
CF <sub>3</sub>	NaBH <sub>4</sub> , <i>i</i> -PrOH, 0°C	59:41
CO <sub>2</sub> Me	NaBH <sub>4</sub> , MeOH, 0°C	61:39

in Tables 4 and 5, the observed axial preference of 2-adamantanones is not as high as those of the 4-substituted *trans*-decalones. The strong  $\sigma_{C2/C6-H_{ax}} \rightarrow \sigma^{*}\#$  interactions possible in 4-substituted *trans*-decalones *vis-à-vis* the corresponding but relatively weak  $\sigma_{C-C} \rightarrow \sigma^{*}\#$  interactions in 5-substituted 2-adamantanones are likely to contribute to the higher axial selectivity in the former class of molecules. Further, 5-hydroxy-2-adamantanone exhibits largely equatorial selectivity. This cannot be explained within the ambit of Cieplak's  $n \rightarrow \sigma^{*}\#$  hypothesis. An alternate rationale is therefore required. It is likely that the carbinol function is transformed into alkoxide under the alkaline conditions of  $\text{NaBH}_4$  reduction. This renders  $\sigma_{C-O}$  electron-donor to increase the electron densities of the ring  $\sigma_{C-C}$  bonds and, thus, support the equatorial attack.

In order to explain the selectivity observed in cyclohexanones bearing polar substituents at position 4, Cieplak cited the reactions of 5-phenyl-2-adamantanone with sodium acetylide in liquid  $\text{NH}_3$  shown in Eq. 15 and 5-carbomethoxy-2-adamantanone with  $\text{LiAl}(\text{O}^t\text{Bu})_3\text{H}$  in THF shown in Eq. 16. These reactions proceed with 66:34 and 83:17 selectivity in favor of axial attack. While the example in Eq. 15 may conform to the  $\pi_{Ar} \rightarrow \sigma^{*}\#$  overlap as indicated Fig. 5, it is not clear which nonbonding orbital of the methoxycarbonyl group is so engaged. In terms of vicinal overlap, both the phenyl and methoxycarbonyl groups are electron-attracting to reduce the electron densities of  $\sigma_{C3-C4}$  and  $\sigma_{C1-C6}$  bonds to destabilize the equatorial TS. The methoxycarbonyl group, being more electron-attracting than phenyl, is expected to impart improved axial selectivity, which is indeed observed.

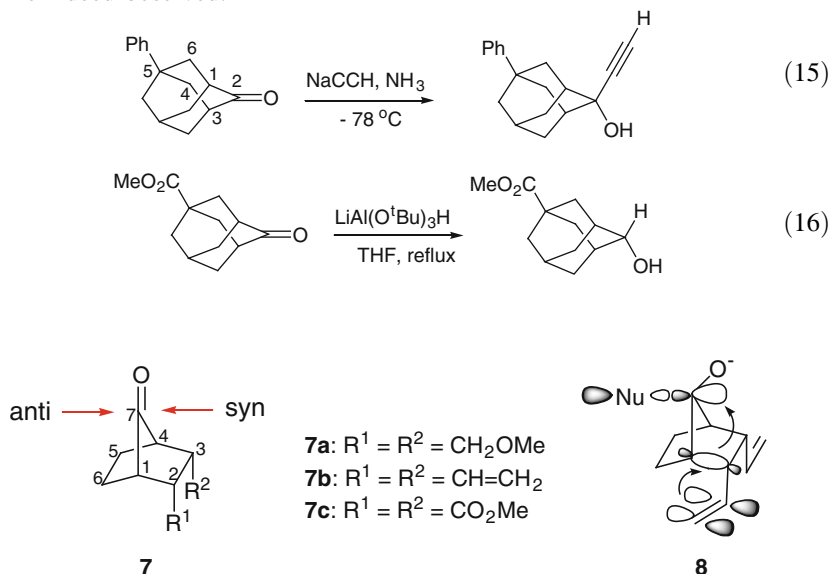


**Fig. 6** The structures of selected norbornan-7-ones **7** and the proposed rigid conformer **8** for the species **7b**

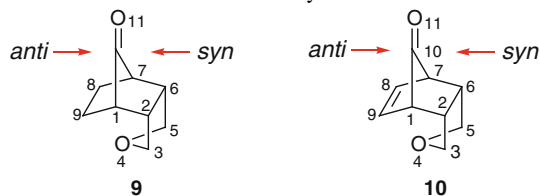
Norbornan-7-ones have been the subject of intense experimental studies for their facial selectivities caused by the *endo* substituents at positions 2 and 3 (Fig. 6). The impetus arose primarily because, unlike cyclohexanones, norbornan-7-ones are rigid and are also devoid of significant geometrical distortions around the carbonyl function [19, 20]. While 2,3-bis(methoxymethyl)norbornan-7-one (**7a**) and 2,3-divinylnorbornan-7-one (**7b**) show *anti* preference for the addition of nucleophiles, 2,3-bis(methoxycarbonyl)norbornan-7-one (**7c**) exhibits *syn* preference. All the three substituents are electron-withdrawing and, thus, the Cieplak model predicts predominantly *syn* addition to all. Mehta and le Noble [21] have attributed the anti-selectivities of **7a** and **7b** to through-space donations from the substituents in rigid conformers such as **8** for the divinyl species. In **8**, the vinyl  $\pi$  bonds lie parallel to  $\sigma_{C1-C2}$  and  $\sigma_{C3-C4}$  bonds. Though this geometrical assumption may appear logical [22, 23], the rigid conformer premise requires verification.

## 4 Houk's Transition State and Electrostatic Models for Diastereoselectivity

From the transition state structures for addition of LiH to a series of 2,3-disubstituted norbornan-7-ones, Houk concluded the followings: (a) the Cieplak's premise of stereoselection controlled by  $\sigma \rightarrow \sigma^*$  interaction is unimportant, and (b) the electrostatic effect constitutes the sole control element [24–27]. Electron-attracting substituents induce positive charges on C2 and C3. These positive charges electrostatically attract the nucleophile on the *syn* face. In contrast, electron-donating substituents induce negative charges on C2 and C3. These negative charges electrostatically repel the nucleophile to result in diminution of attack on the *syn* face. Why do **7a** and **7b** favor *anti* addition and **7c** *syn* addition when the substituents in all of them are electron-withdrawing? Houk considers electrostatic repulsion between a nucleophile and the substituents in **7a** and **7b** and electrostatic attraction in **7c**. The differential treatment of the otherwise electron-withdrawing substituents may, at best, be considered an anomaly.

The rigid conformer argument for the 2,3-bis-methoxymethyl derivative **7a** with the attendant  $n \rightarrow \sigma^*_{C1-C2}$  and  $n \rightarrow \sigma^*_{C3-C4}$  interactions and the 2,3-divinyl species **7b** with the attendant  $\pi \rightarrow \sigma^*_{C1-C2}$  and  $\pi \rightarrow \sigma^*_{C3-C4}$  interactions, as assumed by Mehta and le Noble, was examined by optimum geometry computations and Natural Bond Orbital (NBO) analysis [28, 29]. While the geometrical assumption for **7b** was found to be true with the option of  $\pi \rightarrow \sigma^*_{C1-C2}$  and  $\pi \rightarrow \sigma^*_{C3-C4}$  interactions, the  $n \rightarrow \sigma^*_{C1-C2}$  and  $n \rightarrow \sigma^*_{C3-C4}$  interactions are absent in the 2,3-bis-methoxymethyl derivative **7a**.

The ring oxygen in 4-oxatricyclo[5.2.1.0<sup>2,6</sup>]decan-10-one (**9**) and 4-oxatricyclo[5.2.1.0<sup>2,6</sup>]dec-8-en-10-one (**10**) is indeed held in such a rigid conformation that the electron donation from one of the two lone pair orbitals to  $\sigma^*_{C1-C2}$  and  $\sigma^*_{C6-C7}$  appears a distinct possibility to support *anti*-selectivity. Alternatively, the

**Table 6** The  $\pi$ -Selectivities of hydride reductions of **9** and **10**

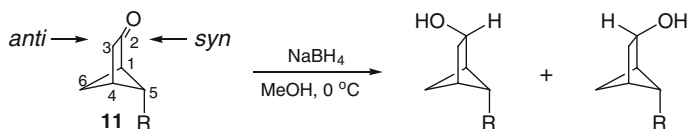
Entry	<b>9/10</b>	Hydride	Solvent	Lewis acid	Time (h)	Yield (%)	<i>anti:syn</i>
1	<b>9</b>	NaBH <sub>4</sub>	MeOH		0.5	>95	1.0:1.0
2	<b>9</b>	NaCNBH <sub>3</sub>	MeOH	pH 3–4	0.5	>95	2.1:1.0
3	<b>9</b>	LiAlH <sub>4</sub>	Et <sub>2</sub> O		2.0	>80	1.1:1.0
4	<b>9</b>	DIBAL-H	Toluene		2.0	>85	2.0:1.0
5	<b>9</b>	DIBAL-H	Toluene	TiCl <sub>4</sub> (3 equiv)	0.5	>85	4.8:1.0
6	<b>9</b>	L-Selectride	THF		1.0	>95	1.0:1.5
7	<b>9</b>	L-Selectride	Toluene		1.0	>85	1.0:8.0
8	<b>9</b>	L-Selectride	Toluene	TiCl <sub>4</sub> (3 equiv)	2.0	>80	1.3:1.0
9	<b>10</b>	NaBH <sub>4</sub>	MeOH		1.0	>85	23:1.0
10	<b>10</b>	NaCNBH <sub>3</sub>	MeOH	pH 3–4	1.0	>95	25:1.0
11	<b>10</b>	LiAlH <sub>4</sub>	Et <sub>2</sub> O		2.0	>95	4.5:1.0
12	<b>10</b>	DIBAL-H	Toluene		2.0	>75	1.8:1.0
13	<b>10</b>	DIBAL-H	Toluene	TiCl <sub>4</sub> (3 equiv)	0.5	>85	>20:1.0
14	<b>10</b>	L-Selectride	THF		1.0	>85	15:1.0
15	<b>10</b>	L-Selectride	Toluene		1.0	>85	2.3:1.0

There is a strong dependence of selectivity on the specific hydride used and the reaction solvent employed. The selectivity of **9** is reversed with the use of L-Selectride. Unlike most other reducing species that favor *anti* addition, L-Selectride favors *syn* addition. The effect of solvent on the reaction with L-Selectride is phenomenal; the selectivity changes from 1:1.5 in THF (entry 6) to 1:8 in toluene (entry 7)

The compound **10** exhibited *anti*-selectivity throughout. The magnitude of selectivity is, again, highly dependent on the source of hydride and the reaction solvent. Throughout, there is no reversal in the selectivity of **10**. This contrasts the results for **9** and demonstrates a dominant role of the  $\pi$ -bond in guiding a nucleophile *syn* to it. Coordination of the  $\pi$ -bond to the nucleophile through the cation followed by delivery of the nucleophile to the carbonyl function *syn* to it appears to be a distinct possibility. The saturation of  $\pi$ -bond in the products formed from **10** generates the same products as those from **9**. Lewis acids promote *anti* addition to both **9** and **10**. The exclusive *anti* addition of DIBAL-H to **10** in the presence of TiCl<sub>4</sub> in toluene (entry 13) is indeed remarkable in comparison to the 1.8:1 selectivity observed in its absence (entry 12)

electron-withdrawing nature of the ring oxygen will be expected to reduce the residual charges on C2 and C6 and support *syn* selectivity in compliance with Houk's electrostatic model. The experimental selectivities of these molecules under different conditions are collected in Table 6 [30]. While the general trend for both the molecules under normal reaction conditions is in favor of *anti* selection, the selectivity of **10** is much higher than that of **9** (see the footnotes of Table 6 for details).



**Table 7** The  $\pi$ -selectivities of different 5-substituted bicyclo[2.1.1]hexan-2-ones

<b>11a</b> , R = CN	75 %	25 %
<b>11b</b> , R = CO <sub>2</sub> Me	66 %	34 %
<b>11c</b> , R = CCH	60 %	40 %
<b>11d</b> , R = CH <sub>2</sub> OH	48 %	52 %
<b>11e</b> , R = CH <sub>2</sub> CH <sub>3</sub>	47 %	53 %
<b>11f</b> , R = CH = CH <sub>2</sub>	44 %	56 %

**Table 8** The residual charges on C5/C6 of **11** at B3LYP/6-31G\* level

<b>11</b> , R=	Charge at C5	Charge at C6
CN	-0.36160	-0.45430
CO <sub>2</sub> Me	-0.35079	-0.45289
CCH	-0.31560	-0.45349
CH <sub>2</sub> OH	-0.27062	-0.45252
CH <sub>2</sub> CH <sub>3</sub>	-0.24412	-0.45088
CHCH <sub>2</sub>	-0.27014	-0.45388

NBO analysis does not show  $n \rightarrow \sigma^*_{C1-C2}$  and  $n \rightarrow \sigma^*_{C6-C7}$  interactions in both **9** and **10**. Clearly, an interpretation of the observed anti-selectivity based on electron donation from the ring oxygen is faulty. Further, C2 or C6 on the *syn* face and C8 or C9 on the *anti* face carry NBO charges of  $-0.29$  and  $-0.47$  in **9**, and  $-0.28$  and  $-0.22$  in **10** [31–33]. These charges predict *syn* addition to **9** and *anti* addition to **10**, according to the Houk's electrostatic model. While the difference of charges in **10** is too small to explain its high *anti* selectivity, the weak *anti*-selectivity of **9** observed with LiAlH<sub>4</sub> is clearly alarming and much against the model. An alternate rationale is therefore required to explain the generally observed *anti*-selectivity.

Mehta et al. [34] introduced 5-substituted bicyclo[2.1.1]hexan-2-ones **11** as a new probe for the experimental as well as computational study of the electronic effects on  $\pi$ -facial selectivity, Table 7. Houk's TS model was discovered to fail in correctly treating correctly the CO<sub>2</sub>Me- and CCH-substrates. The residual charges on C5 and C6 are collected in Table 8. It is clear that C5 is always less negatively charged than C6 and, thus, a nucleophile must always approach the carbonyl group from the direction *syn* to C5. However, this is not always the case. The electrostatic model, therefore, also fails in correctly interpreting the observed diastereoselectivities.

It is amply clear from the foregoing discussions that no single model is sufficient to rationalize the observed facial selectivities of substrates of different skeleton types under varying reaction conditions. Some models have larger applicability and,

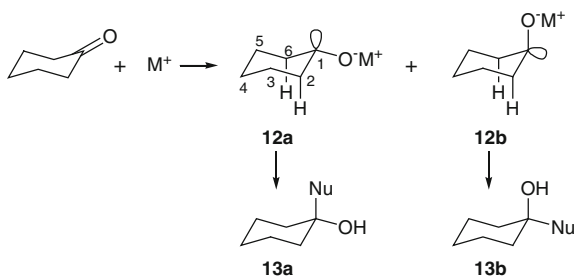
hence, greater appeal than other models. For instance, Cieplak's model based on  $\sigma \rightarrow \sigma^*$  interaction has been verified by many researchers based on the study of substrates of many skeleton types. The transition state model must conceivably work all the times. However, it fails in select instances. Why must the transition state model fail at all? LiH is not known to act as a nucleophile. Is the use of LiH as a nucleophile in the calculation of transition states the source of discrepancy? Is there a need to take solvation effects into consideration? We shall try to find answers to some of these questions in the sections to follow.

## 5 Cation Coordination Model for Diastereoselectivity

A rather simple premise to understand facial selectivity is to consider geometrical changes around the carbonyl carbon upon coordination of the carbonyl oxygen with a positively charged species before the nucleophile is allowed to react. The positively charged species, in effect, is the cation companion of the true nucleophile. This premise is based on the very fact that such a coordination has previously been demonstrated to constitute the initial step [35]. The coordination will reduce  $\pi_{C=O}$  bond order to usher in pyramidalization at the carbonyl carbon, which, in turn, will change the torsion angles of the carbonyl oxygen with select ring positions. This is followed by preferred attack of the nucleophile on the carbonyl carbon on the face with increased torsion angle. Since the changes in torsion angles are expected to depend on the nature and relative orientation and position of a given substituent from the carbonyl group, the approach appears to hold promise for the prediction of selectivity. In applying this concept to cyclohexanone, and considering complete tetrahedral pyramidalization at the carbonyl carbon for the sake of simplicity, two scenarios that emerge and lead to **12a** and **12b** as shown in Fig. 7.

In **12a**, the empty orbital is antiperiplanar to  $\sigma_{C2-H_{ax}}$  and  $\sigma_{C6-H_{ax}}$  bonds. In **12b**, the empty orbital is antiperiplanar to  $\sigma_{C2-C3}$  and  $\sigma_{C5-C6}$  bonds. Since the  $\sigma_{C-H}$  bond is a better electron-donor than the  $\sigma_{C-C}$  bond, the principle of stereoelectronic effect dictates that **12a** is of lower energy than **12b**. The electron-rich nucleophile (a Lewis base) is expected to be electrostatically drawn toward the empty orbital (a Lewis acid) on the axial face in **12a**, leading to the formation of the equatorial

**Fig. 7** The two scenarios that arise as a consequence of coordination of carbonyl oxygen in cyclohexanone with metal ion  $M^+$



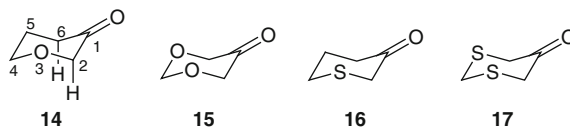


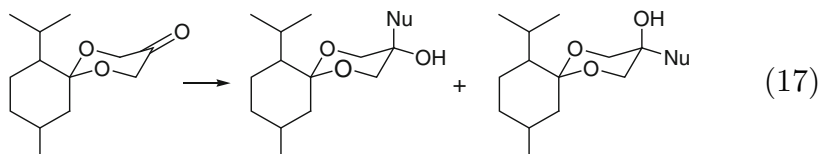
**Fig. 8** Structures of 3-oxacyclohexanone, 3,5-dioxacyclohexanone and the corresponding thia-analogs

alcohol **13a**. The axial alcohol **13b** should be derived from **12b**. A quick support for this analysis comes from the observation that a conformationally locked and sterically unbiased cyclohexanone generates the equatorial alcohol predominantly. The species **12a** and **12b** are products of axial and equatorial pyramidalization, respectively.

In 3-oxacyclohexanone **14**, the interactions of  $\sigma_{C2-Hax}$  and  $\sigma_{C6-Hax}$  with the axially oriented empty orbital on carbonyl carbon is more energy-lowering than the interactions of  $\sigma_{C2-O3}$  and  $\sigma_{C5-C6}$  with the equatorially oriented empty orbital. The  $\sigma_{C2-O3}$  is electron-withdrawing for the electron-attracting nature of the oxygen atom. Consequently, axial pyramidalization [36] and, thus, predominantly axial attack takes place in excellent agreement with the experimental observations [7]. From an extrapolation of these arguments to 3,5-dioxacyclohexanone (**15**), one predicts better axial selectivity than observed with 3-oxacyclohexanone, which is in complete agreement with the experimental results [36–38] (Fig. 8).

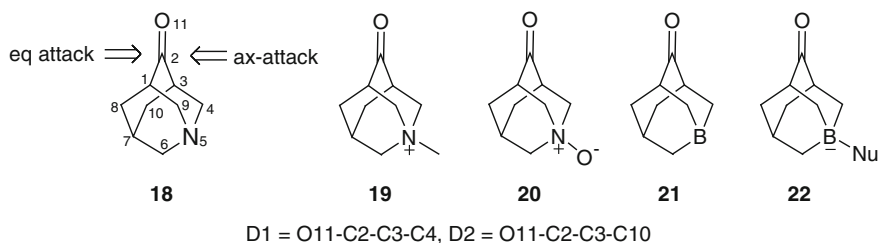
A  $\sigma_{S-C}$  bond is highly electron-donating from sulfur to carbon, so much so that the sum of the (antiperiplanar) interactions of one  $\sigma_{C-C}$  and one  $\sigma_{S-C}$  with an equatorially oriented empty orbital is significantly larger than the sum of the antiperiplanar interactions of the two  $\sigma_{C-Hax}$  bonds with the axially oriented empty orbital. This being so, the situation reverses from 3-oxacyclohexanone **14** to 3-thiacyclohexanone **16** and from 3,5-dioxacyclohexanone **15** to 3,5-dithiacyclohexanone **17**. Both **16** and **17** have been found to exhibit high equatorial selectivity [7]. Indeed, cation coordination leads to axial pyramidalization in **14** and **15** as opposed to significant equatorial pyramidalization in **16** and **17** [38].

As the Lewis acid strength of the cation increases, its complexation with the carbonyl oxygen becomes stronger with corresponding increase in carbonyl pyramidalization. This, in turn, leads to larger diastereoselectivity. Conversely, cation remaining the same, the selectivity must not vary significantly for an insignificant change in the steric requirement of the nucleophile. Indeed, the ax:eq selectivity varies from 7.7:1 to 16:1 to >25:1 in the reactions of the 3,5-dioxacyclohexanone derivative, shown in Eq. 17, with  $LiAlH_4$ , DIBAL-H and a Grignard reagent, respectively [36]. The intensity of coordination is expected to improve in that order by following the HSAB principle. Further, in keeping with the argument above, the selectivity remains at >25:1 when the nucleophile is varied from  $MeMgX$  to  $n-BuMgX$  to  $PhMgX$  [36].



In the event that the cation possesses a poor coordinating ability because of either diffused positive charge or large size, the level of diastereoselection is low due to reduced pyramidalization and, thus, less defined axial versus equatorial disposition of the electron-deficient orbital on the carbonyl carbon. In conformity with this argument, 3-oxacyclohexanone exhibits 90 and 85 % axial selectivity on reaction with  $\text{AlH}_4^-$  possessing, respectively,  $\text{Li}^+$  and  $(n\text{-C}_8\text{H}_{17})_3(n\text{-Pr})\text{N}^+$  as the cation.  $\text{Li}^+$  complexes better with the carbonyl oxygen than the large ammonium ion [36]. 4-Methylcyclohexanone exhibits predominantly axial selectivity in reactions with  $\text{LiAlH}_4$  and  $\text{NaBH}_4$ . However, the selectivity turns in favor of equatorial in reactions with K-Selectride (88 %) and Li-Selectride (80.5 %), due largely to their very large sizes that cause significant steric interactions in the TS for axial attack [39]. The marginally higher equatorial selectivity (i.e., less axial selectivity) observed with K-Selectride is likely to be due to somewhat inferior coordinating ability of  $\text{K}^+$  over  $\text{Li}^+$ .

We shall now consider the diastereoselectivities of 5-aza-2-adamantanone **18**, *N*-methyl-5-aza-2-adamantanone **19**, 5-aza-2-adamantanone *N*-oxide **20** and 5-bora-2-adamantanone **21**, Fig. 9. The 5-substituted 2-adamantanones, investigated thoroughly by William le Nobel [40, 41], allow us to test the validity of the model. In the application of cation coordination model, we are required to measure the torsion angles D1 and D2. An increase in D1 with a corresponding decrease in D2 supports axial attack for the heteroatom-containing ring. On the contrary, an increase in D2 with a corresponding decrease in D1 supports equatorial attack. By taking  $\text{H}^+$  as a representative cation, these torsion angles are collected in Table 9. The proton, i.e.,  $\text{H}^+$  was used as a substitute for a metal cation merely for computational simplicity.



The ax- and eq-attacks are in respect of the heteroatom-containing cyclohexanone unit.

**Fig. 9** The 5-aza- and 5-bora-2-adamantanones and derivatives studied for the selectivity profile

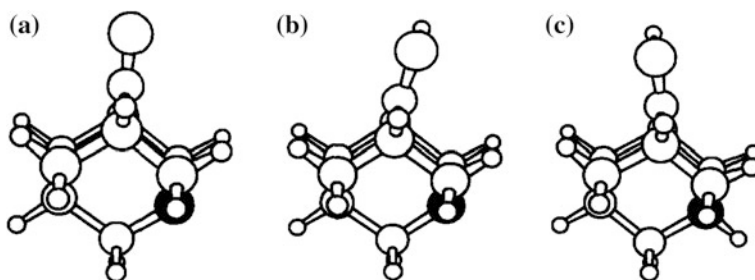
**Table 9** Selected torsion angles of 5-aza- and 5-bora-2-adamantanones and their cation complexes

Entry	Substrate	D1	D2
1	5-aza-2-adamantanone	120.88	122.10
	5-aza-2-adamantanone; C = O...H <sup>+</sup>	108.53	137.77
	5-aza-2-adamantanone; C = O...H <sup>+</sup> and N...H <sup>+</sup>	135.50	107.55
2	N-methyl-5-aza-2-adamantanone	123.00	117.87
	N-methyl-5-aza-2-adamantanone; C = O...H <sup>+</sup>	135.30	107.70
3	5-aza-2-adamantanone <i>N</i> -oxide	123.66	117.98
	5-aza-2-adamantanone <i>N</i> -oxide; C = O...H <sup>+</sup>	128.82	114.99
4	5-bora-2-adamantanone	118.17	122.18
	5-bora-2-adamantanone; C = O...H <sup>+</sup>	123.27	119.40
	5-bora-2-adamantanone; B...H <sup>-</sup> and C = O...H <sup>+</sup>	100.91	142.88

### 5-aza-2-adamantanone, 18

The reduction in the torsion angle D1 by  $>12^\circ$  and enhancement in the torsion angle D2 by  $>15^\circ$  on carbonyl protonation (Fig. 10b) suggests equatorial pyramidalization and, hence, a preference for equatorial nucleophilic attack. The bonds  $\sigma_{C3-C4}$  and  $\sigma_{C1-C9}$  are more electron-rich than  $\sigma_{C1-C8}$  and  $\sigma_{C3-C10}$  as a consequence of being antiperiplanar to the equatorial lone pair orbital on the nitrogen atom. This situation is similar to those in 5-trimethylsilyl- and 5-trimethylstannyl-2-adamantanones, which have been shown to exhibit, respectively, 45:55 and 43.5:56.5 selectivity in favor of equatorial attack on reduction with NaBH<sub>4</sub> in isopropanol [40, 41]. The selectivity is slightly higher at 35:65 in the reaction of the tin-derivative with MeLi in Et<sub>2</sub>O. Both  $\sigma_{C-Si}$  and  $\sigma_{C-Sn}$  bonds are good electron donors.

The above trend with 5-aza-2-adamantanone reverses on allowing protonation of the nitrogen as well. This results in enlarged D1 by  $>14^\circ$  and reduced D2 correspondingly as shown in Fig. 10c. If so, the axial attack must prevail, as was observed by le Noble. The 68:32 (ax:eq) ratio on reduction by NaBH<sub>4</sub> in both methanol and water was considered by le Noble to have involved a hydrogen-bonded amine center [40, 41]. The overall effect of hydrogen-bonding is,

**Fig. 10** a 18, b 18 with C = O...H<sup>+</sup>, and c 18 with C = O...H<sup>+</sup> and N...H<sup>+</sup>

more or less, akin to protonation. It is just that the latter represents the end game of the former in a dynamic situation. Why must one consider protonation of nitrogen at all?

From NBO analysis, the nitrogen atom bears nearly as much negative charge ( $-0.50$ ) as the carbonyl oxygen ( $-0.54$ ). As such, a healthy competition between the two heteroatoms for a cation appears to be a genuine possibility. Protonation makes the nitrogen electron-deficient which, in turn, renders the  $\sigma_{C3-C4}$  and  $\sigma_{C1-C9}$  bonds electron-poor in comparison to  $\sigma_{C1-C8}$  and  $\sigma_{C3-C10}$  bonds. This allows a preferred axial orientation of the empty orbital on carbonyl carbon and, thus, the observed preference in favor of axial selectivity.

The Cieplak model fails at predicting the correct selectivity in the reduction of 5-aza-2-adamantanone because it predicts equatorial selectivity by taking into account the electron-donating nature of the nitrogen lone pair orbital. This model, however, appears to succeed if only the electron-attracting  $\sigma_{C-N}$  bonds are considered to be important. The calculated geometry of the carbonyl-protonated 5-aza-2-adamantanone, Fig. 10b, establishes, with certainty, that the stereoelectronic effect caused by the nitrogen lone pair orbital is more significant than the electron-attracting nature of  $\sigma_{C-N}$  bonds.

### *N*-Methyl-5-aza-2-adamantanone, 19

The  $> 12^\circ$  increase in D1 and  $>10^\circ$  decrease in D2 on protonation of the carbonyl oxygen favor axial selectivity. This is in agreement with the observed 96:4 selectivity noted in the reduction with  $\text{NaBH}_4$  in isopropanol. Like the *N*-protonated 5-aza-2-adamantanone above, the positively charged nitrogen renders the  $\sigma_{C3-C4}$  and  $\sigma_{C1-C9}$  bonds electron-deficient in comparison to  $\sigma_{C1-C8}$  and  $\sigma_{C3-C10}$  bonds. This allows the empty orbital on the carbonyl carbon to orient in an antiperiplanar geometry to the latter two bonds and, thus, the nucleophile attacks predominantly from the axial direction. The computed 3D structures of *N*-methyl-5-aza-2-adamantanone and its protonated derivative are shown in Fig. 11.

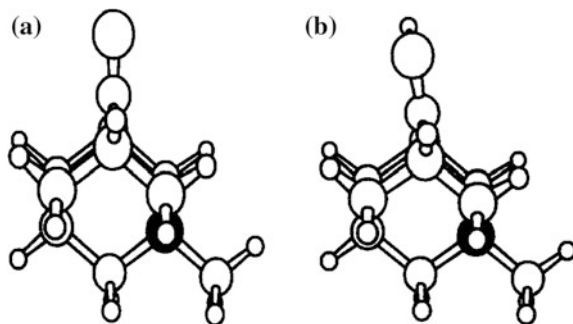


**Fig. 11** **a** *N*-methyl-5-aza-2-adamantanone and **b** protonated *N*-methyl-5-aza-2-adamantanone

### 5-aza-2-adamantanone *N*-oxide, 20

The 5° increase in D1 and 3° decrease in D2 on protonation of the carbonyl oxygen indicates preference for axial selectivity. The axial selectivity is supplemented additionally by the coordination of *N*-oxide oxygen with a cation. This prospect appears genuine because the residual charge on this oxygen,  $-0.71$ , is actually larger than that on the carbonyl oxygen,  $-0.52$ . This additional coordination renders the  $\sigma_{C3-C4}$  and  $\sigma_{C1-C9}$  bonds even more electron-poor than those in the only carbonyl oxygen protonated species and, thus, results in an enhanced axial selectivity. The high axial selectivity expected from 5-aza-2-adamantanone *N*-oxide is in agreement with the experimental observations [40, 41].

Like the *N*-methyl-2-adamantanone species above, 5-aza-2-adamantanone *N*-oxide exhibits axial selectivity by a margin of 96:4 on reduction with  $\text{NaBH}_4$  in isopropanol. Cieplak model predicts axial selectivity for the overall electron-attracting character of the  $\text{N}^+-\text{O}^-$  bond. The Anh-Felkin model fails as it is opposite of the Cieplak model in concept and allows attack of a nucleophile anti to the more electron-deficient bond on the  $\alpha$  carbon. The computed 3D structures of 5-aza-2-adamantanone *N*-oxide and its protonated derivative are shown in Fig. 12.

### 5-Bora-2-adamantanone, 21

This molecule is truly appealing because a nucleophile is expected to add on to the boron atom before any addition to the carbonyl carbon to give **22** (Fig. 9) [16]. This is so because the boron atom is  $>1.5$  times more electron-deficient than the carbonyl carbon. This will have consequences on the observed selectivity. On using hydride ion as the nucleophile to add to boron and  $\text{H}^+$  for carbonyl group protonation, D2 is discovered to be  $>40^\circ$  larger than D1 and, hence, an eminent equatorial attack [17]. This analysis is in agreement with the result observed for

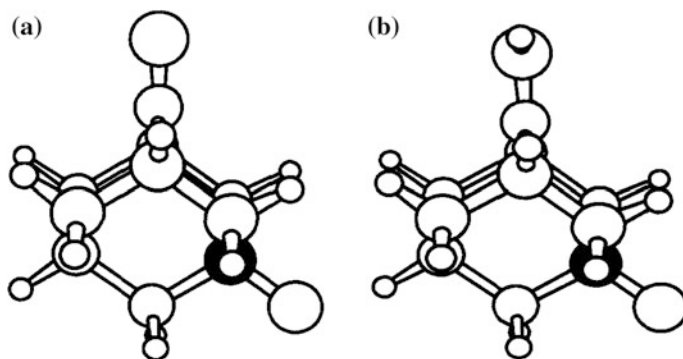


Fig. 12 a 5-aza-2-adamantanone *N*-oxide and b 5-aza-2-adamantanone with  $\text{C}=\text{O}-\text{H}^+$

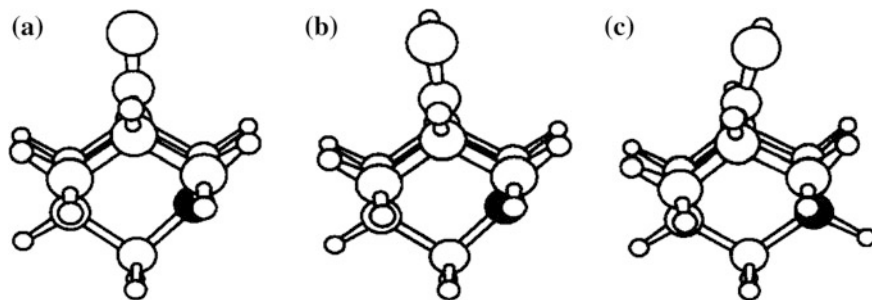


Fig. 13 a **21**, b **21** with  $C = O \dots H$ , and c **21** with  $C = O \dots H^+$  and  $B \dots H^-$

5-pyridyl-5-bora-2-adamantyl radical in its capture of deuterium from  $n\text{-Bu}_3\text{SnD}$ , the ax:eq selectivity is 35:65. An orbital with one electron is very similar to the empty orbital on a carbonyl carbon because both are electron-poor and, therefore, similar stereoelectronic arguments apply.

The Cieplak model fails as it predicts axial attack for the electron-attracting nature of the boron atom. For the same reason, however, the Anh–Felkin model succeeds in predicting the equatorial selection. Houk’s TS model also succeeds in predicting the equatorial preference. Since D2 is  $4^\circ$  larger than D1 in 5-bora-2-adamantanone, less destabilizing interactions in the TS for equatorial attack over those in the TS for axial attack are expected. The computed 3D structures of 5-bora-2-adamantanone and its above derivatives are shown in Fig. 13.

Depending upon the substituents in the vicinity of the carbonyl group, the carbonyl carbon is expected to undergo some pyramidalization due to  $\sigma \rightarrow \pi^*_{C=O}$  type interactions. This pyramidalization is noticeably enhanced on complexation with a cation. Thus, it is possible that one can look at just the  $\sigma \rightarrow \pi^*_{C=O}$  type interactions in a given molecule and predict its diastereoselectivity.

### 2,3-Endo,endo-dimethylnorbornan-7-one and the Corresponding Diethyl Analogue

Both 2,3-endo,endo-dimethylnorbornan-7-one **23** and 2,3-endo,endo-diethylnorbornan-7-one **24** are anti-selective. However, the anti-selectivity of the diethyl derivative is significantly superior to that of the dimethyl derivative. For instance, on reduction with  $\text{LiAlH}_4$ , the *anti:syn* selectivity is 79:21 for **24** and only 55:45 for **23**. If  $\sigma_{\text{vicinal}} \rightarrow \sigma^*_{\text{C-H}}$  interaction, as advocated by Cieplak, is indeed the control element, both molecules will be predicted to exhibit *syn* selectivity because: (a)  $\sigma_{\text{C-H}}$  is more electron-donating than  $\sigma_{\text{C-C}}$  and (b) the anti side has two *endo*  $\sigma_{\text{C-H}}$  bonds in lieu of the two *endo*  $\sigma_{\text{C-C}}$  bonds on the *syn* side. Consequently, the  $\sigma_{\text{C1-C6}}$  and  $\sigma_{\text{C4-C5}}$  bonds, both on the anti side, must be more electron-rich than the  $\sigma_{\text{C1-C2}}$



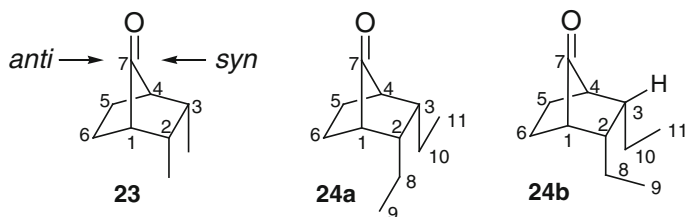


**Fig. 14** Structures of 2,3-*endo,endo*-dimethylnorbornan-7-one **23** and the two low energy conformers **24a** and **24b** of 2,3-*endo,endo*-diethylnorbornan-7-one **24**

**Table 10** Calculated torsion angles D1–D4 in **23**, **24**, and their protonated derivatives at B3LYP/6-31G\* level (D1 = O-C7-C1-C2, D2 = O-C7-C1-C6, D3 = O-C7-C4-C3 and D4 = O-C7-C4-C5)

Substrate	D1	D2	D3	D4
<b>23</b>	121.63	125.06	121.63	125.06
<b>23-H<sup>+</sup></b>	115.33	132.28	115.69	131.97
<b>24a</b>	121.22	125.59	121.22	125.59
<b>24a-H<sup>+</sup></b>	112.57	135.20	113.18	134.60
<b>24b</b>	122.46	124.50	120.75	126.40
<b>24b-H<sup>+</sup></b>	114.21	133.68	112.34	135.86

and  $\sigma_{C3-C4}$  bonds on the *syn* side. Obviously, the Cieplak model, in its original form, fails at not only predicting the correct selectivity of these molecules, but also at explaining the differential selectivity profile (Fig. 14).

In the conformer **24a**,  $\sigma_{C8-C9}$  and  $\sigma_{C10-C11}$  bonds are antiperiplanar to  $\sigma_{C2-C3}$  bond. In the conformer **24b**, the  $\sigma_{C8-C9}$  bond is almost antiperiplanar to  $\sigma_{C1-C2}$  bond, and  $\sigma_{C10-C11}$  bond is almost synperiplanar to the *exo*  $\sigma_{C3-H}$  bond. The conformer **24a** is more stable than **24b** by almost 3.40 kcal mol<sup>-1</sup>. In application of the cation coordination model, the torsion angles D1–D4, both before and after carbonyl protonation, are found to support anti pyramidalization [42]. These torsion angles are collected in Table 10. The calculated 3D structures of **23** and **24**, and their H<sup>+</sup>- and Li<sup>+</sup>-coordinated species are shown in Fig. 15 for a ready visualization of the expected diastereoselectivity.

The origin of the above anti-selectivity lies in the antiperiplanar interactions collected in Table 11. In **23**, one of the three  $\sigma_{C-H}$  bonds of each methyl group is antiperiplanar to the  $\sigma_{C1-C2}$  and  $\sigma_{C3-C4}$  bonds, which allows an interaction energy worth 3.53 kcal mol<sup>-1</sup> each. This interaction increases to 4.16–4.24 kcal mol<sup>-1</sup> on protonation of the carbonyl oxygen. The increased electron densities of  $\sigma_{C1-C2}$  and  $\sigma_{C3-C4}$  bonds allow increased anti pyramidalization of the carbonyl group and, thus, increased anti-selectivity. A similar situation exists in **24a**. One of the two methylene  $\sigma_{C-H}$  bonds is antiperiplanar to the  $\sigma_{C1-C2}$  and  $\sigma_{C3-C4}$  bonds. However, the resultant  $\sigma_{C-H} \rightarrow \sigma^*_{C1-C2}$  or  $\sigma_{C-H} \rightarrow \sigma^*_{C3-C4}$  interaction is somewhat higher at 3.93 kcal mol<sup>-1</sup> and increases to 4.61–4.71 kcal mol<sup>-1</sup> on protonation of the carbonyl oxygen. The stronger interactions in **24a** and its protonated derivative over

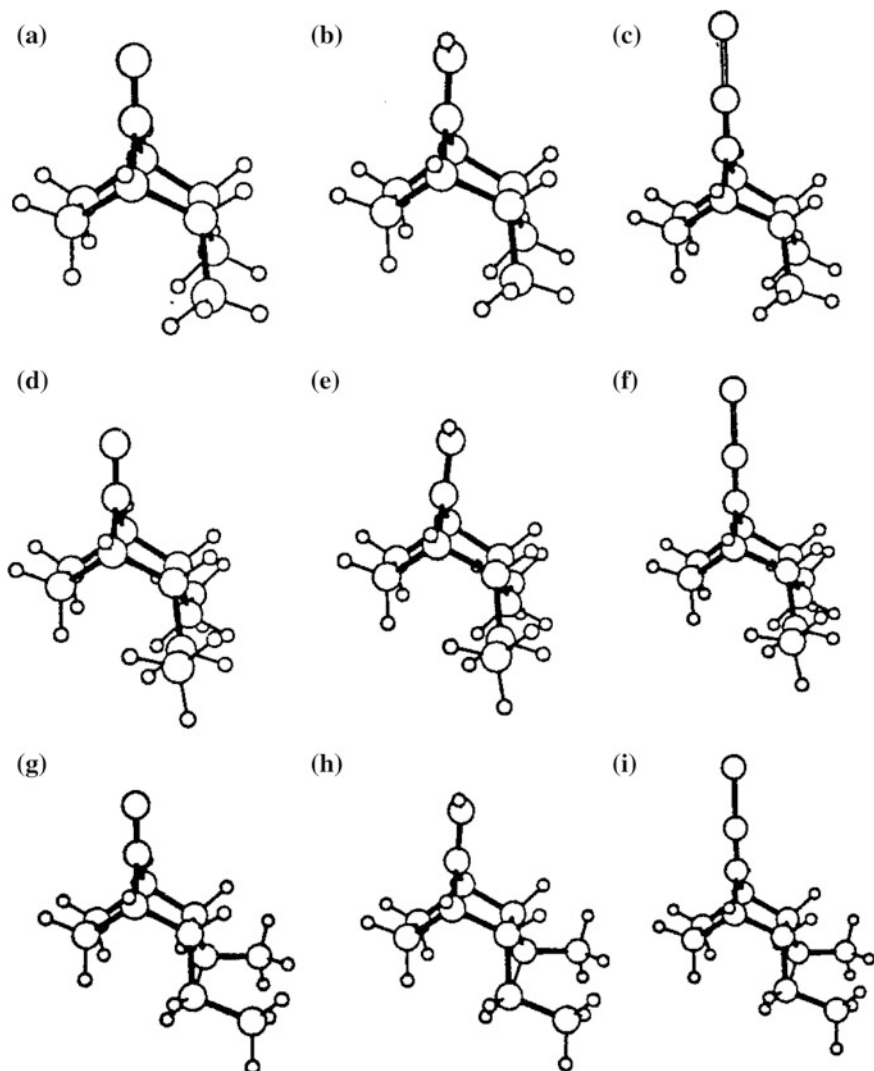


**Fig. 15** Calculated 3D structures: **a** **23**, **b** **23-H<sup>+</sup>**, **c** **23-Li<sup>+</sup>**, **d** **24a**, **e** **24a-H<sup>+</sup>**, **f** **24a-Li<sup>+</sup>**, **g** **24b**, **h** **24b-H<sup>+</sup>**, and **i** **24b-Li<sup>+</sup>**

those in **23** and its protonated derivative ensure larger anti pyramidalization in the former and, thus, the observed improved selectivity.

The sum of  $\sigma_{C1-C2} \rightarrow \pi^*_{C=O}$  and  $\sigma_{C3-C4} \rightarrow \pi^*_{C=O}$  interactions is more than the sum of  $\sigma_{C1-C6} \rightarrow \pi^*_{C=O}$  and  $\sigma_{C4-C5} \rightarrow \pi^*_{C=O}$  interactions in both **23** and **24**, and their protonated species to indicate *anti*-selectivity. Moreover, since the difference of the *anti*- and *syn*-favoring interactions is more in protonated **24** than in protonated **23**, larger *anti*-selectivity of the former compared to that of the latter is in

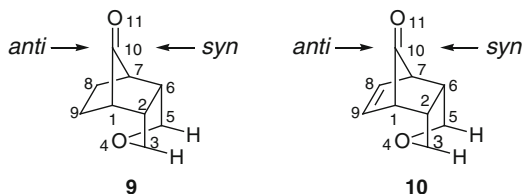
**Table 11**  $\sigma \rightarrow \pi^*_{C=O}$  interactions in **23** and **24**, and their protonated species

Substrate	$\sigma_{C1-C2} \rightarrow \pi^*_{C=O}$	$\sigma_{C1-C6} \rightarrow \pi^*_{C=O}$	$\sigma_{C3-C4} \rightarrow \pi^*_{C=O}$	$\sigma_{C4-C5} \rightarrow \pi^*_{C=O}$	$\sigma_{C8-H} \rightarrow \sigma^*_{C1-C2}$	$\sigma_{C10-H} \rightarrow \sigma^*_{C3-C4}$	$\sigma_{C8-C9} \rightarrow \sigma^*_{C1-C2}$	$\sigma_{C10-C11} \rightarrow \sigma^*_{C3-C4}$
<b>23</b>	3.43	3.27	3.43	3.27	3.53	3.53		
<b>23-H<sup>+</sup></b>	8.60	5.66	8.82	5.66	4.24	4.16		
<b>24a</b>	3.48	3.25	3.38	3.25	3.93	3.93		
<b>24a-H<sup>+</sup></b>	9.20	5.30	9.39	5.32	4.71	4.61		
<b>24b</b>	3.33	3.45	3.69	3.06			1.83	1.24
<b>24b-H<sup>+</sup></b>	8.42	5.79	10.3	4.79			2.19	1.57

order. Thus, the  $\sigma_{C-C} \rightarrow \pi^*_{C=O}$  interaction alone offers a good way of predicting and also explaining the observed differential selectivity [42]. The effect of interaction of remote bonds is inherent in the vicinal  $\sigma_{C-C}$  bonds.

### 4-Oxatricyclo[5.2.1.0<sup>2,6</sup>]decan-10-one, **9**, and 4-oxatricyclo[5.2.1.0<sup>2,6</sup>]dec-8-en-10-one, **10**

We return now to the substrates **9** and **10**, wherein  $n \rightarrow \sigma^*_{C1-C2}$  and  $n \rightarrow \sigma^*_{C6-C7}$  interactions, as previously speculated by Mehta and le Noble, were not noticed from NBO analysis. The prominent  $\sigma_{C-C} \rightarrow \pi^*_{C=O}$  interactions relevant to the selectivity are listed in Table 12. The sum of the interactions  $\sigma_{C1-C2} \rightarrow \pi^*_{C=O}$  and  $\sigma_{C6-C7} \rightarrow \pi^*_{C=O}$  (6.64 kcal mol<sup>-1</sup> in **9** and 7.02 kcal mol<sup>-1</sup> in **10**) is superior to the sum of the interactions  $\sigma_{C1-C9} \rightarrow \pi^*_{C=O}$  and  $\sigma_{C7-C8} \rightarrow \pi^*_{C=O}$  (6.38 kcal mol<sup>-1</sup> in **9** and 5.52 kcal mol<sup>-1</sup> in **10**) in both the species [30]. Noticeably, the difference in these interactions is larger in **10** (1.5 kcal mol<sup>-1</sup>) than in **9** (0.26 kcal mol<sup>-1</sup>). This could be taken to support larger anti-selectivity in **10** as compared to that in **9**. Additional factors, of course, may also be responsible for the higher selectivity in **10** over that in **9** (*wide infra*).



Let us understand why  $\sigma_{C1-C2} \rightarrow \pi^*_{C=O}$  and  $\sigma_{C6-C7} \rightarrow \pi^*_{C=O}$  interactions are superior to  $\sigma_{C1-C9} \rightarrow \pi^*_{C=O}$  and  $\sigma_{C7-C8} \rightarrow \pi^*_{C=O}$  interactions. The geometrical feature of the heterocyclic ring in both **9** and **10** is such that one the two electron pair orbitals on the oxygen is antiperiplanar to  $\sigma_{C2-C3}$  and  $\sigma_{C5-C6}$ , and the other to a  $\sigma_{C-H}$  bond on both C3 and C5. This geometry results in  $n \rightarrow \sigma^*_{C2-C3}$  and  $n \rightarrow \sigma^*_{C5-C6}$  interactions (1.91 kcal mol<sup>-1</sup> in **9** and 2.15 kcal mol<sup>-1</sup> in **10**) and also  $n \rightarrow \sigma^*_{C3-H}$  and  $n \rightarrow \sigma^*_{C5-H}$  interactions (7.16 kcal mol<sup>-1</sup> in **9** and 7.47 kcal mol<sup>-1</sup> in **10**). The latter interactions raise the electron densities of the  $\sigma_{C-H}$  bonds. Since these  $\sigma_{C-H}$  bonds are antiperiplanar to  $\sigma_{C1-C2}$  and  $\sigma_{C6-C7}$  bonds, they interact in  $\sigma_{C3-H} \rightarrow \sigma^*_{C1-C2}$  and  $\sigma_{C5-H} \rightarrow \sigma^*_{C6-C7}$  manner and, thus, raise the electron densities of the latter bonds by 2.94 kcal mol<sup>-1</sup> in **9** and 2.83 kcal mol<sup>-1</sup> in **10**. The anti-selectivity, therefore, appears eminent.

The  $\pi$ -route predicts *syn* selectivity for **10** by consideration of  $\pi \rightarrow \pi^*_{C=O}$  interaction. The  $\pi \rightarrow \pi^*_{C=O}$  barrier must be disrupted by the nucleophile to enter from the *anti* face [43, 44]. Additionally, the electrostatic repulsion between the olefin and the nucleophile, both being electron-rich, also favors *syn* addition [45]. However, there exists a good possibility for olefin-cation coordination to guide the

**Table 12** Interactions relevant to the  $\pi$ -selectivities in **9** and **10**

Substrate	$\sigma_{C1-C2} \rightarrow \pi^*_{C=O}$	$\sigma_{C6-C7} \rightarrow \pi^*_{C=O}$	$\sigma_{C1-C9} \rightarrow \pi^*_{C=O}$	$\sigma_{C7-C8} \rightarrow \pi^*_{C=O}$	$\sigma_{C3-H} \rightarrow \sigma^*_{C1-C2}$	$\sigma_{C5-H} \rightarrow \sigma^*_{C6-C7}$
<b>9</b>	3.32	3.32	3.19	3.19	2.94	2.94
<b>10</b>	3.51	3.51	2.76	2.76	2.83	2.83

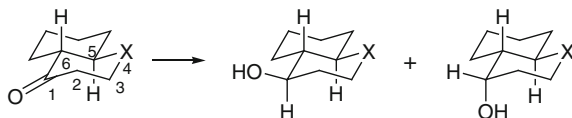
delivery of the nucleophile *syn* to the  $\pi$  bond itself to account for the very high *anti*-selectivity observed in this molecule when compared to that in **9**.

### Trans-2-heterobicyclo[4.4.0]decan-5-ones

The axial transition states with LiH were computed for the aza-, oxa-, and thia-derivatives and subjected to NBO analysis to explore  $n \rightarrow \sigma^*$  interaction as advocated by Cieplak in support of the observed axial preference. Such an interaction was found to be absent. The corresponding equatorial transition states were found to be devoid of the  $n \rightarrow \sigma^*$  interaction. The energy differences in the axial and equatorial transition states are collected in Table 13. These energy profiles point to poorest axial selectivity for the thia-species and highest axial selectivity for the oxa-species. The axial selectivity of the aza-species is predicted to be intermediate of the other two. However, this contrasts the experimental findings in as much as the aza-species exhibited the highest axial selectivity.

The inductively electron-withdrawing N and O atoms are expected to reduce the electron densities of the ring bonds  $\sigma_{C2-C3}$  and  $\sigma_{C5-C6}$ . This reduces the magnitudes of  $\sigma_{C2-C3} \rightarrow \pi^*_{C=O}$  and  $\sigma_{C5-C6} \rightarrow \pi^*_{C=O}$  interactions, leading to higher axial selectivity. On the contrary,  $\sigma_{C-S}$  is electron-donating. The consequent increase in the electron densities of  $\sigma_{C2-C3}$  and  $\sigma_{C5-C6}$  bonds results in increased  $\sigma_{C2-C3} \rightarrow \pi^*_{C=O}$  and  $\sigma_{C5-C6} \rightarrow \pi^*_{C=O}$  interactions to support equatorial attack and, thus, a loss in the axial selectivity is anticipated. The higher axial selectivity in the aza-species in comparison to the oxa-species is likely to be due to the hydrogen-bonding of nitrogen atom with the reaction medium (methanol for borohydride reduction), which renders nitrogen effectively more electron-withdrawing than oxygen. The prospect of such a hydrogen-bonding has previously been suggested by le Noble to explain the predominant *syn* selectivity of 5-aza-2-adamantanone [40, 46–48]. The decrease in the electron densities of  $\sigma_{C2-C3}$  and  $\sigma_{C5-C6}$  bonds has indeed been established by computational studies of the aza-species wherein the nitrogen atom is allowed for hydrogen-bonding with water [16].

**Table 13** Energy differences in the axial and equatorial TSs of *trans*-2-heterobicyclo[4.4.0]decan-5-ones with LiH



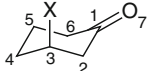
Substrate X =	$[E_{\text{ax-TS}} - E_{\text{eq-TS}}]$ kcal/mol HF/6-31G*	$[E_{\text{ax-TS}} - E_{\text{eq-TS}}]$ kcal/mol HF/6-31 + G*
X = NMe	-1.26	-1.10
X = O	-1.58	-1.47
X = S	-1.07	-0.83

### 3-Halocyclohexanones

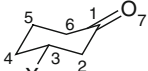
Finally, let us consider the selectivity in nucleophilic additions to 3-halocyclohexanones. The Cieplak model predicts axial attack irrespective of whether the halogen is axial or equatorial for similar inductive electron-withdrawal from  $\sigma_{C2-C3}$ . From transition state calculations, Frenking has predicted equatorial attack in 3-ax-fluorocyclohexanone and axial attack in the corresponding 3-eq-species [49]. The equatorial attack is favored over the axial attack by  $2.3 \text{ kcal mol}^{-1}$ . Likewise, the axial attack on 3-eq-fluorocyclohexanone is favored over the equatorial attack by  $2.7 \text{ kcal mol}^{-1}$ . While the preferred axial attack on cyclohexanones bearing equatorial electron-withdrawing substituents at position 3 is known experimentally [7], Frenking's prediction of equatorial attack on 3-ax-fluorocyclohexanone has not been verified due to conformational mobility of the ring system.

In application of the cation coordination model, the carbonyl groups in 3-chloro- and 3-fluorocyclohexanones were allowed for protonation and the torsion angles O7-C1-C2-C3 and O7-C1-C6-C5 were calculated [50]. These torsion angles are collected in Table 14. The reduction in these torsion angles in the protonated 3-ax-chlorocyclohexanone predicts equatorial attack. In contrast, the same torsion angles increase in the protonated 3-eq-chlorocyclohexanone to signal axial attack. The increase in torsion angles in protonated 3-eq-chlorocyclohexanone is considerably larger than the corresponding reduction in the protonated 3-ax-chlorocyclohexanone. Consequently, 3-eq-chlorocyclohexanone is predicted to exhibit improved selectivity in comparison to 3-ax-chlorocyclohexanone. In the same vein, 3-ax- and 3-eq-fluorocyclohexanones are predicted to exhibit equatorial and axial preferences, respectively. These selectivity predictions are in excellent agreement with the predictions based on the transition state energy calculations.

**Table 14** The torsion angle changes upon protonation of the carbonyl group in 3-ax- and 3-eq-chlorocyclohexanones



3-ax-halocyclohexanone



3-eq-halocyclohexanone

Substrate	Torsion angle O7-C1-C2-C3	Torsion angle O7-C1-C6-C5
3-ax-chlorocyclohexanone	140.47	138.27
3-ax-chlorocyclohexanone, protonated	133.93	135.62
3-eq-chlorocyclohexanone	134.33	134.18
3-eq-chlorocyclohexanone, protonated	145.64	144.89
3-ax-fluorocyclohexanone	139.77	138.07
3-ax-fluorocyclohexanone, protonated	136.68	139.44
3-eq-fluorocyclohexanone	134.59	133.58
3-eq-fluorocyclohexanone, protonated	149.67	147.04

The transition state is known to be of two types, the early transition state and the late transition state. The early transition state structure is reactant-like, wherein the incipient bond ( $\sigma^\ddagger$ ) has not yet begun to form. In contrast, the formation of the incipient bond has progressed to a reasonable extent in the late transition state structure and, hence, it is product-like. In view of this, the Cieplak's vicinal  $\sigma \rightarrow \sigma^\ddagger$  model need not apply to those reactions that proceed through early transition states. Indeed, the vicinal  $\sigma \rightarrow \sigma^\ddagger$  interaction has been found to be absent in several early transition structures with  $\sigma \rightarrow \pi^*_{C=O}$  interaction controlling the selectivity. In contrast, the late transition structures have been found to be devoid of  $\sigma \rightarrow \pi^*_{C=O}$  type interaction with  $\sigma \rightarrow \sigma^\ddagger$  interaction controlling the selectivity [51].

## References

1. Cram DJ, Abdelhafez FA (1952) *J Am Chem Soc* 74:5828
2. Cherest M, Felkin H (1968) *Tetrahedron Lett* 2205
3. Anh NT (1980) *Top Curr Chem* 88:145
4. Baker JW (1952) *Hyperconjugation*. Oxford University Press, London
5. Taft RW, Lewis IC (1959) *Tetrahedron* 5:210
6. Edlund U (1978) *Org Magn Res* 11:516
7. Cieplak AS (1981) *J Am Chem Soc* 103:4540
8. Cieplak AS, Taft BD, Johnson CR (1989) *J Am Chem Soc* 111:8447
9. Rei M-H (1979) *J Org Chem* 44:2760
10. Meakins GD, Young RN (1968) R K Percy. *J Chem Soc C*, E E Richards, p 1106
11. Rocquet F, Battioni JP, Capmau M-L, Chodkiewicz WCR (1969) *Hebd Seances Acad Sci Ser C* 268:1449
12. Cazaux L, Jugie G (1977) *J Mol Struct* 39:219
13. Terasawa T, Okada T (1978) *J Chem Soc Perkin Trans* 1:1252
14. Kobayashi YM, Lambrecht J, Jochims JC (1978) *U Burkert Chem Ber* 111:3442
15. Agami C, Fadlallah M, Kazakos A (1979) *J Levisalles Tetrahedron* 35:969
16. Balamurugan R, Sriramurthy V, Yadav Vk (2007) *Ind J Chem* 46B:509
17. Wu YD, Tucker JA, Houk KN (1991) *J Am Chem Soc* 113:5018
18. Cheung CK, Tseng LT, Lin MH, Srivastava S, le Noble WJ (1986) *J Am Chem Soc* 108:1598
19. Mehta G, Khan FA (1990) *J Am Chem Soc* 112:6140
20. Mehta G, Khan FA (1991) *J Chem Soc Chem Commun* 18
21. Li H, Mehta G, Padma S, le Noble WJ (2006) *J Org Chem* 1991:56
22. Laube T, Ha T-K (1988) *J Am Chem Soc* 110:3511
23. Kost D (1989) H Egozy *J Org Chem* 54:409
24. Paddon-Row MN, Wu Y-D, Houk KN (1992) *J Am Chem Soc* 114:10638
25. Wong SS, Paddon-Row MN (1990) *J Chem Soc Chem Commun* 456
26. Wong SS, Paddon-Row MN (1991) *J Chem Soc Chem Commun* 327
27. Wu Y-D, Tucker JA, Houk KN (1991) *J Am Chem Soc* 113:5018
28. Yadav VK, Balamurugan R (2001) *J Chem Soc Perkin Trans* 2:1
29. NBO 3.1 program: Glendening ED, Reed AE, Carpenter JE, Weinhold F (1990) *QCPE Bull*, 10:58. For detailed information, see: Reed AE, Curtiss LA, Weinhold F (1988) *Chem Rev* 88:8899
30. Yadav VK, Balamurugan R (2002) *J Org Chem* 67:587



31. All geometry optimizations and calculations of NBO charges were performed at the B3LYP/6-31G\* level using the program Gaussian 94, Revision C.2. Frish MJ, Trucks GW, Schlegel HB, Jones PMW, Johnson BG, Robb MA, Cheeseman JR, Keith T, Petersson GA, Montgomery JA, Raghavachari K, Al-Laham MA, Zakrzewski VG, Ortiz JV, Foresnan JB, Cioslowski J, Stefanov BB, Nanayakkara A, Challacombe M, Peng CY, Ayala PY, Chen W, Wong MW, Andres JL, Replogle ES, Gomperts R, Martin RL, Fox DJ, Binkley JS, Defrees DJ, Baker J, Stewart JP, Head-Gordon M, Gonzalez C, Pople JA, Gaussian Inc, Pittsburgh, PA, 1995
32. Becke AD (1993) *J Chem Phys* 98:5648
33. Lee C, Yang W, Parr RG (1988) *Phys Rev B* 37:785
34. Mehta G, Singh SR, Gagliardini V, Priyakumar UD, Sastry GN (2001) *Tetrahedron Lett* 42:8527
35. Ashby EC, Dobbs FR, Hopkins HP (1975) *Jr J Am Chem Soc* 97:3158
36. Harada T, Nakajima H, Ohnishi T, Takeuchi M, Oku A (1992) *J Org Chem* 57:720
37. Ashby EC, Boone JR (1976) *J Org Chem* 41:2890
38. Jeyaraj DA, Yadav A, Yadav VK (1997) *Tetrahedron Lett* 38:4483
39. Brown HC, Krishnamurthy S (1972) *J Am Chem Soc* 94:7159
40. Xie M, le Noble W (1989) *J Org Chem* 54:3836
41. Hahn JM, le Noble W (1916) *J Am Chem Soc* 1992:114
42. Yadav VK (2001) *J Org Chem* 66:2501
43. Nickon A, Jones SS, Parkhill BJ (1989) *Heterocycles* 28:187
44. Eaton PE, Hudson RA (1965) *J Am Chem Soc* 87:2769
45. Clark F, Warkentin J (1971) *Can J Chem* 49:2223
46. Ameer F, Drews SE, Freese S, Kaye PT (1988) *Synth Commun* 18:495
47. Marku IE, Giles PR (1015) N T Hindley *Tetrahedron* 1997:53
48. Yamada YMA (2000) S Ikegami *Tetrahedron Lett* 41:2165
49. Frenking G, Kohler KF, Reetz MT (1991) *Angew Chem Int Ed Engl* 30:1146
50. Jeyaraj DA, Yadav VK (1997) *Tetrahedron Lett* 34:6095
51. Yadav VK, Gupta A, Balamurugan R, Sriramurthy V, Naganaboina VK (2006) *J Org Chem* 71:4178

# Chapter 4

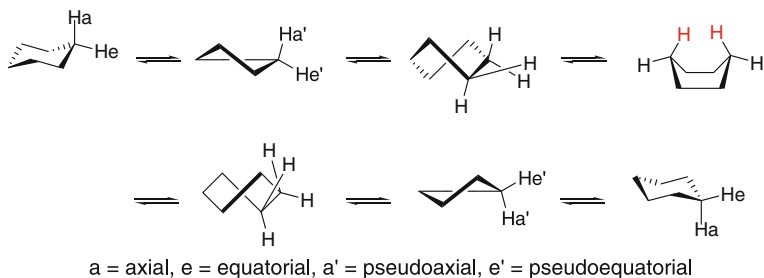
## A<sup>(1,2)</sup> and A<sup>(1,3)</sup> Strains

**Abstract** The A<sup>(1,2)</sup> and A<sup>(1,3)</sup> strains and their control on the conformational and reactivity profiles of substrates are discussed. The application of A<sup>(1,3)</sup> strain to the facial selectivity of reactions such as [2,3] and [3,3] sigmatropic shifts, intramolecular S<sub>N</sub>2 reactions, hydroboration, enolate alkylation, etc. is highlighted. The high diastereoselectivity observed in the reactions of enolates derived from 4-substituted *N*-alkanoyl-1,3-oxazolidinones (Evans enolates) with electrophiles is discussed.

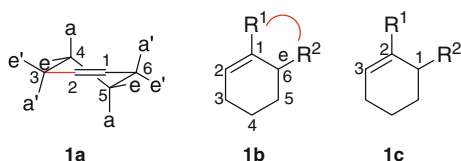
**Keywords** A<sup>(1,2)</sup> strain · A<sup>(1,3)</sup> strain · Enamine · Epimerization · [2,3] and [3,3] sigmatropic shifts · Intramolecular S<sub>N</sub>2 reaction · Iodolactonization · Hydroboration · Conjugate addition · 1,3-oxazolidinones · Diastereoselectivity

### 1 Introduction

Six-membered ring is the most preferred form of a transition state, as it is an intrinsically strain-free system. It also allows us the discussion of stereochemistry and steric interactions. Chair → twist boat → boat → the other twist boat → the other chair are the recognized events en route ring-flip from one chair to the other. In this process, a substituent changes its position from axial to equatorial and from equatorial to axial. In between the chair and the twist boat forms, there is the half chair form. The twist boat and the boat conformers are, respectively, 5.5 and 6.5 kcal mol<sup>-1</sup> above the chair conformer. The two hydrogen atoms in red color in the boat conformer, called flagpole hydrogen atoms, come close enough to raise its energy by 1.0 kcal mol<sup>-1</sup>. This energy value is the same as the σ<sub>C-H</sub> → σ<sub>C-H</sub> bond pair repulsion energy in the eclipsed conformer of ethane. The positions occupied by the flagpole hydrogen atoms are called flagpole positions. The highest energy difference, about 10.5 kcal mol<sup>-1</sup> at STP, between the chair and the half chair is about the energy required to flip one chair into the other.

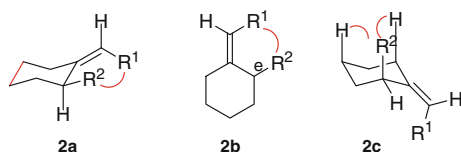


Cyclohexene exists in the half chair [1] conformation **1a** as confirmed from the X-ray structures of many species including morphine [2] and cholesteryl iodide [3]. Relative to cyclohexane, cyclohexene is flattened and only C4 and C5 bear the truly axial and equatorial bonds. The bonds on C3 and C6, which are slightly off from the truly axial and equatorial positions, are called pseudo-axial (a') and pseudo-equatorial (e'), respectively. The dihedral angle between a substituent on C1 (like  $R^1$  in the structure **1b**) and an equatorial substituent on position C6 (like equatorial  $R^2$  in the structure **1b**) is about  $43\text{--}44^\circ$  (significantly less than the normal value of  $60^\circ$ ). This allows them to interfere with each other sterically.



The magnitude of the above interaction will depend on the sizes of the substituents  $R^1$  and  $R^2$ . Each of these substituents being larger than a hydrogen atom, the resultant interaction is called  $A^{(1,2)}$  interaction or  $A^{(1,2)}$  strain as the substituents are positioned on atoms 1 and 2 of an allylic system. The numbering commences from the allylic position and moves to the olefinic linkage as demonstrated in structure **1c**. Some conformational change must occur to avoid or minimize such an energy-enhancing interaction.

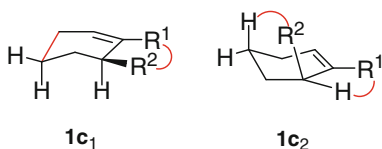
A similar picture emerges from the consideration of a cyclohexane ring bearing an exocyclic methylene group. The two substituents  $R^1$  and  $R^2$  in the 3D conformer **2a** or the planar conformer **2b** are nearly coplanar with a dihedral angle within a few degrees and, thereby, dangerously close to each other to result in steric interaction. As above with the conformer **1a**, the severity of the interaction will increase with the increase in the sizes of the substituents  $R^1$  and  $R^2$ . This interaction is christened  $A^{(1,3)}$  interaction or  $A^{(1,3)}$  strain because the substituents involved are located on positions 1 and 3 of the allylic system. The system will, therefore, tend to adopt a conformer different from **2a** wherein the two substituents are held as far apart from each other as geometrically possible. The obvious choice is the conformer **2c** wherein the substituent  $R^2$  is oriented axial.



For  $R^1 = R^2 = \text{Me}$ , the conformer **2c** is about  $3.7 \text{ kcal mol}^{-1}$  lower than the conformer **2a**. The energy of the conformer **2c** is raised by approximately  $2 \times 0.9 = 1.8 \text{ kcal mol}^{-1}$  on account of two 1,3-diaxial interactions, as shown. Were these 1,3-diaxial interactions not present, the energy of **2c** would be  $3.7 + 1.8 = 5.5 \text{ kcal mol}^{-1}$  lower than that of **2a**. Thus, the strain energy present in **2a** due to the van der Waals interaction between the two methyl groups comes to be about  $5.5 \text{ kcal mol}^{-1}$ . In this calculation, the overall energy-lowering arising from the hyperconjugation effects between the axial  $\sigma$  bonds on C2 and C6 and the  $\pi$  bond have been ignored.

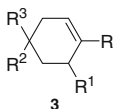
## 2 A<sup>(1,2)</sup> Strain

The molecule **1c** with both the substituents  $R^1$  and  $R^2$  being larger than hydrogen will be expected to exist as an equilibrium mixture of the conformers **1c<sub>1</sub>** and **1c<sub>2</sub>**. This equilibrium involves flip from one half-chair to the other half-chair. It is to be noted that unlike the conformer **1c<sub>2</sub>**, the conformer **1c<sub>1</sub>** benefits from the energy-lowering hyperconjugation effects arising from the interaction of the axial  $\sigma_{\text{C-H}}$  on the allylic carbon and the  $\pi$  bond ( $\sigma_{\text{C-H}} \rightarrow \pi_{\text{C=C}}^*$  and  $\pi_{\text{C=C}} \rightarrow \sigma_{\text{C-H}}^*$ ). Must the sizes of the substituents  $R^1$  and  $R^2$  be such that the steric interaction between them in the conformer **1c<sub>1</sub>** minus the above stabilizing hyperconjugative interaction be larger than the sum of the steric interactions between  $R^1$  and H and between  $R^2$  and H as shown in the conformer **1c<sub>2</sub>**, the conformer **1c<sub>2</sub>** will predominate. Here also, to keep the matter simple, we shall ignore the hyperconjugative effects from further discussions.



Garbisch has demonstrated, from the application of NMR spectroscopy, that many 1,6-disubstituted cyclohexenes existed predominantly in the conformer having the C6-substituent axial [4]. Garbisch also noted that the 6-equatorial substituent in 1-aryl cyclohexenes was held more nearly in C2–C1–C6 plane (due to conjugation effects) than the 6-equatorial substituent in 1-alkyl cyclohexenes. The interaction between the aryl group and C6-equatorial substituent leads to a

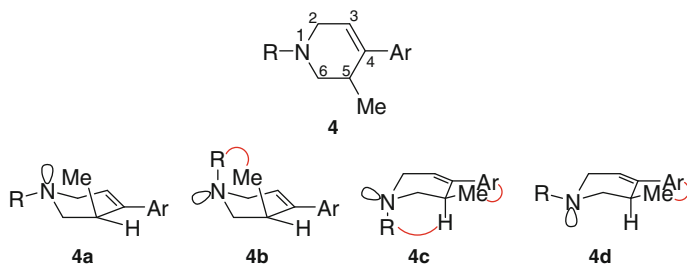
preference for the conformer bearing the C6-substituent axial, i.e., **1c<sub>2</sub>**. The results for specific examples of the general structure **3** are collected in the Table below. From the examples at entries 4 and 6, it is obvious that the 1,3-diaxial interaction (between Me<sub>2</sub>COH and Me in entry 4 and between COMe and Me in entry 6) is stronger than the A<sup>(1,2)</sup> interaction, so much so that the C6-substituent occupies the equatorial position preferentially.



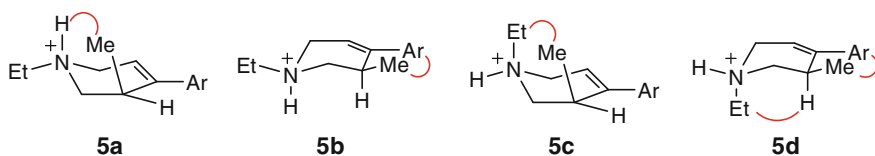
	R	R <sup>1</sup>	R <sup>2</sup>	R <sup>3</sup>	Preferred orientation of R <sup>1</sup>
1	Ph	Me <sub>3</sub> C	H	H	Axial
2	Ph	Ph	H	H	Axial
3	Ph	Me <sub>2</sub> COH	H	H	Axial
4	Ph	Me <sub>2</sub> COH	Me	Me	Equatorial
5	Ph	COMe	H	H	nep*
6	Ph	COMe	Me	Me	Equatorial
7	Me	COMe	H	H	nep*
8	Ph	NO <sub>2</sub>	H	H	Axial
9	Me	NO <sub>2</sub>	H	H	Axial
10	Me	Br	H	H	Axial
11	OMe	Br	H	H	Axial

\*nep = no conformational preference

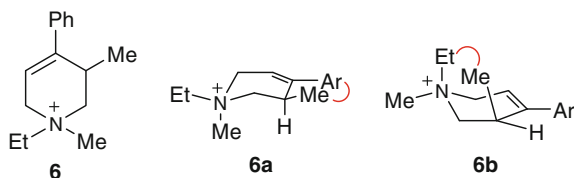
There could be four conformers in all for a molecule of the type **4**. Beckett et al. [5–7] have observed that the conformer **4a** is preferred over the conformers **4b**, **4c** and **4d**. The 1,3-diaxial interaction between the electron pair orbital on nitrogen and the methyl substituent in **4a** is considered to be small. The conformer **4b** is destabilized by the 1,3-diaxial interaction between the methyl group and the substituent R on the nitrogen. The conformer **4c** is destabilized by the 1,3-diaxial interaction between the axial H on C5 and the axial substituent R on the nitrogen. Both the conformers **4c** and **4d** are destabilized by A<sup>(1,2)</sup> strain also.



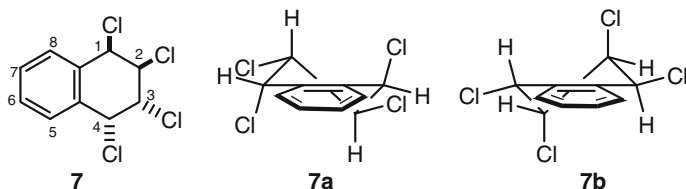
Beckett and coworkers have also discovered that protonation reduced the population of the conformer with C5-axial methyl to less than 50 % of the total [5–7]. Only the conformers **5a** and **5b** (**5a:5b** = 43:57) were detected in the case of the *N*-ethyl salt **5**. The increased interaction of the C5-axial-methyl group with the axial hydrogen atom on the nitrogen as against the electron pair orbital in the conformer distribution. The conformers **5c** and **5d** are destabilized due to severe 1,3-diaxial interactions as shown. The conformer **5d** is destabilized by A<sup>(1,2)</sup> strain as well.



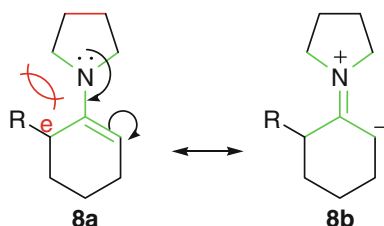
Beckett and coworkers [5–7] found that quaternization of **4** with alkyl halides reversed the conformational equilibrium even further and, for a system like **6**, the conformer **6a** with the C5-substituent occupying the equatorial position predominated. Obviously, the A<sup>(1,2)</sup> strain present in **6a** is less than the steric strain arising from 1,3-diaxial interaction between the ethyl and methyl substituents in the conformer **6b**.



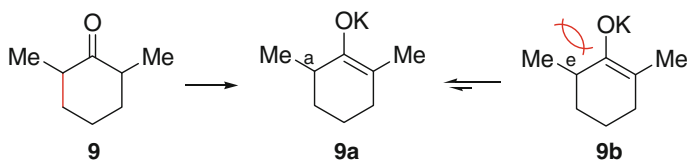
The conformational profile of *cis,trans,cis*-1,2,3,4-tetrachlorotetrahydronaphthalene, **7** (R, R = -CH=CH-CH=CH-), is influenced by A<sup>(1,2)</sup> strain. Of the two conformers **7a** and **7b**, **7a** constitutes the nearly exclusive conformer at equilibrium [8]. It is important to note that both the chlorine atoms on the allylic positions in **7a** are (pseudo)axial and, thus, significantly away from the hydrogen atoms on C5 and C8 *peri* positions to avoid the otherwise eminent A<sup>(1,2)</sup> strain.



Enamine constitutes an excellent example of  $A^{(1,2)}$  strain. Because of the  $\mathbf{8a} \leftrightarrow \mathbf{8b}$  resonance involving overlap of lone pair of electrons on the nitrogen with the  $\pi$ -bond, the bonds shown in green color in  $\mathbf{8a}$  are, more or less, in a single plane that brings the methylene group attached to the nitrogen atom and the substituent R, must it be equatorial, very close to each other to result in severe steric interactions. Consequently, the enamine  $\mathbf{8a}$  adopts a conformation wherein the substituent R occupies axial position [9–11].

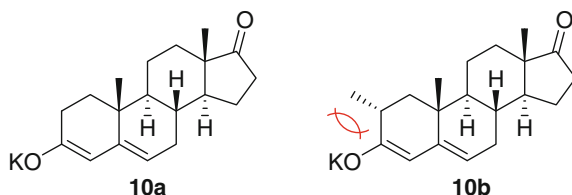


Enolates formed from certain substituted cyclohexanones are very close to enamines in their display of  $A^{(1,2)}$  strain and, hence, the preferred conformer distribution. The equilibrium composition of the potassium enolate conformers  $\mathbf{9a}$  and  $\mathbf{9b}$  is solvent dependent [12]. The bulkier and also the more cation-coordinating the solvent, the larger is the concentration of the conformer  $\mathbf{9a}$ . The interaction of the solvated ion pair  $\text{O}^- \text{K}^+$  with the equatorial methyl group at C6, as in  $\mathbf{9b}$ , is the apparent cause. The greater this interaction is, the greater will be the contribution of  $\mathbf{9a}$  to the equilibrium. However, there ought to be a point where the solvated  $\text{O}^- \text{K}^+$  may begin to substantially interact with the axial methyl group as well, i.e., the system has reached the limiting equilibrium point.

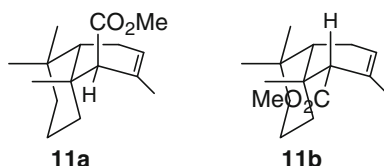


A similar effect has been noted in the generation of the potassium enolate of 2 $\alpha$ -methyl androst-4-ene-3,17-dione  $\mathbf{10b}$ . This enolate was discovered to be  $\sim 1.4 \text{ kcal mol}^{-1}$  less stable than  $\mathbf{10a}$ , the enolate without the 2 $\alpha$ -methyl substituent [13]. It is to be recognized that the 2 $\alpha$ -methyl substituent in  $\mathbf{10b}$  is located at equatorial position and, hence, is in steric interaction with the solvated ion pair

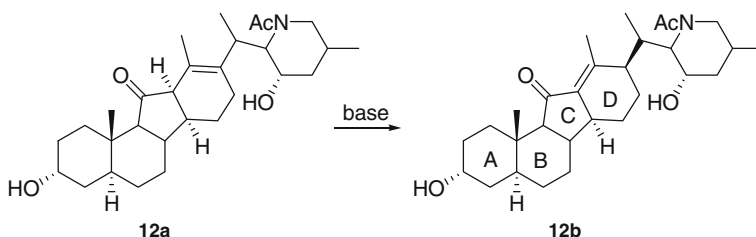
O<sup>-</sup>K<sup>+</sup> as discussed above. A 2 $\beta$ -methyl group occupies the axial position in which it is free from interaction with the ion pair, i.e., devoid of A<sup>(1,2)</sup> interaction but in severe 1,3-diaxial interaction with the nearby angular methyl group.



The methyl ester of bicyclofarnesic acid **11a** was discovered unchanged on being treated with sodium methoxide at 150–160 °C for 24 h [14]. The necessity for an axial carbomethoxy group in **11a** is the interaction between the methyl group on the olefinic bond and the carbomethoxy group in the equatorial isomer **11b**.



Base-catalyzed isomerization of **12a** furnished **12b** wherein the large side chain on ring D was axially oriented to avoid A<sup>(1,2)</sup> strain with the methyl group on the adjacent sp<sup>2</sup> carbon [15].



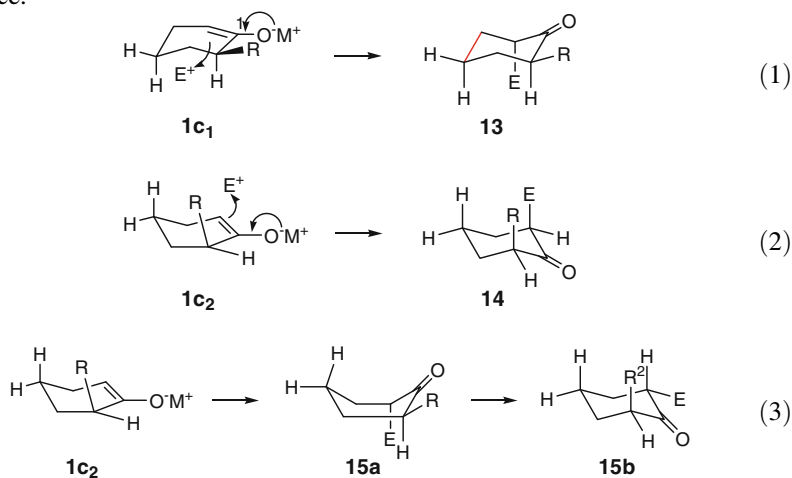
### 3 Stereocontrol in Reactions on Account of A<sup>(1,2)</sup> Strain

An interesting aspect of the **1c<sub>1</sub>**/**1c<sub>2</sub>** conformational change is the steric resistance offered to an approaching reagent when the substrate is a reactive species such as an enamine or enolate. This approach will be controlled by two factors: (a) the stereoelectronic effect which demands as much continuous orbital overlap as possible in the TS and (b) the steric resistance that will be offered to the reagent's approach.

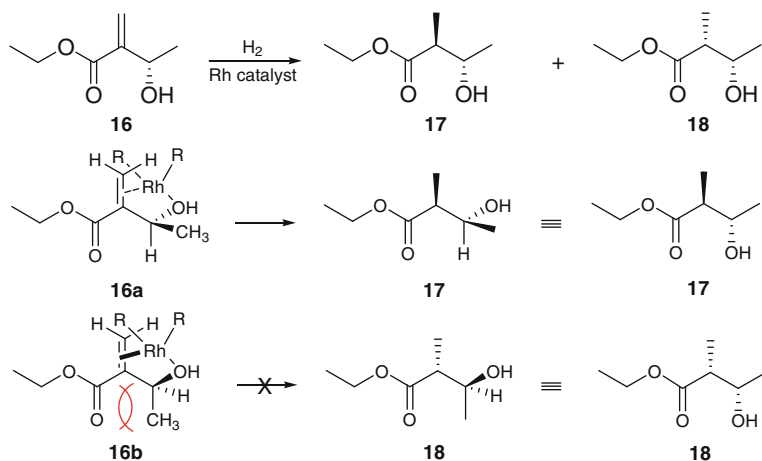
In **1c<sub>1</sub>** (R<sup>1</sup> = O<sup>-</sup>M<sup>+</sup> and R<sup>2</sup> = R), there is absolutely no resistance to a reagent's axial approach and an electrophile is expected to attack C2 on the lower face to



generate **13**, as shown in Eq. (1). In **1c<sub>2</sub>** ( $R^1 = O^-M^+$  and  $R^2 = R$ ), attack on C2 on the upper face will be favored on account of stereoelectronic effect to generate **14**, as shown in Eq. (2). The direction of attack by the electrophile being axial, the TS is chair-like. It is to be noted that the upper face approach to **1c<sub>2</sub>** is opposed by R on account of steric interactions. Thus, must R be very large, attack on the lower face may prevail to generate **15b**, as shown in Eq. (3). However, this attack requires adoption of the boat conformer **15a** by the ring at some point during the course of the reaction which is energy demanding. The lower face attack will therefore be expected to prevail only if the energy required for adoption of this boat conformer is lower than the energy required for the reagent to pass by R in its approach to **1c<sub>2</sub>** on upper face.



In a smart application of the  $A^{(1,2)}$  strain on the conformer distribution, Brown studied Rh-catalyzed hydrogenation the chiral allylic alcohol **16** to discover a very high degree of diastereocontrol in furnishing **17** and **18** in 99:1 ratio [16]. The catalyst must form a complex with the carbinol function in **16** for the reaction to occur. For being coplanar, the  $A^{(1,2)}$  strain present between the methyl substituent and the carbonyl oxygen in **16b** causes it to be much less populated than **16a** wherein the hydrogen is placed *syn* to the carbonyl group to avoid  $A^{(1,2)}$  interaction.

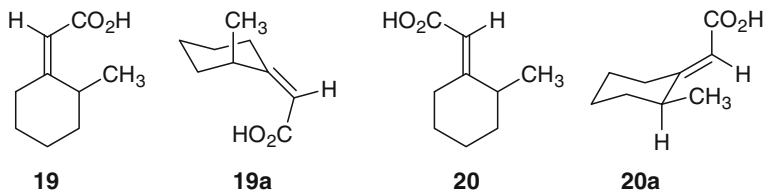


#### 4 A<sup>(1,3)</sup> Strain

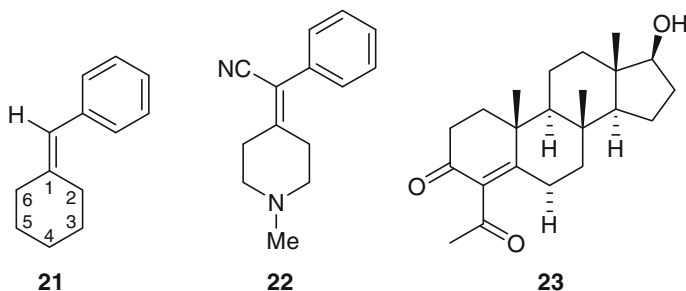
With  $R^1 = H$  and  $R^2 = CH_3$  in **2**, the conformer **2a** is more stable than the conformer **2c** by  $0.90 \text{ kcal mol}^{-1}$  at  $6-31G^*$  level of Hartree-Fock theory, respectively. This result may be taken to understand that the A<sup>(1,3)</sup> interaction in the conformer **2a** is not significant enough to subvert the conformer distribution in favor of **2c**.

With  $R^1 = R^2 = CH_3$  in **2**, the total energy difference between **2a** and **2c** is  $3.71 \text{ kcal mol}^{-1}$  at the  $6-31G^*$  level of the Hartree-Fock theory. The energy of the conformer **2c** with the methyl group axial is lower than the energy of the conformer **2a** with the methyl group equatorial. Were the 1,3-diaxial interaction of the  $CH_3$  group in **2c** (one such interaction raises the energy by  $0.9 \text{ kcal mol}^{-1}$ ) absent, its energy would be lower than that of **2a** by  $-(3.71 + 1.80) = -5.51 \text{ kcal mol}^{-1}$ . Thus, the  $CH_3-CH_3$  interaction energy in **2a** will compute to  $5.51 \text{ kcal mol}^{-1}$ . Clearly, with the increase in the bulk of either  $R^1$  or  $R^2$  or both, the conformer **2c** will be favored. Since the conformer **2a** is also stabilized by hyperconjugative interactions arising from the axial  $\sigma_{C-H}$  bonds on the allylic carbons, the A<sup>(1,3)</sup> interaction must be somewhat larger than even the above value.

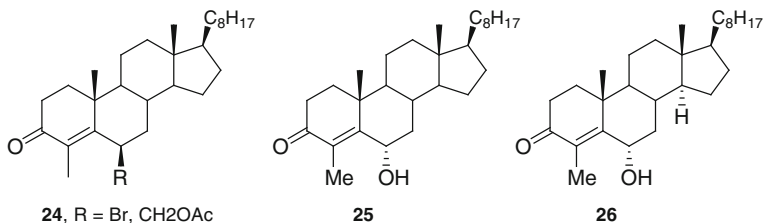
NMR studies have revealed that *syn*-2-methylcyclohexylideneacetic acid **19** exists predominantly as the conformer **19a** with the methyl group axial, whereas the corresponding *anti*-isomer **20** adopts predominantly the conformer **20a** with the methyl group equatorial [17].



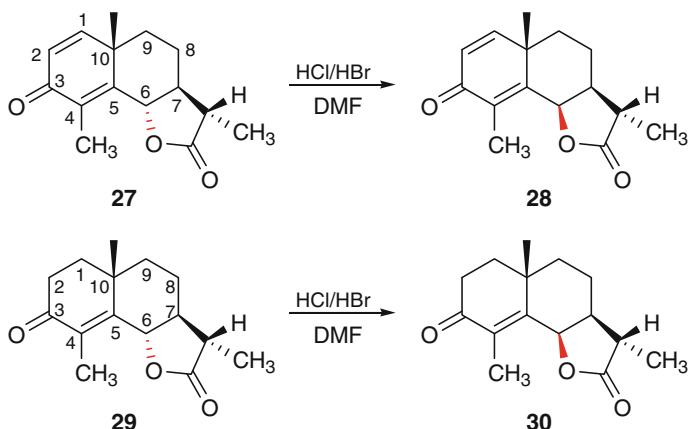
The phenyl group in **21** is twisted out of the plane of the double bond by  $\sim 52^\circ$  in an apparent attempt to avoid steric interaction that would otherwise result between the phenyl group and the equatorial hydrogen atom on C2 if the phenyl group were planar with the  $\pi$  bond. Such a subtle but definite manifestation of A<sup>(1,3)</sup> strain was indeed demonstrated in instances such as **22** and **23**. The phenyl group in **22** [18] and the acetyl group in **23** [19] were found from ultraviolet measurement studies to be twisted out of the plane of the  $\pi$  bond to varying degrees [18, 19]. The phenyl group in **22** is twisted out of the plane of the  $\pi$  bond by  $63^\circ$  at the 6-31G\* level of the Hartree-Fock theory.



From examination of a number of 6-substituted 4-methylcholest-4-enes, it was noted that the isomerization of **24** (R = Br/CH<sub>2</sub>OAc), through hydrolysis of the corresponding dienol acetates, failed and that only the 6 $\beta$ -isomer was recovered [20]. Also, an attempted isomerization of **24** (R = Br) on treatment with hydrogen chloride in glacial acetic acid returned only the starting isomer. In contrast, the 6 $\alpha$ -hydroxy species **25** isomerized completely to the 6 $\beta$ -hydroxy species **26** when simply left in contact with silica gel. The lability of the 6 $\alpha$ -isomer is apparently due to the significant A<sup>(1,3)</sup> interaction between the methyl group at C4 and the  $\alpha$  substituent on C6.



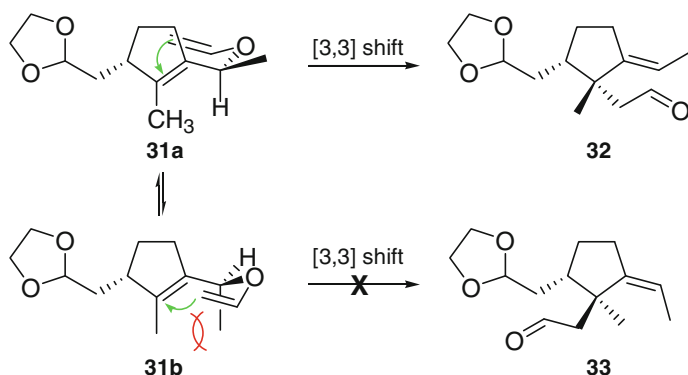
A solution of hydrogen chloride or hydrogen bromide in dimethylformamide causes smooth isomerization of (–)- $\alpha$ -santonin, **27**, into santonin-C, **28**. Likewise,  $\alpha$ -dihydrosantonin, **29**, also isomerizes to **30**. Although the conversion of the *trans*-lactone to *cis*-lactone itself is an exothermic process, a good part of the driving force for these isomerizations must come from A<sup>(1,3)</sup> strain that exists between the C4-methyl group and the C6-equatorial oxygen substituent since the products **28** and **30** themselves have a fairly strong 1,3-diaxial interaction between the C6-axial oxygen atom and the C10-axial methyl group.



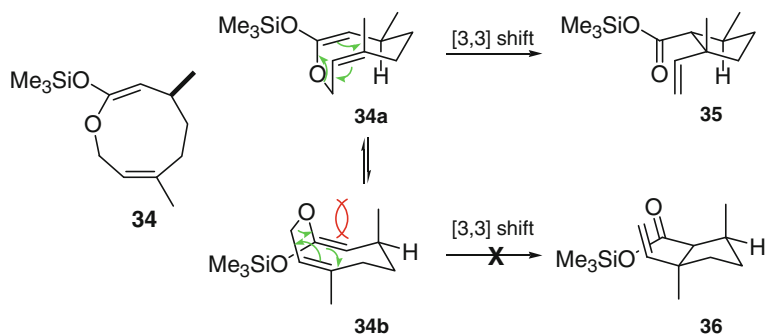
## 5 Stereocontrol in Reactions on Account of A<sup>(1,3)</sup> Strain

A<sup>(1,3)</sup> strain is capable of stabilizing/destabilizing the transition state of a reaction and thus influencing the product distribution. The compound **31** can organize in two different ways, **31a** and **31b**, to undergo [3,3] sigmatropic shift to generate **32** and **33**, respectively. However, since the transition state resembling **31b** is of higher energy than the transition state resembling **31a** due to the A<sup>(1,3)</sup> strain between the two methyl groups as shown, the reaction funnels through **31a** and **32** is formed

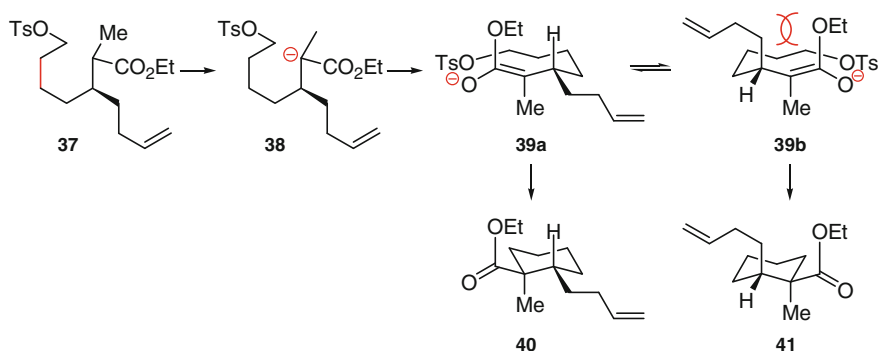
exclusively [21]. Thus, one of the two faces of the alkene in the allyl unit reacts in preference to the other face.



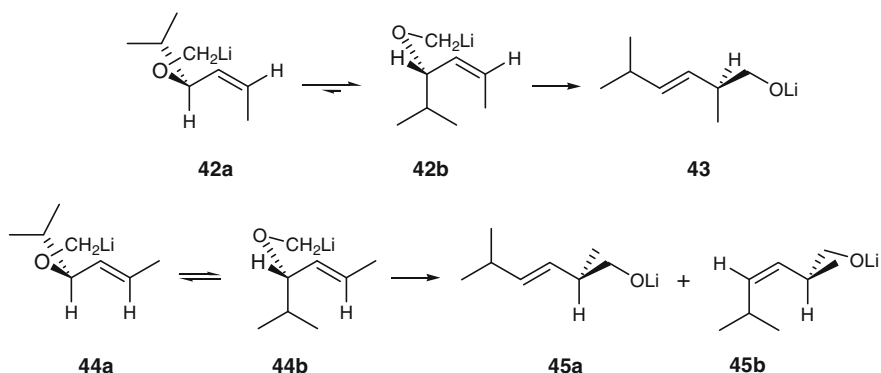
The Claisen rearrangement of **34** proceeds through a transition state resembling **34a** to generate **35**, wherein the two methyl substituents on the resultant cyclopentane ring are *syn* oriented. The transition state resembling **34b** encounters  $A^{(1,3)}$  strain between a methyl substituent and the oxygen of the vinyl ether unit as shown and, thus, the product **36** is not formed. Note that the two methyl substituents are now *anti* oriented [22, 23].



$A^{(1,3)}$  strain determines the degree of selectivity in the intramolecular alkylation of **37**. The enolate formed from the carbanion **38** can adopt the two different transition state conformations **39a** and **39b**, leading to **40** and **41**, respectively. However, the transition state resembling **39b** is destabilized by  $A^{(1,3)}$  interaction between the 3-butenyl group and either the ethoxy group (as shown) or the oxy anion in the *Z*-enolate (not shown) by virtue of being *cis* to each other. The transition state resembling **39a** is therefore favored over the transition state resembling **39b** and it leads to the diastereoisomer **40** predominantly [24].

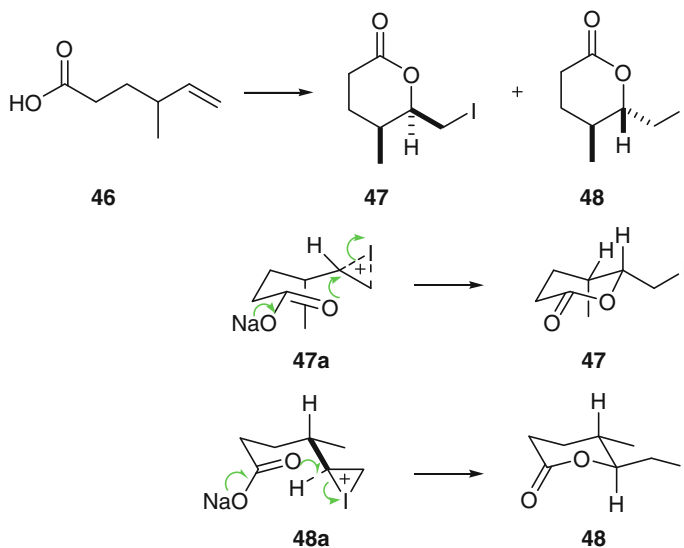


[2,3] Sigmatropic rearrangement proceeds through a conformationally flexible five-membered cyclic transition state and, hence, it is difficult to attain high stereocontrol. In certain instances, however, the use of A<sup>(1,3)</sup> strain may be the only reliable way to achieve a high level of diastereoselection. Accordingly, the level of chirality transfer from the allylic carbon in the reactant to the allylic carbon in the product was discovered to increase from an (*E*)-allylic system to the corresponding (*Z*)-allylic system, as evident from the reactions of **42** and **44** [25, 26]. The species **42** reacted with full diastereocontrol and **43** was formed as the sole product. In contrast, the species **44** was transformed into a 50:50 mixture of two products **45a** and **45b**. The conformer **42b** is destabilized because of the A<sup>(1,3)</sup> strain between the Me and isopropyl substituents and, hence, its concentration at equilibrium is negligible. Only the conformer **42a** is available for the reaction and the product **43** is formed exclusively. The conformers **44a** and **44b** contribute equally due to lack of A<sup>(1,3)</sup> strain. These conformers therefore react with equal ease to generate **45a** and **45b**, respectively.

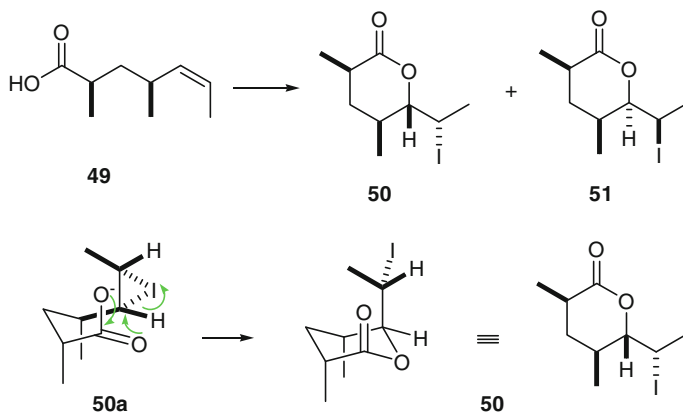


Iodolactonization is often used to functionalize a double bond with the generation of a new stereocenter. Kinetically controlled iodolactonization (I<sub>2</sub>, CH<sub>3</sub>CN,

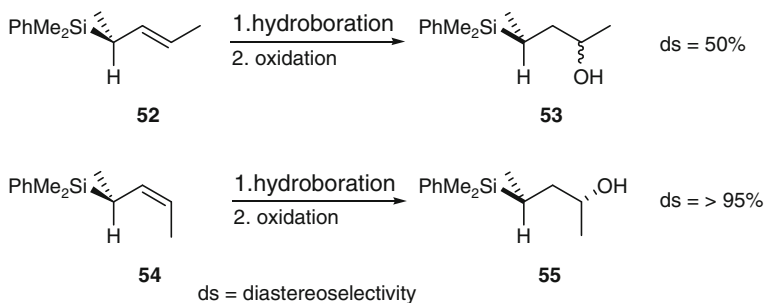
$\text{NaHCO}_3$ ,  $0\text{ }^\circ\text{C}$ ) of **46** resulted in a 70:30 mixture of **47** and **48** [27, 28]. The major product **47** is formed through the six-membered cyclic transition state wherein the iodonium ion is formed under the steric guidance of the methyl substituent, i.e., on the anti face of the double bond as in **47a**. The minor product **48** could be envisioned to be derived from the transition state resembling **48a**. The transition state **47a** is favored over the transition state **48a** on account of the absence of  $A^{(1,3)}$  strain for having the methyl substituent oriented axial, though the strain is small.



In comparison, the iodolactonization of **49** proceeds with very high diastereoselectivity and a 95:5 mixture of the products **50** and **51** is obtained [27, 28]. The diastereoselectivity is tightly controlled by  $A^{(1,3)}$  strain between the methyl group on the terminal olefinic carbon and the other methyl group on the allylic carbon so much so that it allows the reaction to proceed primarily through the transition state **50a**.



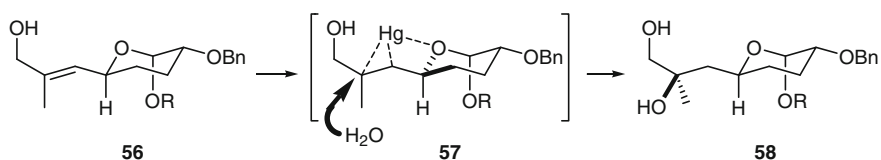
The hydroboration of a double bond next to a stereocenter results in high diastereoselectivity when one of the groups at the stereocenter shields one side of the double bond effectively. It requires fixation of the conformation around the bond between the stereocenter and the double bond. A<sup>(1,3)</sup> strain plays an important role as demonstrated from the reactions of **52** and **54** [29, 30]. The cooperative effect of both the bulk and the stereoelectronic effect of the dimethylphenylsilyl group ( $\sigma_{\text{C-Si}}$  orients perpendicular to the  $\pi$  bond for an effective  $\sigma_{\text{C-Si}}-\pi^*$  interaction) allows selective attack on one face of the olefin. Possibly, the A<sup>(1,3)</sup> strain rigidifies the conformation as in **54** and then the large bulk of the dimethylphenylsilyl group directs the reagent to the opposite less hindered side of the double bond. With the bulky 9-BBN as the hydroboration reagent, high asymmetric induction can be achieved with the *E*-olefins also [29, 30].



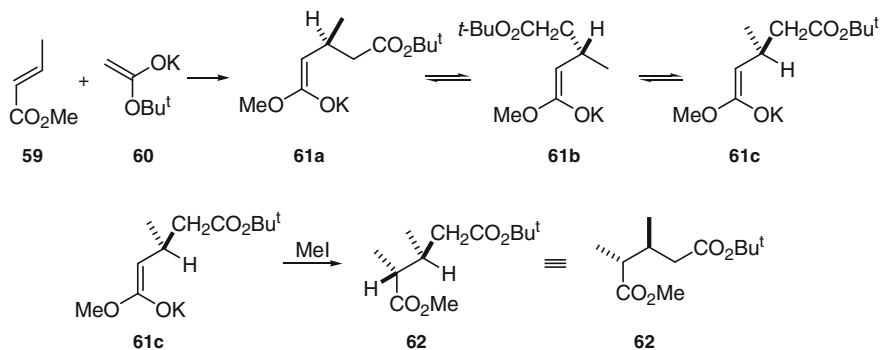
The allyl alcohol **56** furnished **58** predominantly on oxymercuration in aqueous tetrahydrofuran followed by reductive demercuration using  $\text{NaBH}_4$  [31]. Assisted by chelation with both the ring oxygen and the carbinol function, mercuration on the  $\alpha$ -face allows water to approach from the  $\beta$ -face, as shown in **57**, to form the product **58** selectively. In aligning the methyl group on the double bond with the



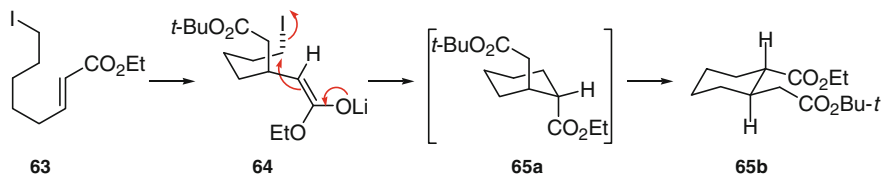
axial hydrogen on the allylic ring carbon, the molecule in conformation **56** avoids A<sup>(1,3)</sup> strain.



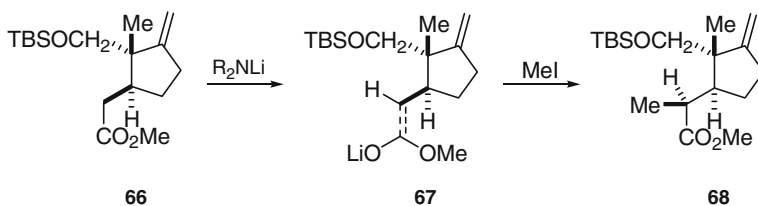
An admixture of the unsaturated ester **59** with the K-enolate **60** generates yet another K-enolate, which could exist as a mixture of the conformers **61a**, **61b** and **61c**. On account of A<sup>(1,3)</sup> interaction between either of the substituents, except hydrogen, on the allylic carbon and the solvated OK (or even OMe if one considers the other geometry of the enolate), the conformer **61c** will be considered to be the most stable. In **61c**, the  $\sigma_{\text{C-H}}$  at the allylic carbon is nearly cisoid to the double bond of the enolate to avoid A<sup>(1,3)</sup> strain. The electrophile, MeI in the present instance, approaches the double bond from anti to the large  $\text{CH}_2\text{CO}_2\text{Bu}^t$  substituent and the predominant product **62** is formed [32].



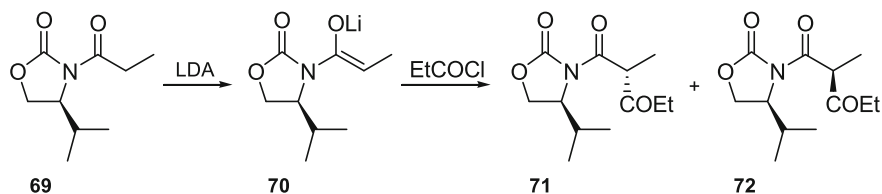
The Li-enolate formed from *tert*-butyl acetate reacts with the unsaturated ester **63** in a conjugate manner to generate an enolate, which must adopt the conformation **64** to avoid A<sup>(1,3)</sup> interaction between  $\text{CH}_2\text{CO}_2\text{Bu}^t$  and OEt in the *E*-enolate, as shown, or solvated OLi in the *Z*-enolate (not shown). The intramolecular S<sub>N</sub>2 reaction with the alkyl iodide through a transition state resembling **64** generates **65a**, which undergoes a quick ring flip to the more stable conformer **65b**. In the said transition state, the axis of the p orbital on the internal olefinic carbon of the enolate must be parallel to  $\sigma_{\text{C-I}}$  bond for a proper S<sub>N</sub>2 attack. The *trans* disposition of the two ring substituents may please be noted [33].



The Li-enolate of **66** adopts the conformation **67** in which the  $\pi$  bond is almost *syn* to  $\sigma_{C-H}$  on the adjacent ring carbon to avoid the otherwise strong A<sup>(1,3)</sup> interaction with either of the two substituents on the quaternary ring carbon. Since one face of the enolate is blocked by this quaternary carbon, an electrophile like MeI approaches the enolate from the front, i.e., from the direction opposite to the quaternary carbon and **68** is formed exclusively [34].

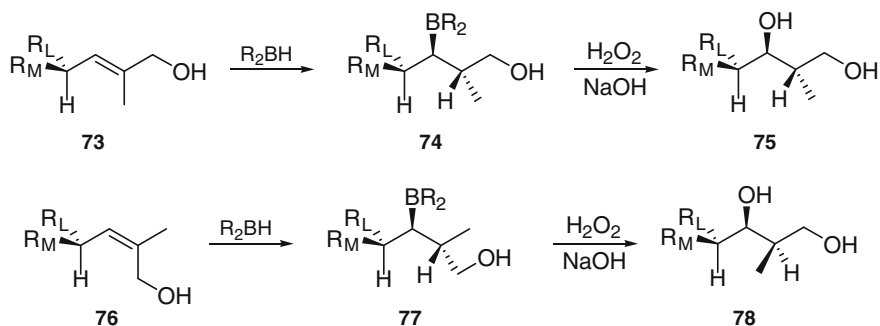


The alkylation of the lithium enolate formed from *N*-propanoyl-1,3-oxazolidinone **69** proceeds with very high selectivity to result primarily in a single diastereomer. The *Z*-enolate **70** is generated, in preference to the *E*-enolate, on reaction with LDA to avoid A<sup>(1,3)</sup> interaction between the methyl group on the olefinic bond and the isopropyl-containing substituent on the nitrogen. The predominant formation of the *Z*-enolate and the steric resistance offered by the isopropyl group to an electrophile in its approach from the top face control the transition state so very well that **71** and **72** are formed in 96:4 ratio on reaction with propanoyl chloride [35, 36]. The absolute stereochemistry of the product is thus determined by the absolute stereochemistry of the isopropyl-containing carbon of 1,3-oxazolidinone.

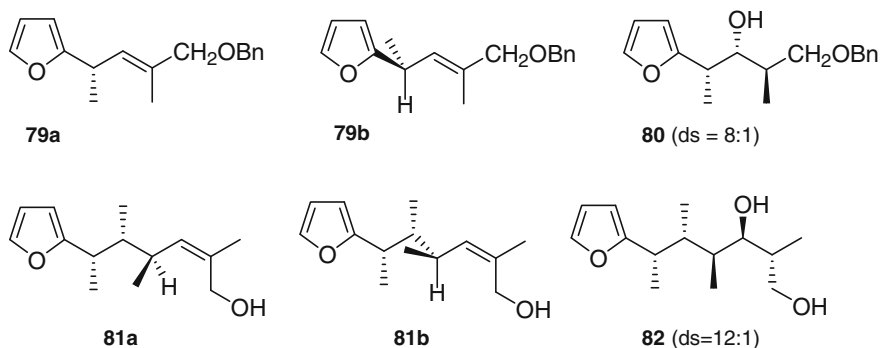


The consequences of A<sup>(1,3)</sup> strain could also be seen under hydroboration conditions. For instance, the conformations **73** and **76** are preferred to other

conformations to avoid the above strain in having the smallest substituent hydrogen in the plane of the double bond. Hydroboration is expected to proceed from the side of the medium size group to generate, after oxidative cleavage of  $\sigma_{C-B}$  bond, **75** and **78**, respectively. Please note that the hydroboration takes place in Markovnikov fashion whereby the boron is attached to the lesser substituted olefinic carbon.

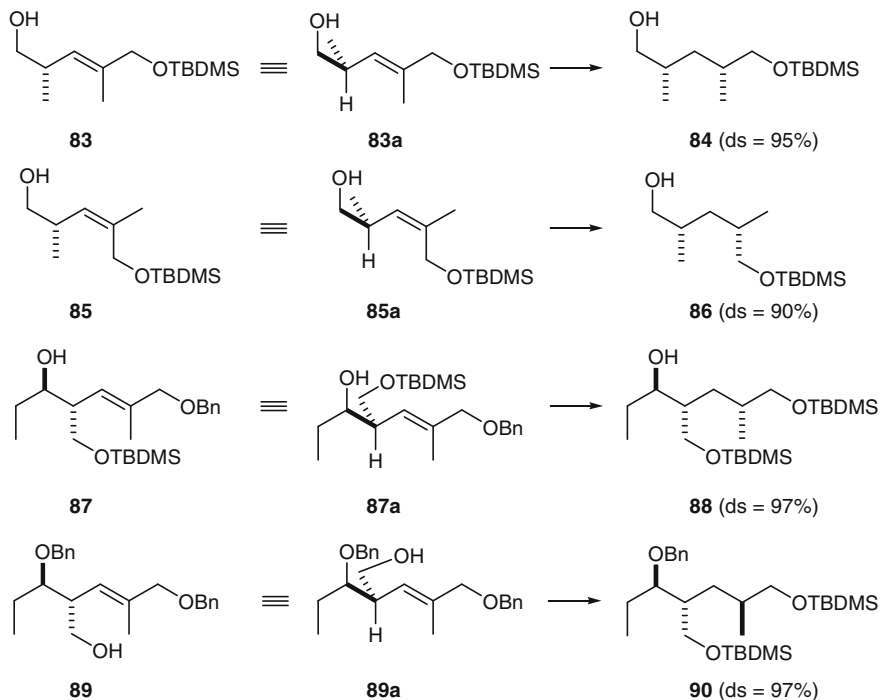


Indeed, **79a**, which must exist predominantly in the conformation **79b** to avoid A<sup>(1,3)</sup> strain with the methyl substituent on the olefinic carbon, allows approach of the hydroboration reagent on the face *syn* to the methyl substituent on the allylic carbon and, thus, the product **80** is formed with a selectivity of 8:1 after oxidative cleavage of the  $\sigma_{C-B}$  bond. A similar analysis applies to **81** and guides us to consider **81b** as the conformer preferred to **81a**. Hydroboration *syn*-to-methyl on the allylic carbon followed by oxidative cleavage of the  $\sigma_{C-B}$  bond leads to **82** as the predominant product. Indeed, **82a** and **82b** are formed in 12:1 diastereoisomeric ratio [37].

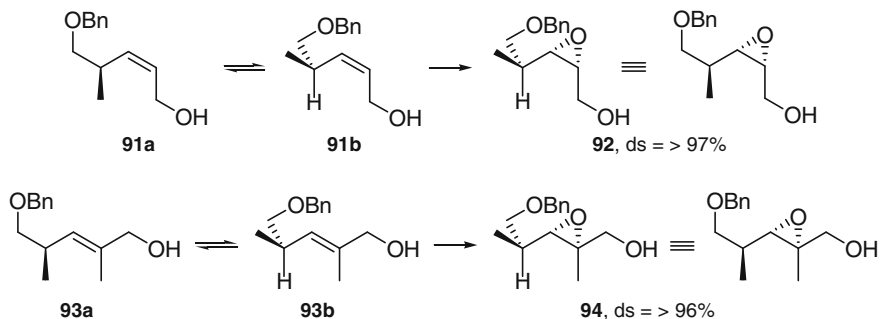


Having controlled the preferred geometry of an allylic system, A<sup>(1,3)</sup> strain influences the stereochemistry of catalytic hydrogenation of substituted allylic alcohols in a manner that is analogous to the control by A<sup>(1,2)</sup> strain. With the prior

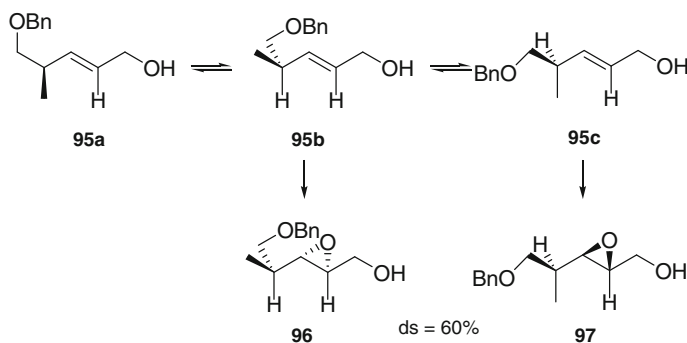
coordination of the carbinol function with the metal catalyst, Rh(Diphos-4)<sup>+</sup>, the observed high diastereoselectivities of the transformations of **83**, **85**, **87** and **89** into **84**, **86**, **88** and **90**, respectively, can be easily understood. The conformers **83a**, **85a**, **87a** and **89a** constitute the reacting conformers that are also free from A<sup>(1,3)</sup> strain.



In tune with hydroboration and hydrogenation above, A<sup>(1,3)</sup> strain controls the diastereoselectivity of epoxidation reaction as well by exercising control on the preferred conformer distribution. The direction of epoxidation by *m*-CPBA is also controlled through additional coordination of the peracid to a nearby ether group. For instance, conformational equilibrium between **91a** and **91b** favors **91b** in order to avoid A<sup>(1,3)</sup> strain by virtue of having the  $\sigma_{C-H}$  bond *syn* to the CH<sub>2</sub>OH group. Coordination of *m*-CPBA with the ethereal oxygen followed by delivery of the peroxygen from the face *syn* to it allows formation of the epoxide **92**. Likewise, **93** exists predominantly in the conformer **93b** to avoid A<sup>(1,3)</sup> interactions between methyl and methyl, and also methyl and CH<sub>2</sub>OBn. Coordination-controlled epoxidation leads to the formation of **94** with >96 % diastereoselectivity.

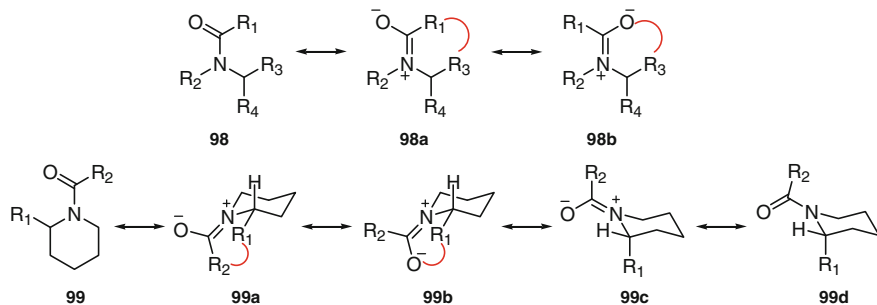


The  $A^{(1,3)}$  strain in *trans*-olefins is not as high as in *cis*-olefins. Accordingly, the conformer **95c** competes well with the conformer **95b** at the equilibrium and coordination-controlled delivery of peroxygen generates a mixture of the epoxides **96** and **97** with an overall 60 % diastereoselectivity.

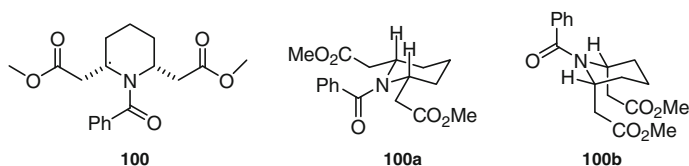


## 6 $A^{(1,3)}$ Strain in Amides and Its Consequences on Diastereoselectivity

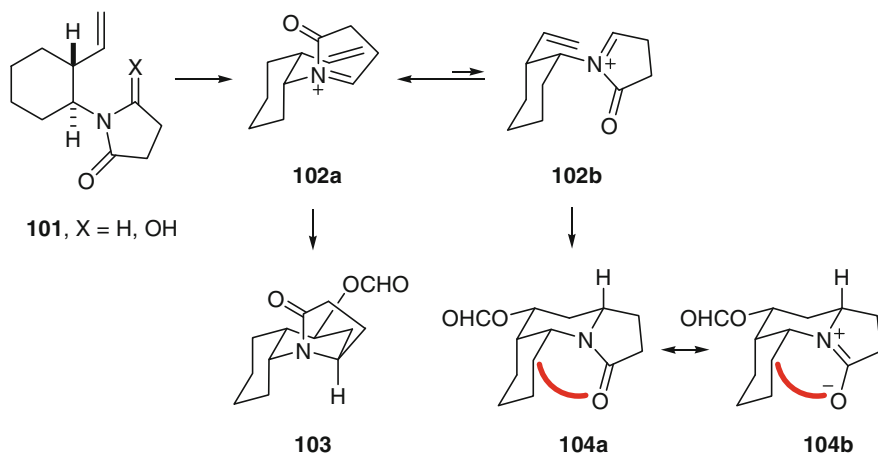
$A^{(1,3)}$  strain is experienced by amides as well. This is on account of the conjugation of the lone pair of electrons on nitrogen with the carbonyl function to generate enolate-like species such as **98a** and **98b** from **98**. The  $A^{(1,3)}$  interactions present in these species are as shown. When applied to cyclic systems such as **99**, the conformers **99a** and **99b**, both with the substituent  $R_1$  equatorial, are expected to suffer from intense  $A^{(1,3)}$  strain, so much so that the conformer **99c**, which is equivalent to **99d**, turns out to be the most favored conformer.



The A<sup>(1,3)</sup> strain experienced by amides is so very strong that the *cis*-2,6-disubstituted amide **100** exists exclusively as the conformer **100b**. In this conformer, both the CH<sub>2</sub>CO<sub>2</sub>Me substituents are axial, which leads to strong 1,3-diaxial interactions. Apparently, the overall raise in energy due to the 1,3-diaxial interactions in **100b** is still less than the A<sup>(1,3)</sup> strain present in **100a** [38].



Treatment of **101** with formic acid furnished the tricyclic lactam **103** exclusively [39]. The cyclization proceeds through an *N*-acyliminium ion, which can adopt either of the conformations **102a** and **102b**. The transformation **102a** → **103** is faster than the transformation **102b** → **104a** owing to the development of A<sup>(1,3)</sup> strain in the latter product. Upon mixing of the electron pair on nitrogen with the  $\pi$ -electrons of the adjacent carbonyl group, we arrive at the double bond in **104b**. The oxy anion and the methylene group of the non-nitrogen-containing ring, as shown in **104b**, are close enough to result in serious A<sup>(1,3)</sup> interactions. Consequently, the equilibrium between **102a** and **102b** is expected to largely favor **102a**.



There are many examples of other reaction types that proceed with high level of selectivity on account of allylic strain. The reader is directed to an exhaustive review [40] and other sources [41] for more detailed studies.

## References

1. Beckett CW, Freeman NK, Pitzer KS (1948) *J Am Chem Soc* 70:4227
2. Lindsay JM, Barnes WH (1955) *Acta Cryst* 8:227
3. Carlisle CH, Crowfoot D (1945) *Proc Roy Soc (Lond)* 64:A184
4. Garbisch EW Jr (1962) *J Org Chem* 27:4249
5. Beckett AH, Casy AF, Iorio MA (1966) *Tetrahedron* 22:2745
6. Beckett AH, Casy AF, Youssef HZ (1965) *Tetrahedron Lett* 537
7. Casy AF, Beckett AH, Iorio MA, Youssef HZ (1966) *Tetrahedron* 3387
8. de la Mare PB, Johnson MD, Lomas JS, del Olmo VS (1966) *J Chem Soc B* 827
9. Williamson WRN (1958) *Tetrahedron* 3:31
10. Johnson F, Whitehead A (1964) *Tetrahedron Lett* 3825
11. Malhotra SK, Johnson F (1965) *Tetrahedron Lett* 4027
12. Malhotra SK, Johnson F (1965) *J Am Chem Soc* 87:5513
13. Subramaniam G, Malhotra SK, Reingold HJ (1966) *J Am Chem Soc* 88:1332
14. Stork G, Burgstahler AW (1955) *J Am Chem Soc* 77:5068
15. Wintersteiner O, Moore M (1965) *Tetrahedron* 21:779
16. Brown JM (1987) *Angew Chem Int Ed Engl* 26:190
17. Hauth H, Stauffacher D, Nicklaus P, Melera A (1987) *Helv Chim Acta* 1965:48
18. Lee CM, Beckett AH, Sugden JK (1966) *Tetrahedron Lett* 272
19. Gorodetsky M, Mazur Y (1964) *J Am Chem Soc* 86:5213
20. Shoppee CW, Johnson FP, Lack RE, Rawson RJ, Sternhell S (1965) *J Chem Soc* 2476
21. Takahashi T, Yamada H, Tsuji J (1982) *Tetrahedron Lett* 23:233
22. Abelman MM, Funk RL, Munger JD Jr (1982) *J Am Chem Soc* 104:4030
23. Beslin P, Perrio S (1989) *J Chem Soc Chem Commun* 414
24. Ahn SH, Kim D, Chun MW, Chung W-K (1986) *Tetrahedron Lett* 27:943
25. Nakai T, Mikami K (1986) *Chem Rev* 86:88

26. Chan KK, Saucy G (1977) *J Org Chem* 42:3828
27. Bartlett PA, Richardson DP, Meyerson J (1984) *Tetrahedron* 40:2317
28. Williams DR, Osterhout MH, McGill JM (1989) *Tetrahedron Lett* 30:1327
29. Fleming I (1988) *Pure Appl Chem* 60:71
30. Fleming I, Lawrence NJ (1988) *Tetrahedron Lett* 29:2077
31. Isobe M, Ichikawa Y, Goto T (1985) *Tetrahedron Lett* 26:5199
32. Yamaguchi M, Tsukamoto M, Hirao I (1984) *Chem Lett* 375
33. Yamaguchi M, Tsukamoto M, Hirao I (1985) *Tetrahedron Lett* 26:1723
34. Hutchinson JH, Money T (1986) *Chem Commun* 288
35. Evans DA, Ennis MD, Le T (1984) *J Am Chem Soc* 106:115
36. Evans DA, Clark JS, Metternich R, Novack VJ, Sheppard GS (1990) *J Am Chem Soc* 112:866
37. Schmid G, Fukuyama T, Kishi Y (1979) *J Am Chem Soc* 101:259
38. Quick J, Mondello C, Humora M, Brennan T (1978) *J Org Chem* 43:2705
39. Hart DJ, *Am J* (1980) *Chem Soc* 102:397
40. Hoffmann RW (1841) *Chem Rev* 1989:89
41. <http://euch6f.chem.emory.edu/allylicstrain.html>



# Chapter 5

## The Conservation of Orbital Symmetry (Woodward–Hoffmann Rules)

**Abstract** A discussion on conservation of orbital symmetry and its application to select pericyclic reactions is presented. Initially, effort is made to explore the symmetry characteristics of the  $\sigma$ ,  $\sigma^*$ ,  $\pi$  and  $\pi^*$  molecular orbitals (MOs). This is followed by a description of the MOs and their symmetry characteristics for allyl cation, allyl radical, allyl anion, and 1,3-butadiene. This concept is applied to  $\pi^2 + \pi^2$ ,  $\pi^4 + \pi^2$  (Diels–Alder) and electrocyclic reactions.

**Keywords** Conservation of orbital symmetry rules · Mirror plane symmetry ·  $C_2$  symmetry ·  $\pi^2 + \pi^2$  reaction · Electrocyclic reactions ·  $\pi^4 + \pi^2$  reaction

### 1 Introduction

In the projected synthesis of vitamin B<sub>12</sub>, the plan called for the construction of a key intermediate by the stereospecific cyclization of a stereochemically well-defined 1,3,5-triene to the corresponding 1,3-cyclohexadiene. From the inspection of molecular models, Woodward and his colleagues were confident that the minimization of angle strain coupled with appropriate orbital overlap would favor a conrotatory cyclization. While the reaction was indeed found to be highly stereospecific, it took the disrotatory path instead. To explain the observed contradiction, it was necessary to recognize a new control element that Woodward and Hoffmann christened ‘conservation of orbital symmetry’ [2, 3].

*Reactions occur readily when there is congruence between the orbital symmetry characteristics of the reactants and the products, and only with difficulty when that congruence does not obtain.* In other words, the orbital symmetry is conserved in concerted reactions. How exactly is the orbital symmetry conserved and what are its further ramifications are important issues which we will examine in detail by considering a few examples. For a better grasp of the subject, let us first understand orbitals and their interactions in relation to  $\pi$  and  $\sigma$  bond formation.

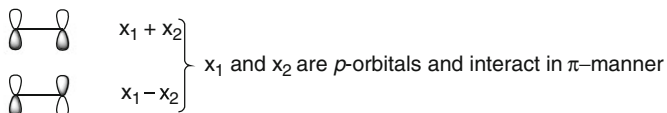
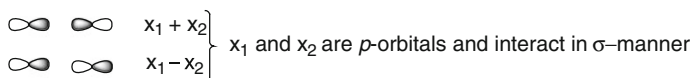
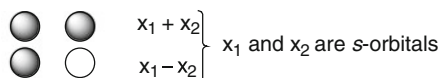
## 2 Orbitals and Symmetry Considerations

A  $\pi$  bond is formed from the overlap of two  $p$  orbitals that are adjacent and parallel to each other across a  $\sigma$  bond, and a  $\sigma$  bond is the result of coaxial approach of two atomic orbitals such as  $s$  and  $s$ ,  $s$  and  $p$ , and  $p$  and  $p$ . A molecular orbital (MO) is the result of a linear combination of the constituent atomic orbitals and each MO can then be populated by a maximum of two electrons. For a total of  $n$  atomic orbitals, there shall be  $n/2$  bonding and an equal number of anti-bonding MOs with  $n$  being an even number. With  $n$  being an odd number, there shall be  $(n - 1)/2$  bonding MOs with an equal number of anti-bonding MOs and one nonbonding orbital.

If  $x_1$  and  $x_2$  are two atomic orbitals,

- $x_1 + x_2$  shall represent the bonding combination characterized by positive overlap with maximum electron density localized in the region between the two nuclei, and
- $x_1 - x_2$  shall represent the anti-bonding combination characterized by negative overlap with a nodal plane in the region between the two nuclei where the electron density is nil.

For example,

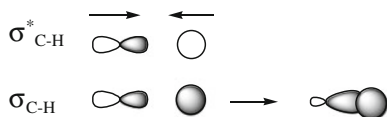


Because an orbital is a mathematical representation of a wave function and because multiplying an entire wave function by  $-1$  does not change its energy characteristics, overlap of a minus lobe with another minus lobe is precisely the same as the overlap of a plus lobe with another plus lobe, i.e.,  $x_1 + x_2$  is the same bonding MO as the bonding MO represented by  $-x_1 - x_2$ . In the construction of a  $\sigma$  bond from the overlap of two  $p$  orbitals, this shall be represented as follows:



The overlap of a hydrogen  $s$  orbital with a carbon  $p$  orbital to result in  $\sigma_{\text{C-H}}$  and  $\sigma_{\text{C-H}}^*$  MOs shall be represented as follows. Here, it must be made very clear that two

$sp^3$  hybrid orbitals may also combine to result in either a  $\pi$  bond or a  $\sigma$  bond, depending upon whether they approach parallel or collinear to each other.



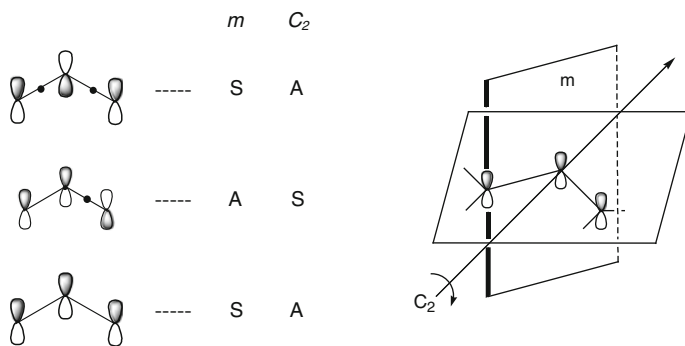
In understanding the principle of conservation of orbital symmetry, we ought to comprehend various MO levels in a chemical entity and their symmetry properties in terms of selected symmetry operators. For the sake of discussion, let us consider the simple molecule of ethylene, which has four  $\sigma_{C-H}$  bonds, one  $\sigma_{C-C}$  bond, and one  $\pi_{C=C}$  bond. The four  $\sigma_{C-H}$  bonds are undoubtedly of equal energy and, hence, they are placed at a single energy level. Because the energy of a  $\sigma_{C-C}$  bond is expected to be only a little different from that of a  $\sigma_{C-H}$  bond, the  $\sigma_{C-C}$  level may also be placed at the  $\sigma_{C-H}$  level. Corresponding to these five bonding  $\sigma$  levels, we shall have five anti-bonding levels which we designate as  $\sigma^*$ . For the remaining  $\pi_{C=C}$  bond, we shall have both the bonding  $\pi$  and the anti-bonding  $\pi^*$  levels. On the energy scale, the  $\pi$  level is higher than the  $\sigma$  level in the bonding domain but lower in the anti-bonding domain. Given below is a graphical representation of this analysis. The symmetry properties of all the MOs (bonding and anti-bonding) in respect of two symmetry elements, namely mirror plane  $m$  and  $C_2$  axis, are also given.

It should be remembered that (a) a mirror plane  $m$  is a plane which is perpendicular to the plane of the molecule/orbital and also bisects it and (b) a  $C_2$  axis of symmetry is a line that bisects the molecule/orbital through the center and is in plane with it. We will understand these more by considering the symmetry properties of the MOs of an allyl system.

			$m$	$C_2$
$\sigma^*$		-----	A	A
$\pi^*$		----	A	S
$\pi$		----	S	A
$\sigma$		-----	S	S

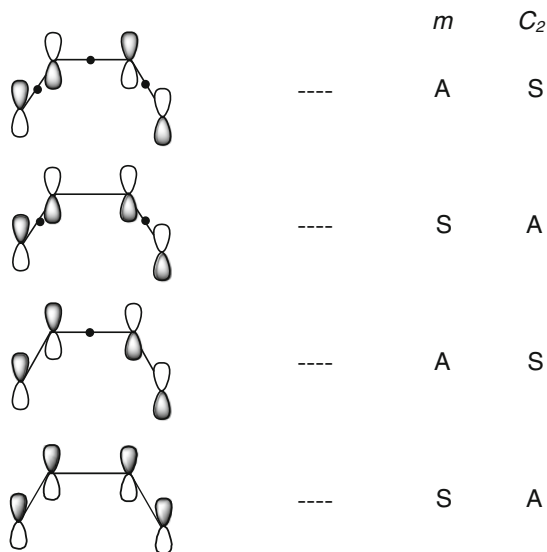
MOs of ethylene and their symmetry characteristics  
(A = antisymmetric, S = symmetric)

Consider all the three carbons in the plane of the paper with the  $p$  orbitals perpendicular to it. All the substituents are therefore in the same plane as the carbons by virtue of resonance present in such systems. The mirror plane is orthogonal to the plane of the paper and passes through the central carbon atom. The mirror plane shall therefore be parallel to the  $p$  orbitals on either side. The  $C_2$  axis also passes through the central carbon atom and it is in the plane of the paper. The  $C_2$  axis is therefore orthogonal to the plane of the  $p$  orbitals and, hence, to the  $\pi$  bond. If the reflection to the right of an orbital on the left side of a mirror is the same, the orbital is said to be symmetric. In the absence of such a relationship, the orbital is called antisymmetric. In order to determine the symmetry properties with respect to a  $C_2$  axis, the MO in question is rotated, clockwise or anticlockwise, around this axis by  $180^\circ$  to see whether or not the same MO is generated. In the former event, i.e., when the same MO is received back, it is said to be symmetric. The antisymmetric situation arises otherwise. Very clearly, a MO that is symmetric with respect to a mirror plane is antisymmetric with respect to a  $C_2$  axis and vice versa. Also, the symmetry characteristic with respect to a given symmetry element alternates in going from the lowest lying energy level to the highest one.



MOs of the allylic system (cation, anion and radical) and their symmetry characteristics

Two electrons in the lowest orbital with the other two levels empty is what characterizes an allyl cation. Allyl radical has an additional one electron in the middle orbital and the same shall possess two electrons in an allyl anion. In all of these, the highest level is always empty in the ground state of the species.



MOs of 1,3-butadiene and their symmetry characteristics

We are now well equipped to consider the various MOs and the symmetry characteristics present in *s-cis*-butadiene. The two  $\pi$  bonds are comprised of four atomic  $p$  orbitals, their allowed combinations give rise to a set of four MOs, two bonding and two anti-bonding. These MOs and their symmetry properties with respect to two symmetry elements, namely  $m$  and  $C_2$ , are given below.

Once again, it should be noted that the symmetry of the orbital alternates and also the energy increases with the increase in the number of nodes. In moving from the lowest MO to the highest MO, the nodes increase in number from 0 to 3. These nodal points are shown by thick dots along the C–C bonds. The symmetry properties with respect to one symmetry element are clearly opposite to the symmetry properties with respect to the other symmetry element. In the ground state 1,3-butadiene, the lower two MOs are filled by two electrons each and the higher two levels are empty.

### 3 $\pi^2 + \pi^2$ Reaction

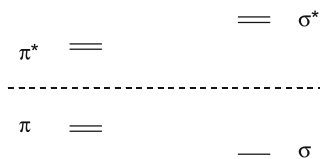
We are now equipped to consider a pericyclic reaction to see how best we can accommodate the principle of conservation of orbital symmetry. For this, we shall associate the relevant reactant orbitals and the product orbitals with a certain symmetry element. Let us first consider the  $\pi^2 + \pi^2$  [2 + 2] reaction of two simple ethylene molecules to form cyclobutane as shown below. We create two  $\sigma$  bonds in the product at the expense of two  $\pi$  bonds in the reactants. The energy level

correlation is as follows. The  $\sigma$  and  $\sigma^*$  and also the  $\pi$  and  $\pi^*$  levels are equidistant from the nonbonding level.



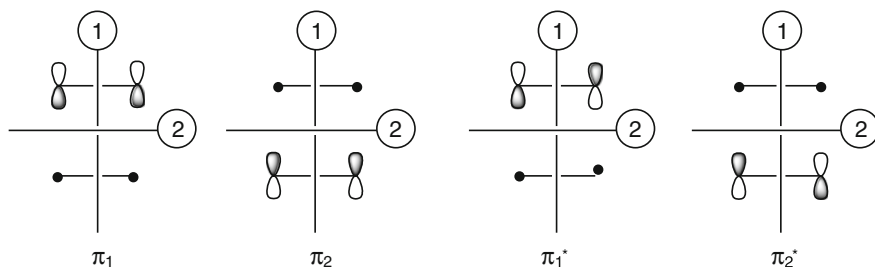
$\pi^2 + \pi^2$  reaction of two alkenes to form cyclobutane

A pericyclic reaction is a reaction wherein the transition state has a cyclic geometry and the reaction progresses in a concerted fashion, i.e., the breaking of some bonds and the formation of some other bonds take place simultaneously without any discrete intermediate being ever involved. The reactant passes through a single transition state and falls to the product. The major classes of pericyclic reactions are electrocyclic reactions such as the transformation of 1,3-butadiene to cyclobutene, cycloadditions such as  $\pi^2 + \pi^2$  and  $\pi^4 + \pi^2$  reactions and sigmatropic shifts such as [1,5]-hydrogen shift. In general, these reactions are considered to be equilibrium processes. However, it is possible to push the reaction in one direction by designing a reactant whose product is at a significantly lower energy level than the reactant itself.

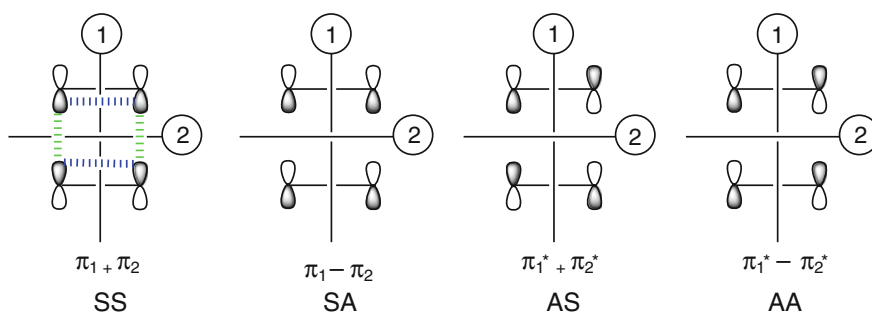


Approximate energy levels of the MOs involved. The dashed horizontal line is the nonbonding level which is approximately the same as that of a free 2p orbital with one electron in it. The two  $\pi$  and  $\sigma$  levels, both bonding and antibonding, will be the same for ethylene and other symmetrically substituted alkenes but slightly different for unsymmetrical alkenes.

The two localized  $\pi$  bonds,  $\pi_1$  and  $\pi_2$ , of the two reactant ethylene molecules are shown below. Corresponding to these, there are the  $\pi_1^*$  and  $\pi_2^*$  levels, also shown below. The orbital cross section is shown in the plane of the paper.



Let us now consider the MOs of two ethylene molecules approaching each other. Knowing well that an anti-bonding level shall not mix with a bonding level, there can be a total of four combinations in all: the plus (+) and minus (-) combinations of the two bonding levels, i.e.,  $\pi_1 + \pi_2$  and  $\pi_1 - \pi_2$ , respectively, and the plus and minus combinations of the two anti-bonding levels, i.e.,  $\pi_1^* + \pi_2^*$  and  $\pi_1^* - \pi_2^*$ , respectively. These combinations are shown below. For each combination, we shall consider two mirror plane symmetry elements represented by the encircled digits 1 and 2. As evident, the  $\pi_1 + \pi_2$  is symmetric with respect to the reflections in both the planes,  $\pi_1 - \pi_2$  is symmetric with respect to the reflection in mirror plane 1 but antisymmetric with respect to the reflection in mirror plane 2. From the anti-bonding combinations, while  $\pi_1^* + \pi_2^*$  level is antisymmetric with respect to the reflection in mirror plane 1 but symmetric with respect to the reflection in mirror plane 2, the  $\pi_1^* - \pi_2^*$  combination is antisymmetric with respect to both the mirror planes. These symmetry properties are given just below each combination. The first symmetry property is with respect to the mirror plane 1 and the second with respect to the mirror plane 2. It is important to recognize that on the energy scale, the  $\pi_1 + \pi_2$  combination shall be lower than the  $\pi_1 - \pi_2$  combination in the bonding region. Likewise, in the anti-bonding region, the combination  $\pi_1^* + \pi_2^*$  shall be lower than the combination  $\pi_1^* - \pi_2^*$ .

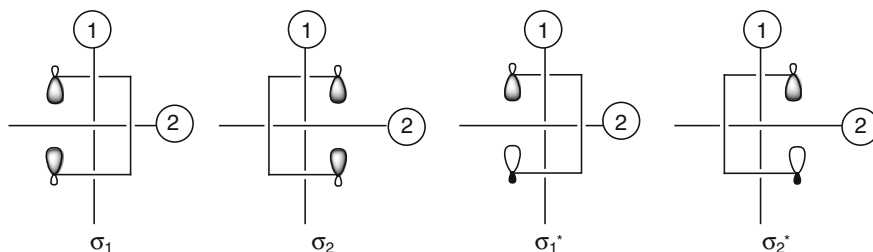


The criterion to make the above energy distinction is very simple. Think of the situation where the two  $\pi$  bonds have come close enough to begin some interaction for  $\sigma$  bond formation. For the  $\pi_1 + \pi_2$  combination, not only the interactions for the formation of both the  $\sigma$  bonds (vertical coaxial overlap shown by broken green lines) are constructive but the  $p$  orbitals are also properly disposed for constructive  $\pi$ -type overlap (horizontal blue lines) to result in the formation of  $\pi$  bonds. For the  $\pi_1 - \pi_2$  combination, the above two  $\sigma$ -type overlaps (green type) are absent. The  $\pi_1 + \pi_2$  situation is naturally more energy lowering than the  $\pi_1 - \pi_2$  situation and, thus,  $\pi_1 + \pi_2$  MO shall appear lower than  $\pi_1 - \pi_2$  MO on the relative energy scale. Likewise, in between the two anti-bonding combinations, both are devoid of  $\pi$ -type overlaps (being the anti-bonding levels). However,  $\pi_1^* + \pi_2^*$  benefits from two constructive  $\sigma$ -type overlaps but  $\pi_1^* - \pi_2^*$  does not. The combination  $\pi_1^* + \pi_2^*$  is, therefore, lower on the energy scale than the combination  $\pi_1^* - \pi_2^*$ . A note of

caution: combinations of the anti-bonding levels remain in the anti-bonding region and, likewise, combinations of the bonding levels remain in the bonding region and, most definitely, the energy of a bonding level orbital is lower than the energy of an orbital in the anti-bonding domain. In brief, we have the following constructive overlaps across the four MOs of the reactants.

combination	$\pi$ -type overlaps (constructive)	$\sigma$ -type overlaps (constructive)
$\pi_1 + \pi_2$	2	2
$\pi_1 - \pi_2$	2	0
$\pi_1^* + \pi_2^*$	0	2
$\pi_1^* - \pi_2^*$	0	0

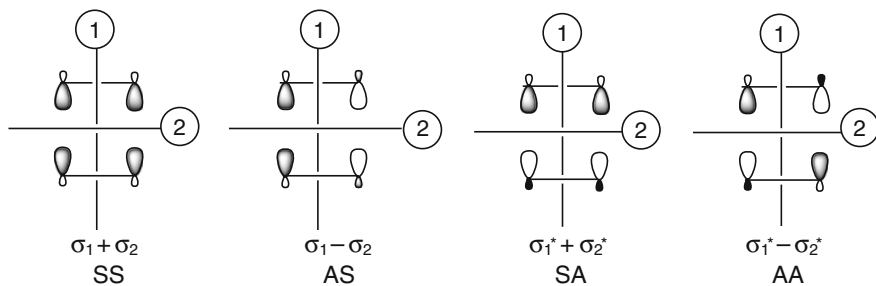
It may appear a priori that whereas  $\pi_1^* + \pi_2^*$  combination enjoys from two  $\sigma$ -type of interactions,  $\pi_1 - \pi_2$  combination benefits from two  $\pi$ -type of interactions, and since a  $\sigma$  bond resulting from  $\sigma$ -interaction is lower in energy than a  $\pi$  bond originating from  $\pi$ -interaction,  $\pi_1^* + \pi_2^*$  must be lower on the energy scale in comparison to the  $\pi_1 - \pi_2$  level. The fact, however, remains that this  $\sigma$ -interaction is in the very early stage and, hence, its contribution to lowering of the energy is considerably small.



The  $\sigma$  and  $\sigma^*$  orbitals in the formation of cyclobutane

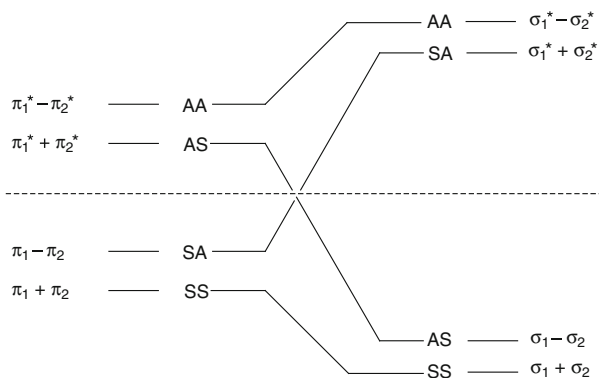
Now, we shall analyze the situation in cyclobutane in an analogous manner. The two localized  $\sigma$  orbitals,  $\sigma_1$  and  $\sigma_2$ , and their anti-bonding levels  $\sigma_1^*$  and  $\sigma_2^*$ , respectively, are given above. The possible allowable combinations  $\sigma_1 + \sigma_2$ ,  $\sigma_1 - \sigma_2$ ,  $\sigma_1^* + \sigma_2^*$  and  $\sigma_1^* - \sigma_2^*$  and their symmetry properties in respect of the same two planes as above are shown below. As above, the  $\sigma_1 + \sigma_2$  combination is lower than  $\sigma_1 - \sigma_2$  combination in the bonding region and, likewise, the  $\sigma_1^* + \sigma_2^*$  combination is lower than the  $\sigma_1^* - \sigma_2^*$  combination in the anti-bonding region. For relative energy considerations, the criteria discussed above for  $\pi$  combinations will apply.





The possible combinations of  $\sigma_1$  and  $\sigma_2$  and  $\sigma_1^*$  and  $\sigma_2^*$  in the formation of cyclobutane

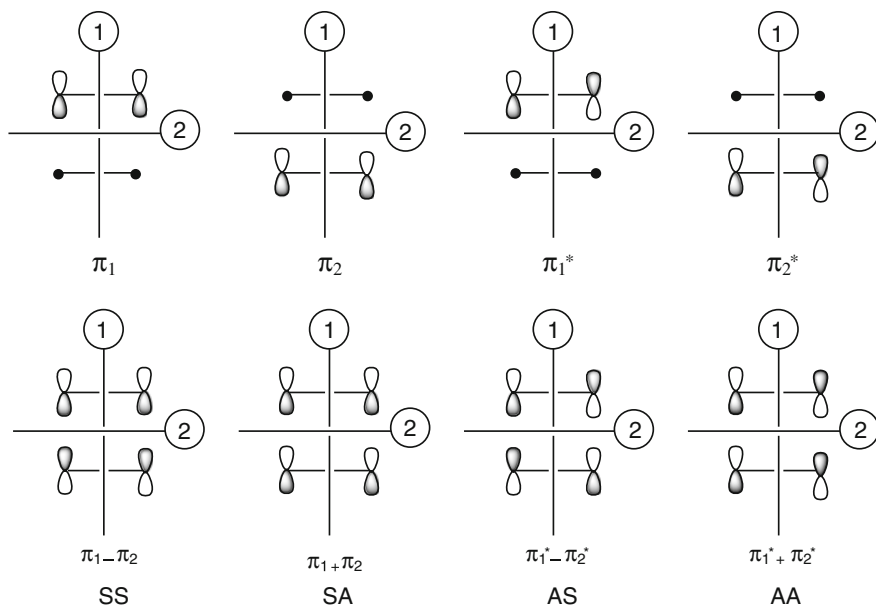
Now, we can draw the correlation diagram for the reaction of two ethylene molecules to result in the formation of cyclobutane. We must bear in mind that a  $\sigma$  level is lower than a  $\pi$  level on a relative energy scale. By the same token, a  $\sigma^*$  level ought to be higher than a  $\pi^*$  level. For the reaction in the direction of cyclobutane, we must focus on the two bonding MOs of cyclobutane,  $\sigma_1 + \sigma_2$  and  $\sigma_1 - \sigma_2$ , and then search for their symmetry correspondence with MOs on the reactant side. In doing so, we soon discover that while the SS symmetry of the lowest bonding cyclobutane orbital  $\sigma_1 + \sigma_2$  corresponds to that of the bonding level reactant orbital  $\pi_1 + \pi_2$ , the symmetry of the higher bonding cyclobutane orbital  $\sigma_1 - \sigma_2$  correlates with that of the lowest anti-bonding reactant orbital  $\pi_1^* + \pi_2^*$ . So, if the orbital symmetry is indeed to be conserved, one product orbital is to be derived from one ethylene molecule in its ground state which is  $\pi_1 + \pi_2$  and the other bonding product orbital from the other ethylene molecule in its first excited state which is  $\pi_1^* + \pi_2^*$ . The reaction, therefore, is photochemical. It cannot be thermal because it is impossible to thermally promote a ground level molecule into its first excited state because the energy requirement is truly very large.



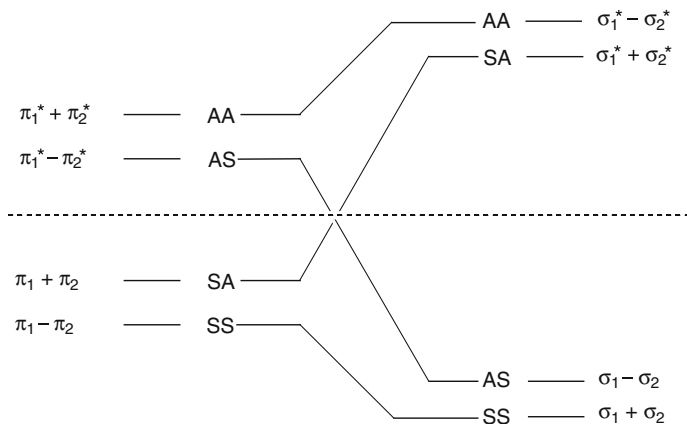
Orbital symmetry correlation for the  $\pi^2 + \pi^2$  reaction leading to cyclobutane  
 S = Symmetric and A = antisymmetric

Following the principle of microscopic reversibility, the transformation of cyclobutane into two ethylene molecules must also be photochemical. This notion is beautifully borne out from the above correlation diagram. Whereas  $\pi_1 + \pi_2$  is derived from the still lower lying reactant orbital  $\sigma_1 + \sigma_2$ ,  $\pi_1 - \pi_2$  is derived from the  $\sigma_1^* + \sigma_2^*$ . Since, the energy difference between  $\sigma$  and  $\sigma^*$  levels is larger than the energy difference of  $\pi$  and  $\pi^*$  levels, the transformation of a cyclobutane into two ethylene molecules should be expected to be more energy requiring than the coupling of two ethylene molecules to generate cyclobutane. Consequently, with a light of suitable wavelength, it should be possible to prepare cyclobutane from ethylene in a good quantum yield. There is a large symmetry-imposed barrier in either direction for the reaction to occur in the ground state.

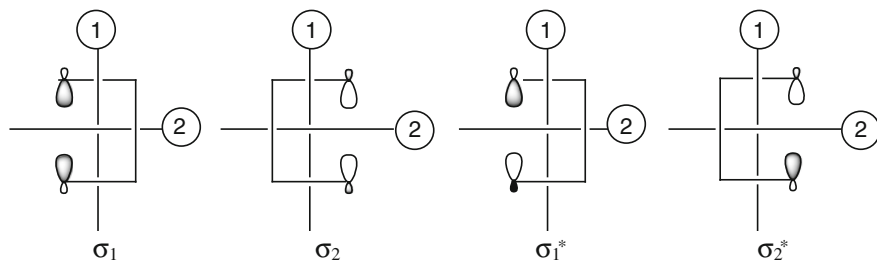
In the discussion of the above reaction in terms of the conservation of orbital symmetry, one may be tempted to use the following localized  $\pi_1$  and  $\pi_2$  orbitals. This is to be understood that this should not change the overall analysis because only the placement of the combinations of localized orbitals on the relative energy scale will change. The anti-bonding  $\pi_1^*$  and  $\pi_2^*$ , the four possible  $\pi$ -combinations and their symmetry properties in respect of the same mirror planes 1 and 2 are given below.



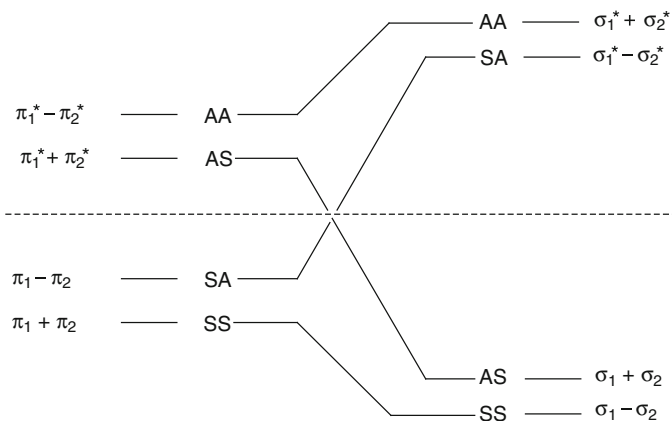
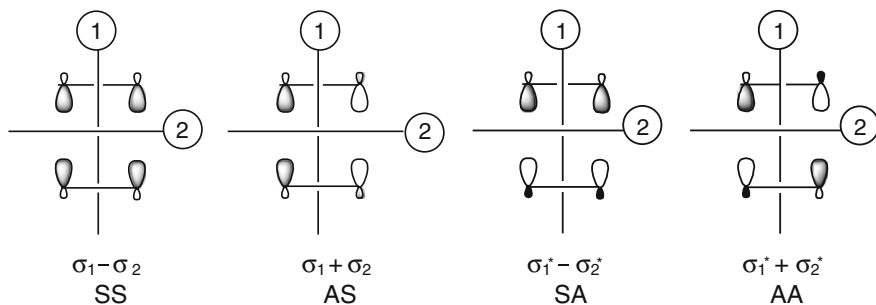
Now,  $\pi_1 - \pi_2$  is lower than  $\pi_1 + \pi_2$  and, likewise,  $\pi_1^* - \pi_2^*$  is lower than  $\pi_1^* + \pi_2^*$ . These situations were opposite in the previous analysis. These  $\pi$  combinations and their symmetry properties are placed together with the previously taken  $\sigma_1$  and  $\sigma_2$  and their combinations in the following correlation diagram.



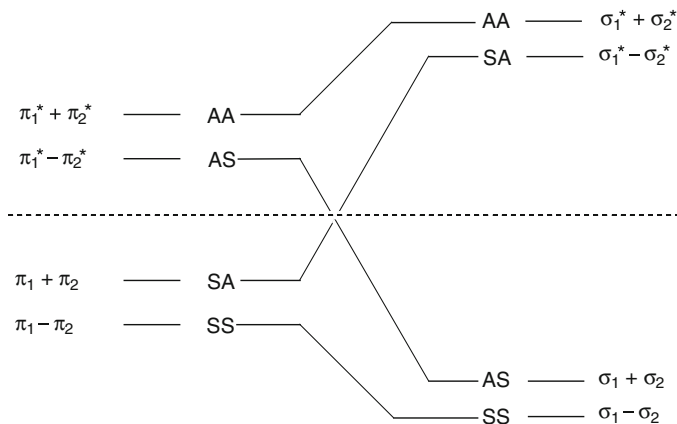
In a fashion similar to the above, one may like to consider the following localized  $\sigma$  orbitals for their possible combinations. Their respective anti-bonding variants are also shown.



The  $\sigma$  combinations in the increasing order of energy and the correlation of these with the  $\pi$  combinations used in the very first instance above is the followings. The overall analysis and the photochemical nature of the reaction did not change.

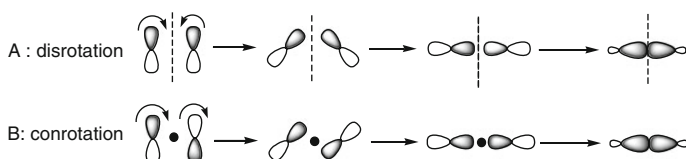


The correlation diagram for the second sets of the  $\pi$  and the  $\sigma$  combinations given above shall be as follows. Clearly, no matter in which way we perceive the localized reactant and product orbitals, the eventual correlation feature remained unchanged. The only thing which changed was the notations of the various levels. By recognizing the fact that the energy levels remained unaltered, we can confidently conclude that nothing ever changed except our perception of the localized orbitals.



## 4 Electrocyclic Ring Closure and Ring Opening Reactions

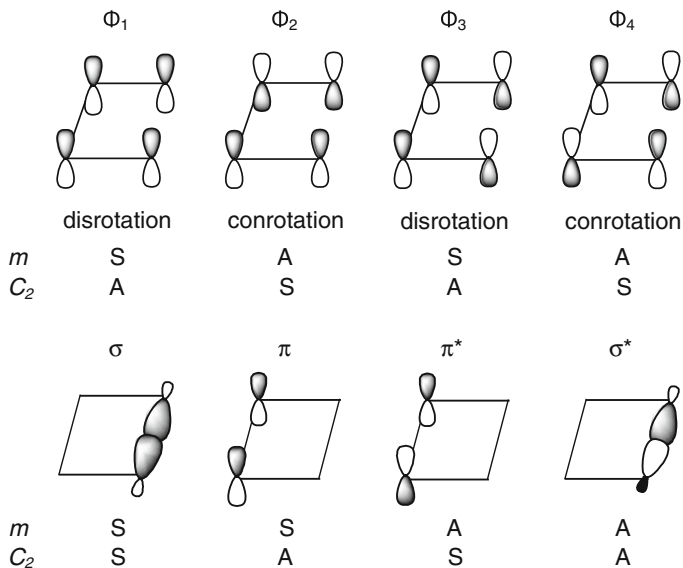
Let us now consider the interaction of two  $p$  orbitals in the construction of a  $\sigma$  bond and let us also consider that these two  $p$  orbitals are, to begin with, parallel to each other. Two situations, say A and B, arise. In situation A, one  $p$  orbital must rotate clockwise and the other anticlockwise to place the lobes of similar signs in a coaxial manner to overlap and result in the desired  $\sigma$  bond. In situation B, a bonding  $\sigma$  bond shall result when both the  $p$  orbitals would rotate either clockwise or anticlockwise. The former rotation is known as disrotation for the two orbitals rotate in mutually opposite directions and the latter rotation is known as conrotation for the two orbitals rotating in the same direction. Whereas mirror plane symmetry is maintained during disrotation,  $C_2$  symmetry is retained during conrotation maintains. Incidentally, a bonding  $\sigma$  bond orbital is symmetric to both the mirror plane and the  $C_2$  axis.



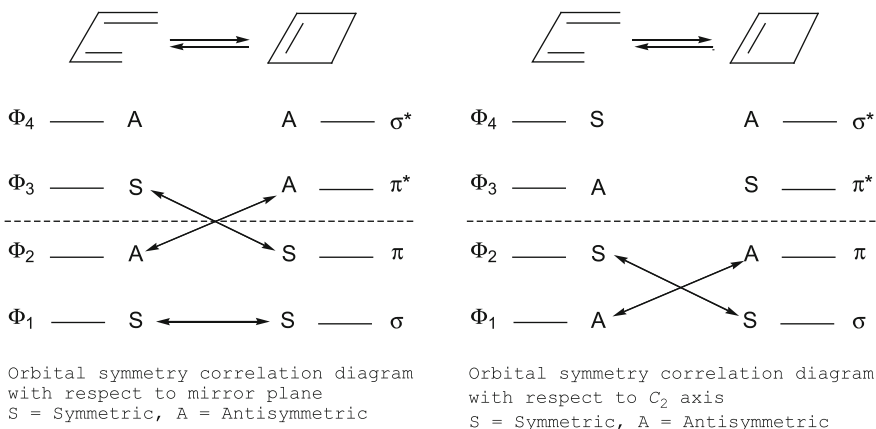
We now consider the transformation of conjugated  $k\pi$  ( $k = 4q$  or  $4q + 2$ ,  $q = 1, 2, 3, \dots$  etc.) polyenes to cyclic products. Such a reaction is popularly known as electrocyclic ring closure in which the rotation of the two  $p$  orbitals at the termini is either disrotatory or conrotatory. Either mode of ring closure is symmetry allowed. It is the mirror plane symmetry during disrotation and  $C_2$  symmetry during conrotation that are preserved. We wish to explore the conditions for both ring closing pathways by invoking conservation of orbital symmetry.

### *1,3-Butadiene* $\rightarrow$ *Cyclobutene*

Let us first consider the conversion of 1,3-butadiene into cyclobutene. In this transformation, two new bonds, one  $\sigma$  and the other a  $\pi$  bond, are generated at the expense of two  $\pi$  bonds in butadiene. All the other bonds in butadiene remain unaltered but for changes in hybridization, the bond lengths and bond angles. The most important point to note is that their symmetry properties remain unchanged. So, for simplicity of the correlation diagram, we will consider only the two  $\pi$  bonds on the reactant side and one  $\pi$  and one  $\sigma$  bond on the product side. The MOs of the reactant and the product and their symmetry properties in respect of mirror plane and  $C_2$  axis are given below. The reaction requires sometimes disrotation and sometimes conrotation, depending upon the given MO, to result into a bonding  $\sigma$  bond.



$\Phi_1$  and  $\Phi_2$  are the two bonding and  $\Phi_3$  and  $\Phi_4$  are the two anti-bonding MOs of the reactant. The energies of these MOs increase in going from  $\Phi_1$  to  $\Phi_4$ . The ring closure mode of these MOs to result in a ground state  $\sigma$  bond is indicated below each MO. Now, we can draw the correlation diagram between the orbitals of 1,3-butadiene and cyclobutene in respect of both the symmetry elements, the mirror plane and  $C_2$  axis, separately.

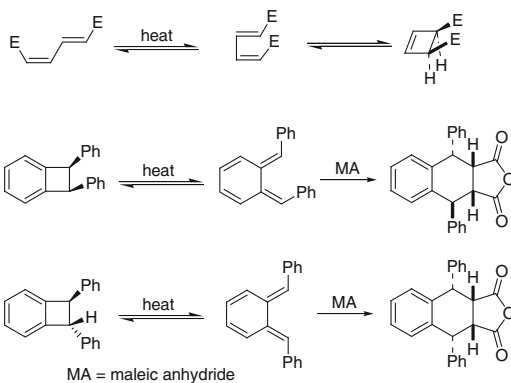


Again, for cyclobutene formation, we must focus on the two bonding MOs in it (i.e.,  $\sigma$  and  $\pi$ ) and then search for their symmetry correspondence with the MOs of 1,3-butadiene. In reference to mirror plane symmetry, which amounts to disrotation,

the symmetry of the lower lying anti-bonding orbital  $\Phi_3$  is the same as that of the higher lying bonding orbital  $\pi$  of cyclobutene. Therefore, in order for cyclobutene to form from 1,3-butadiene, the  $\Phi_2$  level must first be promoted to the  $\Phi_3$  level. The reaction, therefore, is photochemical. Likewise, for the reverse reaction, we concentrate on the bonding  $\Phi_1$  and  $\Phi_2$  MOs of 1,3-butadiene and note their symmetry correspondence with  $\sigma$  and  $\pi^*$ , respectively. The  $\pi$  level of cyclobutene must, therefore, be promoted to  $\pi^*$  level before the reaction could take place. It is to be noted that the  $\Phi_1$  and  $\sigma$  have the same symmetry property in respect of the mirror plane. We can now conclude that the disrotatory ring closure of 1,3-butadiene to cyclobutene or the disrotatory ring opening of cyclobutene to 1,3-butadiene could be accomplished only photochemically.

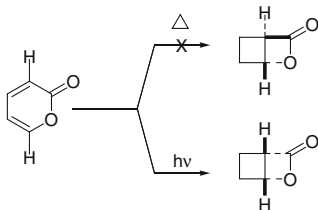
In the other correlation diagram, where  $C_2$  symmetry has preserved, we note that the symmetry properties of both the bonding level MOs on either side correlate and that there is no crossover of the nonbonding level. The reaction in either direction must, therefore, proceed thermally. Thus, *the conrotatory ring closure of 1,3-butadiene to cyclobutene or the conrotatory ring opening of cyclobutene to 1,3-butadiene takes place thermally*. In other words, *the thermal ring closure of 1,3-butadiene to cyclobutene and the thermal ring opening of cyclobutene to 1,3-butadiene involve conrotatory motion*.

We can consolidate the above two analyses: In the transformation of a 1,3-diene into a cyclobutene or vice versa, the reaction must be accomplished photochemically if the desire is to effect a disrotatory ring closure or thermally to allow a conrotatory ring closure. The choice of one rotation over the other is dependent purely on the stereochemical requirement of the product. This notion becomes amply clear from the following transformations.

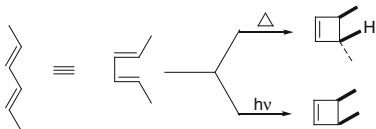


A conrotatory ring closure under thermal conditions shall furnish this cyclobutene derivative having the two ester functions cis on the ring framework as shown. A photochemical disrotatory ring closure shall have these two ester functions trans.

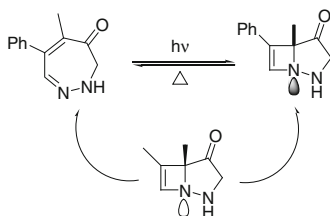
Both of these reactions involve conrotatory thermal ring opening of the benzocyclobutenes, which differ in the relative stereochemistry of the two phenyls. The resultant quinodimethanes are then trapped by MA in a Diels-Alder cyclization fashion to furnish the adducts wherein the relative stereochemistry of the two phenyls in each case is easily determined as shown. The observed stereochemical relationships confirm the predictions one makes based on conrotatory ring openings.



Although both reactions are symmetry allowed, the thermal pathway is disfavored simply for the geometrically difficult *trans* nature of the resultant ring junction.



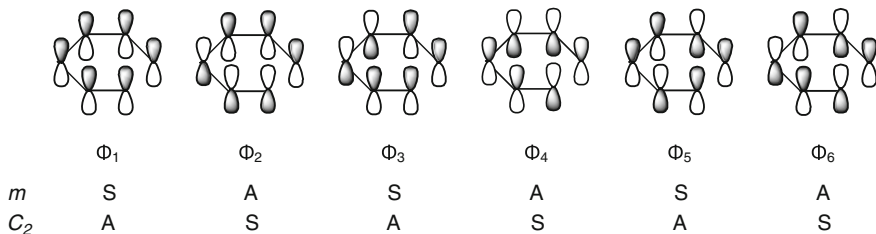
If the requirement is that of *trans*-3,4-dimethyl-1-cyclobutene, one will choose to perform the reaction thermally. The reaction must be achieved photochemically for the generation of the *cis*-isomer.



The photochemical forward reaction is fine and we understand it in view of what has been discussed above. However, if we were to believe in the principle of microscopic reversibility, the reverse thermal reaction does not seem to fit in place. Inversion of nitrogen at the ring junction to produce a *trans*-fused ring following thermal conrotatory ring opening explains the observation. The inversion at N is not difficult due to its pyramidal nature.

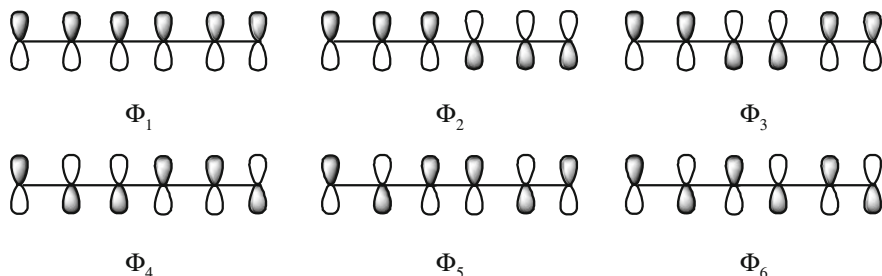
### 1,3,5-Hexatriene $\rightarrow$ 1,3-Cyclohexadiene

Further, for still better understanding, we shall consider the conversion of 1,3,5-hexatriene into 1,3-cyclohexadiene. We shall explore whether thermal or photochemical a given mode of cyclization reaction ought to be by imposing the symmetry considerations. In the said reaction, we derive one  $\sigma$  and two new  $\pi$  bonds in the product 1,3-cyclohexadiene from a total of three  $\pi$  bonds in the reactant 1,3,4-hexatriene. Given below are the six MOs ( $\Phi_1 - \Phi_6$ ) of hexatriene and their symmetry properties in relation to both the mirror plane and  $C_2$  axis.

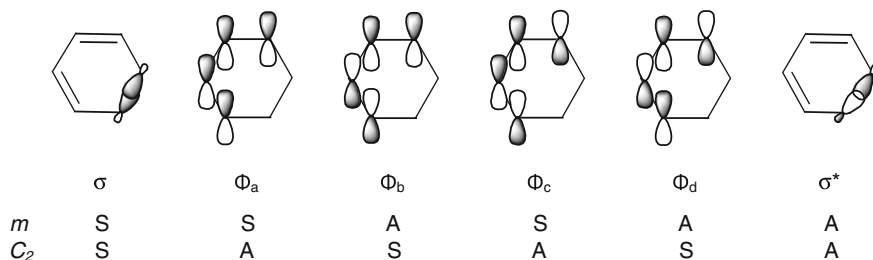




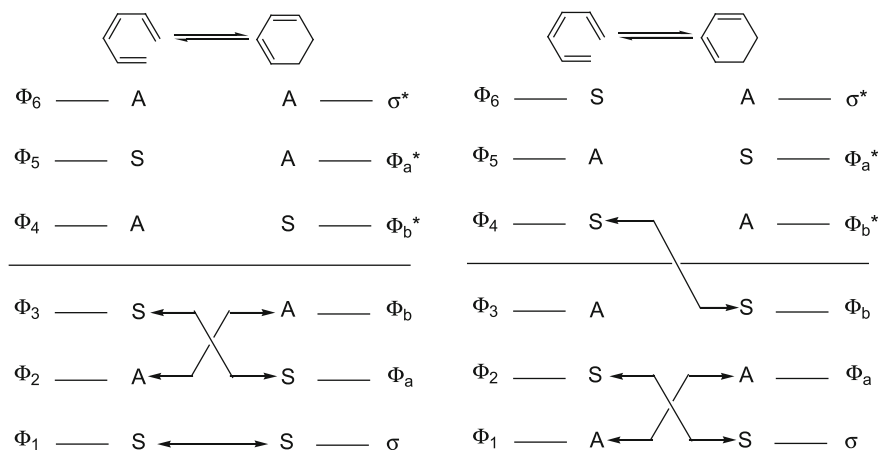
For an easier depiction of the MOs and recognition of their symmetry elements, the above six MOs may be represented in the following fashion as well.



Now, we have one  $\sigma$  and two bonding  $\pi$  orbitals,  $\Phi_a$  and  $\Phi_b$ , and the associated anti-bonding levels on the product side. The four  $\pi$  levels are the same as in 1,3-butadiene discussed above. These six MOs along with their symmetry properties in respect of both the mirror plane and  $C_2$  axis are shown below.



The separate correlations of the above reactant and product MOs in respect of mirror plane and  $C_2$  axis are shown below.



orbital symmetry correlation diagram  
with respect to mirror plane  
S = Symmetric, A = Antisymmetric

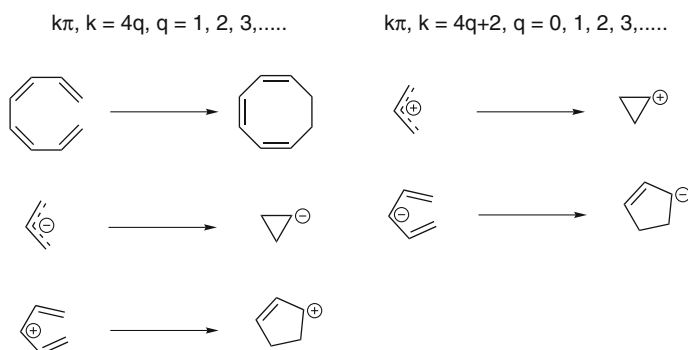
orbital symmetry correlation diagram  
with respect a  $C_2$  axis  
S = Symmetric, A = Antisymmetric

Obviously, while the disrotatory ring closure with conservation of mirror plane symmetry will take place thermally, the conrotatory ring closure with conservation of  $C_2$  axis of symmetry will be photochemical. Whether indeed there is such a predicted mode of ring closure, and it certainly is, can be deduced easily from product's stereochemistry. It must be noted that there is a switch in the mode of ring closure in moving from transformation 1,3-butadiene  $\rightarrow$  cyclobutene to the transformation 1,3,5-hexatriene  $\rightarrow$  1,3-cyclohexadiene. It is important for the central  $\pi$  bond in 1,3,5-hexatriene to have *Z*-geometry for the 1,3,5-hexatriene  $\rightarrow$  1,3-cyclohexadiene transformation to succeed. Several such cases could be examined to emerge with the following general understanding.

$k\pi$  electron system:

		Thermal reaction	Photochemical reaction
For $k = 4q$	$(q = 0, 1, 2, 3, \dots)$	Conrotatory	Disrotatory
For $k = 4q + 2$	$(q = 0, 1, 2, 3, \dots)$	Disrotatory	Conrotatory

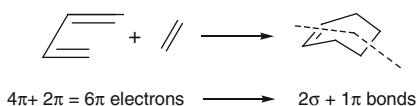
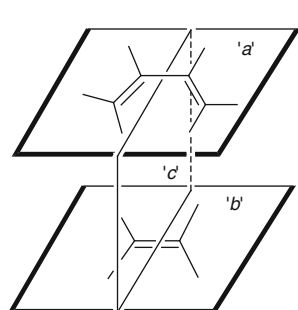
Under the category of  $k\pi$ ,  $k = 4q$ , electrons system, we can cite the ring closures of allyl anion to cyclopropyl anion, 1,3- and 1,4-pentadienyl cation to cyclopentenyl cation, and 1,3,5,7-octatetraene to 1,3,5-cyclooctatetraene. Under the category  $k\pi$ ,  $k = 4q + 2$ , we can quote the ring closures of allyl cation to cyclopropyl cation and 1,3- and 1,4-pentadienyl anion to cyclopentenyl anion. The chemical equations for these transformations are given below.



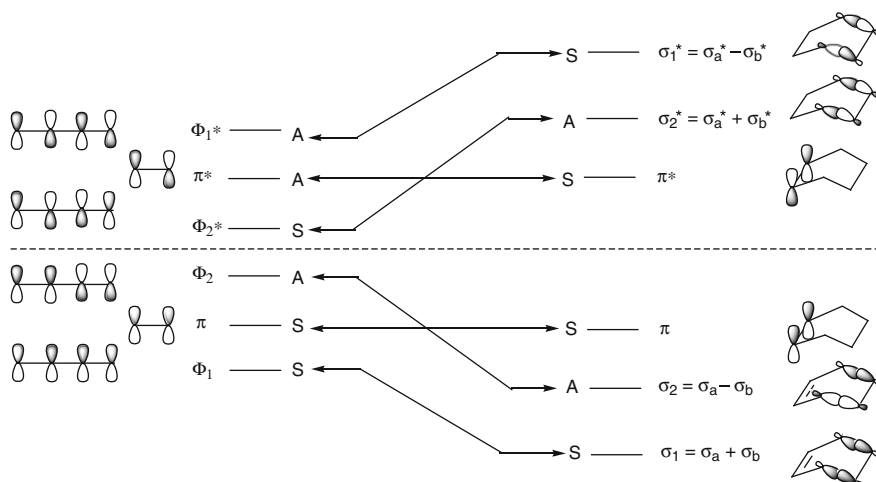
## 5 Diels–Alder Reaction ( $\pi^4 + \pi^2$ Reaction)

Diels–Alder reaction involves the cycloaddition of 1,3-dienes with alkenes in a pericyclic manner to generate six-membered ring products. We know that this reaction is thermal and is never accomplished photochemically. Now, we seek for a

rational to comprehend the only thermal nature of the reaction. Let us consider the reaction of 1,3-butadiene with ethylene to result in cyclohexene, and we impose the preservation of mirror plane symmetry on the course of the reaction. We have six MOs coming from the reactants, four from 1,3-butadiene comprising two bonding and two anti-bonding MOs and two from the alkene consisting one bonding  $\pi$  and one anti-bonding  $\pi^*$  MO. In the product cyclohexene, we have constructed two new  $\sigma$  bonds, say  $\sigma_a$  and  $\sigma_b$ , to lead to the bonding combinations  $\sigma_a + \sigma_b$  and  $\sigma_a - \sigma_b$  and the anti-bonding combinations  $\sigma_a^* + \sigma_b^*$  and  $\sigma_a^* - \sigma_b^*$ . For the new  $\pi$  bond in the product cyclohexene, there will be the bonding  $\pi$  MO and the associated  $\pi^*$  MO. It is to be understood that the energy levels of the reactant alkene MOs shall be, in the present case, almost the same as those of the product  $\pi$  levels. For substituted alkenes and 1,3-dienes, these shall, however, be different. The overall symmetry-driven conclusion, however, does not change. The entire picture of this reaction and the symmetry correlation is given below.



1,3-butadiene and ethylene are both planar molecules and they are shown to lie in two separate planes marked 'a' and 'b', but parallel to each other. The third plane marked 'c' is the mirror plane which is orthogonal to the plane of the paper and also to the above two planes. During the reaction, bond formation occurs between the terminal  $sp^2$  carbons of the diene and  $sp^2$  carbons of the alkene. Because these bonds are  $\sigma$  bonds, the overlap of the involved  $p$  orbitals must be coaxial.



As there is no symmetry-imposed barrier in the ground state MOs of both the reactants and the product, the reaction is thermal in nature. Although there is one-to-one symmetry correspondence among all the anti-bonding MOs of the reactants and the product, there is a huge energy-imposed barrier to the reaction because the first excited state of the diene-alkene complex, i.e.,  $\Phi_2^*$ , does not correlate with the first excited state of cyclohexene, i.e.,  $\pi^*$ .

The  $\pi$  levels on both sides being more or less the same, the fact that the  $\sigma_1$  and  $\sigma_2$  levels are considerably lower than the  $\Phi_1$  and  $\Phi_2$  levels, the reaction should be expected to be exothermic and, hence, smooth. The reaction however, still requires some  $20 \text{ kcal mol}^{-1}$  as activation energy. This energy requirement is not related to orbital symmetry conservation but to factors such as energy changes accompanying rehybridization in the levels, bond length extensions and contractions, and angle distortions.

## References

1. Woodward RB (1967) Aromaticity. The Chemical Society. London, p 217 (Special Publication No. 21)
2. Woodward RB, Hoffmann R (1970) The conservation of orbital symmetry. Academic Press, New York (and references cited therein)
3. Woodward RB, Hoffmann R (1969) *Angew Chem Int Ed Engl* 08:781

# Chapter 6

## The Overlap Component of the Stereoelectronic Factor Vis-à-Vis the Conservation of Orbital Symmetry Rules

**Abstract** The integration of conservation of orbital symmetry and the orbital overlap effect serves as a powerful tool to reliably predict the stereochemical course of pericyclic reactions as exemplified in this chapter. The orbital overlap factor has been discussed with a variety of examples such as the thermal fragmentations of cyclopropanated and cyclobutanated *cis*-3,6-dimethyl-3,6-dihydropyridazine, and [1,5] sigmatropic shifts in *cis*-2-alkenyl-1-alkylcyclopropanes and *cis*-2-alkenyl-1-alkylcyclobutanes.

**Keywords** Orbital overlap factor · Fragmentation · [1,5] sigmatropic shift · Epimerization · Reverse ene reaction · Cope rearrangement · *E/Z*-isomerization

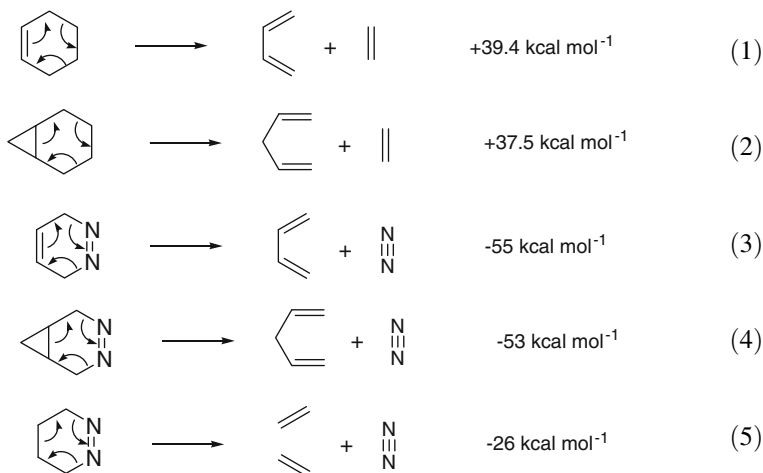
### 1 Introduction

We have understood the stereoelectronic factor as a tool to cause reactions to proceed fast when certain spatial relationships exist between the electrons involved in the bonds formed and broken [1]. The ‘certain spatial relationships’ are, in fact, the mutual orientations of the reactive sites such as the collinearity of the three atoms involved in  $S_N2$  reactions and the near coplanarity of the four ligands on the developing double bond in vicinal eliminations to allow orbital overlap throughout, etc. Combine this orbital overlap factor with the conservation of orbital symmetry factor and we have an extremely powerful tool in our hands to help us delineate the stereochemistry of certain reactions that would otherwise be difficult to explain if left to the stereoelectronic factor alone.

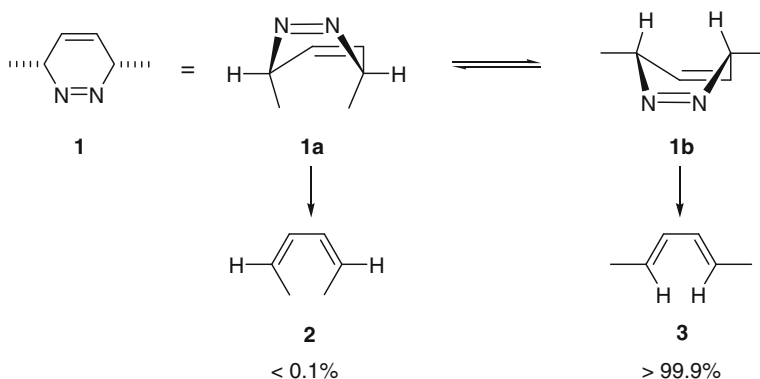
The significance of combining the conservation of orbital symmetry factor with the orbital overlap factor was felt first from the observation that the cyclization of a stereochemically well defined 1,3,5-triene to the corresponding cyclohexadiene in a projected synthesis of vitamin B<sub>12</sub> took exclusively what we today call the disrotatory pathway instead of the much expected conrotatory pathway. The conrotatory ring closure was expected on account of minimization of (a) angle strain and (b)  $\pi$ -uncoupling, i.e., the orbital overlap factor. To explain this contradiction, at that time, it became necessary to recognize a new stereoelectronic control element

which Woodward and Hoffmann called the conservation of orbital symmetry. Today, we know that 1,3,5-trienes undergo disrotatory ring closure under thermal conditions and conrotatory ring closure under photochemical conditions.

In the backdrop of the orbital symmetry rules, a need was felt to evaluate the strength of the orbital overlap component of the stereoelectronic effect by designing experiments in which both the competing pathways are orbital symmetry allowed but one pathway is preferred to the other pathway for better orbital overlap. Berson has explored this avenue exhaustively by replacing one double bond of a simple model system by a cyclopropane ring because such a structural change was expected to cause one of the two orbital symmetry-allowed pathways to enjoy better orbital overlap than the other pathway (see below).



Let us first collect some background information to address the orbital overlap issue better. The fragmentation of cyclohexene into 1,3-diene and alkene takes place in a process known as the retro-Diels-Alder reaction as shown in Eq. 1. The unsubstituted version of the reaction is endothermic by 39.4 kcal mol<sup>-1</sup>, a number that is considerably high to make the reaction very slow. A similar difficulty is present in the retro-homo-Diels-Alder reaction shown in Eq. 2. In contrast, the corresponding fragmentations of 3,6-dihydropyridazine, Eq. 3, and its homologue, Eq. 4, proceed rapidly because formation of the very stable N<sub>2</sub> makes the reaction >90 kcal mol<sup>-1</sup> more exothermic than the reaction in Eq. 1 [2, 3]. The extraordinary rate enhancements associated with the dihydropyridazines, whose fragmentations are many orders of magnitude faster than those of 3,4,5,6-tetrahydropyridazines as shown in Eq. 5, are consistent with concerted mechanisms for the reactions given in Eqs. 3 and 4.



**Scheme 1** Thermal fragmentation of *cis*-3,6-dimethyl-3,6-dihydropyridazine

## 2 Steric Effects in the Thermal Fragmentation of *Cis*-3,6-Dimethyl-3,6-Dihydropyridazine

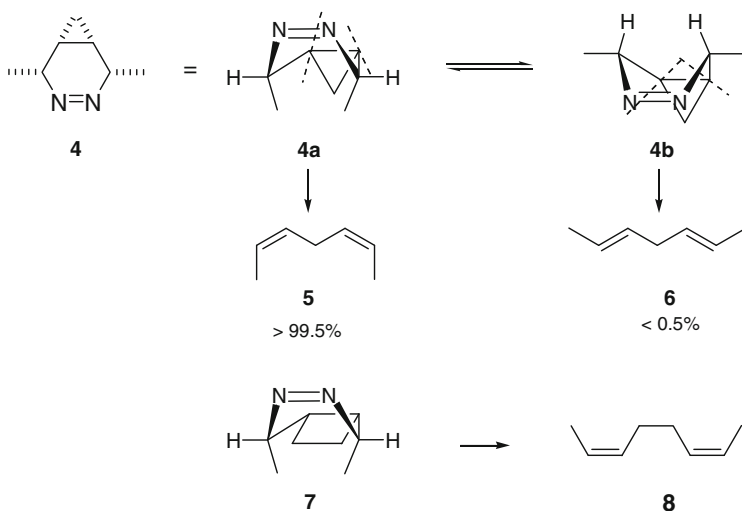
The 3,6-dihydropyridazines are appropriate substrates to bring together the steric effect and the orbital overlap effect while maintaining the conservation of orbital symmetry principle. We bring in the steric effect first. The fragmentation of *cis*-3,6-dimethyl-3,6-dihydropyridazine **1** (Scheme 1) can proceed through two different symmetry-allowed pathways. While the reaction proceeding through the TS resembling the conformation **1a** will generate the *cis,cis*-2,4-hexadiene **2**, the reaction proceeding through the TS resembling the conformation **1b** will generate the *trans,trans*-2,4-hexadiene **3**. Since the two methyl groups strongly interfere with each other in the conformer **1a**, the reaction will be expected to proceed largely through the conformer **1b**. Indeed, the sole product of fragmentation of **1** is the *trans,trans*-2,4-hexadiene **3**. The steric effect is so large that one of the two orbital symmetry-allowed pathways is preferred by a factor of >1000.

## 3 Orbital Overlap Effects in the Thermal Fragmentation of Cyclopropanated and Cyclobuanated *Cis*-3,6-Dimethyl-3,6-Dihydropyridazine

Now, we couple the above steric effect with the overlap effect by replacing the carbon-carbon double bond in **1** with a cyclopropane ring such that it acts in tandem with the steric effect arising from the methyl substituents to allow evaluation of the strength of the orbital overlap effect as in the substrate **4**. The conformer **4a** suffers from steric interactions involving the methyl groups and the methylene group of the cyclopropane ring and, thus, it results in a preference for the uncrowded conformer

**4b**. The preference for **4b** over **4a** ought to be significantly larger than the preference for **1b** over **1a** and, therefore, **4** will be expected to fragment predominantly to the *trans,trans*-diene **6** if the steric factors alone were the dominant control factor. It was, however, the *cis,cis*-diene **5** that predominated over **6** by a margin of >200:1. Obviously, there has to be some very powerful effect at work in the TS resembling **4a** that reversed the normal steric preference.

The above powerful effect has been shown to have its origin in the superior orbital overlap in **4a**-like TS wherein the breaking  $\sigma_{C-N}$  bonds are aligned parallel to the orbital axes of the cyclopropane ring (dashed lines in **4a**). In the alternate **4b**-like TS, orbital overlap is unsatisfactory because the axes of the involved orbitals are essentially perpendicular. Thus, the cyclopropane has synthetically compelled the choice of one pathway and controlled the stereochemical course of the reaction at the sites of the two newly generated  $\pi$  bonds. Such a feature was observed from the cyclobutane derivative **7** as well as it fragmented to the *cis,cis*-diene **8** with a stereospecificity that was too high to measure. However, the reaction **7**  $\rightarrow$  **8** was much slower than the reaction **4**  $\rightarrow$  **5** for the comparatively poorer parallel alignment of the cyclobutane ring orbitals with the cleaving  $\sigma_{C-N}$  bond orbitals.

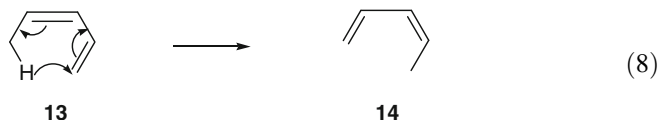
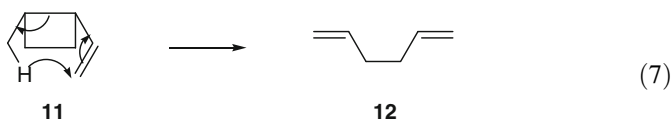
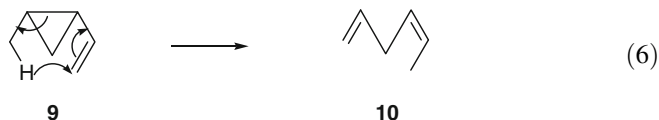


Thermal fragmentation of cyclopropanated and cyclobutanated 3,6-dimethyl-3,6-dihydropyridazines

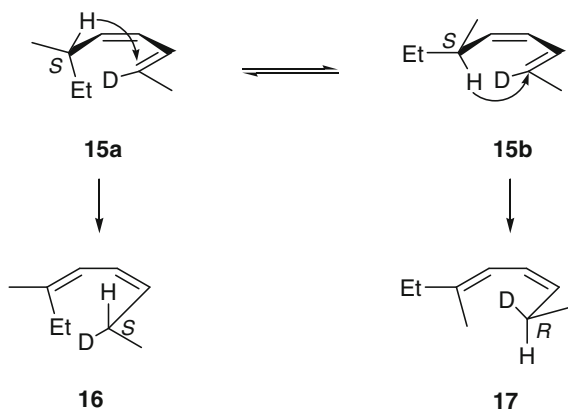


## 4 Orbital Overlap Effects in [1,5] Sigmatropic Shifts

The above overlap effect generated by the anisotropic influence of a small ring should apply to other concerted pericyclic reactions as well. Let us consider the hydrogen shifts in *cis*-2-alkenyl-1-alkylcyclopropanes (**9**  $\rightarrow$  **10**, Eq. 6) and the analogous *cis*-2-alkenyl-1-alkylcyclobutanes expressed by the transformation (**11**  $\rightarrow$  **12**, Eq. 7). These reactions may be considered analogous to the [1,5]-hydrogen shift **13**  $\rightarrow$  **14** (Eq. 8) [4, 5].



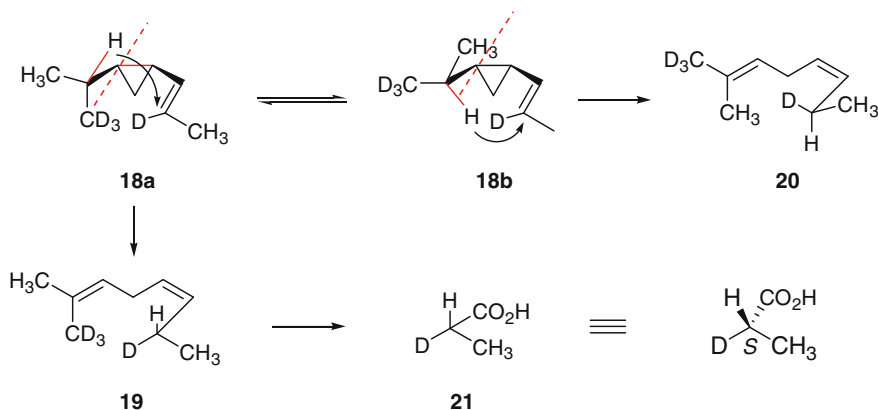
Let us first understand the steric effect during the hydrogen shift in 6(*S*),2(*E*),4(*Z*)-2-deuterio-6-methyl-2,4-octadiene **15** that can exist as an equilibrium mixture of the conformers **15a** and **15b** (Scheme 2) [6]. The sigmatropic shift is suprafacial



**Scheme 2** [1,5]-Hydrogen shift in 6(*S*),2(*E*),4(*Z*)-2-deuterio-6-methyl-2,4-octadiene

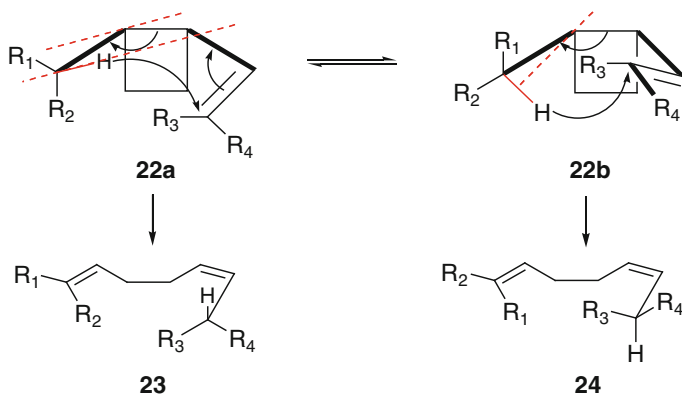
from orbital symmetry rules and it can generate two products, **16** from **15a**, and **17** from **15b**. The electron distribution above and below the plane of the reactant diene **15** is essentially isotropic (it will be exactly so were it not for the stereogenic center). Product **17** is favored over the product **16** by a factor of 1.5 probably because of the slightly smaller steric requirement of methyl than ethyl. It is the ethyl group that is closer to the D-containing terminus of the double bond in **15a** and methyl group in **15b**. The reader is advised to understand this closeness from inspection of the models. It is important to note that the migration origin and the migration terminus must be close to each other by virtue of being *cis* across the central double bond for the concerted process to occur. Furthermore, the migration terminus-derived double bond has always the *Z*-geometry.

Now, we bring in the overlap effect by replacing the central double bond by a small ring such as cyclopropane and consider the optically homogeneous molecule **18** [7, 8]. This molecule may be considered to undergo [1,5]-hydrogen shift through the conformers **18a** and **18b**. The conformer **18a** will lead to **19** wherein the newly generated asymmetric center will have the *S*-configuration. In contrast, the conformer **18b** will generate **20** with the new asymmetric center possessing *R*-configuration. It is to be noted that only in the conformer **18a**, the breaking  $\sigma_{C-H}$  at the asymmetric center and the  $\sigma_{C-C}$  orbital on the adjacent cyclopropane carbon are parallel to each other to allow for an effective overlap to culminate finally into a double bond. These orbitals are orthogonal to each other in the conformer **18b** to allow none or very slow reaction. The product obtained was subjected to oxidative cleavage to isolate a carboxylic acid that was analyzed to possess *S*-configuration. Very clearly, **18** reacted only through the conformer **18a** and the orbital overlap factor controlled the reaction pathway exclusively. Only the isotopic difference between the two substituents at the donor site (CH<sub>3</sub> and CD<sub>3</sub>) minimized any possible steric bias to the configuration of the donor-derived double bond in the product.



[1,5]-Hydrogen shift in *cis*-2(*S*)-[2(*S*)-isopropyl-1-*d*<sub>3</sub>]-1(*S*)-[1-(*E*)-propenyl-2-*d*]-cyclopropane **18**

In application of the above to hydrogen shift in the corresponding cyclobutane derivative **22**, one will expect **22a** as the most reactive conformer on account of better orbital overlap of the breaking  $\sigma_{C-H}$  bond and the cyclobutane  $\sigma_{C-C}$  bond, as shown by parallel dotted lines in red color required for  $\pi$  bond formation, to generate **23**. The conformer **22b** will be the least reactive to generate **24**. The difference in the geometries of the donor-derived double bonds and also the reversal in the configuration on the acceptor-derived carbon must specifically be noted.



## 5 Difficulties Experienced with the [1,5] Sigmatropic Shift in Cyclobutanated Species

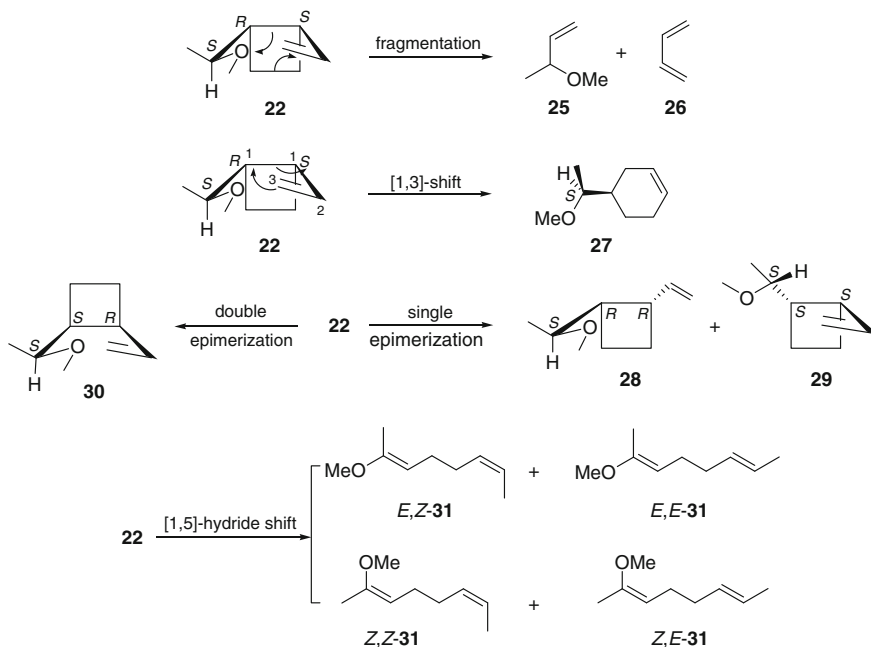
The following factors, however, make a clean realization of such a reaction more difficult than in the corresponding cyclopropane analog for the following reasons:

- The reverse ene reaction of a *cis*-1-alkenyl-2-alkylcyclobutane is much slower than that of the cyclopropane counterpart. Consequently, fragmentation, epimerization and sigmatropic rearrangement, which are not seen in the cyclopropane system, now compete with the reverse ene reaction of the cyclobutane system whose products are depositories of the required stereochemical information in the corresponding reactants.
- Since the primary product of the reverse ene reaction is 1,5-diene, one may expect a secondary transformation via the Cope rearrangement.
- At the high temperature (250 °C and above) at which the reaction is carried out, the *E/Z*-isomerization is a very likely and, in fact, an observed event.

Fortunately, the problem arising from the secondary Cope rearrangement could be suppressed by the choice of a methoxy group as a stereochemical marker as in **22** ( $R_1=CH_3$ ,  $R_2=OMe$ ,  $R_3=R_4=H$ ), **22** ( $R_1=OMe$ ,  $R_2=CH_3$ ,  $R_3=R_4=H$ ), **22** ( $R_1=CH_3$ ,  $R_2=OMe$ ,  $R_3=D$ ,  $R_4=CH_3$ ) and **22** ( $R_1=OMe$ ,  $R_2=CH_3$ ,  $R_3=D$ ,  $R_4=CH_3$ ). This is so because a hydrogen shift leads to an enol ether whose subsequent Cope rearrangement

is insignificant under the reaction conditions [9, 10]. Although investigation of the full stereochemical features of this reaction requires a substrate with specified configuration at three stereocenters such as in **22** ( $R_1=CH_3$ ,  $R_2=OMe$ ,  $R_3=D$ ,  $R_4=CH_3$ ) and **22** ( $R_1=OMe$ ,  $R_2=CH_3$ ,  $R_3=D$ ,  $R_4=CH_3$ ), the substrates **22** ( $R_1=CH_3$ ,  $R_2=OMe$ ,  $R_3=R_4=H$ ) and **22** ( $R_1=OMe$ ,  $R_2=CH_3$ ,  $R_3=R_4=H$ ) that terminate in stereochemically uninformative  $CH_2$  group can provide valuable partial solutions in as much as the stereochemistry of the donor-derived double bond is concerned.

Berson has studied the thermal reaction of the substrate **22** ( $R_1=OMe$ ,  $R_2=CH_3$ ,  $R_3=R_4=H$ ) and identified the products arising from different channels such as fragmentation to **25** and **26**, [1,3]-sigmatropic shift to **27**, single epimerization to **28** and **29**, double epimerization to **30** and the much desired [1,5]-hydride shift leading to all possible double bond isomers of **31** as outlined below. From the temperature dependence of the overall rate of disappearance of the reactant and the product distribution, the activation parameters for the individual pathways were determined. It was discovered that the activation energy for the [1,5]-hydride shift was lower than those of the other competing pathways, i.e., epimerization, fragmentation, and [1,3]-sigmatropic shift. This finding is consistent with a difference in the mechanism for the overall two sets of reactions, a concerted pathway for the [1,5]-hydride shift and a stepwise biradical pathway for some or all of the other pathways.



[1,5]-Hydrogen shift and various other reactions of *cis*-1-alkenyl-2-alkylcyclobutane **22** ( $R_1 = OMe$ ,  $R_2 = CH_3$ ,  $R_3 = R_4 = H$ )

The epimerization at both the ring stereogenic centers causes the diastereomeric interconversion **22**↔**30**. Since the rates of [1,5]-hydride shifts in these two diastereomers are comparable, some of the product formed from the pyrolysis of **22** must actually arise from **30** and vice versa. After making corrections for the concurrent double epimerization by following an established procedure [9, 10], it was shown that the mechanistically significant ratio of the products *E,Z*-**31** and *Z,Z*-**31** formed directly from **22** was >220:1. Very clearly, the orbital overlap controlled the reaction of the stereochemically well defined reactant **22** and caused one symmetry-allowed pathway to take prominence over the other symmetry-allowed pathway.

To sum up the above discussion, we have witnessed that the orbital overlap component of the stereoelectronic effect is indeed a very powerful tool as it controls both the stereochemistry and the rates of a range of pericyclic reactions by allowing exclusively one of the two possible symmetry-allowed pathways for the very simple reason of better overlap of the breaking bonds.

## References

1. Eliel EL (1962) Stereochemistry of carbon compounds. McGraw-Hill, New York, p 227
2. Berson JA, Petrillo EW (1974) *J Am Chem Soc* 96:636
3. Berson JA, Olin SS, Petrillo EW Jr, Bickart P (1974) *Tetrahedron* 30:1639
4. Wolinsky J, Chollar B, Baird MB (1962) *J Am Chem Soc* 84:2775
5. Gajewski JJ (1981) Hydrocarbon thermal isomerizations. Academic Press, New York, p 106
6. Roth WR, König J, Stein K (1970) *Chem Ber* 103:426
7. Parziale PA, Berson JA (1990) *J Am Chem Soc* 112:1650
8. Parziale PA, Berson JA (1991) *J Am Chem Soc* 113:4595
9. Getty SJ, Berson JA (1990) *J Am Chem Soc* 112:1652
10. Getty SJ, Berson JA (1991) *J Am Chem Soc* 113:4607

## Chapter 7

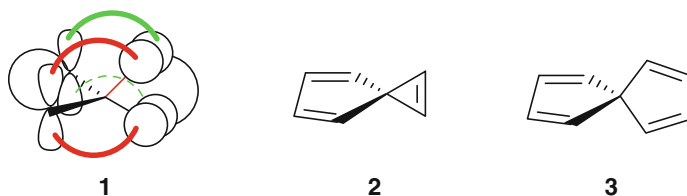
# Miscellaneous

**Abstract** The control elements that did not find mention in the earlier chapters are dealt with here. The prominent among these elements are spiroconjugation, periselectivity in pericyclic reactions, torquoselectivity in conrotatory-ring openings, ambident nucleophiles and electrophiles,  $\alpha$ -effect in nucleophilicity, carbene addition to 1,3-dienes, Hammett's substituent constants, Hammond postulate, Curtin–Hammett principle, and diastereotopic, homotopic, and enantiotopic substituents.

**Keywords** Spiroconjugation · Periselectivity · Carbenes · Ketenes · Torquoselectivity · Ambident nucleophiles and electrophiles ·  $\alpha$ -effect · Hammett's substituent constants · Hammond postulate · Curtin–Hammett principle · Diastereotopic · Homotopic · Enantiotopic substituents

### 1 Spiroconjugation

When one conjugated system is held at a right angle to another conjugated system, as in the case of a spirostructure, the  $p$  orbitals of one conjugated system can overlap with those of the other conjugated system, as indicated by the red curved lines on the front lobes and green curved lines on the rear lobes in structure **1**, with a small overlap integral. In the situation when the symmetries match, the interaction leads to two new orbitals, one raised and the other lowered in energy, in the usual fashion that we have previously learnt elsewhere. However, when the symmetry elements do not match, the overlap is considered to have no effect.



Let us consider spiroheptatriene **2** with the unperturbed orbitals of the cyclopentadiene component shown on the left and that of the cyclopropene component shown on the right in Fig. 1. It is easy to see that the only orbitals that can interact are  $\psi_2$  on the left and  $\pi^*$  on the right and that all the other orbitals possess wrong symmetry. For example, the top lobes of  $\psi_1$  and the upper  $p$  orbital of  $\pi$  (one lobe in the front and the other in the back) have one interaction in phase and the other out of phase, exactly cancelling each other. A similar situation exists between the lower lobes of  $\psi_1$  and the lobes of the lower  $p$  orbitals of  $\pi$  on the right.

The interaction  $\psi_2 \rightarrow \pi^*$  creates two new orbitals, one raised and the other lowered in energy. Since there are only two electrons (originating from  $\psi_2$ ) to go into these orbitals and, also, since these two electrons will occupy the lowered orbital, the overall energy of the system is lowered. This lowering in energy,  $\Delta E$ , is small because of poor overlap which is necessarily on account of having the two interacting orbitals significantly apart in energy. Nevertheless, it is generally

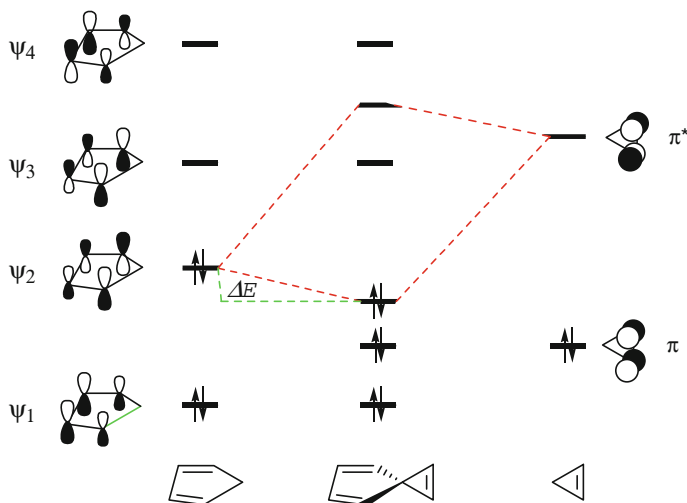


Fig. 1 Molecular orbitals of spiroheptatriene

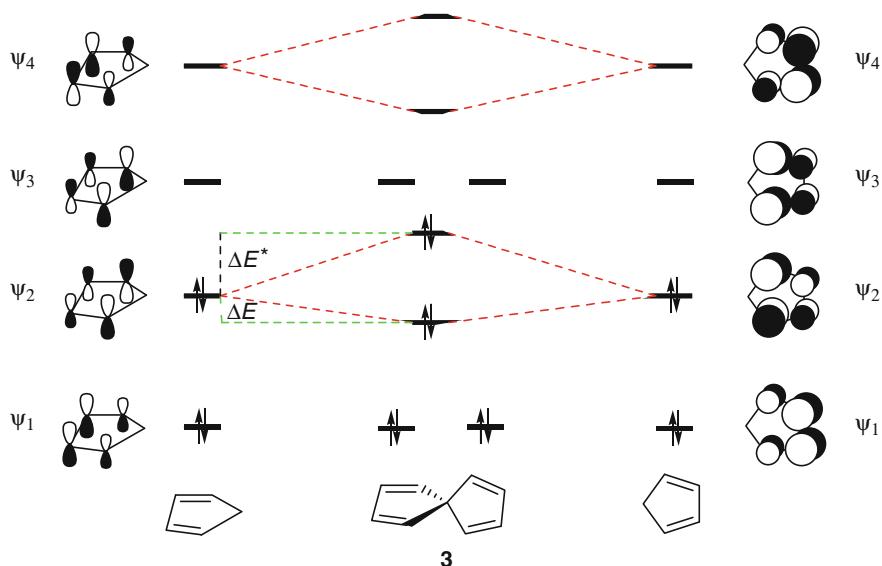


Fig. 2 Molecular orbitals of spirononatetraene

concluded that if the total number of  $\pi$  electrons is  $4n + 2$  ( $n \neq 0$ ), the spiro system is stabilized, leading to the concept of *spiroaromaticity*.

*Spiroantiaromaticity* arises when the total number of  $\pi$  electrons is  $4n$  ( $n \neq 0$ ), as in spirononatetraene **3**. Ignoring the interactions of the unfilled  $\Psi_3$  and  $\Psi_4$  orbitals that have no effect on energy because there are no electrons in them, the only MOs with right symmetry to interact constructively are  $\Psi_2$  on each side, Fig. 2. The  $\Psi_2 \rightarrow \Psi_2$  interaction leads to two new orbitals, each occupied by two electrons. The net effect is a raise in the overall energy because, according to the theory of perturbation, the bonding combination is lowered less than the raise in the antibonding combination, i.e.,  $\Delta E < \Delta E^*$ . The energy levels  $\Delta E$  and  $\Delta E^*$  have been measured to be 1.2 eV apart. This, in turn, is expected to impart exceptional reactivity to the molecule. Indeed, this is in agreement with the increase in (a) the overall energy of the molecule, (b) the energy of the HOMO and, hence, (c) the overall reactivity of the substrate [1].

## 2 Periselectivity

In the cycloaddition of a conjugated system, there are three different situations to be considered: (a) the entire conjugated array of electrons is involved, (b) a large part of the conjugated array of electrons is involved, and (c) only a small part of the



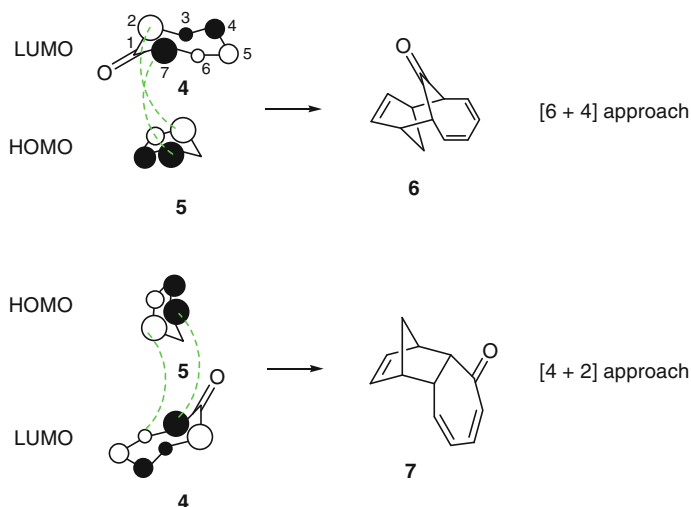
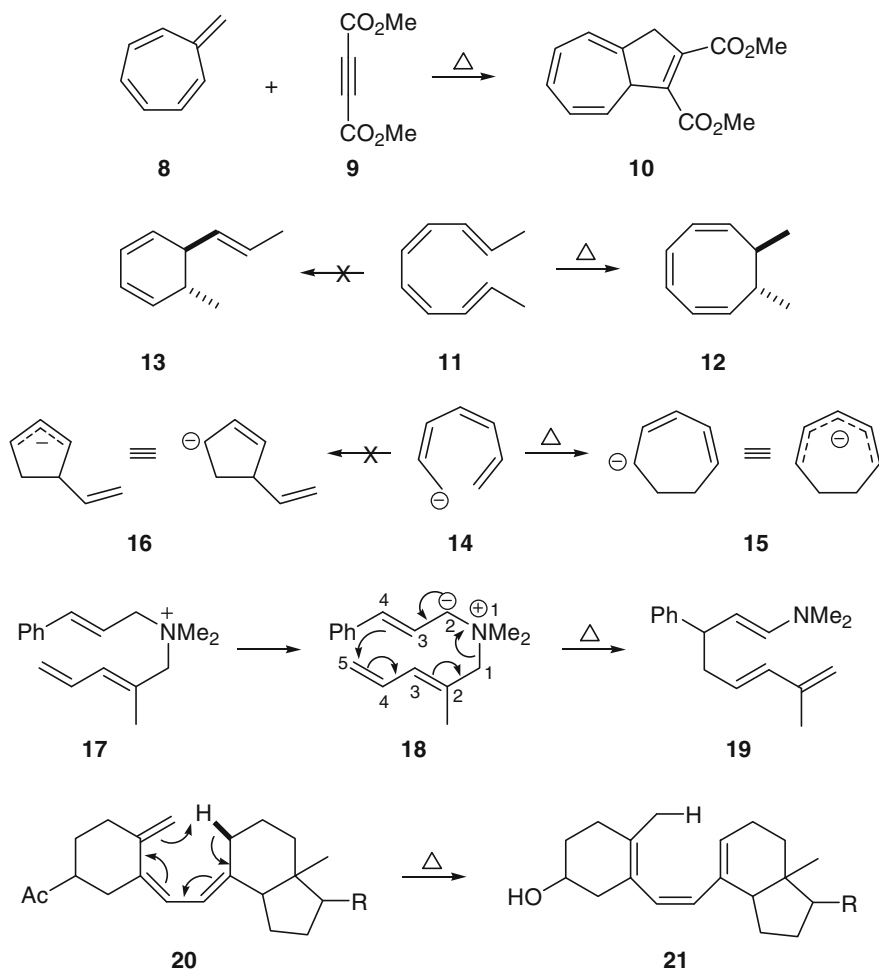


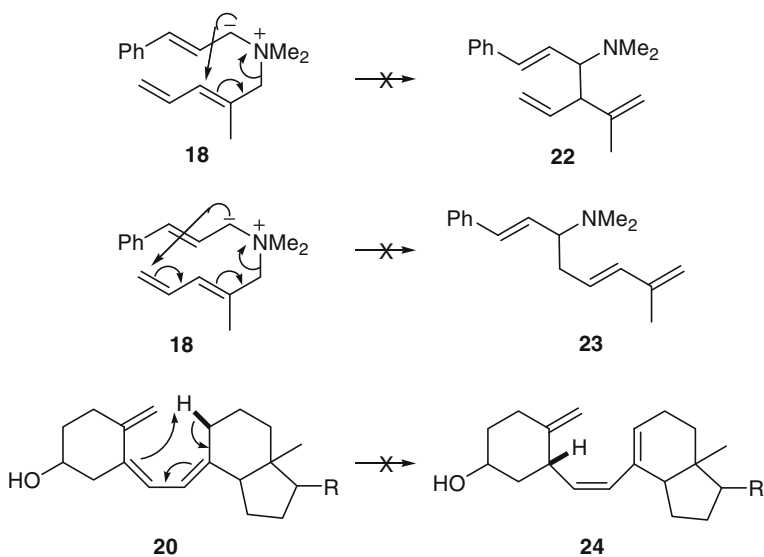
**Fig. 3** The FMOs of troponone and cyclopentadiene placed together for [6 + 4] and [4 + 2] cycloadditions

conjugated array of electrons is involved. The principle of conservation of orbital symmetry rules restricts the total number of electrons to 6, 10, 14, 18, etc., in suprafacial reactions, but it is silent on which of these electrons would be preferred if they were all geometrically feasible. For instance, cycloaddition of troponone **4** with cyclopentadiene **5** may be expected to give a mixture of the [6 + 4] adduct **6** and the [4 + 2] adduct **7**, Fig. 3. However, the adduct **6** is formed in preference to **7** in a process called *periselectivity*. We will try to understand the origin of this selectivity.

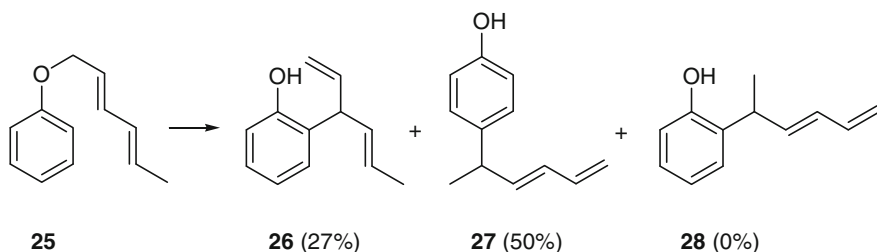
The frontier molecular orbital (FMO) approach makes the longer conjugated system in troponone more reactive than any other shorter conjugated system, because the largest LUMO coefficients are concentrated at C2 and C7, which allows bonding to these sites more energy lowering as in the [6 + 4] approach, leading to **6**, than bonding to the C2 and C3 sites as in the [4 + 2] approach, leading to **7**. In general, the termini of a conjugated system carry the largest frontier orbital coefficients, and we can, therefore, expect pericyclic reactions to occur with the longest conjugated system. The latter is evidently more compatible with the conservation of orbital symmetry rules and, of course, the geometrical feasibility.



The cycloaddition of **8** with dimethyl acetylene dicarboxylate **9** to generate **10** [2, 3], the electrocyclic ring closures **11**  $\rightarrow$  **12** and **14**  $\rightarrow$  **15** (8 electron conrotatory ring closures) [4, 5] under thermal conditions and the sigmatropic rearrangements **18**  $\rightarrow$  **19** [6] and **20**  $\rightarrow$  **21** [7, 8] are some of the many examples to support the observation that the largest possible number of electrons are mobilized when smaller, but equally allowed, numbers could have been used instead. The transformations **18**  $\rightarrow$  **19** and **20**  $\rightarrow$  **21** are example of [4,5] and [1,7] sigmatropic shifts, respectively. Please note that **18** could also have undergone [2,3] and [2,5] sigmatropic shifts to generate **22** and **23**, respectively. However, neither of these products was formed. Likewise, **24**, which could have formed from **20** via a suprafacial [1,5] sigmatropic shift, as shown, was also not formed.

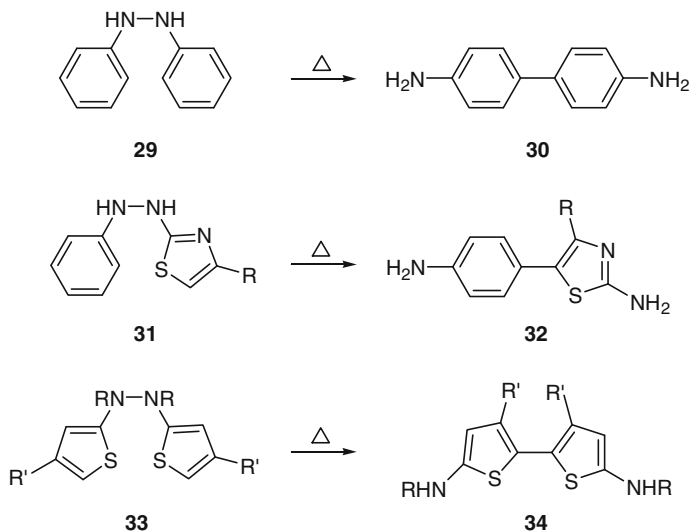


The 2,4-pentadienyl phenyl ether **25** makes an interesting case [9]. The indicated products **26**, **27**, and **28** arise from [3,3], [5,5], and [3,5] sigmatropic shifts, respectively. When the reaction was conducted, only the products **26** and **27** were formed. Thus, unlike all the above examples, the [3,3] sigmatropic shift, which involved only a small part of the conjugated array of electrons, competed reasonably well with the product **26** derived from [5,5] sigmatropic shift, which involved the entire conjugated array of electrons. Another possible product **28**, which involved a large part of the conjugated array of electrons, was not observed.



The exclusive acid-catalyzed transformations of hydrazobenzene **29** into 4,4'-diaminodiphenyl **30**, *N*-phenyl-*N'*-(2-thiazolyl)hydrazine **31** into 2-amino-5-

(*p*-aminophenyl)thiazole **32** and *N,N'*-bis(2-thiazolyl)hydrazine **33** into 5,5'-bis(2-aminothiazole) **34** are some other examples of [5,5] sigmatropic shifts, where the entire array of electrons are used. The products from [3,3] and [3,5] sigmatropic shifts (not shown) were not observed in either instance [10].

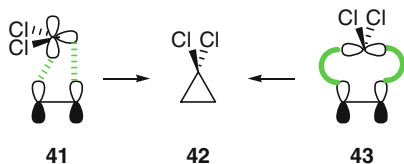
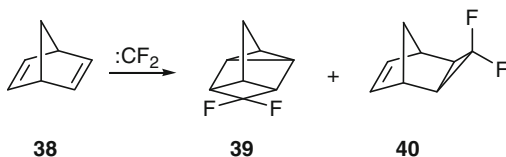
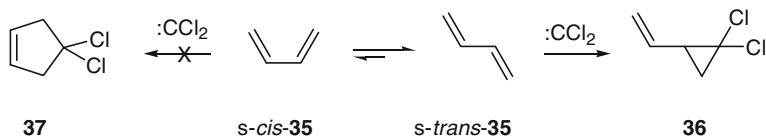


It is important to understand whether indeed the above predominant selectivity arises solely on account of the FMO coefficients consideration or the thermodynamic factor, the thermodynamic stability of the product in particular, has any role in it. The species **6** and **15** are calculated to be more stable than the species **7** and **16** by 9.2 and 24.08 kcal mol<sup>-1</sup>, respectively, at the HF/6-31G\* level of theory. Further, the species **19** is more stable than the alternate species **22** and **23** by 13.8 and 2.53 kcal mol<sup>-1</sup>, respectively. From the observation that only the most stable products **6**, **15**, and **19** are formed, one may tend to infer that the thermodynamic factor may also have contributed to the observed selectivity.

On the contrary, the species **12** is less stable than **13** by 6.2 kcal mol<sup>-1</sup> and yet **12** is formed predominantly. Likewise, **26** is less stable than **27** by 4.1 kcal mol<sup>-1</sup> and yet the formation of **26** competes reasonably well with the formation of **27** so much so that both **26** and **27** are formed in about 1:2 ratio. It is equally noteworthy that **28** is more stable than both **26** and **27** by 4.6 and 0.53 kcal mol<sup>-1</sup>, respectively, and yet none of **28** is formed.

Taking into consideration the observed selectivity and the product stability together, it can be argued that the latter per se is not a significant factor to have a bearing on the success of the reaction. In the instance, where the selectivity feature based on the FMO coefficients is matched by the product stability, the reaction will, at best, be predicted to be relatively faster than when the match is absent. It is expected that the energy of the TS which involves the entire array of conjugated electrons is lower than the energy of the TS which involves a shorter array of conjugated electrons and it is this feature that contributes most to the selectivity.

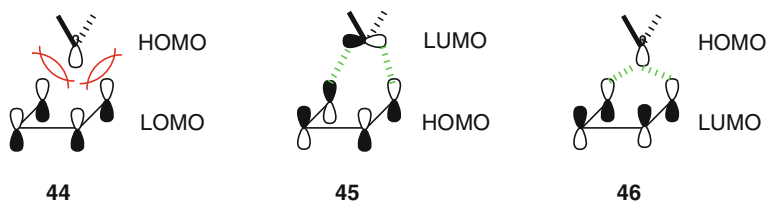
In contrast, carbenes reacts with 1,3-dienes such as **35** to give vinylcyclopropanes **36**. The symmetry-allowed [4 + 2] cycloaddition to cyclopentenes such as **37** does not occur. An exception to this general observation is the reaction of difluorocarbene with norbornadiene **38** where [2 + 2 + 2] reaction, leading to **39**, competes with the [2 + 2] reaction which leads to the formation of **40** [11]. The cyclopropanation reaction requires nonlinear approach of a carbene to the double bond as shown in **41**. As the reaction progresses, both the substituents tilt upward to occupy positions where they will be in the product **42**. In the corresponding linear approach, as shown in **43**, the carbene comes straight down to the middle of the double bond with its substituents already lined up where they will be in the product. There is experimental evidence for the nonlinear approach based on isotope effects [12]. Calculations also support the nonlinear approach even though they suggest two steps by way of a short-lived diradical for the reaction [13, 14]. So, one needs to understand why a nonlinear approach giving vinyl cyclopropane is preferred over the linear approach giving cyclopentene when the cyclopentene formation is likely to benefit from overlap of the atomic orbitals of carbene with the two large coefficients at the ends of 1,3-diene.



In considering reaction of a carbene with 1,3-diene, three different situations are likely to emerge:

- Overlap of HOMO of the carbene with the lowest occupied MO (LUMO) of the 1,3-diene, as shown in **44**, must be repulsive because both the orbitals are filled (please note that the phases of the orbitals appear to match which could be mistaken for a constructive overlap).
- Overlap of LUMO of the carbene and HOMO of the 1,3-diene, as shown in **45**, is constructive.
- Overlap of HOMO of the carbene with LUMO of 1,3-diene, as shown in **46**, is also constructive.

Calculations show that the repulsive forces in **44** are much stronger than the attractive forces in either **45** or **46** which prevent the [1 + 4] addition. On the contrary, the nonlinear approach of the LUMO of a carbene to the HOMO of an alkene as in **41** is virtually barrierless and, hence, cyclopropanation takes place rapidly and predominantly [15].

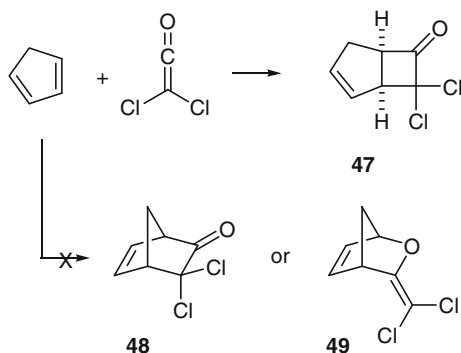


Additional factors that may be responsible for cyclopropanation reaction are as follows:

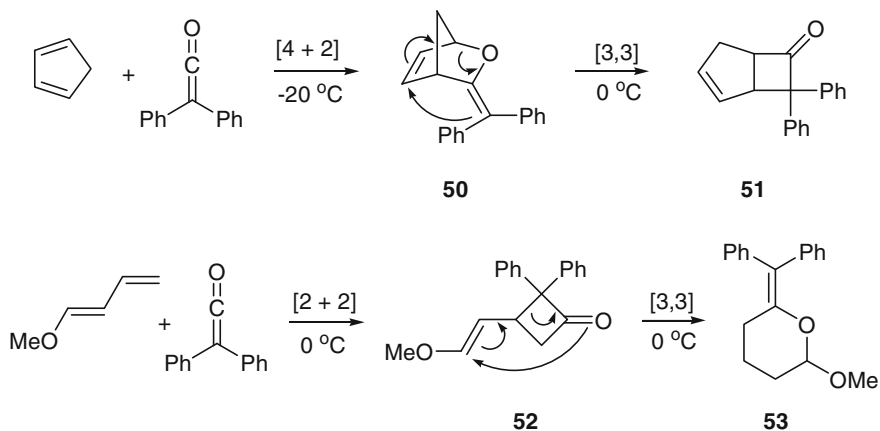
- The probability of *s-cis* conformation of the diene necessary for the overlap to develop simultaneously at both ends is low. Since cyclopropanation can take place in any conformation, it goes ahead without waiting for the diene to change from the predominant *s-trans* conformation to the *s-cis* conformation.
- The cyclic dienes such as cyclopentadiene are fixed in the *s-cis* conformation, and yet they react to give cyclopropanes predominantly. This is probably because the alternative would create a strained bicyclo[2.1.1]hexene system.
- Cyclic dienes in larger rings also form cyclopropanes, probably because they have the two ends of the diene held so far apart that both cannot easily be reached by the single carbon atom of the carbene.

Ketenes avoid the higher FMO coefficients in their reactions with 1,3-dienes and undergo exclusive [2 + 2] cycloaddition in a suprafacial manner to form adducts such as **47** from cyclopentadiene [16]. Neither **48** nor **49**, both being products of [4 + 2] cycloaddition, is formed. The orthogonal disposition of the *p* orbitals of  $\pi_{C=C}$  and  $\pi_{C=O}$  does not allow  $\pi_{C=C}$  to have a lowlying LUMO. The energy of this LUMO is raised even further from its mixing with the lone pair orbital on the oxygen atom. The  $\pi_{C=C}$  of ketene is, therefore, not a good dienophile and, hence,

the [4 + 2] cycloaddition giving **48** does not occur. The [4 + 2] addition in which the carbonyl group acts as dienophile to generate **49** is unfavorable just as any other [4 + 2] cycloaddition with a normal carbonyl group is unfavorable. In the [2 + 2] cycloaddition giving **47**, it is the LUMO of  $\pi_{C=O}$  which is involved in the formation of the leading  $\sigma_{C-C}$  bond for being lowlying on account of its conjugation with the two  $\sigma_{C-Cl}$  bonds [17].



However, the equivalent of **49** is known from the reaction of diphenyl ketene with cyclopentadiene. The adduct **50**, formed at low temperature, rearranges through [3,3] sigmatropic shift to form what appears to be the [2 + 2] adduct **51**. The reaction of 1-methoxybutadiene with diphenyl ketene to form **52** at low temperature is akin to [2 + 2] reaction involving  $\pi_{C=C}$  of the ketene. However, this species also rearranges further by [3,3] sigmatropic shift to form **53**, which is akin to [4 + 2] cycloaddition of the butadiene with  $\pi_{C=O}$  of the ketene, just as in **49** [18].

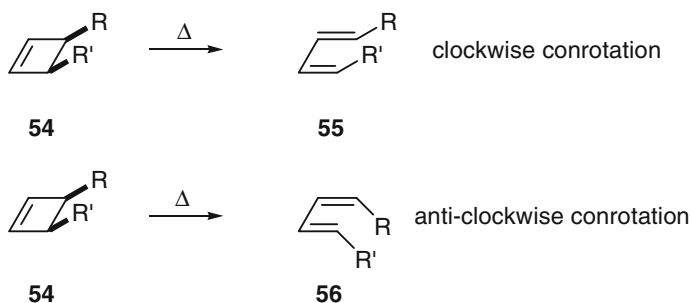


In conclusion, reactions generally take the path that uses the longest array of the conjugated system in compliance with orbital symmetry control. However, several

other factors such as spatial separation of the ends of the conjugated system, entropy changes required to attain the requisite geometrical disposition on the way to transition state, and steric factors that operate during this progression must also be taken into consideration [19].

### 3 Torquoselectivity

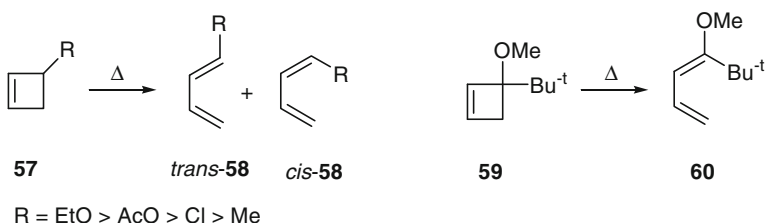
Let us consider the ring opening of **54** in a conrotatory fashion. The substituent R will be located on the *trans*-double bond and R' on the *cis*-double bond in the conrotatory clockwise ring opening **54**  $\rightarrow$  **55**. In the alternate anticlockwise ring opening as in **54**  $\rightarrow$  **56**, the situation changes because the substituent R is now located on the *cis*-double bond and R' on the *trans*-double bond. Both the pathways are one and the same when R = R' because the transition states are enantiomeric and, hence, there is no difference in their energies. However, when R  $\neq$  R', there is a remarkable level of selectivity, called torquoselectivity, that ascertains in which substituent will turn up on the *cis*-double bond and in which one on the *trans*-double bond. The overall observation is that an electron-donating substituent selectively moves outward to be on the *trans*-double bond and an electron-attracting substituent moves inward to be on the *cis*-double bond.



The torquoselectivity is not driven only by the steric effects, because there is stronger preference for the formation of *trans*-**58** with a more powerful electron-donating substituent on the cyclobutene **57**. The *trans*-**58**:*cis*-**58** ratio decreases gradually as R changes from EtO to AcO to Cl to Me group [20]. Of course, the electron-donating ability of these groups also decreases in the same order. The activation energy for ring opening is calculated to be lower when the electron-donating substituent rotates outward than the activation energy for the ring opening of cyclobutene itself. The activation energy for ring closing is similarly lower when there is an electron-donating substituent in the outside position of the diene and, likewise, an electron-attracting group in the inside position of the diene. For instance, the ring opening of **59** places the methoxy group in the outside

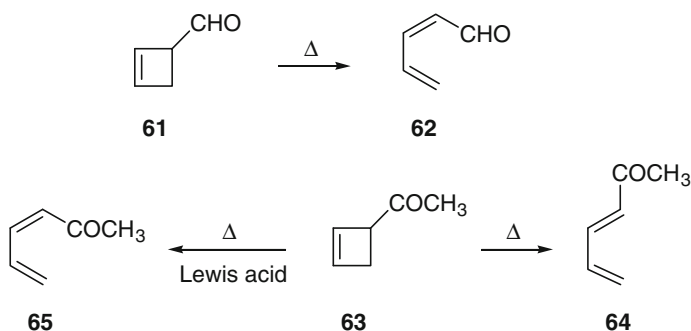


position even when the *tert*-butyl group occupies the much hindered inside position in the diene **60** [21].



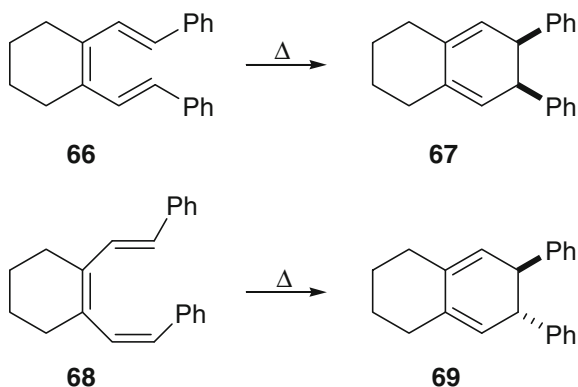
In comparison to the TS energy for the ring opening of cyclobutene itself being  $46.94 \text{ kcal mol}^{-1}$ , the TS energies for 3-methyl, 3-chloro, 3-acetoxy, 3-methoxy, and 3-*tert*-butyl-3-methoxycyclobutene species are, respectively, 45.15, 43.68, 41.98, 38.39, and  $36.63 \text{ kcal mol}^{-1}$ . Thus, 3-*tert*-butyl-3-methoxycyclobutene is expected to rearrange fastest among these substrates for having the lowest TS energy.

An example of electron-withdrawing substituent moving inward is the transformation **61**  $\rightarrow$  **62**, where the electron-withdrawing aldehyde group has moved inward exclusively [22]. The TS leading to inward movement of the carbonyl group is  $4.7 \text{ kcal mol}^{-1}$  lower in energy than the TS leading to outward movement. Contrast this with the methyl ketone **63** which gives the *trans*-ketone **64** exclusively under purely thermal conditions. True that the outward TS is  $2.9 \text{ kcal mol}^{-1}$  lower than the corresponding inward TS, the complete switch over in torquoselectivity in the transformation **63**  $\rightarrow$  **64** is not understood. However, in the presence of a Lewis acid, when coordination to the carbonyl group turns it into a more powerful electron-withdrawing substituent, the ring opening gives the *cis*-ketone **65** exclusively even when the substituent is much larger on coordination [23]. The strong electronic effect, therefore, steers the reaction to very high torquoselectivity.



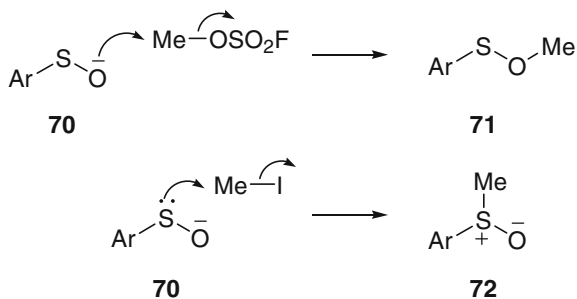
In the conrotatory ring openings of substituted cyclobutenes, the transition states have been calculated to be antiaromatic when a filled p-orbital moves inside leading to a three-center four-electron conjugated system as in **57**  $\rightarrow$  *cis*-**58** and aromatic when an empty orbital moves inside leading to a three-center two-electron conjugated system as in **61**  $\rightarrow$  **62** and **63**  $\rightarrow$  **65** [24].

The torquoselectivity on account of electronic effects is less pronounced in the disrotatory ring opening of 5,6-disubstituted 1,3-hexadienes. The effect is rather more steric in nature than electronic, and the larger substituents move outward [25, 26]. For instance, a hexatriene with both 1- and 6-substituents on *trans*-double bonds reacts faster than a hexatriene with one substituent on a *trans*-double bond and the other substituent on a *cis*-double bond. The transformation **66**  $\rightarrow$  **67** has been estimated to proceed 20 times faster than the transformation **68**  $\rightarrow$  **69** under otherwise identical reaction conditions.

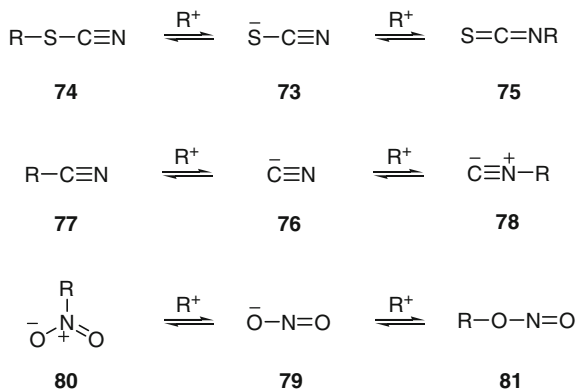


## 4 Ambident Nucleophiles

Nucleophiles with two sites that could react with electrophiles are called ambident nucleophiles. The Hard and Soft Acids and Bases (HSAB) principle applies because a hard electrophile reacts at the harder nucleophilic site and a soft electrophile at the softer nucleophilic site. For instance, the sulfenate ion **70** is an ambident nucleophile, because it reacts (a) with methyl fluorosulfonate, a hard electrophile, at the oxygen atom, where most of the negative charge is concentrated, to give the sulfenate ester **71** and (b) with methyl iodide, a soft electrophile, to give the sulfoxide **72**. Sulfur atom is the softer of the two nucleophilic sites available in the sulfenate ion and, furthermore, it is rendered more nucleophilic by the  $\alpha$ -effect arising from the adjacent oxygen atom.



The thiocyanate, cyanide, and nitrite ions are also ambident nucleophiles. The thiocyanate ion is softer on the sulfur atom and harder on the nitrogen atom. Likewise, the cyanide ion is softer on the carbon atom and harder on the nitrogen atom, and the nitrite ion is harder on the oxygen atom and softer on the nitrogen atom. Depending on the nature of the electrophile  $\text{R}^+$  and also the reaction conditions, each of these ions can react to give either of the two possible products: the thiocyanate **74** or the isothiocyanate **75** from the thiocyanate ion **73**, the nitrile **77** or the isonitrile **78** from the cyanide ion **76**, and the nitroalkane **80** or the alkyl nitrite **81** from the nitrite ion **79**.

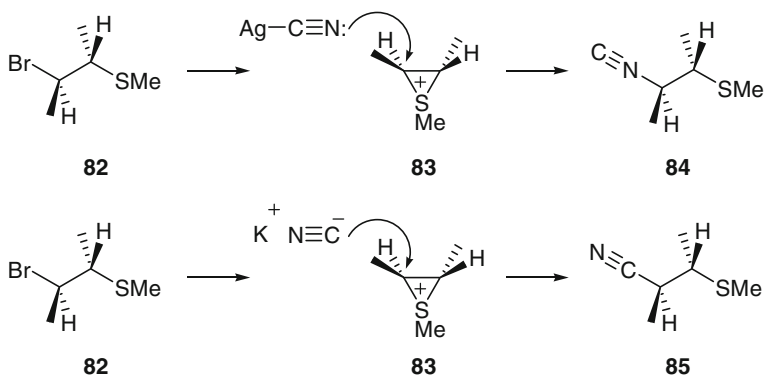


We tend to expect that a harder electrophile will form isothiocyanate, isonitrile, and nitrite. However, other factors also play significant roles. For instance, the thiocyanate **74** is the kinetically preferred product in alkylation by alkyl halides and carbocationic species even when a carbocation constitutes a hard electrophile by virtue of being charged. This is partly explained by the relatively small changes in the bond lengths and in the electronic reorganization required in going from the thiocyanate ion to the thiocyanate product. However, a thiocyanate isomerizes rapidly to the corresponding isothiocyanate which is thermodynamically more

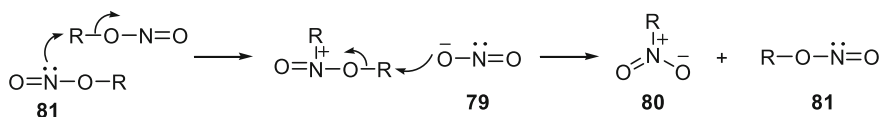
stable. A tertiary alkyl thiocyanate rearranges by the  $S_N1$  pathway (ionization followed by recombination) [27], and a primary alkyl thiocyanate by the  $S_N2$  pathway (the nitrogen of one thiocyanate attacks the alkyl group of another thiocyanate from the rear) [28].

Just as with the thiocyanate ion **73**, the cyanide ion **76** reacts with soft alkyl halides in  $S_N2$  fashion and with hard carbocations in  $S_N1$  fashion to give, almost always, the nitrile **77**, which is thermodynamically more stable than the corresponding isonitrile **78**. The isonitrile product is formed along with the nitrile product when (a) the cation is so very reactive that the rate of reaction reaches diffusion-controlled limit and (b) the reversible reaction that equilibrates the isonitrile and nitrile products is very slow. Since the reaction of a cyanide ion with a carbocation falls in the domain of ion-to-ion reaction, it is indeed very fast. For such a barrierless combination of ions, the kinetic factors associated with the HSAB principle are not applicable.

The isonitrile product is formed under special conditions. For example, silver cyanide reacts with the bromide **82** to form the isonitrile **84**, whereas potassium cyanide gives only the nitrile **85** [29]. Both the reactions proceed through the episulfonium ion **83** to allow overall retention of configuration. These observations are explained as follows: the relatively soft silver is attached to the carbon end of the cyanide ion, leaving the nitrogen end free to participate as a nucleophile, whereas potassium is not so attached. Likewise, trimethylsilyl cyanide sometimes gives the isonitrile product from reaction with a carbocation that is stabilized only by alkyl groups. It happens perhaps because (a) the silyl group is attached to the carbon atom at the time of the reaction and/or (b) the formed isonitrile rearranges very slowly to the corresponding nitrile.



Nitrite ion generally gives nitroalkane **80** as the major product. Since a nitroalkane is thermodynamically more stable than the corresponding alkyl nitrite, the alkyl nitrite isomerizes to the corresponding nitroalkane in a manner as shown below.



As with the cyanide ion, when the reaction of nitrite ion with a carbocation reaches diffusion-controlled limit, the alkyl nitrite may be detected and it may even be the predominant product. Nitrite ion gives mixture of nitroalkane and alkyl nitrite in  $S_N2$  reactions even when the alkyl electrophile is relatively soft. For instance, the  $S_N2$  reaction of nitrite ion with methyl iodide, trimethyloxonium ion, and methyl triflate gives, respectively, 30:70, 50:50, and 60:40 mixtures of methyl nitrite and nitromethane. The gradual increase in the methyl nitrite component is in keeping with the gradual increase in the hardness of the electrophile [30]. Likewise, the nitrite to nitroalkane ratio increases from 16:84 to 30:70 to 61:39 in the  $S_N2$  reactions of silver nitrite with primary benzyl bromides as the *p*-substituent on the benzene ring is changed from  $\text{NO}_2$  to H to OMe, respectively [31–33]. Silver, being soft, is bound largely to the nitrogen of the nitrite ion, leaving the oxygen as the more available nucleophilic species. As the hardness of the electrophile rises in the order that the substituent on the benzene ring is changed, more of the alkyl nitrite is formed. The OMe substituent imparts more cationic character to the benzyl bromide through conjugation effect.

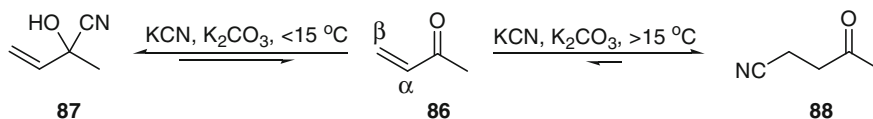
## 5 Ambident Electrophiles

There are molecules that have two-electron deficient centers capable to react with nucleophiles. Such molecules are called ambident electrophiles. The reactivity profile is susceptible to the same kind of analysis as the one we have had above for the reaction of ambident nucleophiles with electrophiles. In the reaction of an electrophile with a nucleophile, it is the LUMO of the electrophile that interacts with the HOMO of the nucleophile. As such, the higher the HOMO and/or the lower the LUMO to reduce energy gap between the two, the faster will be the reaction. Alternatively, the better the match of the HOMO and LUMO coefficients, the more effective will be the reaction.

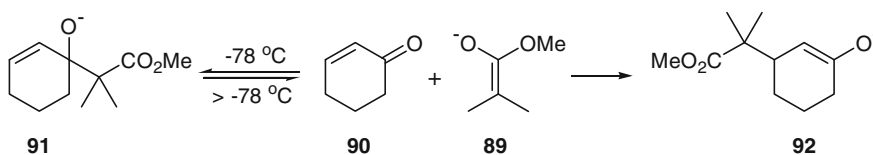
### *$\alpha,\beta$ -Unsaturated Carbonyl Compounds*

Most nucleophiles attack  $\alpha,\beta$ -unsaturated ketones faster at the carbonyl carbon than at the  $\beta$ -carbon. The attack at the  $\beta$ -carbon is generally the result of a slower, but

thermodynamically more favorable, reaction. For the  $\beta$  mode of attack to predominate, it is necessary that the first step is reversible. Well-stabilized anions and higher temperatures aid this reversibility. For instance, reaction with cyanide ion at a temperature below 15 °C leads to reaction largely at the carbonyl carbon and cyanohydrin (**86**  $\rightarrow$  **87**) is formed. However, the same reaction, when conducted at a temperature above 15 °C, turns largely in favor of conjugate addition to result in a  $\beta$ -cyanoketone (**86**  $\rightarrow$  **88**) [34].



Likewise, the lithium enolate **89** reacts with cyclohexenone **90** at  $-78\text{ }^\circ\text{C}$  to give the product of attack at the carbonyl carbon (direct attack) **91**. However, warming the reaction mixture to room temperature allows this step to revert to the starting materials, which react again to form the thermodynamically more stable product of conjugate addition **92** [35]. The enolates formed from  $\beta$ -dicarbonyl compounds do not allow the isolation of the product of direct attack because the first step is even more easily reversible in these instances.

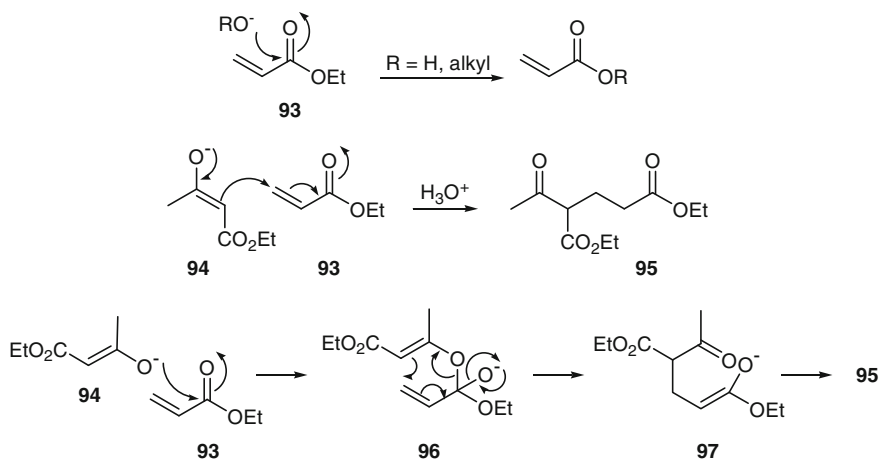


In the simplest  $\alpha,\beta$ -unsaturated carbonyl compound acrolein, though there is greater  $\pi$ -electron deficiency at the carbonyl carbon, but the LUMO coefficient is larger at the  $\beta$  carbon [36]. Thus, if any nucleophile is to attack directly at the  $\beta$  carbon, it must be soft in response to frontier orbital term. This is borne out by the observation that radicals, which are inherently soft, add to the  $\beta$  carbon exclusively. Further, the relatively soft Grignard reagents react more in conjugate fashion than the relatively hard organolithium reagents [37].

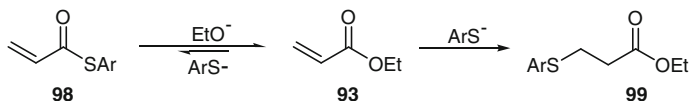
Many additions to  $\alpha,\beta$ -unsaturated carbonyl compounds, take advantage of coordination to the oxygen by a metal cation or a proton, or even just a hydrogen bond. This is true for hydrides and carbon nucleophiles. In such a situation, the LUMO coefficient is largest at the carbonyl carbon, but not at the  $\beta$  carbon. Thus, even soft nucleophiles can be expected to attack directly at the carbonyl carbon when Lewis or protic acid catalysis is involved. It is likely that the difference in the

levels of selectivity shown by Grignard and lithium reagents is largely due to the difference in the effectiveness of coordination by the metal than the difference in the hardness and softness of the nucleophiles. For instance, the ratio of direct to conjugate attack to cyclohexenone by  $\text{LiAlH}_4$  in ether is 98:2. However, on sequestering the lithium ion by a cryptand, the selectivity changes to 23:77 [38].

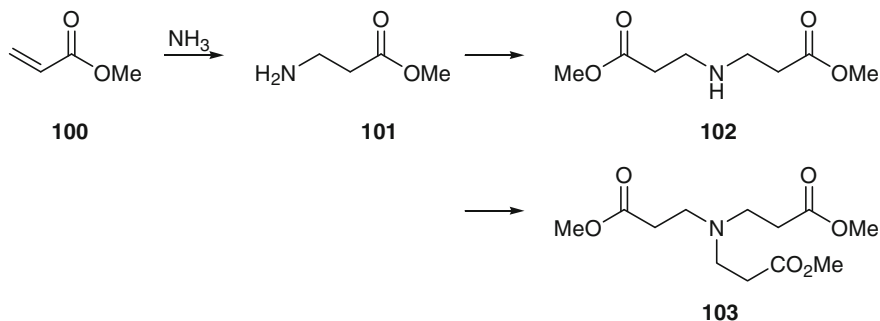
Hydroxide and alkoxide ions, both hard nucleophiles, react with ethyl acrylate **93**, an  $\alpha,\beta$ -unsaturated ester, by direct attack at the carbonyl carbon to bring about ester hydrolysis and ester exchange, respectively. However, the enolate **94**, a soft nucleophile, reacts in conjugate manner to form **95** predominantly. In an alternate pathway, it is also likely that the enolate **94** reacts through the oxy anion (hard nucleophile) directly at the carbonyl carbon (hard electrophile) to generate the species **96**, which rearranges in an oxy anion accelerated [3.3] sigmatropic shift manner, as shown, to form **97** and, thus, the above product **95**. However, it is not certain that such a direct attack by the enolate is not more rapid and reversible.



The thiolate anion ( $\text{RS}^-/\text{ArS}^-$ ) does not react with  $\alpha,\beta$ -unsaturated esters to give  $\alpha,\beta$ -unsaturated thioesters **98** because the equilibrium favors the ester. However, reaction with esters gives the products of conjugate addition **99** exclusively. The relative rate of attack at both the sites can, therefore, not be measured. It is likely that the conjugate attack is kinetically controlled.



Ammonia, a soft nucleophile for being neutral, reacts with methyl acrylate **100** in methanol in conjugate manner to give the primary amine **101**. The reaction continues in the same sense and the secondary amine **102** and the tertiary amine **103** are formed successively [39]. It is to be noted that ammonia, and other primary and secondary amines, do not react with simple esters to form amides. Combine this with the known observation that attack at the carbonyl group is irreversible and also rate determining [40], the above conjugate addition must necessarily be a product of kinetic control, supported by HOMO-LUMO interaction.

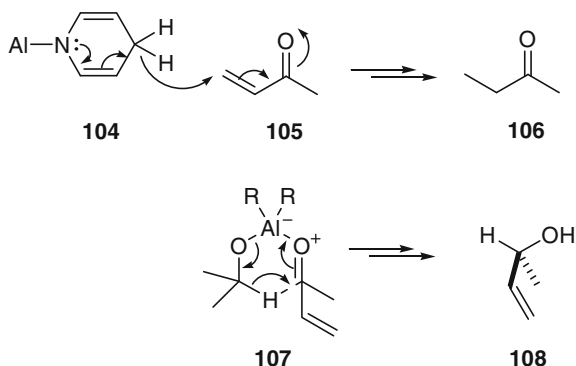


Making the carbonyl group more electrophilic by protonation or coordination with a metal cation increases the possibility of direct attack at the carbonyl carbon. Contrary to this, a reduction in the electrophilicity, which indeed happens in the corresponding cyclohexyl imine, increases the chances of conjugate addition. For instance, acryloyl chloride, which is like protonated acrolein, reacts with ammonia directly at the carbonyl group to result in acrylamide exclusively. Contrary to this, the cyclohexyl imine derivative reacts with organolithiums exclusively in the conjugate manner.

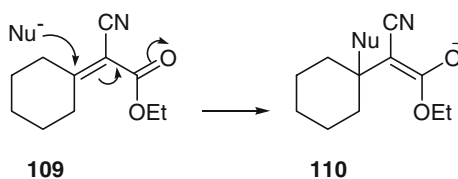
The ratio of the products of conjugate and direct reductions increases with the increase in the softness of the hydride reagent. This softness increases in the order: aluminum hydrides < boron hydrides < carbon hydrides. It is this difference that brings about exclusive conjugate addition when an  $\alpha,\beta$ -unsaturated ketone is allowed for reduction using lithium aluminum hydride in pyridine [41]. In the process, pyridine is first reduced by lithium aluminum hydride to **104** which then delivers hydride ion to the substrate in the manner shown below to form the saturated ketone. The reduction using Hantzsch ester (diethyl 1,4-dihydro-2,6-dimethyl-3,5-pyridinedicarboxylate) is very similar to this [42–51]. Contrast this with the Meerwein-Ponndorf-Verley reduction wherein the hydride delivery is constrained by the six-membered ring transition structure **107** to give the product of



direct reduction **108** [52]. Even though electronically favored, the conjugate addition is avoided because it would involve an eight-membered ring transition structure.

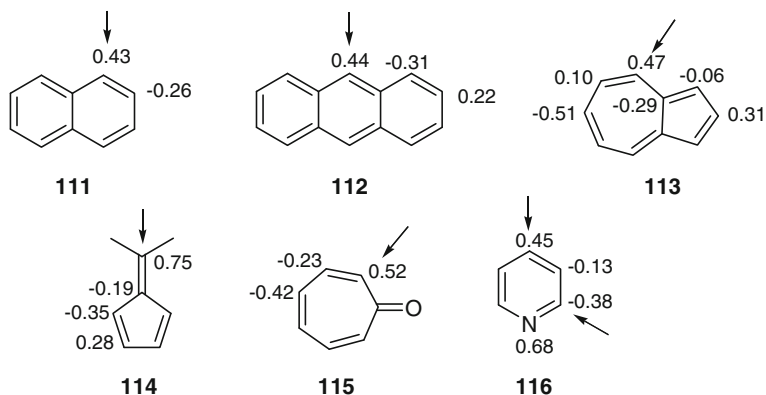


Olefins with two activating substituents, as in the ester **109**, undergo fast conjugate reduction and also conjugate addition of carbon nucleophiles. The stability of the conjugated enolate species **110** and frontier orbital factors, i.e., largest LUMO coefficient at the  $\beta$ -carbon explain this selectivity.

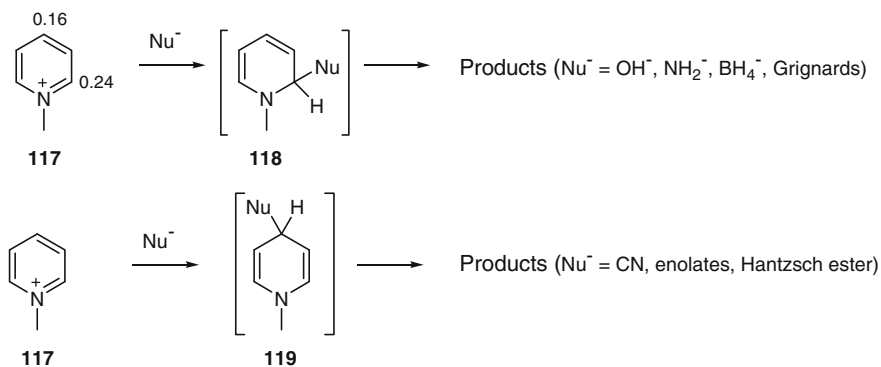


### *Aromatic Electrophiles*

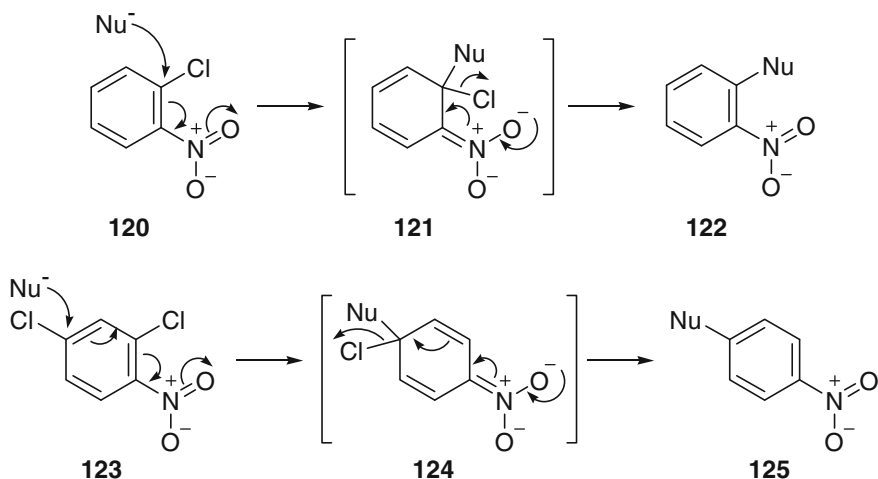
Considering the LUMO of the conjugated system and the HOMO of the nucleophile as the important FMOs for the reaction, the electrophilic site (or sites) of a select group of aromatic compounds **111–116** is indicated by the arrow(s). In each case, there is high LUMO coefficient at the site of attack, each such site also has a high total electron deficiency and, with the possible exception of pyridine, the tetrahedral intermediate formed from such an attack is lower in energy than attack at an alternate site.



The pyridinium cation **117** is even more readily attacked by nucleophiles at C2 and C4 than pyridine itself. On the product side of the reaction, the linearly conjugated intermediate **118**, which also benefits from an anomeric effect should the nucleophile be an electronegative heteroatom, and will therefore be the product of thermodynamic control. Since this step is not always reversible, the frontier orbitals and the charge distribution in the starting material are likely to be important when the reaction is kinetically controlled. Charge control, taken together with the high  $\pi$  electron deficiency at C2, will favor reaction with hard nucleophiles at this site. This is indeed the case with hard nucleophiles such as the hydroxide ion, amide ion, borohydride ion, and Grignard reagents as shown [53, 54]. In contrast, the LUMO coefficient is larger at C4 than at C2 and, hence, the soft nucleophiles such as cyanide ion, enolates, and the hydride ion derived from the carbon atom of the Hantzsch ester attack faster at C4 than at C2 [55].



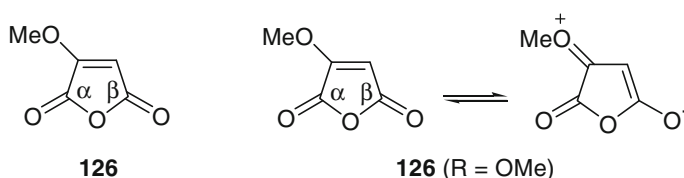
We know that the *ortho*- and *para*-halogenonitrobenzenes are readily attacked by nucleophiles. The first step is generally ratedetermining. As discussed above, the product development control should favor faster attack at the *ortho* position than at the *para* position because the intermediate **121** with linear conjugation is lower in energy than the intermediate **124** with cross conjugation. The electrostatic factor also favors attack at the *ortho* position because of greater  $\pi$  electron deficiency at this position than the *para* position. However, since the LUMO coefficient is larger at the *para* position than the *ortho* position, attack by a soft nucleophile at the *para* position must be faster than that at the *ortho* position. Indeed, DABCO (neutral and, hence, a soft nucleophile) attacks at the *para* position in *p*-chloronitrobenzene 250 times faster than the *ortho* position in *o*-chloronitrobenzene.



### Unsymmetrical Anhydrides

The selectivities demonstrated by unsymmetrical maleic and phthalic anhydrides for attack of a nucleophile on one carbonyl group rather than on the other are large enough to demand explanation. In principle, maleic anhydride **126** can undergo attack by a nucleophile at either of the two carbonyl carbons C<sub>α</sub> and C<sub>β</sub>. However, there is exclusive attack at C<sub>α</sub> by lithium aluminum hydride when R is a methoxy group. The ratio of attack at C<sub>α</sub> versus C<sub>β</sub> reduces only slightly to 88:12 when R is a

methyl group. Being electron-donating and/or electron-releasing, both these groups are in conjugation with the  $\beta$  carbonyl group. This results in reduction in the LUMO coefficient at  $C_\beta$ . Consequently,  $C_\alpha$  is more electrophilic than  $C_\beta$  and, hence, the preferential attack, in spite of the greater steric demand imposed by the substituent. Calculations show that the LUMO coefficient at  $C_\alpha$  is slightly smaller in the methyl derivative than in the methoxy species and, hence, the difference in the observed selectivities [56]. The difference in the LUMO coefficients at  $C_\alpha$  is in line with the known fact that methoxy is a more powerful electron-donating group than methyl.

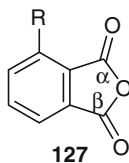


LUMO coefficients at  $C_\alpha$  versus  $C_\beta$

R	$C_\alpha$	$C_\beta$
MeO	0.39	-0.34
Me	0.36	-0.35
Ph	0.22	-0.25

The selectivity changes in favor of attack at  $C_\beta$  in the reaction with a phosphorus yield when the substituent is methyl ( $C_\alpha:C_\beta = 6:94$ ) and phenyl ( $C_\alpha:C_\beta = 0:100$ ), although still in favor of exclusive attack at  $C_\alpha$  when R is a methoxy group ( $C_\alpha:C_\beta = 100:0$ ). It appears that the inherent LUMO controlled reactivity at  $C_\alpha$  is preserved with the better electron-donating group, but steric effects override with the others. The methoxy group may additionally help by coordination to deliver the nucleophile to the nearer carbonyl group, i.e.,  $C_\alpha$ .

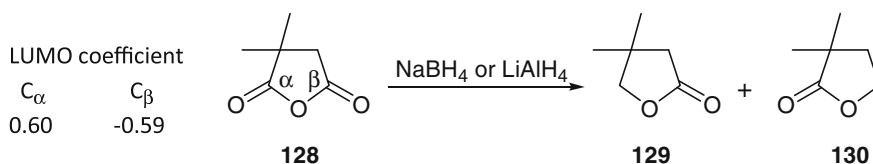
The above analysis, however, is not applicable to phthalic anhydride **127**. The electron-donating and electron-withdrawing substituents should make the reaction selective for attack at  $C_\beta$  and  $C_\alpha$ , respectively, due to the relatively larger LUMO coefficients on these positions. Except for R = Me, when the values are hardly different, the LUMO coefficients match this expectation. However, in spite of being sterically disfavored, the attack by  $\text{NaBH}_4$  takes place preferably at  $C_\alpha$  of all the three substrates:  $C_\alpha:C_\beta = 87:13$  for R = OMe, 57:43 for R = Me, and 83:17 for R =  $\text{NO}_2$ . Thus, the overall situation remains unclear and no suitable rationale could be offered to explain the observed selectivity.



LUMO coefficients at  $C_\alpha$  versus  $C_\beta$

R	$C_\alpha$	$C_\beta$
MeO	-0.26	0.30
Me	-0.33	0.33
NO <sub>2</sub>	-0.21	0.08

The selectivity observed from the reaction of the unsymmetrical succinic anhydride **128** is remarkably in favor of attack at  $C_\alpha$ . The electronic difference between the two-carbonyl groups is that while  $C_\alpha$  is in hyperconjugative interaction with a  $CMe_2$  group, and  $C_\beta$  is in hyperconjugative interaction with a  $CH_2$  group. Since  $\sigma_{C-H}$  is more electron-donating than a  $\sigma_{C-C}$  bond,  $C_\alpha$  must have larger LUMO coefficient than  $C_\beta$ . Calculations indeed place larger LUMO coefficient at  $C_\alpha$  than that at  $C_\beta$  and, hence, the observed selectivity. The composition **129:130** is 95:5. With a Grignard reagent, with which the steric effects are more important, attack takes place at the less hindered  $C_\beta$ . However, when the two substituents are exchanged for chlorine atoms, attack is completely selective for  $C_\alpha$ . Due to the negative hyperconjugation caused by the electronegative chlorine atoms, the LUMO at  $C_\alpha$  turns fairly large and, hence, the observed selectivity.

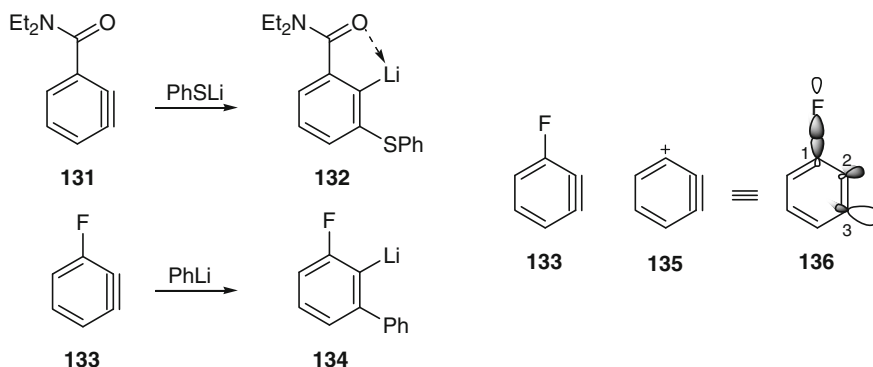


## Arynes

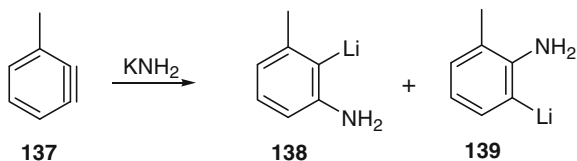
*o*-Benzynes show synthetically useful regioselectivity in reactions with nucleophiles and, therefore, it is desirable to reflect upon its origin. The two in-plane *p* orbitals are bent apart, making their interaction considerably less than the interaction of the two *p* orbitals in forming the  $\pi$  bond of an alkene. Consequently, the

HOMO is raised and the LUMO lowered in energy relative to those of alkenes or linear alkynes. The nucleophilic addition to a benzyne is rendered favorable by the low energy of this LUMO. Even though the HOMO is raised in energy, arynes do not normally react with electrophiles. A likely rationale for this discrepancy may be found from an analysis of the products. The product of nucleophilic attack on an aryne is aryl anion which is stable relative to a tetrahedral anion. This is one of the reasons why acetylenes react more readily than alkenes with nucleophiles. In contrast, the product of electrophilic attack on an aryne is aryl cation which is high in energy. The high energy of this aryl cation is possibly the main reason why acetylenes are generally less reactive than alkenes toward electrophiles.

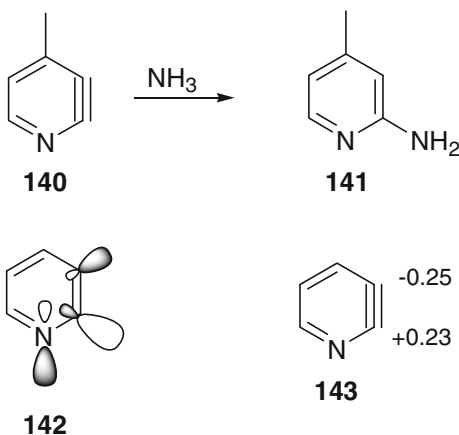
The regioselectivity of *o*-benzyne is controlled by the electronic and steric effects of the substituent. A major factor is the relative stability of the regioisomeric products, with the benzyne **131** giving the lithium intermediate **132** and the benzyne **133** giving the lithium intermediate **134**. These two substituents are excellent at stabilizing the neighboring  $\sigma_{\text{C-Li}}$  bond, the former by coordination to lithium, as shown, and the latter by conjugation between the  $\sigma_{\text{C-F}}$  and  $\sigma_{\text{C-Li}}$  bonds. In the latter instance, an alternate argument also holds. Being highly electron-withdrawing,  $\sigma_{\text{C-F}}$  bond in **133** has some of the character of a cation on a carbon **135**, in which the empty *p* orbital will be conjugated to the in-plane bent *p* orbital on the adjacent carbon. The LUMO will, therefore, resemble that of an allyl cation with its largest coefficient on C3 as indicated in **136**. Additionally, C3 is also the site with less steric hindrance, but it is clear from cycloadditions that steric hindrance at C2 is not the reason why nucleophiles attack at C3.



With an alkyl substituent, the two regioisomeric product anions are not substantially different, nor are the LUMO coefficients on C2 and C3. Such systems are therefore expected to show poor selectivity, if at all. Indeed, the benzyne **137** is attacked equally at C2 and C3, except when the nucleophile is substantially large.



Pyridynes are inherently unsymmetrical. Nucleophiles attack 4-methyl-2,3-pyridyne **140** exclusively at C2. Since, the nitrogen electron pair is in the same plane as the two  $p$  orbitals in the plane of the ring, the situation resembles an allyl anion. Like the allyl anion, the large LUMO coefficient is on C2 than at C3, as shown in **142** [57]. Also, the total charge distribution, as shown in **143**, is such that C2 bears a partial positive charge. The overall result is that nucleophiles attack preferably at C2 because both electrostatic and frontier orbital forces favor attack at this site. Additionally, in terms of product analysis, the product 3-pyridyl anion is more stable than 2-pyridyl anion due to hyperconjugative interaction between the electron pair orbital on C3 and the electronegative  $\sigma_{\text{C-N}}$  bond, both being antiperiplanar to each other across the  $\sigma_{\text{C2-C3}}$  bond.



## 6 $\alpha$ -Effect

The  $pK_a$  of the conjugate acid of a given nucleophile is a good measure of the rate at which it attacks hard electrophiles. A plot, known as Brønsted plot, of the log of the rate constant for nucleophilic attack on a carbonyl group against the  $pK_a$  of the conjugate acid of the nucleophile is a good straight line only when the nucleophilic atom is the same. In other words, there is a straight line for every nucleophilic atom. However, nucleophiles such  $\text{HO}_2^-$ ,  $\text{ClO}^-$ ,  $\text{HONH}_2$ ,  $\text{N}_2\text{H}_4$ , and  $\text{R}_2\text{S}_2$  are unique because they are more nucleophilic than one would expect from the  $pK_a$  values of

their conjugate acids. Consequently, these nucleophiles do not fit on the Brønsted plots. The nucleophilic site in each of  $\text{HO}_2^-$ ,  $\text{ClO}^-$ ,  $\text{HONH}_2$ ,  $\text{N}_2\text{H}_4$ , and  $\text{R}_2\text{S}_2$  is attached to a heteroatom bearing an electron pair orbital. The electron pair orbital on the nucleophilic atom overlaps with the electron pair orbital on the adjacent atom. This interaction raises the energy of the HOMO relative to its position in the unsubstituted nucleophile and, thus, results in an increase in the nucleophilicity, called the  $\alpha$ -effect, which could be quite dramatic sometimes. The  $\alpha$ -effect becomes more noticeable when the reactions are carried out in dipolar aprotic solvents because these solvents do not stabilize anions through solvation [58].

The LUMO of the triple bond of a nitrile is lower than the LUMO of the double bond of a carbonyl group. Further, the LUMO of the double bond of a carbonyl group is lower than the LUMO of a  $\sigma_{\text{C-Br}}$  bond. Thus, the relative rate of reaction of  $\text{HO}_2^-$  versus  $\text{HO}^-$  ( $k_{\text{HO}_2^-}/k_{\text{HO}^-}$ ) decreases when the substrate is changed from benzonitrile ( $k_{\text{HO}_2^-}/k_{\text{HO}^-} = 10^5$ ) to methyl *p*-nitrobenzoate ( $k_{\text{HO}_2^-}/k_{\text{HO}^-} = 10^3$ ) to benzyl bromide ( $k_{\text{HO}_2^-}/k_{\text{HO}^-} = 50$ ) [59].

The raised HOMO also provides an explanation for a single electron transfer mechanism as it allows an electron to be easily transferred to the LUMO of an electrophile to generate a radical pair to further couple to the product. Since the removal of a single electron from one of the two electron pair orbitals on nucleophilic atom leaves behind a stabilized radical, the rate constant for the reaction of a nucleophile with  $\alpha$ -effect is likely to be more sensitive to the LUMO energy of the electrophile than the rate constant for a nucleophile with a normal lone pair [60]. This is indeed so in the rates of *N*-methylation of a series of *N*-phenylhydroxylamines, which are higher than the rates in comparable anilines [61].

The  $\alpha$ -effect influences the thermodynamic stability of the species as well. For instance, overlap of the lone pair on nitrogen with  $\pi^*_{\text{C=O}}$  is responsible, in large part, for the higher stability of amides such as **144** relative to the corresponding ketones. In the hydroxamic acid **145**, the effect of lone pair on the oxygen is to raise the energy of the lone pair on nitrogen which, in turn, makes its overlap with  $\pi^*_{\text{C=O}}$  more effective and, thus, more energy-lowering. Consequently, hydroxamic acids are more stable than the corresponding amides. It is the  $\alpha$ -effect in oximes and hydrazones that makes them less electrophilic than imines. The overlap of the lone pair on the second heteroatom, oxygen in oximes, and nitrogen in hydrazones, with the developing lone pair on the nitrogen atom of the imine during the progress of the reaction is destabilizing. However, it is also true that the same lone pair is conjugated to  $\pi_{\text{C=N}}$  of the imine, which is stabilizing.

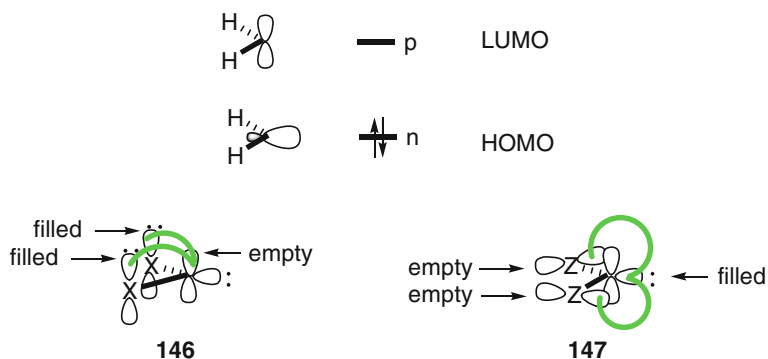




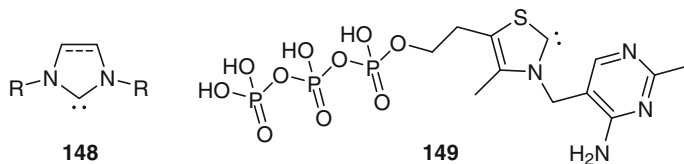
## 7 Carbenes

Carbenes can act both as nucleophilic and electrophilic species. The HOMO is a filled  $p$  orbital, high in energy because of its closeness to an isolated  $p$  orbital. The LUMO is an unfilled  $p$  orbital, orthogonal to HOMO. The high energy of the HOMO makes the carbene very reactive as a nucleophile. Likewise, the low energy of the LUMO makes the carbene very reactive as an electrophile.

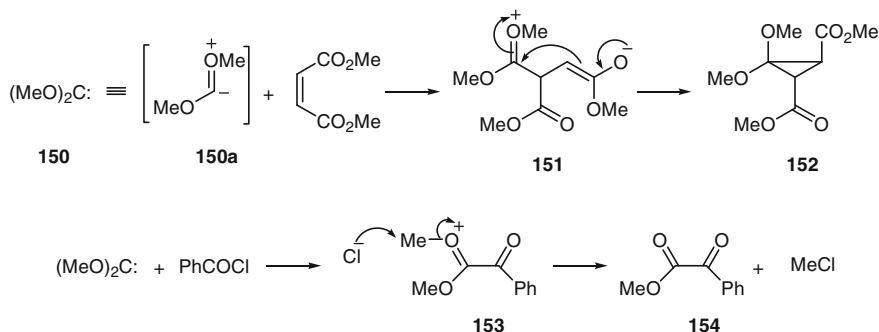
A donor substituent lowers the energy, if it is conjugated to the LUMO as shown in **146**. Likewise, an electron-withdrawing substituent will lower the energy, if it is conjugated to the HOMO as shown in **147**. Since, the above interactions leave the other orbital more or less unchanged for the orthogonal disposition of the two, the situation in **146** is left with a high energy HOMO and, likewise, the situation in **147** is left with a low energy LUMO. The species **146** and **147** are, therefore, nucleophilic and electrophilic, respectively [62].



The donor substituents have more remarkable effect than electron-withdrawing substituents because they make it possible to isolate a good range of carbenes such as **148** [63–65]. The carbene **149** is the key intermediate in the metabolic pathways catalyzed by the thiamine coenzymes. These reactions proceed by the nucleophilic addition of the carbene to the substrates such as aldehydes [66].

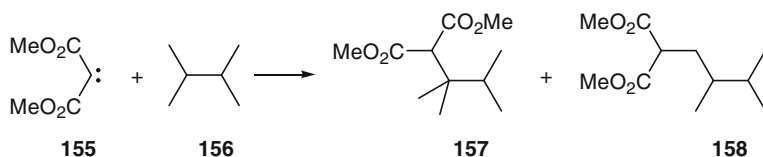


Dimethoxycarbene **150** is known to react with dimethyl maleate and benzoyl chloride to give the intermediates **151** and **153** and, thus, the products **152** and **154**, respectively. While the transformation **151**  $\rightarrow$  **152** involves an intramolecular  $S_N2$  reaction leading to the formation of a cyclopropane ring as shown, the transformation **153**  $\rightarrow$  **154** involves an intermolecular  $S_N2$  reaction. Thus, for all practical purposes, dimethoxycarbene behaves primarily like the ionic species **150a**. Please note that dimethoxycarbene does not insert into isolated alkenes to form cyclopropanes.

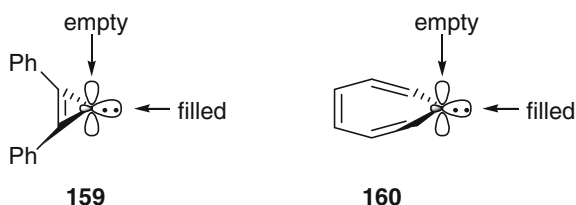


The insertion of a carbene into an alkene is a result of the simultaneous interaction of the HOMO of the alkene with the LUMO of the carbene or the LUMO of the alkene with the HOMO of the carbene. It is the HOMO of a nucleophilic carbene that interacts predominantly with the LUMO of the alkene and, likewise, the LUMO of an electrophilic carbene that interacts predominantly with the HOMO of the alkene. In the case of the highly nucleophilic dimethoxycarbene, the interaction of HOMO of the carbene with the LUMO of the alkene is so very strong that it gives zwitterionic intermediates such as **151**, which results in the loss of stereochemistry in going from a *cis*-alkene to a *trans*-cyclopropane. With the less nucleophilic carbenes, the geometrical integrity of the alkene is retained in the product. Additionally, nucleophilic carbenes do not insert  $\sigma_{C-H}$  bonds.

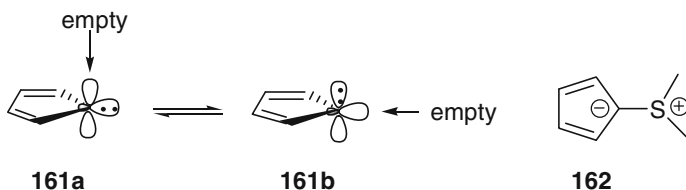
In contrast to nucleophilic carbenes, the electrophilic carbenes with low energy LUMO react with alkenes with high energy HOMO stereospecifically to form cyclopropanes. The electrophilic carbenes also insert  $\sigma_{C-H}$  bonds, tertiary  $\sigma_{C-H}$  bonds in particular. As an example, bis(methoxycarbonyl)carbene **155** reacts with 2,3-dimethylbutane **156** to form the malonate **157** selectively (**157:158** = 97:3) even though there are only two tertiary  $\sigma_{C-H}$  bonds competing against twelve primary  $\sigma_{C-H}$  bonds. The selectivity for the tertiary  $\sigma_{C-H}$  bond is taken to presume a substantial cationic charge on the carbene carbon in the transition state structure which results in electrophilic attack on the hydrogen atom [67, 68].



The cyclopropenylidene carbene **159** has the empty *p* orbital conjugated with the  $\pi$  bond, making it a two-electron three-center cyclic system and, hence, aromatic like the cyclopropenyl cation. Likewise, the cycloheptatrienylidene carbene **160** has the empty *p* orbital conjugated with three  $\pi$  bonds, making it a six-electron seven-center cyclic system and, hence, aromatic like the tropylium cation. In both these instances, the filled HOMO orbital of the carbene remains unaltered to impart enough nucleophilic character. Both these carbenes, therefore, must possess highly nucleophilic character and react readily with electrophilic alkenes but not with the simple alkenes. Indeed, **160** reacts faster with styrenes having electron-attracting substituents and slower with those having no such substituents or donor substituents.

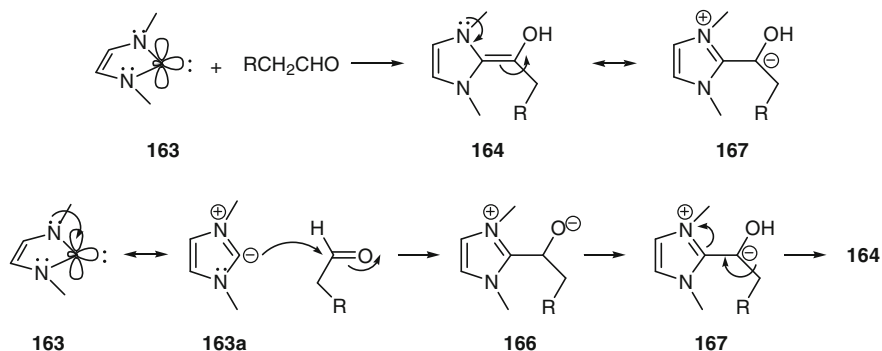


Cyclopentadienylidene carbene is different from **159** and **160**. This is so because the configuration of the carbene may change from **161a** to **161b**. In the configuration **161a**, the empty *p* orbital of the carbene is in conjugation with the two  $\pi$  bonds, leaving the filled *p* orbital to act as a nucleophile. However, in the configuration **161b**, the filled *p* orbital of the carbene is conjugated with the two  $\pi$  bonds, making it like a cyclopentadienyl anion and, hence, aromatic in character. The configuration **161b** can act only as electrophile. Overall, the carbene **161** is only somewhat electrophilic as it reacts with more substituted alkenes at, more or less, the same rate as with the less substituted alkenes. The predominant **161b** character is evident in the reaction with dimethyl sulfide when the zwitterion **162** is formed smoothly [69].



Two distinct scenarios arise for dichlorocarbene. First, the inductive withdrawal along  $\sigma_{\text{C}-\text{Cl}}$  bond lowers the electron density on the carbon to such an extent that the carbene is rendered largely electrophilic in nature. Second, a situation similar to that shown in **146** emerges and the electron pairs on chlorine atoms conjugate with the unfilled LUMO, leaving the filled HOMO to act as a nucleophile. It has been discovered from calculations that the former situation prevails over the latter, allowing dichlorocarbene to exhibit the electrophilic character largely [70].

The carbene **163** is stable enough to be isolated [71]. Carbenes such as **163** are employed as reagents to achieve many transformations and also as preferred ligands for catalyst design. With the six electrons, two from the  $\pi$  bond and two each from the two nitrogen lone pairs, forming an aromatic sextet through the carbene LUMO, the HOMO remains available to impart nucleophilic character. For instance, the species **163** combines with an aldehyde to form the enol species **164** which is in resonance with the zwitterionic species **165**. The species **165** is capable of reacting through the carbanion to form products [72].



The carbene **163** exists in resonance with the species **163a**. The nucleophilic reaction of **163a** with an aldehyde, as shown, forms the 1,4-zwitterion **166**. Now, proton transfer from carbon to oxygen generates the 1,3-zwitterion **167**, which collapses to **164** after electron reorganization.

## 8 Hammett Substituent Constants

The electronic property of an aromatic substituent is expressed by the Hammett substituent constant,  $\sigma$ . This constant for a given substituent is arrived at by measuring its effect on the dissociation of benzoic acid. Benzoic acid itself is a weak acid and it ionizes into benzoate ( $\text{C}_6\text{H}_5\text{CO}_2^-$ ) and proton only partially in water. The relative proportions of the ionized and nonionized species at equilibrium

is known as the equilibrium or dissociation constant  $K_H$ , where the subscript H indicates that there is no substituent on the aromatic ring.

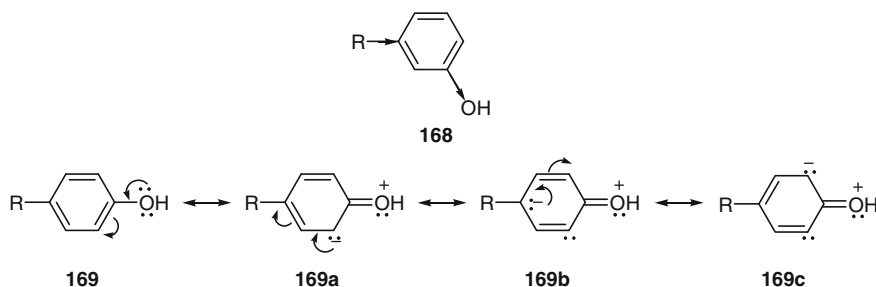
$$K_H = \frac{[\text{PhCO}_2^-][\text{H}_3\text{O}^+]}{[\text{PhCO}_2\text{H}]}$$

A substituent on the aromatic ring will affect the equilibrium. An electron-withdrawing group will stabilize the carboxylate ion to shift the equilibrium to the ionized form, and lead to a larger equilibrium constant, i.e.,  $K_R > K_H$ . In contrast, an electron-donating group will destabilize the carboxylate ion and shift equilibrium to the nonionized form and leads to a smaller equilibrium constant, i.e.,  $K_R < K_H$ . The Hammett constant  $\sigma_R$  for a given substituent R is given by the following equation:

$$\sigma_R = \log \frac{K_R}{K_H} = \log K_R - \log K_H = (pK_a)_H - (pK_a)_R$$

$$(pK_a)_H = pK_a \text{ of unsubstituted acid, } (pK_a)_R = pK_a \text{ of R-substituted acid}$$

The following conclusions emerge from the above discussion: (a) the constant  $\sigma$  for a given substituent is accurate only for the molecular structure from which it is derived and (b) an electron-withdrawing substituent will have a positive  $\sigma$  value and an electron-donating substituent a negative  $\sigma$  value. The Hammett constant is based on benzoic acid and it takes into consideration both the inductive and resonance effects of the substituent and, thus, the value depends on whether the substituent is positioned *meta* ( $\sigma_m$ ) or *para* ( $\sigma_p$ ) to the ionizing group. A *m*-substituent will exert inductive effect and a *p*-substituent the resonance effect largely. Let us consider phenol as an example. The property of the substituent R is influenced by the inductive effect of OH in **168** and the resonance effect in **169**, as shown.



The constants  $\sigma_m$  and  $\sigma_p$  for a host of substituents are collected in Table 1. It is to be noted that both  $\sigma_m$  and  $\sigma_p$  for alkyl substituents such as methyl, ethyl, isopropyl, *tert*-butyl, and  $\text{CH}_2\text{SiMe}_3$  are negative as they exert only the positive

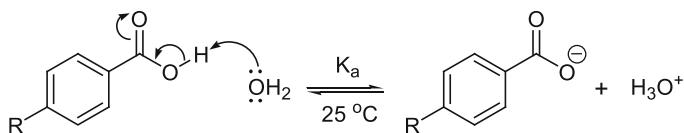
**Table 1** Hammett constants,  $\sigma$ , based on the ionization of benzoic acids<sup>a</sup>

Substituent	$\sigma_m$	$\sigma_p$	$\sigma^+$	$\sigma^-$	Substituent	$\sigma_m$	$\sigma_p$	$\sigma^+$	$\sigma^-$
CH <sub>3</sub>	-0.07	-0.17	-0.31	-	N <sub>2</sub> <sup>+</sup>	+1.76	+1.91		
CH <sub>2</sub> CH <sub>3</sub>	-0.07	-0.15			NMe <sub>3</sub> <sup>+</sup>	+0.88	+0.82		
CHMe <sub>2</sub>	-	-0.15			NO <sub>2</sub>	+0.71	+0.78	+0.79	+1.24
CMe <sub>3</sub>	-0.10	-0.20			CN	+0.56	+0.66	+0.66	+0.90
CH <sub>2</sub> SiMe <sub>3</sub>	-0.16	-0.21			CF <sub>3</sub>	+0.43	+0.54		
SiMe <sub>3</sub>	-0.04	-0.07			COMe	+0.38	+0.50	-	+0.87
NH <sub>2</sub>	-0.16	-0.66	-1.30	-	CO <sub>2</sub> H	+0.37	+0.45	+0.42	-
NHMe	-	-0.84			SH	+0.25	+0.15		
NMe <sub>2</sub>	-	-0.83			SCN	-	+0.52		
NHCOMe	+0.21	+0.00			SCOMe	+0.39	+0.44		
OH	+0.12	-0.37	-0.92	-	SMe	+0.15	+0.00		
OMe	+0.12	-0.27	-0.78	-0.20	SMe <sub>2</sub> <sup>+</sup>	+1.00	+0.90		
OCOMe	+0.39	+0.31			SOMe	+0.52	+0.49		
F	+0.34	+0.06	-0.07	-0.02	SO <sub>2</sub> Me	+0.60	+0.72		
Cl	+0.37	+0.23	+0.11	-	SO <sub>2</sub> NH <sub>2</sub>	+0.46	+0.57		
Br	+0.39	+0.23	+0.15	-	SO <sub>3</sub> <sup>-</sup>	+0.05	+0.09		
I	+0.35	+0.18	+0.13	-	-				

<sup>a</sup>The values in the table are taken from Leffler and Grunwald [75]. The  $\sigma^+$  and  $\sigma^-$  values are given for the *para* substituents only. The  $\sigma^+$  values for selected meta substituents have been measured, but they do not differ appreciably from the  $\sigma_m$  values

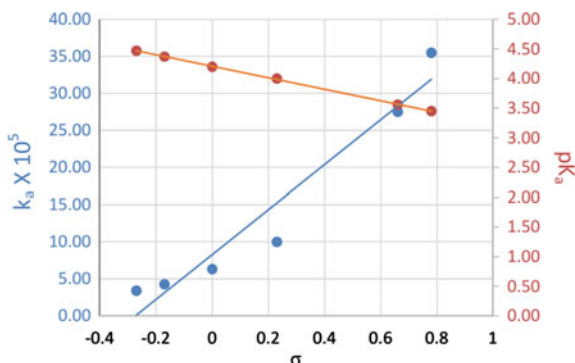
inductive effect and, thus, destabilize the carboxylate ion. Both  $\sigma_m$  and  $\sigma_p$  are negative also for the nitrogen-based substituents such as NH<sub>2</sub>, NHMe, and NMe<sub>2</sub>. These substituents exert their effect largely through strong resonance with the  $\pi$  electrons of the ring such that, irrespective of the *meta* or *para* positioning, there is enough negative charge residence on the ring carbon bearing the carboxylic acid group. This reduces ionization. Unlike the nitrogen substituents, OH and OMe exert largely inductive effect when located at the *meta* position to turn  $\sigma$  positive and resonance effect when at the *para* position to turn  $\sigma$  negative. It is not that the lone pair on oxygen in OH or OMe at the *meta* position is not in resonance with the ring's  $\pi$  electrons, but just that the accumulation of negative charge on the carboxy-bearing carbon through this exercise is negligible. The substituent SH is unique as it exerts only the inductive effect (electron withdrawal) from both the positions. This is largely because of mismatch of the orbital coefficient on the sulfur atom and the *p* orbital coefficient on the adjacent ring carbon to result in poor or no overlap.

The equilibrium ionization constants  $K_a$  for selected *p*-substituted benzoic acids including benzoic acid, their  $pK_a$  values, and Hammett's constants are collected in Table 2. The plots of  $K_a \times 10^5$  and also  $pK_a$  against  $\sigma$  for these acids are shown in Fig. 4. The data in Table 2 and the plots in Fig. 4 demonstrate their linear relationships. As  $K_a$  increases,  $pK_a$  decreases, and  $\sigma$  increases.

**Table 2** Equilibrium ionization constant  $K_a$ ,  $pK_a$  values, and Hammett constants  $\sigma$  of selected acids

R	$K_a$	$pK_a$	$\sigma$
$\text{NO}_2$	$3.55 \times 10^{-4}$	3.45	0.78
CN	$2.75 \times 10^{-4}$	3.56	0.66
Cl	$1.00 \times 10^{-4}$	4.00	0.23
H	$6.31 \times 10^{-5}$	4.20	0.00
Me	$4.27 \times 10^{-5}$	4.37	-0.17
OMe	$3.39 \times 10^{-5}$	4.47	-0.27

Hammett [84]

**Fig. 4** plots  $\sigma$  versus  $K_a \times 10^5$  and  $pK_a$  for the substrates in Table 2

Please note that the  $\sigma$  values are so designed that a plot of  $\log_{10} (K_R/K_H)$  versus the  $\sigma$  constant gives a straight line with a slope of unity. The substituent effects found from the ionizations of substituted benzoic acids are applicable to other similar acid ionizations. For instance, a plot of  $\log_{10} (K_R/K_H)$  for a number of ring-substituted phenylacetic acids ( $\text{RC}_6\text{H}_4\text{CH}_2\text{CO}_2\text{H}$ ) vis-à-vis the unsubstituted phenylacetic acid ( $\text{PhCH}_2\text{CO}_2\text{H}$ ) against the  $\sigma$  values obtained for those substituents from the ionization of substituted benzoic acids ( $\text{RC}_6\text{H}_4\text{CO}_2\text{H}$ ) is a straight line but with a slope of less than unity (0.489) [73, 74]. A similar exercise with the ring-substituted 3-arylpionic acids gives  $\rho$  a value of 0.212 [73, 74]. Such diminutions in the substituent effect relative to the effect in benzoic acids are due to the greater separation between the substituent and the acid group. This differential feature is accommodated by Eq. 1, in which  $\rho$  is the slope of the line. This

relationship is applicable to a large number of other equilibria of substituted acids. The closely related Eq. 2 applies to the reaction rates of a large number of substituted aromatic compounds. Both Eqs. 1 and 2 are known as Hammett equations.

$$\rho\sigma_{\text{R}} = \log_{10}(K_{\text{R}}/K_{\text{H}}) \quad (1)$$

$$\rho\sigma_{\text{R}} = \log_{10}(k_{\text{R}}/k_{\text{H}}) \quad (2)$$

The  $\sigma$  values are always those determined from the ionization of substituted benzoic acids, but the  $\rho$  values are different for each substrate type and also for each reaction type because they reflect the sensitivity of the substrate to the electronic effect of the substituent. With  $\rho > 1$ , the ionization or reaction rate is more sensitive to substituent's electronic effects than is the ionization of benzoic acids. With  $\rho < 1$ , electron-withdrawing groups will increase the equilibrium constant or rate, but less than in benzoic acid dissociation. A negative  $\rho$  indicates that electron-donating groups increase the reaction constant. In consideration of reaction rates, a small  $\rho$  often indicates that the reaction involves either radical intermediates or some other pathway that requires little charge separation.

Hammett equation is a linear free energy relationship and we will now see how it is so. The equilibrium constant  $K$  is related to free energy by the equation  $\Delta G^{\circ} = -RT \ln K = -2.303RT \log_{10} K$ , where  $R$  is the gas constant and  $T$  is the temperature in Kelvin. This translates into  $\log_{10} K = -(\Delta G^{\circ}/2.303RT)$ . If the free energy change for the ionization of a R-substituted acid is  $(\Delta G^{\circ})_{\text{R}}$  and that of the unsubstituted acid is  $(\Delta G^{\circ})_{\text{H}}$ , then, Eq. 1 could be modified as below:

$$\begin{aligned} \rho\sigma_{\text{R}} &= \log_{10}K_{\text{R}} - \log_{10}K_{\text{H}} \\ \text{i.e., } \rho\sigma_{\text{R}} &= \left[ \left( \frac{(\Delta G^{\circ})_{\text{R}}}{2.303RT} \right) \right] - \left[ \left( \frac{(\Delta G^{\circ})_{\text{H}}}{2.303RT} \right) \right] \\ \text{i.e., } 2.303RT\rho\sigma_{\text{R}} &= \left[ -(\Delta G^{\circ})_{\text{R}} + (\Delta G^{\circ})_{\text{H}} \right] \\ \text{i.e., } (\Delta G^{\circ})_{\text{R}} - (\Delta G^{\circ})_{\text{H}} &= -2.303RT\rho\sigma_{\text{R}} \end{aligned}$$

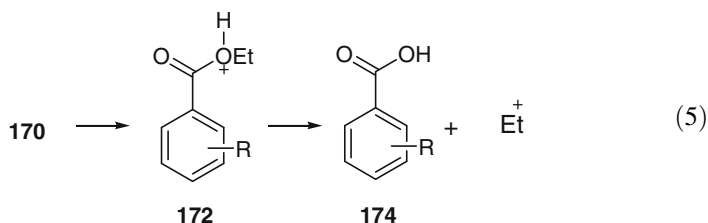
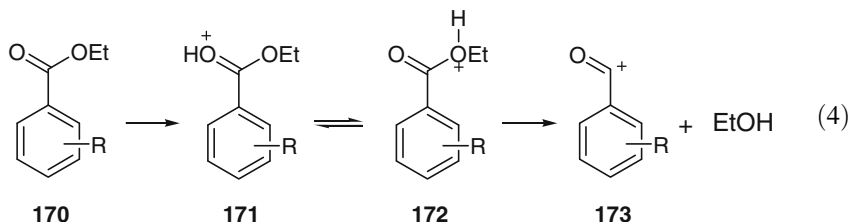
If the free energy changes in the ionizations of a substituted and unsubstituted benzoic acids are represented by  $(\Delta G^{\circ})_{\text{R}}$  and  $(\Delta G^{\circ})_{\text{H}}$ , respectively, we obtain the relationship  $(\Delta G^{\circ})_{\text{R}} - (\Delta G^{\circ})_{\text{H}} = -2.303RT\rho\sigma_{\text{R}}$  on account of the above derivation. Substituting this into the above equation, we get,

$$(\Delta G^{\circ})_{\text{R}} - (\Delta G^{\circ})_{\text{H}} = r(\Delta G^{\circ})_{\text{R}} - (\Delta G^{\circ})_{\text{H}} \quad (3)$$

This equation states that the extent to which the free energy change of a particular equilibrium is altered by adding a substituent R is linearly related to the extent to which the free energy change of ionization of benzoic acid is altered by putting the same substituent on the benzene ring.

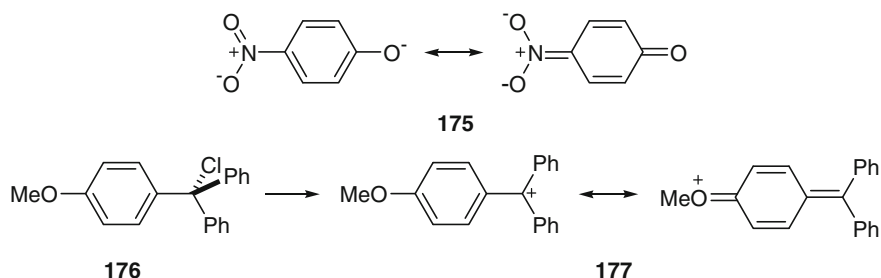


A linear correlation of  $\log_{10} (K_R/K_H)$  or  $\log_{10} (k_R/k_H)$  with  $\sigma$  implies that the position of transition state does not change on changing the substituent. A curved line implies constant change in the position of the transition state. Two intersecting straight lines imply a sharp change from one distinct transition state to another distinct transition state. However, neither transition state changes its position with minor changes in the nature of the substituent. For instance, the rate of hydrolysis of ethyl benzoate **170** in 99.9 %  $\text{H}_2\text{SO}_4$  first decreases as the substituents are made more electron-withdrawing. Then, a break occurs and the rate increases again [75]. It is apparent that the mechanism with electron-donating and weakly electron-withdrawing substituents is the one shown in Eq. 4. However, it changes the one shown in Eq. 5 when the substituents are strongly electron-withdrawing. Electron-donating substituents stabilize the acyl cation **173** and the weakly electron-withdrawing substituents are not likely to change the prospects of such acyl cation formation and, hence, the pathway in Eq. 4. Highly electron-withdrawing substituents do not allow the formation of the acyl cation due to its high instability and, thus, the pathway shown in Eq. 5 sets in rapidly.

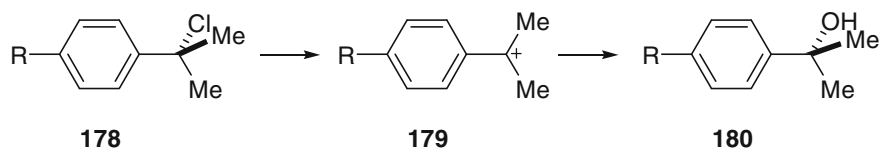


The constant  $\sigma$  is defined from the ionization of benzoic acids wherein the negative charge of the carboxylate ion is not in conjugation with the ring and/or the substituent through the ring. The Hammett equation, therefore, need not apply to equilibria or reaction rates in which the substituent comes into direct resonance interaction with the reaction site. For instance, the *p*-nitro group increases the ionization constant of phenol much more than what would normally be predicted from the  $\sigma_{\text{p-NO}_2}$  constant obtained from the ionization of *p*-nitrobenzoic acid. The product *p*-nitrophenoxide ion **175** has a resonance structure in which the nitro group

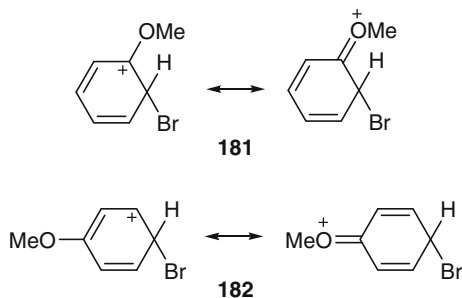
participates with the oxide ion through resonance, as shown. The resultant extra stabilization of the oxy anion is not included in the  $\sigma_{p-\text{NO}_2}$  constant. In yet another example, a *p*-methoxy group is much more effective at increasing the ionization rate of triphenylmethyl chloride **176** than what would be predicted from the  $\sigma_{p-\text{OMe}}$  constant obtained from the ionization of benzoic acids.



It was therefore felt that the rate and equilibria constants could be correlated better by the Hammett equation if two new types of  $\sigma$  constants were introduced. When there is resonance between a reaction site that becomes electron-rich and an electron-withdrawing substituent,  $\sigma^-$  constant is used. The standard reactions for the evaluation of  $\sigma^-$  constants are the ionization of *p*-substituted phenols and *p*-substituted anilinium ions [75]. Likewise, when there is resonance between a reaction site that becomes electron-deficient and an electron-donating substituent,  $\sigma^+$  constant is used. The standard reaction for the evaluation of  $\sigma^+$  constants is the solvolysis of *p*-substituted *tert*-cumyl chlorides **178** using 90 % aqueous acetone [76]. Selected  $\sigma^+$  and  $\sigma^-$  values are included in Table 1.



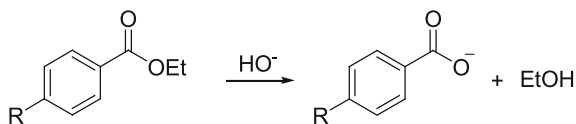
The utility of the  $\sigma^+$  and  $\sigma^-$  values in comparison to the  $\sigma$  values could be understood from the plots of  $\log_{10}(k_{\text{R}}/k_{\text{H}})$  for the bromination of monosubstituted benzenes *versus*  $\sigma$  and  $\sigma^+$ . While the plot  $\log_{10}(k_{\text{R}}/k_{\text{H}})$  *versus*  $\sigma$  is a scatter of points, the plot  $\log_{10}(k_{\text{R}}/k_{\text{H}})$  *versus*  $\sigma^+$  is a straight line [76]. Bromination of anisole, at both *ortho* and *para* positions, demonstrates how a substituent, electron-donating by resonance, can stabilize the positive charge in the intermediate cations **181** and **182** and, therefore, the respective transition states.



The  $\sigma$  value alone can, of course, be used to understand the mechanism of those reactions which do not come under the ambit of  $\sigma^+$  and  $\sigma^-$  values. For instance, the base hydrolysis of a benzoic acid ester may take two different pathways: (a) nucleophilic attack of hydroxide ion on the carbonyl carbon to result in a tetrahedral intermediate, in a rate determining step, followed by its collapse into carboxylic acid or (b) nucleophilic attack of hydroxide ion on the alkyl carbon of the ester function, leading to the formation of the carboxylate directly. Since the carbonyl carbon is closest to the ring, the effect of a substituent felt by it must be much larger than the effect felt by the alkyl carbon. Hence, the rate of hydrolysis will be expected to increase much more in the former instance than in the latter with the increase in the substituent's  $\sigma$  value. This is indeed the case as evident from the  $\sigma$  versus rate constant  $k$  given in Table 3. The large increase in the rate of hydrolysis with the increase in  $\sigma$  could be justified only if the tetrahedral pathway is involved. The correlation of  $\sigma$  with  $\log k$  is linear as seen from the plot in Fig. 5.

Likewise, the substituent constants in the aliphatic series have also been measured from the rates of hydrolysis of a series of aliphatic esters ( $\text{RCH}_2\text{CO}_2\text{CH}_3$ ), where methyl acetate ( $\text{CH}_3\text{CO}_2\text{CH}_3$ ) is the parent ester. The effect of the substituent R

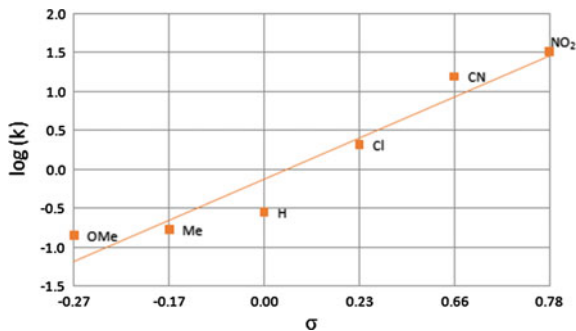
**Table 3** Hammett constant  $\sigma$  versus the rate of base hydrolysis of a benzoic acid ester



R	$\sigma$	$k$ ( $\text{M}^{-1}\text{s}^{-1}$ )
$\text{NO}_2$	0.78	0.329
CN	0.66	0.157
Cl	0.23	0.210
H	0.00	0.289
Me	-0.17	0.172
OMe	-0.27	0.143

Hammett [84]

**Fig. 5** Plot  $\sigma$  versus  $\log k$  for the substrates given in Table 3



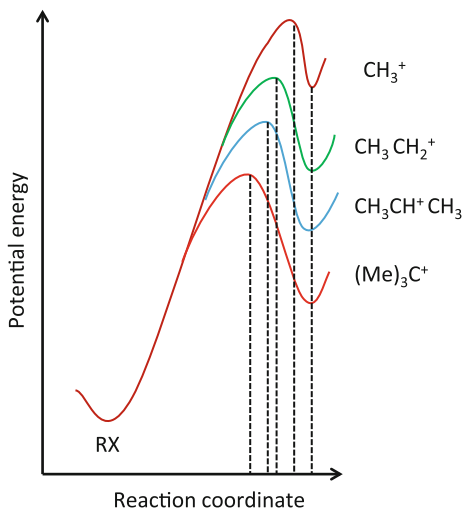
arises purely from the inductive effect. An electron-withdrawing group increases the rate of hydrolysis by (a) making the carbonyl carbon more electrophilic and (b) better stabilization of the resultant carboxylate ion. The Hammett constant therefore has a positive value. For reasons opposite to the above, an electron-donating group makes the constant negative. A bulky substituent is likely to exert steric effect as well on the rate of hydrolysis by shielding the carbonyl group from attack. A compilation of Hammett constants for the aliphatic series of substrates is available [77].

## 9 Hammond Postulate

The transition states of reactions cannot be characterized directly by experimental means because they are only transient in nature. Therefore, any guiding principle that can provide some guess of the chemical structure of a transition state is useful. Hammond postulated, "If two states, as for example, a transition state and an unstable intermediate, occur consecutively during a reaction process and have nearly the same energy, their inter-conversion will involve a small reorganization of the molecular structures." In other words, the transition state most resembles the adjacent reactant, intermediate, or product that is closest to it in energy, but only for as long as the energy difference between the transition state and the adjacent structure is not too large.

Accordingly, the transition state must resemble, respectively, the reactants and the products in highly exothermic and endothermic processes. For the thermoneutral processes, the transition state is in between the reactants and the products. This allows us, more or less, to accurately predict the shape of a reaction coordinate, and also an insight into the structure of the transition state. We generally place the transition state higher than the reactant and the product on the energy scale. Please note that the Hammond postulate predicts only the relative position of the transition state as the reaction progresses but not the height of the energy barrier compared to the reactant and the product.

**Fig. 6** Plot demonstrating Hammond's postulate



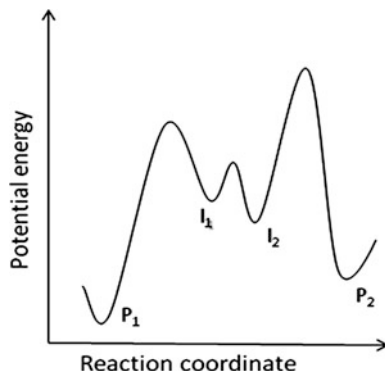
In the most well-known example of the application of Hammond postulate, we consider the comparison of structures of the various carbocations in  $S_N1$  reaction. The relative stabilities of the carbocations decrease in the order  $3^\circ > 2^\circ > 1^\circ > \text{Me}^+$ . According to the Hammond postulate, and as shown in Fig. 6, the transition state shifts toward the product cation as the stability of the cation decreases. Also, coupled with this, the transition state energy is lowered with the increase in the stability of the resultant cation [78–81].

## 10 Curtin–Hammett Principle

The Curtin–Hammett principle is concerned with the products ratio when there are two or more competing pathways originating from fast inter-converting isomers, conformers, or intermediates. Of course, each product is derived from a different transition state. According to this principle, the ratio of the products is ascertained by the relative heights of the transition states leading to different products, and is not significantly influenced by the relative energies of the isomers, conformers, or intermediates formed prior to the transition states. Let us understand this principle by examining the reaction coordinate diagram given in Fig. 7. Here, the intermediates  $I_1$  and  $I_2$  equilibrate readily because the energy barrier between them is much smaller than the exit barriers  $I_1 \rightarrow P_1$  and  $I_2 \rightarrow P_2$ . The intermediate  $I_2$  is lower in energy than the intermediate  $I_1$ . So being the case, the predominant product arises from the less stable structure  $I_1$  because the barrier for  $I_1 \rightarrow P_1$  conversion is less than the barrier for  $I_2 \rightarrow P_2$  conversion [82, 83].

Let us consider the nucleophilic addition to a carbonyl group adjacent to a stereogenic center. Following Anh-Felkin's modification of Cram's model for asymmetric induction, the reaction can follow either of the pathways shown in

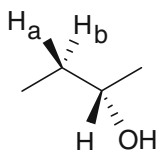
**Fig. 7** Plot demonstrating Curtin–Hammett principle whereby  $I_1 \rightarrow P_1$  predominates over  $I_2 \rightarrow P_2$



Eqs. 4 and 5 of Chap. 3. Since the pathway shown in Eq. 5 involves attack *syn* to the smallest size group and, thus, proceeds through a lower energy transition state than the pathway shown in Eq. 4 which involves attack *syn* to the medium size group due to the steric interaction between the nucleophile and the medium size substituent in the latter, the former process must predominate. Since the rotation barrier between the two reactant conformers is much too small compared to the transition state energies of 8–15 kcal/mol for the additions of hydride and Grignard reagents to carbonyl groups, they equilibrate much more rapidly with each other than pass on to the products on reaction with nucleophiles. Since, we only analyzed the product distribution on account of the relative energies of the transition states, the Curtin–Hammett principle applies to reactions taking place solely under kinetic control.

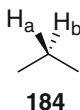
## 11 Diastereotopic, Homotopic, and Enantiotopic Substituents

When identical groups or atoms on the same carbon are in in-equivalent environments, they are termed diastereotopic. For instance, the hydrogen atoms labeled  $H_a$  and  $H_b$  in (*S*)-2-butanol **183** are diastereotopic. There is no symmetry operation that can interconvert these two hydrogen so that one assumes the characteristics of the other. These hydrogen atoms are different from each other in all meaningful ways, such as NMR shifts,  $\sigma_{C-H}$  bond lengths and, hence, bond dissociation energies.

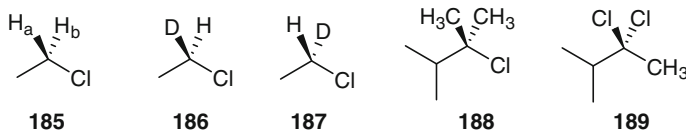


**183**

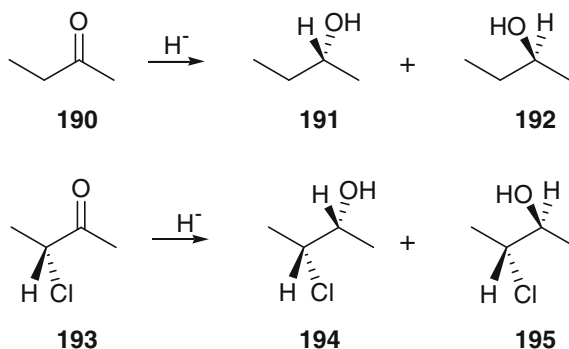
Unlike the above, the two hydrogen atoms labeled  $H_a$  and  $H_b$  in propane **184** are homotopic because a  $C_2$  operation converts one into the other, so that they are considered to be equivalent in all possible ways. Even if one of these hydrogen atoms is replaced by a substituent other than methyl and hydrogen, resultant molecule is not chiral. Homotopic groups remain indistinguishable under chiral influence, i.e., in the presence of chiral ligands.



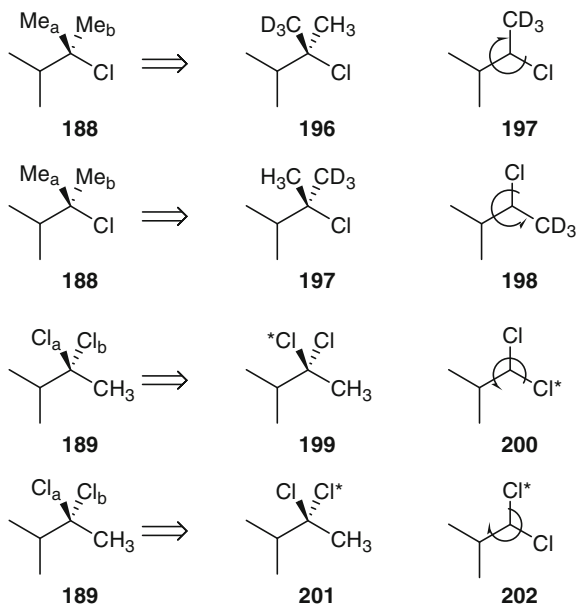
Unlike the case of propane above, replacement of one of the two hydrogen atoms labeled  $H_a$  and  $H_b$  in chloroethane **185** by a substituent different from methyl and chlorine leads to one enantiomer and, likewise, replacement of the other hydrogen atom leads to the other enantiomer. For instance, while the replacement of  $H_a$  by deuterium (D) forms (*R*)-**186**, a similar replacement of  $H_b$  by D forms (*S*)-2-**187**. Such hydrogens are called enantiotopic hydrogens. The enantiotopic groups need not be hydrogen atoms alone. For instance, the two methyl groups in 2-chloro-2,3-dimethylbutane **188** and the two chloro groups in 2,2-dichloro-3-methylbutane **189** are also enantiotopic. The enantiotopic hydrogens are distinguishable under chiral influence, i.e., in the presence of chiral ligands.



The topicity concept is also important in the reactions of trigonal centers, such as carbonyls and alkenes. In consideration of carbonyls, for example, the two faces are homotopic in a symmetrically substituted ketone, such as acetone or 2-pentanone, because the molecule has  $C_2$  symmetry. However, the faces are enantiotopic in an unsymmetrically substituted ketone, such as 2-butanone **190**. While the reaction with hydride on the top face of the carbonyl group forms (*R*)-2-butanol **191**, the reaction on the bottom face forms (*S*)-2-butanol **192**. Extending this argument further, the two faces are diastereotopic in an unsymmetrical ketone bearing a chiral center elsewhere in it, e.g., (*R*)-3-chloro-2-butanone **193**. The delivery of hydride ion to the top face of the carbonyl group forms 2(*R*),3(*R*)-3-chloro-2-butanol **194** and the delivery to the bottom face forms 2(*S*),3(*R*)-3-chloro-2-butanol **195**. The molecules **194** and **195** are diastereoisomers.

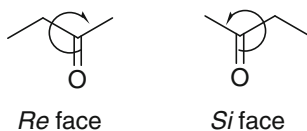


The topicity is described in yet another way also. Here, we use something similar to the *R/S* notation in an attempt to connect it to the topicity. For the  $\text{CH}_2$  group, we take the hydrogen that is to be assigned a descriptor and mentally replace it by a deuterium. Now, we assign the configuration in the normal way. If the result is that the newly formed stereogenic center is *R*, the hydrogen that we mentally replaced by deuterium is denoted pro-*R*, and if the new stereogenic center is *S*, the hydrogen is denoted pro-*S*. For instance, in chloroethane **185**,  $\text{H}_a$  is pro-*R* (as in structure **186**) and  $\text{H}_b$  is pro-*S* (as in structure **187**). Likewise, in **188** and **189**, we replace  $\text{CH}_3$  by  $\text{CD}_3$  and  $\text{Cl}$  by its higher isotope, say  $\text{Cl}^*$ , to distinguish the  $\text{CH}_3$  and  $\text{Cl}$  groups. Since  $\text{CD}_3$  takes precedence over  $\text{CH}_3$ , the  $\text{Me}_a$  and  $\text{Me}_b$  in **188** are pro-*R* and pro-*S*, as shown in **197** and **198**, respectively. The least priority group  $\text{CH}_3$  is kept below the plane. Likewise, the  $\text{Cl}_a$  and  $\text{Cl}_b$  in **189** are pro-*S* and pro-*R*, as shown in **200** and **202**, respectively.





The other descriptors that are sometimes used in describing the enantiotopic faces of a carbonyl group are *Re* and *Si* faces. In arriving at these descriptors, we simply place the molecule in the plane of the paper and assign priorities to the three groups as we would normally do to assign *R/S* or *E/Z* configurations. If the result is a clockwise rotation, the face we are looking at is referred to as the *Re* face. However, if it is anticlockwise rotation, the face is the *Si* face. An example using 2-butanone is give below.



## References

1. Batich C, Heilbronner E, Semmelhack (1973) *MF Helv Chim Acta* 56:2110
2. Huisgen R, Dahmen A, Huber H (1967) *J Am Chem Soc* 89:7130
3. Bates RB, Deines WH, McCombs DA, Potter DE (1969) *J Am Chem Soc* 91:4608
4. Huisgen R, Dahmen A, Huber H (1967) *J Am Chem Soc* 89:7130
5. Bates RB, Deines WH, McCombs DA, Potter DE (1969) *J Am Chem Soc* 91:4608
6. Laird T, Ollis WD, Sutherland IO (1980) *J Chem Soc Perkin Trans* 1:2033
7. Schlatmann JLMA, Pot J, Havinga E (1964) *Rec Trav Chim Pays Bas* 83:1173
8. Akhtar M, Gibbons CJ (1965) *Tetrahedron Lett* 509
9. Fráter G, Schmid H (1968) *Helv Chim Acta* 51:190
10. Lee BW, Lee SD (2000) *Tetrahedron Lett* 41:3883
11. Jefford CW, de los Heros V, Gehret J-CE, Wipff G (1980) *Tetrahedron Lett* 21:1629
12. Keating AE, Merrigan SR, Singleton DA, Houk KN (1999) *J Am Chem Soc* 121:3933
13. Houk KN, Rondan NG, Mareda J (1985) *Tetrahedron* 41:1555
14. Bernardi F, Bottoni A, Canepa C, Olivucci M, Robb MA, Tonachini G (1997) *J Org Chem* 62:2018
15. Schoeller WW, Yurtsever E (1978) *J Am Chem Soc* 100:7548
16. Montaigne R, Ghosez L (1968) *Angew Chem Int Ed Engl* 7:221
17. Woodward RB, Hoffmann R (1969) *Angew Chem Int Ed Engl* 8:167
18. Machiguchi T, Hasegawa T, Ishiwata A, Terashima S, Yamabe S, Minato T (1999) *J Am Chem Soc* 121:4771
19. Fleming I (2010) *Molecular orbitals and organic chemistry reactions*. Wiley, New York
20. Kirmse W, Rondan NG, Houk KN (1984) *J Am Chem Soc* 106:7989
21. Houk KN, Spellmeyer DC, Jefford CW, Rimbault CG, Wang Y, Miller RD (1988) *J Org Chem* 53:2125
22. Rudolf K, Spellmeyer DC, Houk KN (1987) *J Org Chem* 52:3708
23. Niwayama S, Kallel EA, Spellmeyer DC, Sheu C, Houk KN (1996) *J Org Chem* 61:2813
24. Rondan NG, Houk KN (1985) *J Am Chem Soc* 107:2099
25. Schiess P, Seeger R, Suter C (1970) *Helv Chim Acta* 53:1713
26. Evansck JD, Thomas BE IV, Spellmeyer DC, Houk KN (1995) *J Org Chem* 60:7134
27. Iliceto A, Fava A, Mazzucato U (1960) *J Org Chem* 25:1445
28. Fava A, Iliceto A, Bresadola S (1965) *J Am Chem Soc* 87:4791
29. Carretero JC, Ruano JLG (1985) *Tetrahedron Lett* 26:3381

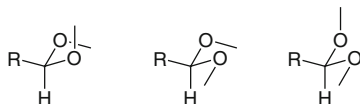
30. Tishkov AA, Schmidhammer U, Roth S, Riedle E, Mayr H (2005) *Angew Chem Int Ed Engl* 44:4623
31. Kornblum N, Smiley RA, Blackwood RK, Iffland DC (1955) *J Am Chem Soc* 77:6269
32. Kornblum N, Jones WJ, Hardies DE (1966) *J Am Chem Soc* 88:1704
33. Kornblum N, Hardies DE (1966) *J Am Chem Soc* 88:1707
34. Braude EA, Evans EA (1956) *J Chem Soc* 3238
35. Schulz AG, Yee YK (1976) *J Org Chem* 41:4045
36. Houk KN, Strozier RW (1973) *J Am Chem Soc* 95:4094
37. Gilman H, Kirby RH (1941) *J Am Chem Soc* 63:2046
38. Loupy A, Seyden-Penne J (1978) *Tetrahedron Lett* 2571
39. Morsch K (1933) *Monatsh Chem* 63:220
40. Jencks WP (1969) *Catalysis in chemistry and enzymology*. McGraw-Hill, New York, p 530
41. Nagamatsu T, Kuroda K, Mimura N, Yanada R, Yoneda F (1994) *J Chem Soc Perkin Trans 1*:1125
42. Ouellet SG, Tuttle JB, MacMillan DWC (2005) *J Am Chem Soc* 7:32
43. Menche D, Hassfeld J, Li J, Menche G, Ritter A, Rudolph S (2006) *Org Lett* 8:741
44. Li G, Liang Y, Antilla JC (2007) *J Am Chem Soc* 129:5830
45. Zhang Z, Schreiner PR (2007) *Synlett* 1455
46. Martin NJA, Ozores L, List B (2007) *J Am Chem Soc* 129:8976
47. Martin NJA, Chen X, List B (2008) *J Am Chem Soc* 130:13862
48. Li G, Antilla JC (1075) *Org Lett* 2009:11
49. Pelletier G, Bechara WS, Charette AB (2010) *J Am Chem Soc* 132:12817
50. Nguyen QPB, Kim TH (1977) *Synthesis* 2012:44
51. Chen L-A, Xu W, Huang B, Ma J, Wang L, Xi J, Harms K, Gong L, Meggers E (2013) *J Am Chem Soc* 135:10598
52. Wilds AL (1944) *Org React* 2:178
53. Ziegler K, Zeiser H (1930) *Ber* 63:1847
54. Lyle RE, Anderson PS (1966) *Adv Heterocycl Chem* 6:45
55. von Doering WE, McEwen WE (1951) *J Am Chem Soc* 73:2104
56. Kayser MM, Breau L, Eliev S, Morand P, Ip HS (1986) *Can J Chem* 64:104
57. Adam W, Grimison A, Hoffmann R (1969) *J Am Chem Soc* 91:2590
58. Um I-H, Oh S-J, Kwon D-S (1995) *Tetrahedron Lett* 36:6903
59. Buncl E, Wilson H, Chuaqui C (1982) *J Am Chem Soc* 104:4896
60. Hoz S (1982) *J Org Chem* 47:3545
61. Fountain KR, Hutchinson LK, Mulhearn DC, Xu YB (1993) *J Org Chem* 58:7883
62. Schoeller WW (1980) *Tetrahedron Lett* 21:1509
63. Arduengo III AJ, Goerlich JR, Marshall WJ (1995) *J Am Chem Soc* 117:11027
64. Alder RW, Allen PR, Murray M, Orpen AG (1996) *Angew Chem Int Ed Engl* 35:1121
65. Denk MK, Thadam A, Hatano K, Lough AJ (1997) *Angew Chem Int Ed Engl* 36:2607
66. Breslow R (1958) *J Am Chem Soc* 80:3719
67. von Doering WE, Knox LH (1989) *J Am Chem Soc* 83:1989
68. Jones M Jr, Ando W, Hendrick ME, Kulczycki A Jr, Howley PM, Hummel KF, Malament DS (1972) *J Am Chem Soc* 94:7469
69. Ando W, Suzuki J, Saiki Y, Migita T (1973) *J Chem Soc Chem Commun* 365
70. Rondan NG, Houk KN, Moss RA (1980) *J Am Chem Soc* 102:1770
71. Bourissou D, Guerret O, Gabbai FP, Bertrand G (2000) *Chem Rev* 100:39
72. Li F, Wu Z, Wang J (2015) *Angew Chem Int Ed* 54:656
73. Dippy JF, Page JE (1938) *J Chem Soc* 357
74. Jaffe HH (1953) *J Chem Phys* 21:415
75. Leffler JE, Greenwald E (1963) *Rates and equilibria of organic reactions*. Wiley, New York
76. Brown HC, Okamoto Y (1958) *J Am Chem Soc* 80:4979
77. Hansch C, Leo A, Taft RW (1991) *Chem Rev* 91:165
78. Hammond GS (1955) *J Am Chem Soc* 77:334
79. Leffler JE (1953) *Science* 117:340

80. Miller AR (1984) *J Am Chem Soc* 1978:100
81. Jencks WP (1985) *Chem Rev* 85:511
82. Seeman JI (1983) *Chem Rev* 83:83
83. Shorter J (1990) *Prog Phys Org Chem* 17:1
84. Hammett LP (1935) *Chem Rev* 17:125

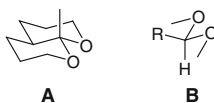
## Questions

Given below are some questions which are designed to test your comprehension of the contents of this book. It is likely that, in doing so, you may be required to read through the relevant chapters in efforts to find solutions.

1. If the energy of *trans*-decalin is equated to zero kcal mol<sup>-1</sup>, what is the energy of *cis*-decalin.
2. PhCHO reacts with excess of MeOH in the presence of a small amount of concentrated sulfuric acid under azeotropic removal of water formed, if any, to form PhCH(OMe)<sub>2</sub>. Write the chemical events that take place during the course of the transformation in such a way that the prevailing stereoelectronic effects are clearly expressed through the structures.
3. Express, through structures only, the more plausible mode of protic cleavage of each of the following acetal conformers. By considering the oxygen atom tetrahedral, write the electron pair orbitals on the oxygen atoms as well.



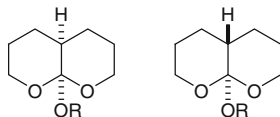
4. Both the acetals **A** and **B** undergo hydrolysis under acidic aqueous condition but with great difficulty. However, the difficulty experienced by the acetal **A** is significantly more severe than that experienced by the acetal **B**, so much so that **A** is practically non-reacting. Provide a crisp rationale for this observation.



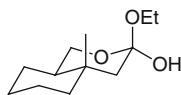
5. Consider all possible ways and arguments to demonstrate that it is fairly unlikely that a  $\gamma$ -lactone will entertain carbonyl oxygen exchange when

subjected to hydrolysis using aqueous  $\text{NaO}^*\text{H}$  [ $\text{O}^*$  denotes labeled oxygen]. The stereochemical relationship, if any, may please be shown meticulously.

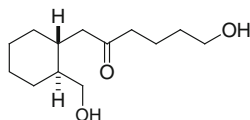
6. You are given a mixture of the following two isomers. How will you separate one from the other? You are allowed to destruct one of the two.



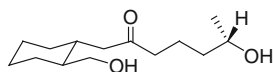
7. The following compound is allowed to stand with very dilute aqueous sulfuric acid for long enough to leave none of this. What product(s) will you expect to form? The rationale could be revealed through suitable stereostructures alone.



8. The following molecule is taken in dry toluene along with a catalytic amount of pyridinium *p*-toluenesulfonate and heated to reflux under azeotropic removal of water, if any formed, to obtain a mixture of two products. Write the stereostructures of these products, calculate the relative energy difference of the two, and predict which one of the two is more likely to constitute the major product.

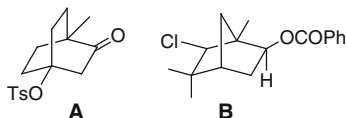


9. Comment, with rationale, on the relative distribution of products formed from the following compound when it has been heated with a trace of *p*-toluenesulfonic acid in toluene under dehydrating conditions. The conformational profile of the products must also be taken into account.

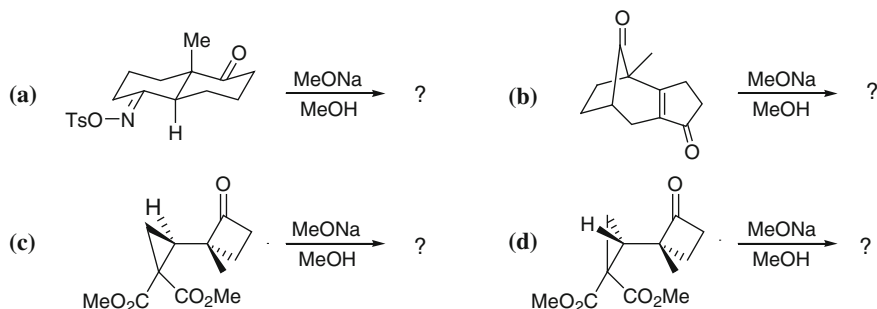


10. In reference to Q8 above, comment upon the scenario that is likely to emerge when the configuration at the Me-containing carbon is reversed.
11. The compound **A** is treated with  $\text{NaBH}_4$  in aqueous  $\text{MeOH}$  and the compound **B** with  $\text{NaOH}$  in aqueous  $\text{MeOH}$  when each one is transformed into a

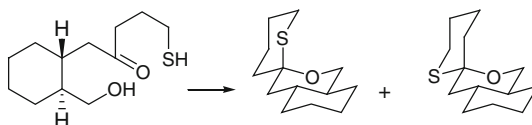
monocyclic product. Show the sequence of reactions and the operating stereo-electronic effects by the movement of arrows.



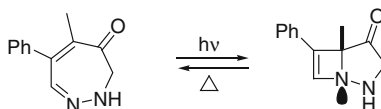
12. Recognize the elements of orbital-orbital interaction in the most appropriate antiperiplanar setup and write the products of the following reactions.



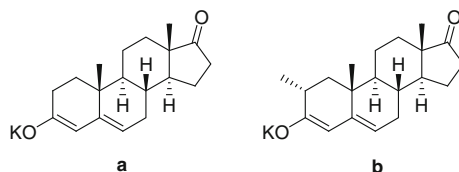
13. Take a look at the following reaction and note the formation of the two isomeric products. Predict, on account of relative energy calculation, the ratio of the two isomers. Please consider the anomeric stabilization arising from electron pair orbital on sulfur the same as that arising from oxygen.



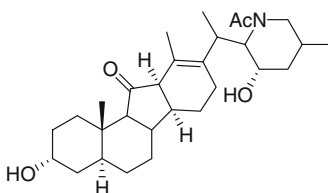
14. The monocyclic material in the following reaction is transformed efficiently into the bicyclic material on exposure to light. Interestingly, the latter reverts to the former on heating at an elevated temperature as shown. How do you account for this observation within the purview of conservation of orbital symmetry rules.



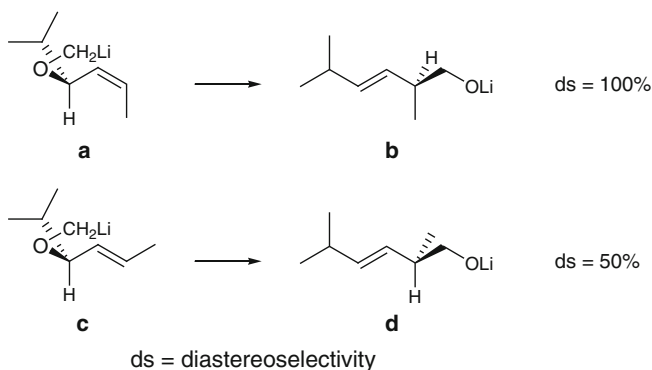
15. Which of the following two enolates is likely to be more easily generated from the corresponding ketone? Explain with rationale.



16. Double bond isomerization to achieve higher conjugation takes place when the following compound is allowed to stand with a dilute solution of caustic soda in aqueous alcohol at 25 °C for extended duration. Write the structure of the product with absolute stereochemical clarity.

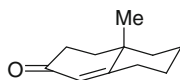


17. Consider the following reactions and offer a brief rationale for the decline in the observed diastereoselectivity.

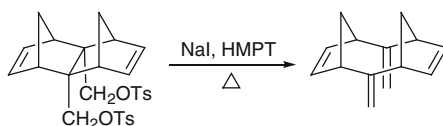


18.  $\delta$ -Lactone is reacted with trimethyloxonium tetrafluoroborate ( $\text{Me}_3\text{O}^+\text{BF}_4^-$ ). The produce is next refluxed with sodium iodide in acetone until complete disappearance of the  $\delta$ -lactone. By taking entropy effects, stereoelectronic effects and the relative ease of  $\text{S}_{\text{N}}2$  reaction on primary versus secondary vs tertiary carbons into consideration, comment on the possible product(s) profile.

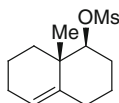
19. The following enone is subjected to dissolving metal reduction in the presence of an appropriate protonating species such *tert*-butanol. Please write the structures of all the possible products and calculate their relative energies. Which product will you predict to predominate if allowed to consider the product's thermodynamic stability as the control factor?



20. The substrate given in question 19 is subjected to reaction with lithium dimethylcuprate. Please write the structures of all the possible products and calculate their relative energies by taking 0.9 kcal/mol for 1,3-diaxial interaction between a methyl and a hydrogen. Which product will you predict to predominate if allowed to consider the product's thermodynamic stability as the primary control factor?
21. On being subjected to Bayer-Villiger oxidation using *m*-chloroperoxybenzoic acid in chloroform as the solvent, 2-norbornanone generates a mixture of two products. One of these products is reluctant to reaction with aqueous ethanolic caustic soda while the other reacts easily to form a product which cannot be extracted out from the alkaline solution by organic solvents such as diethyl ether and dichloromethane. This solvent extraction, however, removes the non-reacting species conveniently. Please try to present an elaborate account of the entire event with structures and arguments.
22. Write the transition state for the following transformation. HMPT's role is that of a high boiling neutral solvent and it, as such, does not take part in the reaction.

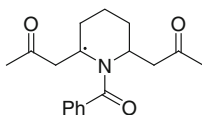


23. The following substrate is subjected to reaction with an equimolar amount of dicyclohexylborane to generate a single boron containing entity in quantitative yield. Without isolation, it is mixed with an equimolar amount of aqueous caustic soda to isolate 1-*trans*-6-*trans*-1-methyl-1,6-cyclodecadiene as the sole product. Please present the events in a schematic fashion with due care of the involved stereochemical features.

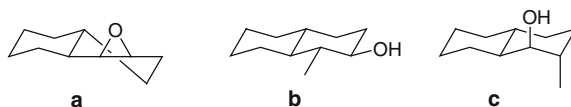




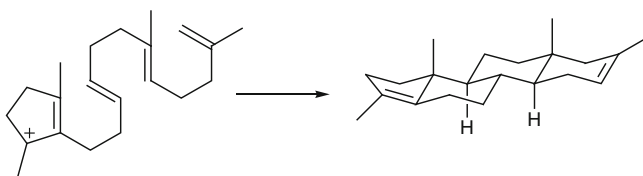
24. The following *cis*-2,6-disubstituted piperidine derivative is expected to exist largely in a single conformation. Please speculate on account of allylic strain and write the said conformer.



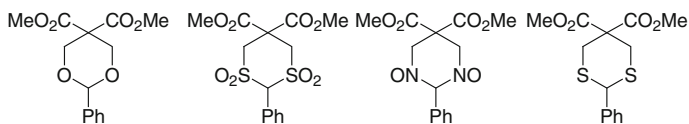
25. Consider reaction of  $\text{Me}_2\text{CuLi}$  with the oxirane **a**. Please steer through the reaction pathways with appropriate stereostructures to the products **b** and **c**. Which product will you expect to be formed as the major product and why?



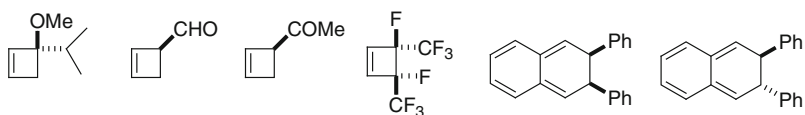
26. Write the 3D geometrical orientation of the reactant which is suitable for the following transformation.



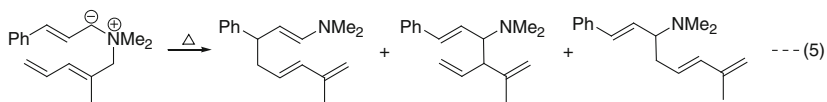
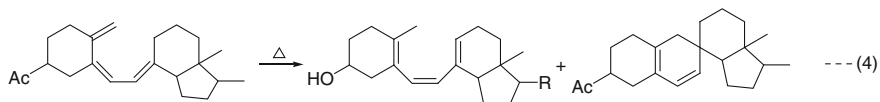
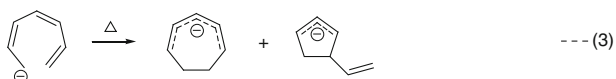
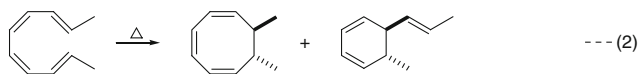
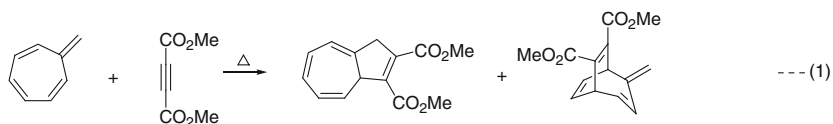
27. Comment on the hydrolysis of the 'stable but devoid of any anomeric effect' conformer of benzaldehyde dimethyl acetal. Write the Newman projection of the cation formed from the first  $\sigma_{\text{C-O}}$  bond cleavage.
28. Write the entire schematic pathway for the change of  $\alpha$ -D-glucose into  $\beta$ -D-glucose under mild acidic condition.
29. Write the chair structures of each of the following substrates and also the major product formed from a single decarboxylation on reaction with  $\text{LiCl}$  in wet DMSO. Please note that the oxygen and sulfur atoms are, respectively, electron-attracting and electron-donating.



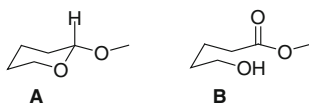
30. Write the major product from each of the following substrates which is formed on heating. You need to consider torquoselectivity which supports an electron-donating substituent to move outside and an electron-attracting substituent to move inside for reasons of greater stabilization of the respective transition states.



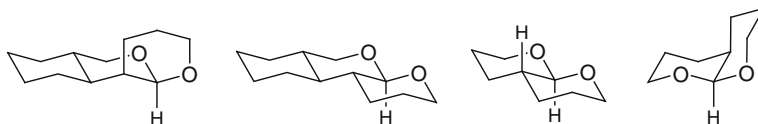
31. Please indicate which of the shown products from each of the following reactions is expected to predominate.



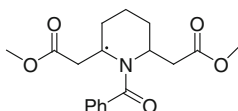
32. The substrate **A** reacts with ozone to form the hydroxy ester **B**. Please write the structure of the transition states that leads to the breakdown of the intermediate hydrotrioxide species into the product in a single step.



33. Which of the following substrates is not likely to react with ozone?

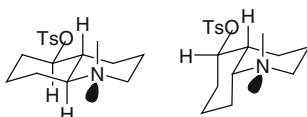


34. Depending fully on the allylic strain, write the preferred conformation of the following *cis*-2,6-disubstituted piperidine derivative.

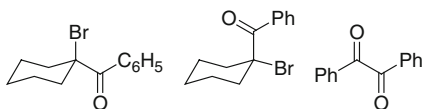


35. (*S*)-2-dimethylphenylsilyl-3(*E*)-pentene and (*S*)-2-dimethylphenylsilyl-3(*Z*)-pentene display, respectively, 50 and >95 % diastereoselectivity on hydroboration followed by oxidative cleavage of the so-formed carbon–boron bond. Please write these transformations and explain the observed difference in the level of selectivity.

36. The following two substrates are subjected to solvolysis in aqueous alcohol and the resultant is subjected to oxidation with IBX. Write the product with full stereo-structure from each.



37. The following compounds are treated with alcoholic aqueous NaOH. Please write the product(s) from each with suitable relative stereochemistry as and where applicable.



38. Write 3D-structures of *cis*- and *trans*-2,10-dioxabicyclo[4.4.0]decalins and calculate the relative energy difference between the two. Please consider the oxygen tetrahedral just like carbon and the value of one anomeric effect arising from oxygen as  $-1.40 \text{ kcal mol}^{-1}$ .

39. 1,9-Dihydroxy-5-nonanone is refluxed in benzene with a catalytic amount of *p*-toluenesulfonic acid monohydrate under azeotropic removal of water formed, if any. Write the stereostructures of all the possible products and calculate the energy of each on a relative scale.
40. Show the progress of acetolysis of the tosylates derived from optically active *erythro*- and *threo*-3-phenyl-2-butanol and also comment on the overall optical activity of the product(s) in each instance.
41. Write the molecular orbitals of allyl anion, allyl radical and allyl cation with the number of electrons in each. Please indicate the symmetry characteristics of each orbital in respect of mirror plane and also  $C_2$  axis of symmetry.
42. The combination of one olefin with another olefin gives rise to the formation of a cyclobutene derivative. Show the molecular orbitals along with the symmetry characteristics with respect to a single mirror plane on both sides of the reaction. Comment on the thermal or photochemical requirement of this reaction.
43. Comment on the nucleophilicity of *t*-BuOO<sup>-</sup> ion vs-à-vis *t*-BuO<sup>-</sup> ion with reason(s) for the difference, if any.
44. Define Hammett's constant for aromatic carboxylic acids and comment on the relationship of this constant with both ionization constant (K) and acid strength (pKa) value.
45. By taking the example of spiro[2.4]heptatriene, explain the concept of spiroaromaticity.
46. An excellent example of spiroantiaromaticity is spiro[4.4]nonatetraene. Please explain how antiaromaticity comes into the picture.
47. Apply Houk's electrostatic model and Cieplak's  $\sigma$ - $\sigma^*$  model to predict the diastereoselectivity of lithium aluminum hydride reduction of *endo,endo*-2,3-dimethylbicyclo[2.2.1]norbornan-7-one.
48. How does the cation complexation model explain the experimental anti-selectivity of *endo,endo*-2,3-dimethylbicyclo[2.2.1]norbornan-7-one and also the higher anti-selectivity of *endo,endo*-2,3-diethylbicyclo[2.2.1]norbornan-7-one over that of *endo,endo*-2,3-dimethylbicyclo[2.2.1]norbornan-7-one?